

**Regulation of a two-pore K<sup>+</sup> channel by multiple functional subunits  
in *Caenorhabditis elegans***

by  
Ignacio Perez de la Cruz

B.S., Biochemistry and Molecular Biology  
Brown University, 1995

Submitted to the Department of Biology  
in partial fulfillment of the requirements for the degree of

DOCTOR OF PHILOSOPHY

at the  
MASSACHUSETTS INSTITUTE OF TECHNOLOGY

September 2002

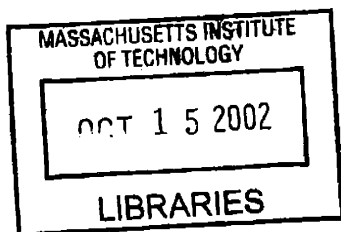
© 2002 Ignacio Perez de la Cruz. All rights reserved.

The author hereby grants MIT permission to reproduce and to distribute publicly  
paper and electronic copies of this thesis document in whole or in part.

Signature of Author: \_\_\_\_\_  
Department of Biology  
August 19, 2002

Certified by: \_\_\_\_\_  
H. Robert Horvitz  
Professor of Biology  
Thesis Supervisor

Accepted by: \_\_\_\_\_  
Alan Grossman  
Chairman of the Graduate Committee  
Department of Biology



ARCHIVES

## **Regulation of a two-pore K<sup>+</sup> channel by multiple functional subunits in *Caenorhabditis elegans***

Submitted to the Department of Biology on August 19, 2002 in partial fulfillment of the  
Requirements for the Degree of DOCTOR OF PHILOSOPHY

### **ABSTRACT**

K<sup>+</sup> channels generate and tune the electrical signals that underlie the functioning of neurons and other excitable cells. We have studied a set of genetically-interacting genes, *sup-9*, *sup-10* and *unc-93*, whose products are predicted to form a protein complex that when misregulated leads to severe muscle paralysis in the nematode *C. elegans*. We cloned *sup-9* and found it encodes a K<sup>+</sup> channel of the recently discovered mammalian two-pore family of voltage-insensitive leak channels, suggesting that SUP-10 and UNC-93, along with multiple UNC-93-like genes in *Drosophila* and humans, are the first regulatory subunits for two-pore K<sup>+</sup> channels. Based on pharmacological data, we propose that gain-of-function mutations in the *sup-9* channel or in its proposed subunits result in muscle paralysis through excessive K<sup>+</sup> efflux and hyperpolarization of muscle cells.

We cloned *sup-18*, a regulator of the channel complex, and show that SUP-18 is a type-three transmembrane protein that colocalizes with SUP-9 in muscle membranes and whose intracellular domain is similar to bacterial NADH nitroreductases that use an FMN cofactor. We identified a mutation in a predicted FMN-binding residue of SUP-18 that both eliminates its *in vivo* function without disrupting its membrane localization and that impairs the enzymatic activity of a related *Thermophilus* enzyme, suggesting that SUP-18 may couple cell metabolism with membrane excitability.

Through genetic and molecular studies, we determined that the SUP-10 subunit acts together with SUP-18 to activate the SUP-9 channel through a novel conserved domain in SUP-9. This domain is not required for the activation of SUP-9 by UNC-93, thus defining two independent modes of activation for a two-pore channel by multiple subunits. We also discovered a second domain in SUP-9, conserved in the human TASK-1 and TASK-3 channels, that integrates multiple regulatory inputs. Finally, our analysis of the subcellular localization of other *C. elegans* two-pore channels suggests that they can be differentially targeted within the cell membrane of muscle cells.

Thesis Supervisor: H. Robert Horvitz

Title: Professor of Biology

## **Acknowledgements**

Becoming a scientist under the tutelage of Bob Horvitz has been a privilege. I thank Bob for tremendous support and freedom in pursuing this project, for his intellectual insights and for demanding the highest standards of scientific inquiry and presentation.

I am indebted to my thesis committee members, Harvey Lodish, Chris Kaiser, Paul Garrity and Steve Cannon, for their support, suggestions and guidance over the years.

I thank members of the Horvitz lab for generating a rigorous yet fun scientific environment. I thank my classmates Rajesh Ranganathan, Craig Ceol, Ho-Yon Hwang and Matt Voas for their support and companionship; my baymates over the years, Gillian Stanfield, Yi-Chun Wu, Hillel Schwartz and Megan Higginbotham, for their patience in “loaning” me their scissors and pens; Peter Reddien for his friendship and lively discussions; Melissa Hunter, Ned Buttner, Mark Alkema, Ewa Davidson, Melissa Harrison and Niels Ringstad for their camaraderie.

While this thesis was completed at MIT, my training as a scientist has its roots in my undergraduate studies at Brown University. Professors David Cane and Philip Rieger inspired me with their “old-school” scientific rigor, while my thesis advisor Dr. Eduardo Nillni afforded me unsurpassed scientific freedom.

Wonderful friends have made the last seven years even more memorable, in particular Magdalena Leuca, Valerie Grabiell, Conny Krause, Flavia Sette da Rocha, Gina Herrera, Juan Carlos Deniz and Shirley Gazabon. Members of the MIT European Club, the IVC volleyball team (especially Chris Melhus and Stefan Gromoll), and the salsa community have balanced the academic demands and allowed me to grow in many ways.

My family has been a source of unwavering love and support. I thank my parents, Mariano and Carmen, for instilling in me the discipline, sacrifice and drive for excellence embodied in this thesis; my siblings Carmen, Cristina and David for believing I would one day graduate and for the joy and companionship they have provided me.

## Table of Contents

Title Page .....	1
ABSTRACT .....	2
Acknowledgments .....	3
Table of Contents .....	4
<b>CHAPTER ONE: K<sup>+</sup> Channels and their Regulatory Subunits</b> .....	11
<b>K<sup>+</sup> Channels in Biology</b> .....	12
<b>Major Discoveries in K<sup>+</sup> Channel Research</b> .....	12
<b>K<sup>+</sup> Channel Families</b> .....	12
<b>6TMD/ 1P Structural Class</b> .....	14
<u>K<sub>v</sub> family</u> .....	14
<u>Eag family</u> .....	15
<u>KCNQ family</u> .....	15
<u>Slo family</u> .....	16
<u>SK family</u> .....	16
<b>2TMD/1P Structural Class</b> .....	17
<b>4TMD/2P Structural Class</b> .....	17
<b>Ion Selectivity and Gating of K<sup>+</sup> Channels</b> .....	20
<b>Regulatory Subunits and K<sup>+</sup> Channel Diversity</b> .....	21
<b>K<sub>v</sub>β Regulatory Subunits</b> .....	21
<b>Slo Regulatory Subunits</b> .....	25
<b>MinK Regulatory Subunits</b> .....	27
<b>SUR Regulatory Subunits</b> .....	29
<b>KchIPs Regulatory Subunits</b> .....	30
<b>K<sup>+</sup> Channel Associated Proteins</b> .....	31
<b>Regulation of Channel-Subunit Interactions</b> .....	32
<b>K<sup>+</sup> Channels in <i>C. elegans</i></b> .....	34
<b><i>sup-9, sup-10, sup-18 and unc-93</i> Interacting Genes</b> .....	35
<b>Acknowledgments</b> .....	36
<b>References</b> .....	37
<b>Figures</b> .....	64
Figure 1. Illustrated Timeline of Significant Developments in the Areas of K <sup>+</sup> Channel and Channel Regulatory Subunit Research .....	64

Figure 2. Human K <sup>+</sup> Channel Families and their Associated Regulatory Subunits .....	68
<b>Chapter TWO: <i>sup-9</i> and <i>unc-93</i> May Encode Components of a Two-Pore K<sup>+</sup> Channel Required to Coordinate Muscle Contraction in <i>C. elegans</i></b> .....	70
<b>Summary</b> .....	71
<b>Introduction</b> .....	72
<b>Results</b> .....	74
Molecular Cloning of <i>sup-9</i> .....	74
<i>sup-9</i> Encodes a Two-pore K <sup>+</sup> Channel .....	74
Characterization of <i>sup-9</i> Mutant Alleles .....	75
<i>sup-9::gfp</i> is Expressed in Muscles and a Subset of Neurons .....	76
<i>unc-93::gfp</i> Is Expressed in Muscles and a Subset of Neurons .....	77
<i>sup-9</i> and <i>unc-93</i> Function in Muscles .....	78
SUP-9 and UNC-93 Colocalize Intracellularly .....	79
Muscimol Can Phenocopy the Rubberband Unc Phenotype .....	79
<i>unc-93</i> Belongs to a Large <i>C. elegans</i> Gene Family and Is Conserved in Flies and Mammals .....	81
<b>Discussion</b> .....	82
<i>sup-9</i> and <i>unc-93</i> Probably Interact Physically .....	82
The SUP-9(gf) K <sup>+</sup> Channel May Be Stabilized in an Open Conformation.....	83
SUP-10 and UNC-93 May Regulate SUP-9 K <sup>+</sup> Channel Activity .....	85
Implications for K <sup>+</sup> Channel Biology .....	86
Experimental Procedures .....	88
Strains and Genetics .....	88
Mapping of the <i>sup-9(n1428)</i> Tc1 Polymorphism .....	88
Cloning of <i>sup-9</i> .....	89
Reverse Transcription PCR/ RACE .....	89
Expression Constructs .....	89
Transgenic Animals .....	90
Antibodies and Immunostaining .....	90
Neuronal Cell Identifications .....	91
Muscimol and Rubberband Unc Assays .....	91
<b>Acknowledgments</b> .....	93
<b>References</b> .....	94

<b>Tables</b> .....	104
Table 1. <i>sup-9</i> loss-of-function mutations .....	104
Table 2. <i>sup-9</i> altered-function mutations .....	107
Table 3. Expression of <i>sup-9</i> and <i>unc-93</i> in muscle rescues their If egg-laying defects .....	108
<b>Figures</b> .....	109
Figure 1. Molecular Cloning, Genomic Structure, and Sequence of the <i>sup-9</i> Gene .....	109
Figure 2. Expression of <i>sup-9::gfp</i> and <i>unc-93::gfp</i> Fusion Proteins .....	111
Figure 3. <i>sup-9</i> and <i>unc-93</i> Muscle-Specific Rescue of Locomotion Defects....	113
Figure 4. Subcellular Colocalization of SUP-9 and UNC-93::GFP .....	115
Figure 5. Muscimol Phenocopies the Rubberband Unc Phenotype of <i>sup-9(gf)</i> , <i>unc-93(gf)</i> and <i>sup-10(gf)</i> Mutants .....	117
Figure 6. Muscimol Responses of <i>sup-9</i> , <i>sup-10</i> , <i>sup-18</i> and <i>unc-93</i> Mutants .....	119
Figure 7. Phylogenetic Tree of UNC-93-like Genes from <i>C. elegans</i> , <i>Drosophila</i> , Mouse and Human .....	121
Figure 8. Proposed Conformational Changes in the Fourth Transmembrane Domain of SUP-9 Underlie Channel Gating .....	123
<b>Appendix to Chapter TWO</b> .....	125
<b>Introduction</b> .....	126
<b>Results/Discussion</b> .....	126
<i>unc-93</i> Is Absolutely Required for Expression of <i>sup-9(gf)</i> Activity .....	126
The Paralysis of <i>twk-18(gf)</i> Mutants Is not Suppressed by <i>unc-93(lf)</i> or <i>sup-10(lf)</i> Mutations .....	128
<b>References</b> .....	128
Table 1. The rubberband Unc paralysis of <i>twk-18(cn110ts) gf</i> mutants cannot be suppressed by If mutations in <i>unc-93</i> or <i>sup-10</i> .....	130
Figure 1. Overexpression of <i>sup-9(gf)</i> Cannot Bypass the Need for <i>unc-93</i> ....	131
<b>Chapter THREE: Regulation of the <i>C. elegans</i> Two-Pore K<sup>+</sup> Channel <i>sup-9</i> by a Nitroreductase-Like Transmembrane Protein</b> .....	133
<b>Summary</b> .....	134
<b>Introduction</b> .....	135

<b>Results</b> .....	137
<i>sup-18</i> is Specifically Required for the Activation of the <i>sup-9</i> Channel by the Proposed <i>sup-10</i> Subunit.....	137
In <i>sup-10(gf)</i> Mutants, the Activity of the SUP-9 Channel is Sensitive to Levels of SUP-18 .....	138
Molecular Cloning of <i>sup-18</i> .....	139
Analysis of <i>sup-18</i> Mutations .....	140
The <i>thermophilus</i> Nox Oxidase Carrying the Equivalent Mutation to <i>sup-18(n1010)</i> is Catalytically Inactive .....	141
SUP-18 Colocalizes with SUP-9 in Muscle Membranes .....	141
Protein Complex Formation .....	142
SUP-18 Membrane Topology .....	143
Overexpression of Catalytically-Impaired SUP-18(n1010) at the Cell Surface Fails to Rescue a <i>sup-18(lf)</i> Null Mutant .....	143
Mouse SUP-18 Cannot Substitute for SUP-18 <i>in vivo</i> .....	144
Overexpression of the Nitroreductase Domain of SUP-18 in Muscle Is Sufficient to Restore <i>sup-18</i> Activity <i>in vivo</i> .....	145
<i>sup-18</i> Overexpression Specifically Enhances the Defects of <i>sup-10(gf)</i> but not those of <i>unc-93(gf)</i> Mutants .....	145
<i>sup-9(n1435)</i> Mutants Are Insensitive to <i>sup-10(gf)/sup-18</i> -Dependent Activation .....	147
The <i>sup-9(n1435)</i> Mutation Affects a Conserved Region in the C-terminal Domain of SUP-9 .....	148
Residue S289 in the SC Box of SUP-9 Is also Required for its Specific Activation by SUP-18.....	149
<b>Discussion</b> .....	151
<i>sup-18</i> Encodes a Muscle Transmembrane Protein with an Intracellular Nitroreductase Domain .....	151
SUP-10(gf) Likely Activates the SUP-9 Two-pore Channel by Creating a Hypersensitivity to SUP-18 .....	153
Activation of the SUP-9 Two-Pore Channel by Multiple Subunits Proceeds through Distinct Domains.....	154
<b>Experimental Procedures</b> .....	157
Strains and genetics.....	157

Mapping and Cloning of <i>sup-18</i> .....	157
Molecular Biology .....	157
Nox Enzymatic Assays .....	159
Antibodies and Immunostaining .....	160
<i>In vivo</i> Pulldown Assays .....	160
Transgenic Animals .....	161
<b>Acknowledgments</b> .....	162
<b>References</b> .....	163
<b>Tables</b> .....	171
Table 1 <i>sup-18(lf)</i> mutations specifically suppress <i>sup-10(gf)</i> locomotion defects .....	171
Table 2 <i>sup-18(lf)</i> mutations are haploinsufficient for suppression of <i>sup-10(gf)</i> but not <i>unc-93(gf)</i> locomotion defects .....	172
Table 3. <i>sup-18</i> loss-of-function mutations .....	173
Table 4. Overexpression of <i>sup-18</i> in muscle enhances the defects of <i>sup-10(gf)</i> but not <i>unc-93(gf)</i> mutants .....	174
<b>Figures</b> .....	175
Figure 1. <i>sup-18</i> Encodes a Protein with Amino Acid Similarity to Bacterial Nitroreductases.....	175
Figure 2. <i>T.t.NOX</i> carrying an S19N mutation Equivalent to <i>sup-18(n1010)</i> Has Greatly Reduced NADH Oxidase Activity .....	177
Figure 3. <i>sup-18</i> Is Expressed Predominantly in Muscle Membranes and Colocalizes with SUP-10::GFP .....	179
Figure 4. Native SUP-18 and SUP-9 Copurify from Worm Membranes .....	181
Figure 5. SUP-18 Is a Type-one Transmembrane Protein whose Nitroreductase Domain Resides Intracellularly .....	183
Figure 6. Overexpression of SUP-18 or of its Intracellular Domain Restores the Locomotion Defect to <i>sup-18(lf); sup-10(gf)</i> Animals .....	185
Figure 7. Overexpression of a <i>sup-18</i> Transgene in <i>sup-10(gf)</i> but not in <i>unc-93(gf)</i> Animals Enhances the Rubberband-Unc Phenotype .....	187
Figure 8. The <i>sup-9(n1435)</i> Mutation Confers Resistance to Channel Activation by <i>sup-18</i> .....	189
Figure 9. Serines 289 and 292 in the Cytoplasmic C-terminal Domain of SUP-9 Are Required for Activation by the <i>sup-10(gf)</i> Subunit .....	191



Figure 10. Biochemical Models of SUP-10/SUP-18 Activation of the SUP-9 Channel .....	193
Figure 11. Activation of K <sup>+</sup> Channels through Multiple Regulatory Inputs .....	195
<b>Appendix to Chapter THREE</b> .....	197
<b>Introduction</b> .....	198
<b>Results/Discussion</b> .....	198
<b>References</b> .....	200
<b>Figures</b> .....	201
Figure 1. A SUP-18::NOX Chimera Does not Rescue <i>sup-18(lf)</i> Mutants.....	201
Figure 2. Overexpression of <i>T.t.NOX</i> in <i>sup-18(lf); sup-10(gf)</i> is Toxic.....	203
<b>Chapter FOUR: Additional Findings</b> .....	205
<b>The <i>sup-9(n3935)</i> Mutation Reveals a Convergence of Activating Signals     from Multiple Regulatory Subunits</b> .....	206
Introduction .....	206
Results .....	207
Screen Rationale.....	207
Isolation of <i>sup-9</i> Alleles.....	207
Discussion.....	209
The Post-4TMD Region of Two-Pore Channels Integrates Multiple Inputs ....	209
Acknowledgments .....	210
References.....	210
Figures .....	213
Figure 1. Gene Assignments of Semidominant Suppressors of <i>sup-10(gf)</i> ...	213
Figure 2. The <i>sup-9(n3935)</i> Mutation in the 4 <sup>th</sup> TMD of SUP-9 Confers Resistance to Activation by <i>sup-18</i> and <i>unc-93(gf)</i> .....	215
Figure 3. <i>C. elegans</i> and Mammalian Two-Pore K <sup>+</sup> channels Integrate Multiple Regulatory Inputs Through a Common Mechanism .....	217
<b>Analysis of Two-Pore K<sup>+</sup> Channel Function and Membrane Localization     in <i>C. elegans</i></b> .....	219
Introduction.....	219
Results/Discussion.....	220
Overexpression of Wildtype or Mutant TWK-4 in Worm Muscle Has no Effect on Locomotion Rates.....	220
TWK-18::GFP Has a Strikingly Different Membrane Localization on Muscle	

Membranes Compared to TWK-4::GFP and SUP-9 .....	220
References.....	222
Table 1.....	226
Figures.....	227
Figure 1. Sequence alignment of SUP-9, TWK-4 and TWK-18 Two-Pore K <sup>+</sup> Channels.....	227
Figure 2. Muscle Expression Patterns in Transgenic Animals Overexpressing GFP Translational Fusions of Various Genes .....	229
<b>Molecular Analysis of <i>sup-10</i> and <i>unc-93</i> mutations.....</b>	<b>231</b>
Mutational Analysis of <i>sup-10</i> .....	231
Mutational Analysis of Second-Site Partial Suppressors of <i>unc-93(e1500)</i> .....	232
References .....	232
Tables .....	233
Table 1. <i>sup-10</i> loss-of-function mutations .....	233
Table 2. <i>unc-93 partial</i> loss-of-function mutations .....	234

## CHAPTER ONE

### **K<sup>+</sup> Channels and their Regulatory Subunits**

## **K<sup>+</sup> Channels in Biology**

Potassium channels are central to biology. They are found in virtually every cell of every organism. The rhythmic beating of the human heart or the complexities of the thinking mind are manifestations of electrical activity that is generated and modified by these highly selective pores. The regulated passage of K<sup>+</sup> ions regulates homeostasis, cell volume, neurotransmitter and hormone secretion and underlies learning and memory. Although the existence of channels had been proposed by Hodgkin and Huxley half a century ago, and many of the currents they generate *in vivo* have been studied for years, it has been only in the past fifteen years that major cloning efforts have led to the molecular identification of dozens of K<sup>+</sup> channels in humans. To achieve the tremendous functional diversity displayed *in vivo*, K<sup>+</sup> channels have acquired regulation through factors as varied as membrane potential, calcium, membrane stretch, pH, phosphorylation by kinases, second messengers and regulatory subunits. Molecular, structural and electrophysiological studies of cloned K<sup>+</sup> channels have elucidated the underlying basis for their ion selectivity and have furthered our understanding of the mechanism by which they are gated. The importance of K<sup>+</sup> channels in the regulation of basic biological processes has been underscored by the identification of human disorders, such as periodic paralysis, cardiac arrhythmia, epilepsy, hypoglycemia and deafness, caused by mutations in these genes.

## **Major Discoveries in K<sup>+</sup> Channel Research**

In reviewing any major area of scientific study, a historical approach serves a dual function: to describe the current state of the field and to frame the intellectual movement that accompanies the science. In a field as broad and intertwined as that of K<sup>+</sup> channels such an approach would be impractical. Whenever possible, experimental findings will be presented historically so as to reflect the thinking at the time, but most of this survey into K<sup>+</sup> channels will be relegated to descriptive terms. Nevertheless, a chronological perspective of major discoveries in the study of K<sup>+</sup> channels is provided as an illustrated timeline (Figure 1). This timeline places an additional emphasis on developments in ion channel regulatory subunits, as they are a major focus of the experimental work contained in this thesis.

## **K<sup>+</sup> Channel Families**

The 67 mammalian K<sup>+</sup> channels identified thus far are classified into seven families (Figure 2) (Wei et al., 1996; Grissmer, 1997). Families can be further grouped into three main structural classes, according to the number of transmembrane domains (TMD) and P-domains they contain (Figure 2). P-domains are highly conserved loops that determine the ion selectivity of K<sup>+</sup> channels (Heginbotham et al., 1994). These classes include the 6TMD/1P, 2TMD/1P and 4TMD/2P classes. A fourth structural class 8TMD/2P is defined by the yeast TOK-1 channel (Ketchum et al., 1995), but as no channels from this class have been identified from any other species it will not be considered further. Likewise, cyclic nucleotide-gated (CNG) channels (reviewed in Broillet and Firestein, 1999) are structurally related to voltage-gated K<sup>+</sup> channels as they have a 6TMD/1P structure, but they are Na<sup>+</sup> and K<sup>+</sup> selective and thus will lie beyond the scope of this survey.

Although K<sup>+</sup> channels display structural diversity, the tetramerization of P-domains to form the K<sup>+</sup> selective pore is regarded as a structural hallmark of K<sup>+</sup> channels (MacKinnon, 1995). This arrangement has been formally shown for the 6TMD/1P class through the use of channel subunits with differing sensitivities to a toxin (MacKinnon, 1991) and for the 2TMD/1P class through experiments with tandem fusions of channels (Yang et al., 1995), chemical crosslinking of native channels (Raab-Graham and Vandenberg, 1998) or by X-ray crystallography (Doyle et al., 1998). Some channels from the 4TM/2P class have been shown to dimerize to form a functional channel (Czirjak and Enyedi, 2002), consistent with a conformation of four P-domains for this class. Voltage-gated Na<sup>+</sup> channels (reviewed in Goldin, 1999) and voltage-gated Ca<sup>2+</sup> channels (reviewed in Catterall, 2000) have a repeating structure of four tandem homologous domains, each resembling a voltage-gated K<sup>+</sup> channel. Thus, the assembly of four P-domains to form a cation-selective pore is conserved through evolution.

The seven K<sup>+</sup> channel families will be introduced in the next section with an emphasis on their regulation and their *in vivo* function as defined by disease. The 4TMD/2P class will be discussed in greater detail since the experimental results in this work are most relevant to this family. A brief discussion of the two basic properties of ion channels, ion selectivity and gating (the conformational changes that lead to channel opening and closing) will follow. The mechanism of channel gating is of particular importance for understanding how mutations in a K<sup>+</sup> channel or in channel regulators may lead to a constitutively open channel. Native K<sup>+</sup> channels are often found

complexed with regulatory proteins that profoundly alter their gating properties. The middle section of this chapter is devoted to a detailed treatment of the five classes of human K<sup>+</sup> channel regulatory subunits identified thus far, highlighting the functionality and diversity generated by regulatory subunits and providing a framework for understanding the function of the three new classes of regulatory subunits discovered in this work. Finally, K<sup>+</sup> channels in *C. elegans* will be introduced together with the mutants that served as a starting point for this study.

### **6TMD/ 1P Structural Class**

The 6TMD/1P structural class encompasses five families of K<sup>+</sup> channels (K<sub>v</sub>, eag, KCNQ, slo, SK) that are generally gated by membrane potential and/or calcium.

K<sub>v</sub> family: The K<sub>v</sub> family is comprised of eight subfamilies, K<sub>v</sub>1 through K<sub>v</sub>7 and K<sub>v</sub>9. The first K<sup>+</sup> channel cloned in any organism was the *Drosophila* voltage-gated Shaker channel (Kamb et al., 1987; Papazian et al., 1987; Tempel et al., 1987). Its mammalian homologs define the K<sub>v</sub>1 subfamily. The Shaker channel and those of the K<sub>v</sub> family are composed of six transmembrane domains, named S1 to S6, and one P-domain between S5 and S6 (Tempel et al., 1988). K<sub>v</sub> channels are generally closed at resting potential, but conduct outward currents upon membrane depolarization (Stuhmer et al., 1988; Christie et al., 1989). The S4 segment contains positively charged residues that drive its movement in response to membrane depolarization to open and close the channel (reviewed in Bezanilla, 2000). A domain at the intracellular N-terminus of K<sub>v</sub> channels called the T1 domain governs the specificity of tetramer formation between members of each subfamily (Shen and Pfaffinger, 1995; Xu et al., 1995) and serves as a binding site for cytoplasmic regulatory subunits (Sewing et al., 1996; Yu et al., 1996; An et al., 2000).

K<sub>v</sub> channels not only open and close in response to membrane potential, but can also become temporarily insensitive to activating signals through inactivation by two independent mechanisms. Fast inactivation (N-type) occurs through the occlusion of the intracellular portion of the pore by a blocking “ball” formed by residues from the extreme N-terminus in a “ball-and-chain” mechanism (Hoshi et al., 1990; Zagotta et al., 1990). Phosphorylation of the inactivating “ball” of K<sub>v</sub>3.4 channels by PKC eliminates their N-type inactivation (Covarrubias et al., 1994), making this form of inactivation a dynamic and regulated process. By contrast, slow inactivation (C-type) occurs at the

outer mouth of the channel through conformational changes in the pore region (reviewed in Yellen, 1998).

Channels from the  $K_v1$  to  $K_v4$  subfamilies can either homomultimerize or heteromultimerize with members of their own subfamily to generate functional  $K^+$  channels when expressed heterologously in *Xenopus* oocytes (Christie et al., 1990; Ruppersberg et al., 1990). When rat  $K_v1.1$ , which is sensitive to the channel blocker tetraethylammonium (TEA), is coexpressed in *Xenopus* oocytes with the TEA-insensitive  $K_v1.2$ , or  $K_v1.3$  channels, heterologomeric channels assemble that display intermediate TEA sensitivities (Christie et al., 1990). Both the  $K_v1.1/K_v1.2$  and  $K_v1.2/K_v1.4$  pairs of channels colocalize in rat axons and can be coimmunoprecipitated from rat brain lysates, indicating that heteromultimers can form *in vivo* (Sheng et al., 1993; Wang et al., 1993). Channels from the  $K_v5$ ,  $K_v6$ ,  $K_v7$  and  $K_v9$  subfamilies are unique in that they do not form homomeric channels *in vitro*, but instead heteromultimerize primarily with channels of the  $K_v2$  subfamily to alter their activation and inactivation kinetics (Salinas et al., 1997a; Salinas et al., 1997b; Kramer et al., 1998; Sano et al., 2002).

Mutations in the human gene encoding  $K_v1.1$  can cause Episodic Ataxia Type-1, a rare autosomal dominant neurological disorder characterized by stress-induced attacks of imbalance and uncoordinated movements (Browne et al., 1994). Similarly, deletion of the  $K_v1.1$  locus in mice results in epilepsy (Smart et al., 1998).

**Eag family:** Several eag family members have been cloned in mammals (reviewed in Ganetzky et al., 1999). Eag channels are related and named after the *Drosophila* eag (ether-a-go-go) channel. By their amino acid sequence they are more related to cation-selective cyclic-nucleotide-gated channels (CNG) than to  $K_v$  channels (Warmke and Ganetzky, 1994). The best-studied eag channel is HERG (Human Ether-a-go-go Related Gene). Expression of HERG in *Xenopus* oocytes results in voltage-dependent  $K^+$  currents that are slowly activating and fast inactivating (Sanguinetti et al., 1995; Smith et al., 1996). HERG underlies the  $I_{kr}$  cardiac current (Sanguinetti et al., 1995) and mutations in the human locus result in LQT2, a form of cardiac arrhythmia (Curran et al., 1995).

**KCNQ family:** Five members of the KCNQ have been identified in humans (reviewed in Robbins, 2001). KCNQ channels can assemble as homomultimers to generate

voltage-gated outward currents when expressed heterologously. However, KCNQ3 can additionally heteromultimerize with KCNQ2 (Wang et al., 1998a), KCNQ4 (Kubisch et al., 1999) or KCNQ5 (Schroeder et al., 2000a) when coexpressed heterologously. KCNQ2/KCNQ3 heteromultimers have been shown to underlie the M-current (Wang et al., 1998a), a slowly-activating and slowly-inactivating neuronal current that is regulated by multiple G-protein coupled receptors, indicating that heteromultimers have functions *in vivo*. Mutations in several KCNQ genes have been shown to cause disease including benign familial neonatal convulsions (BFNC), a form of epilepsy (Schroeder et al., 1998), dominant deafness (Kubisch et al., 1999) and LQT1, a form of cardiac arrhythmia (Wang et al., 1996b).

Slo family: The Slo family of Ca<sup>2+</sup> activated high-conductance K<sup>+</sup> channels (reviewed in Kaczorowski et al., 1996) are named after the *Drosophila slowpoke* channel (Atkinson et al., 1991). Mammalian Slo1 channels are gated by both voltage and by calcium (Butler et al., 1993). Calcium binding to Slo1 channels at a site on their C-terminal tail named the calcium bowl increases their sensitivity to voltage (Schreiber and Salkoff, 1997). A mouse member of this family, Slo3, is not gated by calcium but by pH (Schreiber et al., 1998) and a *C. elegans* channel *slo-2* requires Cl<sup>-</sup> to open (Yuan et al., 2000), indicating that members of these family may generally share dual gating by voltage and by intracellular small molecules not limited to calcium. Although commonly classified in the 6TM/1P structural class, the human Slo1 channel has an additional transmembrane domain at its N-terminus (Wallner et al., 1996). Slo channels underlie the fast afterhyperpolarization (fAHP) following action potentials (Adams et al., 1982; Shao et al., 1999). Although mutations in *C. elegans* (Wang et al., 2001) and *Drosophila* (Kaplan and Trout, 1969) Slo channels result in visible phenotypes, mutations in the human channel have yet to be linked to disease.

SK family: SK channels, or small-conductance Ca<sup>2+</sup> activated K<sup>+</sup> channels (reviewed in Bond et al., 1999), are gated by calcium and are voltage insensitive, even though they contain an S4 voltage-sensing domain (Kohler et al., 1996). SK channels do not bind calcium directly but instead rely on calmodulin for their calcium sensitivity (Xia et al., 1998). SK channels are responsible for the slow afterhyperpolarization (sAHP) that occurs following a train of action potentials (Hirst et al., 1985; Sah, 1996).



## **2TMD/1P Structural Class**

The 2TMD/1P structural class includes only the inward rectifier ( $K_{ir}$ ) family (reviewed in Reimann and Ashcroft, 1999), but like the  $K_v$  family, the  $K_{ir}$  family is large and functionally diverse. These channels contain a P-domain surrounded by two TMDs named M1 and M2.  $K_{ir}$  serve two main purposes *in vivo*,  $K^+$  transport and setting the resting potential of cells near the  $K^+$  equilibrium. Although  $K_{ir}$  channels are intrinsically voltage insensitive, they conduct more current at negative membrane potentials (Ho et al., 1993; Kubo et al., 1993a; Kubo et al., 1993b). This inward rectification is caused by a block of the channel pore by intracellular  $Mg^{2+}$  or polyamines (Matsuda et al., 1987; Ficker et al., 1994; Lopatin et al., 1994). An aspartate residue in M2 has been identified as a candidate binding site for these blockers (Lu and MacKinnon, 1994; Wible et al., 1994). Some  $K_{ir}$  channels are additionally gated by the  $\beta\gamma$  subunits of G-proteins (Krapivinsky et al., 1995) while others can be gated by ATP (Tucker et al., 1997).

Like KCNQ channels,  $K_{ir}$  channels can heteromultimerize to generate  $K^+$  channels with new properties. Examples include the neuronal  $K_{ir}3.1$  and  $K_{ir}3.2$  channels (Kofuji et al., 1995) and the cardiac  $K_{ir}3.1$  and  $K_{ir}3.4$  channels (Krapivinsky et al., 1995). Mutations in  $K_{ir}$  channels underlie several human disorders. Mutations in  $K_{ir}2.1$  result in Andersen's Syndrome, a disorder characterized by periodic paralysis, cardiac arrhythmias and dysmorphic features (Plaster et al., 2001). Other disorders include the renal salt-absorption disorder Bartter's Syndrome by  $K_{ir}1.1$  mutations (Derst et al., 1997), and Persistent Hyperinsulinaemic Hypoglycaemia of Infancy (PHHI) by  $K_{ir}6.2$  mutations (Thomas et al., 1996).

## **4TMD/2P Structural Class**

The 4TMD/ 2P structural class defines the two-pore or twk family, named after the first mammalian member cloned, TWIK-1 (Tandem Two-pore Weakly- Inwardly-Rectifying K<sup>+</sup> Channel) (Lesage et al., 1996a). Two-pore channels resemble a tandem of two  $K_{ir}$  channels and thus contain two P-domains per polypeptide. Fourteen mammalian two-pore channels have been cloned from cDNA libraries and characterized in heterologous systems (reviewed in Goldstein et al., 2001). Expression of two-pore  $K^+$  channels heterologously produces voltage-insensitive, instantaneously-activating and noninactivating  $K^+$  selective currents that are insensitive to conventional  $K^+$  channel blockers such as  $Ba^{2+}$ , TEA and 4-aminopyridine (4-AP) (Patel and Honore, 2001).

Currents with these properties are referred to as “leak” or “background” currents. They set the resting potential of cells and therefore regulate their excitability (Hille, 1992).

Although the currents they produce are insensitive to voltage and do not show the sharp rectification of  $K_{ir}$  channels, two-pore channels show a remarkably diverse regulation by multiple factors. TREK-1(KCNK2), TREK-2(KCNK10) and TRAAK(KCNK4) form a subfamily of two-pore channels that are gated by membrane stretch, free fatty acids and intracellular pH (Fink et al., 1998; Patel et al., 1998; Maingret et al., 1999a; Maingret et al., 1999b; Bang et al., 2000; Lesage et al., 2000). TREK-1 shows additional activation by high temperature, suggesting that it may act as a thermoreceptor (Maingret et al., 2000). TASK-2(KCNK5) and TASK-4(KCNK-17) are both gated by extracellular pH, with TASK-2 being doubly regulated by changes in cell volume (Reyes et al., 1998; Decher et al., 2001; Niemeyer et al., 2001). TASK-1(KCNK3) and TASK-3(KCNK9) form a second subfamily of channels that are also gated by extracellular pH (Duprat et al., 1997; Leonoudakis et al., 1998; Kim et al., 2000; Rajan et al., 2000b). This regulation by pH is mediated by a histidine residue in the first pore domain of TASK-1(Lopes et al., 2001) or TASK-3 (Kim et al., 2000; Rajan et al., 2000b).

TASK-1 has been more extensively studied and shows complex regulation by multiple factors *in vivo*. Channel recordings from rat arterial chemoreceptor cells, which express TASK-1 mRNA, reveal a pH background current with properties similar to those generated by TASK-1 *in vitro* (Buckler et al., 2000). TASK-1 is directly activated by  $O_2$  when expressed heterologously in HEK cells (Lewis et al., 2001). Together, these results suggest that TASK-1 may have a biological role in oxygen sensing.

TASK-1 is also believed to function in at least three neuronal cell types to mediate the modulatory effects of neurotransmitters on cell excitability. Hypoglossal motoneurons (HMs) express TASK-1 at high levels and display a pH-gated background conductance that is identical to that of *in vitro* expressed TASK-1 (Talley et al., 2000). As serotonin and TRH can depolarize HMs through a suppression of the pH-sensitive current, and coexpression of TASK-1 with the Thyrotropin Releasing Hormone (TRH) receptor in HEK cells renders TASK-1 activity suppressible by TRH, TASK-1 has been proposed to underlie the neurotransmitter depolarization of these cells (Talley et al., 2000). Similarly, cerebellar granule neurons (CGNs) express an outward  $K^+$  resting current suppressible by  $M_3$  muscarinic receptors that has identical properties to those of heterologously expressed TASK-1, and TASK-1 currents in *Xenopus* oocytes are

suppressed by activation of endogenous M<sub>3</sub> muscarinic receptors (Millar et al., 2000). Finally, TASK-1 and TASK-3 have also been recently implicated in forming regulated leak currents in serotonergic raphe neurons that may contribute to ventilatory and arousal reflexes (Washburn et al., 2002).

In addition to regulation by multiple cellular factors, two-pore channel activity is sensitive to pharmacological agents of clinical relevance. Inhalational anesthetics, including halothane and isoflurane, activate TREK-1 (Patel et al., 1999), TREK-2 (Lesage et al., 2000), TASK-1 (Patel et al., 1999) and TASK-3 (Meadows and Randall, 2001) channels, while local anesthetics such as bupivacaine, block the K<sup>+</sup> currents of both TASK-1 (Leonoudakis et al., 1998; Kindler et al., 1999) and TASK-3 (Kindler et al., 1999; Meadows and Randall, 2001). The clinical relevance of these effects remains to be established, but they nevertheless attest to the growing potential of these channels as drug targets in the treatment of human disease.

Although fourteen two-pore channels have been cloned to date, three of them do not yield K<sup>+</sup> currents when expressed heterogously. TASK-5(KCNK15) fails to generate K<sup>+</sup> currents when expressed either in *Xenopus* oocytes (Ashmole et al., 2001) or in COS cells (Kim and Gnatenco, 2001). Coexpression of TASK-5 with wildtype TASK-1 or a mutant form of TASK-1 fails to alter TASK-1 currents, suggesting that TASK-5 can not heterodimerize with TASK-1 (Ashmole et al., 2001). Neither the two-pore channel KCNK7 nor its mouse ortholog reach the cell surface when transfected into COS cells, even when the intracellular domain or extracellular loops of mouse KCNK7 are replaced by those of other two-pore channels that express in these cells (Salinas et al., 1999). The THIK-2 (KCNK12) channel reaches the cell surface but fails to produce currents even when coexpressed with the related THIK-1 channel (Rajan et al., 2000a; Girard et al., 2001). As discussed earlier, voltage-gated K<sup>+</sup> channels of the K<sub>v</sub>5 to K<sub>v</sub>9 subfamilies do not express currents on their own but multimerize with K<sub>v</sub>2 channels to yield channels with new properties (Salinas et al., 1997a; Salinas et al., 1997b; Kramer et al., 1998; Sano et al., 2002). As TASK-1 and TASK-3 channels can form functional heterodimers *in vitro* (Czirjak and Enyedi, 2002), these channels may need to heterodimerize with other unidentified K<sup>+</sup> channel subunits to form functional channels. Alternatively, they may need to associate with regulatory subunits (discussed in later sections) to produce functional channels. The work in Chapters 2 and 3 will address the existence of such subunits.

## Ion Selectivity and Gating of K<sup>+</sup> Channels

From a reductionist perspective, K<sup>+</sup> channels have two properties: they discriminate between K<sup>+</sup> and other ions (ion selectivity) and they open and close (gating). The crystal structure of the 2TM/1P channel KcsA from the prokaryote *Streptomyces lividans* has been instrumental in illuminating the mechanisms for both of these processes (Doyle et al., 1998). The general structure of KcsA is that of an inverted teepee, with the activation gate lying in the “smokehole” or the narrowest section where the helix bundles cross each other. The selectivity filter lies above the helix crossing and contains multiple binding sites for K<sup>+</sup> ions, which are stabilized by backbone carbonyl groups rather than by amino acid side chains. The geometry of the binding site coordinates K<sup>+</sup> but not the smaller Na<sup>+</sup> ions. To counteract the attractive forces between K<sup>+</sup> and the pore and thus promote the fast flow of ions, the binding sites are spaced such that electrostatic repulsion between adjacent K<sup>+</sup> ions destabilizes their binding to the pore.

How applicable is the structure of the KcsA pore to other K<sup>+</sup> channel families? Three studies indicate that the KcsA pore structure is conserved with mammalian K<sup>+</sup> channels. First, both KcsA and the Shaker channel bind the scorpion toxin Agitoxin2 at the extracellular entryway of their respective pores, with equivalent mutations in both channels altering the binding affinity (MacKinnon et al., 1998). Second, an experimentally-defined barium-binding site at the intracellular entry of large-conductance Ca<sup>2+</sup>-activated K<sup>+</sup> channels (Neyton and Miller, 1988a; Neyton and Miller, 1988b) is revealed in the crystal structure of barium-soaked KcsA (Jiang and MacKinnon, 2000). Third, substitution of the pore region of a K<sub>v</sub> or K<sub>r</sub> channel for that of KcsA results in hybrid channels that retain voltage-sensitivity and inward rectification respectively, indicating that their pore regions are modular and competent for regulation by the rest of the channel (Lu et al., 2001).

In addition to uncovering the basis for the ion selectivity of K<sub>v</sub> channels, recent studies have sought to define the mechanism by which K<sup>+</sup> channels are gated. The crystal structure of the KcsA channel represents its closed form, with the narrow “smokehole” formed by the inner helices sterically preventing ion flow through the channel (Doyle et al., 1998). Electron paramagnetic spin resonance (EPR) studies of KcsA indicate that the membrane helices that follow the P-domain rotate and tilt near the narrow portion of the channel upon opening (Perozo et al., 1999). Similarly, cysteine modification experiments indicate that the same helices in the Shaker voltage-

gated channel are differentially accessible in the closed and open states (del Camino et al., 2000).

These predicted conformational changes channel gating have been corroborated by the crystal structure of the MthK channel from *Methanobacterium thermoautotrophicum* (Jiang et al., 2002b; Jiang et al., 2002a). MthK is structurally similar to KcsA, as both K<sup>+</sup> channels have two transmembrane domains flanking a P-domain, but unlike KcsA, MthK opens in response to calcium binding to its C-terminal RCK domain (Jiang et al., 2002b). The crystal structure of the open channel bound to calcium confirms a predicted rotation of the inner helices, using a conserved glycine residue as a hinge, to widen the smokehole from 4 to 12Å, thereby allowing K<sup>+</sup> ions to pass through the selectivity filter (Jiang et al., 2002b). In the case of MthK, the energy of Ca<sup>+2</sup> binding to the RCK domains provides the driving force for the rotation of the inner helices (Jiang et al., 2002a). Such a mechanism of inner helix rotation has also been proposed for the mammalian Ca<sup>+2</sup>-gated SK channels based on the crystal structure of calmodulin bound to the channel (Schumacher et al., 2001). Thus, rotation of the inner helices to allow ion access to the selectivity filter may be a conserved mechanism for gating of K<sup>+</sup> channels in response to voltage or small molecule binding.

### **Regulatory Subunits and K<sup>+</sup> Channel Diversity**

As described in the previous sections, K<sup>+</sup> channels comprise an obligatorily diverse superfamily of ion conducting proteins. Each cell in the human body requires a K<sup>+</sup> conductance with properties that are specifically tailored to perform its biological function. A cardiac myocyte requires an orchestrated performance by multiple channels, each firing at specific times and for defined intervals, to generate the action potential underlying a heart beat, whereas a kidney tubule cell requires a constant flow of K<sup>+</sup> out of the cell during renal salt absorption.

Two major mechanisms employed by the organism for generating such functional diversity have already been discussed, namely starting with a large set of genes encoding K<sup>+</sup> channels and heteromultimerization of K<sup>+</sup> channel subunits to generate channels with novel properties. Alternative splicing represents an additional mechanism for generating channels with distinct functional properties (for examples see Kupersmidt et al., 1998; Inanobe et al., 1999; Zhang et al., 2001). As alternative splicing is a general mechanism for increasing diversity in any family of proteins it will not be discussed further. However, it is worth noting that the squid K<sub>v</sub>2 channel

undergoes RNA editing to generate several functionally distinct channels (Patton et al., 1997), but no such regulation has been reported for other K<sup>+</sup> channels.

The third and perhaps the most significant mechanism for generating functional diversity is the association of K<sup>+</sup> channels with auxiliary subunits (Figure 2). Although most K<sup>+</sup> channels generate currents when expressed heterologously, K<sup>+</sup> channels *in vivo* are often found in complexes with other non-channel proteins. Regulatory subunits have a profound impact on channel activity through mechanisms as diverse as modulation of single channel conductances, channel activation and inactivation kinetics, sensitivity to voltage, Ca<sup>2+</sup> or other channel effectors, or through chaperone or cell-trafficking activities. Regulatory subunits or associated proteins have been described that modulate all seven human K<sup>+</sup> channel families with the exception of the two-pore family (Figure 2). In the work described in Chapters 2 and 3, three new putative regulatory subunits of two-pore channels will be described, two of which have *Drosophila* and human counterparts.

The next several sections will describe the five known classes of human K<sup>+</sup> channel regulatory subunits with an emphasis on their identification, structure, and mechanism for modulating channel function.

### **K<sub>v</sub>β Regulatory Subunits**

The identification of the *Drosophila* Shaker K<sup>+</sup> channel led to the rapid homology-based cloning of other mammalian voltage-gated K<sup>+</sup> channels. Expression of these channels in heterologous systems was sufficient to reconstitute K<sup>+</sup> selective currents (Pongs et al., 1988; Christie et al., 1989; Stuhmer et al., 1989). However, several lines of evidence suggested that regulatory subunits likely modulated K<sup>+</sup> channel activity *in vivo*. Biochemical purification of a class of fast-acting, 4-AP sensitive K<sup>+</sup> channels using the snake venom toxin α-dendrotoxin (α-DTX) revealed the presence of a second polypeptide associated with the channel from both rat (Rehm and Lazdunski, 1988) and bovine brain (Parcej and Dolly, 1989). Analysis of the hydrodynamic properties of the channel complex revealed an α<sub>4</sub>β<sub>4</sub> stoichiometry between these two proteins (Parcej et al., 1992). When the α-DTX-sensitive channel was subsequently cloned based on partial peptide sequence of the purified protein, its channel properties when expressed heterologously differed from those of the native channel (Pongs, 1992; Reid et al., 1992). As beta subunits for both voltage-gated Ca<sup>2+</sup> and Na<sup>+</sup> channels had been cloned and shown to alter channel properties (Ellis et al., 1988; Ruth et al., 1989; Jay et al.,

1990; Isom et al., 1992), it was likely that the biochemically-identified associated protein was responsible for altering channel properties of the  $\alpha$ -DTX-sensitive channel *in vivo*. A bovine and two rat beta subunits were subsequently cloned and found to encode cytoplasmic proteins (Rettig et al., 1994; Scott et al., 1994) belonging to the NAD(P)H-dependent oxidoreductase superfamily (McCormack and McCormack, 1994). Co-expression of one of these beta subunits,  $K_v\beta 1$ , with the non-inactivating delayed-rectifier channel  $K_v 1.4$  in *Xenopus* oocytes confers rapid A-type inactivation, while co-expression of  $K_v\beta 1$  with the A-rectifier channel  $K_v 1.4$  accelerates its activation kinetics (Rettig et al., 1994).

In contrast to the biochemical cloning approach employed for mammalian  $K_v\beta$  subunits, a *Drosophila* beta subunit homologous to  $K_v\beta$  subunits was identified through the molecular cloning of the *Hyperkinetic* (*Hk*) locus (Chouinard et al., 1995). *Hk* mutants display an ether-sensitive leg-shaking phenotype similar to that of Shaker  $K^+$  channel mutants (Kaplan and Trout, 1969). Epistasis and other genetic interactions among *Hk*, *Shaker* and *ether-a-go-go*, which was later found to encode a  $K^+$  channel (Bruggemann et al., 1993), formed the basis for proposing that *Hk* encoded a *Shaker* regulatory subunit (Stern and Ganetzky, 1989). Coexpression of *Hk* and *Shaker* in *Xenopus* oocytes results in two-fold larger currents compared to expression of *Shaker* alone, as well changes in Shaker channel activation, inactivation and voltage dependence (Chouinard et al., 1995). Unlike mammalian  $K_v\beta$  subunits, *Hk* can also associate with  $K^+$  channels of the eag family to increase their current amplitudes and modulate gating (Wilson et al., 1998).

A third human subunit ( $K_v\beta 3$ ) as well as splice variants of  $K_v\beta 1$  and  $K_v\beta 2$  have been identified (Majumder et al., 1995; McCormack et al., 1995). The three subunits share approximately 70% amino acid identity, but their N-terminal regions are poorly conserved (Majumder et al., 1995). Through an N-terminal domain that resembles the "ball-and-chain" inactivation particle of Shaker channels,  $K_v\beta 1$  and  $K_v\beta 3$  can confer A-type inactivation to channels that do not inactivate (Rettig et al., 1994; Majumder et al., 1995). By contrast, the predominant  $\beta$  subunit isoform in the brain,  $K_v\beta 2$ , lacks this domain and cannot confer A-type inactivation to noninactivating channels (Rettig et al., 1994; Xu and Li, 1997), but it can accelerate the inactivation of  $K_v 1.4$  channels (McCormack et al., 1995) and the activation time course of  $K_v 1.5$  (Heinemann et al., 1996).

Although its effects in channel gating are limited compared to  $K_v\beta 1$  or  $K_v\beta 3$ ,  $K_v\beta 2$  displays chaperone activity towards  $K_v 1$  channels. Heterologous coexpression of the  $K_v\beta 2$  subunit with either  $K_v 1.2$  or with  $K_v 1.4$  channels increased the amplitude of their currents (Accili et al., 1997b; Accili et al., 1998). Both maturation of the  $K_v 1.2$  channel as monitored by glycosylation status and cell-surface binding sites for the  $\alpha$ -DTX toxin are increased upon  $K_v\beta 2$  coexpression (Shi et al., 1996), indicating that the observed increase in current amplitude is due to an increase in the number of channels at the cell surface. Furthermore, temperature block experiments in transfected cells indicate that the Shaker channel associates with  $K_v\beta 2$  in the Endoplasmic Reticulum (Nagaya and Papazian, 1997). Together, these results argue that  $K_v\beta 2$  may act as a chaperone of  $K_v$  channels.

Although  $K_v\beta 2$  subunit may regulate channel activity through a different mechanism from  $K_v\beta 1$  or  $K_v\beta 3$ , two studies suggest that multiple subunit types may concurrently assemble onto one channel.  $K_v\beta 1$  and  $K_v\beta 2$  interact in two-hybrid assays, and  $K_v\beta 2$  inhibits the  $K_v\beta 1$ -dependent inactivation of Shaker in coexpression studies carried out in mammalian cells (Xu and Li, 1997). In addition, deletion mutants of  $K_v\beta 2$  that failed to physically interact with  $K_v\beta 1$  or Shaker lost their ability to inhibit inactivation (Xu and Li, 1997). In a second study, coexpression of the  $K_v 1.2$  channel together with both wild-type  $K_v\beta 1$  and a truncated form of  $K_v\beta 1$  ( $K_v\beta 1$ -N20) that lost its ability to inactivate resulted in a channel population with intermediate properties to those of  $K_v 1.2/K_v\beta 1$  and  $K_v 1.2/K_v\beta 1$ -N20 channels (Accili et al., 1997a), indicating that coassembly of inactivating and noninactivating  $K_v\beta$  subunits can confer novel properties to a channel.

While the above studies establish that  $K_v\beta$  subunits can regulate the properties of voltage-gated  $K^+$  channels when expressed in heterologous systems, the *in vivo* role of these subunits has been largely unexplored. The disruption of these subunits by genetic means and the characterization of mutant currents and phenotypes in mutant organisms are prerequisites to fully understand their contribution to neuronal and muscle excitability. Patch-clamp recordings of neurons from *Drosophila Hyperkinetic* mutants offers a promising venue for such inquiries (Yao and Wu, 1999). Equally promising are studies assessing the contributions of single and double mutations in  $K^+$  channels or their subunits to specific *Drosophila* behaviors, such as the habituation of the escape circuit (Engel and Wu, 1998). In mammals, a significant step in elucidating  $K_v\beta$  function *in vivo* comes from a  $K_v\beta 2$  knockout mouse (McCormack et al., 2002).



K<sub>v</sub>β2 null mice are viable and fertile, but have a reduced life span and exhibit a cold swim-induced tremor similar to that of K<sub>v</sub>1.1 null mice although less severe. Western blot and immunofluorescence stainings of K<sub>v</sub>1.1 and K<sub>v</sub>1.2 channels in these mutant mice showed no change in their expression levels or localization relative to wild-type animals, suggesting that the mutant phenotypes are not the result of a defective chaperone activity towards these channels. Therefore, K<sub>v</sub>β2 may regulate additional channels or may have additional non-chaperone functions *in vivo*.

A central question in K<sub>v</sub>β research has centered on its putative oxidoreductase activity. Although a weak similarity to aldo-keto reductases has long been noted (McCormack and McCormack, 1994), the crystal structure of the K<sub>v</sub>β2 tetramer has confirmed its assignment to this superfamily (Gulbis et al., 1999). K<sub>v</sub>β2 tetramers are composed of four TIM barrels and a bound NADP<sup>+</sup> cofactor per subunit. The putative catalytic residues, Tyr-90, Lys-118 and Asp-85, are spaced appropriately relative each other and to the NADPH cofactor to support catalysis. In addition to its similarity to oxidoreductases, K<sub>v</sub>β1.2 confers oxygen sensitivity to the K<sub>v</sub>4.2 channels, suggestive of a possible enzymatic role for K<sub>v</sub>β subunits (Perez-Garcia et al., 1999). In spite of the potential for catalytic activity, a substrate for K<sub>v</sub>β2 remains to be identified.

Several recent studies have begun to indirectly address the relevance of the putative oxidoreductase activity of K<sub>v</sub>β subunits by mutating either their catalytic or NADPH-binding residues and testing for disruption of chaperone or inactivation activity (Bähring et al., 2001b; Liu et al., 2001; Peri et al., 2001; Campomanes et al., 2002). A point mutant in K<sub>v</sub>β2 that eliminates NADPH binding does not disrupt tetramer assembly (Liu et al., 2001). Additional mutations in residues that contact NADPH have no effect on the ability of K<sub>v</sub>β2 to accelerate the inactivation in K<sub>v</sub>1.4 channels *in vitro* (Peri et al., 2001), but do diminish its chaperone activity (Peri et al., 2001; Campomanes et al., 2002). Single mutations in the catalytic Tyr, Lys, or Asp residues predicted to eliminate enzymatic activity do not affect the chaperone activity of K<sub>v</sub>β2 on K<sub>v</sub>1.4 channels in transfected COS cells (Campomanes et al., 2002), but catalytic mutations in K<sub>v</sub>β subunits either reduce (Bähring et al., 2001b) or have no effect on accelerating channel inactivation (Peri et al., 2001). Mutant mice carrying an engineered Y90F mutation in the K<sub>v</sub>β2 locus are indistinguishable from wild-type animals, while the knockout mice have spontaneous seizures and reduced lifespans (McCormack et al., 2002), indicating that if K<sub>v</sub>β2 were an enzyme its catalytic activity is dispensable *in vivo*.

## Slo Regulatory Subunits

Like voltage-gated  $K^+$  channels, purification of large-conductance  $Ca^{2+}$ -activated  $K^+$  channel (Slo) from bovine tracheal smooth muscle revealed an associated protein (Garcia-Calvo et al., 1994; Knaus et al., 1994b). Unlike  $K_v\beta$  subunits however, this associated protein was heavily glycosylated, indicating that it was likely a transmembrane protein. Four isoforms of Slo channels have been cloned:  $\beta 1$  (Knaus et al., 1994a);  $\beta 2$  (Wallner et al., 1999);  $\beta 3$  (Xia et al., 1999); and  $\beta 4$  (Brenner et al., 2000a; Meera et al., 2000). Slo subunits span the cell membrane twice, with their N- and C- termini residing intracellularly. Heterologous expression of Slo channels with  $\beta 1$  in *Xenopus* oocytes greatly increases their activation by voltage depolarization and by calcium binding, while single channel conductance and channel expression remain unchanged (McManus et al., 1995). Coexpression of  $\beta 2$  or  $\beta 3$  with Slo channels induces a fast inactivation similar to that induced by the “ball” at the N-termini of Shaker channels or the N- termini of its  $K_v\beta 1$  and  $K_v\beta 3$  subunits (Wallner et al., 1999; Xia et al., 1999). Deletion of the N-terminal 18 amino acids of  $\beta 2$  eliminates this inactivation, and fusion of this domain to the noninactivating  $\beta 1$  subunit induces inactivation, indicating that this domain is necessary and sufficient to confer inactivation (Wallner et al., 1999). Unlike the other three subunits,  $\beta 4$  expression leads to a general decrease in Slo sensitivity to  $Ca^{2+}$  levels and to a pronounced slowing of channel activation (Brenner et al., 2000a). In summary, all four regulatory subunits of Slo channels induce varied changes in channel gating and inactivation, but do not have noticeable effects on channel trafficking or expression.

The site of interaction between Slo and the human  $\beta 1$  subunit has been mapped through chimeras between the human Maxi-K channel and the *Drosophila* Slo channel, whose sensitivity to calcium concentrations is not augmented by human  $\beta 1$  (Wallner et al., 1996). Maxi-K channels have an additional transmembrane domain at their N-terminus when compared to voltage-gated  $K^+$  channels. Addition of this domain to the *Drosophila* Slo channel confers regulation by the human subunit (Wallner et al., 1996).

Slo  $\beta 1$  subunits play a key role in arterial vasoregulation. Membrane electrophysiological recordings from arterial smooth muscle cells of  $\beta 1$  knockout mice reveal a lack of  $K^+$  currents from Slo channels under low micromolar  $Ca^{2+}$  concentrations (Brenner et al., 2000b), consistent with the proposed role of  $\beta 1$  in increasing the sensitivity of Slo to  $Ca^{2+}$ . Furthermore, mutant mice fail to couple bursts of calcium release from intracellular ryanodine channels to membrane

hyperpolarization, leading to higher arterial tone and blood pressure (Brenner et al., 2000b). In addition to coupling intracellular events with membrane hyperpolarization,  $\beta 1$  mediates the vascular relaxation induced by  $17\beta$ -estradiol (estrogen). Slo channels expressed in *Xenopus* oocytes increase their currents in response to treatment with  $17\beta$ -estradiol only when  $\beta 1$  is coexpressed (Valverde et al., 1999). Likewise, the xenoestrogen tamoxifen activates Slo channels in transfected HEK cells only when  $\beta 1$  is coexpressed (Dick et al., 2001). Consistent with the postulated role of  $\beta 1$  in mediating estrogen signaling, single channel recordings from colonic myocytes of  $\beta 1$  knockout mice showed that Slo channels were insensitive to activation by  $17\beta$ -estradiol or tamoxifen (Dick and Sanders, 2001). The role of  $\beta 1$  as a receptor for a hormone illustrates yet another mechanisms by which regulatory subunits confer functional diversity to  $K^+$  channels.

### **MinK Regulatory Subunits**

The minimal  $K^+$  channel (minK or KCNE) proteins comprise the most versatile family of  $K^+$  channel regulatory subunits, both by the breadth of their associations with  $K^+$  channels and by the variety of functional properties conferred by their association. Unlike  $K_v\beta$  subunits that associate only with voltage-gated channels of the  $K_v1$  subfamily or the subunits of Slo channels that regulate only Slo channels, minK proteins have been shown to associate with channels of the  $K_v$ , HERG and  $K_v$  LQT families *in vivo*.

Also unique to minK subunits is the way they were identified. The first minK subunit was cloned through expression cloning of rat kidney mRNA (Takumi et al., 1988). Expression of an mRNA in *Xenopus* oocytes encoding a 130 amino acid single-transmembrane protein generated  $K^+$ -selective voltage-sensitive outward currents upon depolarization. Thus, minK itself was believed to encode a structurally novel  $K^+$  channel. This misconception was further corroborated by the finding that mutations in its transmembrane domain led to alterations in both the ion selectivity and the gating of the currents it generated (Goldstein and Miller, 1991; Takumi et al., 1991). MinK has since been found to be a regulatory  $K^+$  channel subunit that associates with several channels types, and the currents it generated in oocytes were the result of its association with an endogenous  $K^+$  channel. MinK associates with the  $K_v$ LQT1 channel to form the slow repolarizing cardiac current  $I_{ks}$  (Barhanin et al., 1996; Sanguinetti et al., 1996). When coexpressed in mammalian cells, minK increases the magnitude of  $K_v$ LQT1 currents and significantly slows its activation kinetics (Barhanin et al., 1996;

Sanguinetti et al., 1996). Single channel analysis of  $K_v$ LQT1/minK channels indicates that minK reduces the unitary conductance of the channel fifteen-fold, but concurrently leads to a sixty-fold increase in the number of active channels, resulting in an overall increase in total current (Romey et al., 1997). Mutational studies of minK indicate that the transmembrane domain is necessary for its association with  $K_v$ LQT1, and residues within the transmembrane domain and the C-terminal tail are important for its modulation of  $K_v$ LQT1 channel activity (Tapper and George, 2000; Melman et al., 2001).

Four additional minK subunits have been cloned (Abbott et al., 1999; Piccini et al., 1999) and named KCNE2-5. KCNE2 associates with the HERG channel to form the  $I_{kr}$  cardiac potassium currents, and mutations in the human gene underlie a hereditary form of cardiac arrhythmia (Abbott et al., 1999). KCNE3 associates with the voltage-gated  $K^+$  channel  $K_v$ 3.4 to underlie periodic paralysis (Abbott et al., 2001). KCNE3 increases the single-channel conductance of  $K_v$ 3.4 and greatly shifts its voltage-activation threshold to more negative potentials, allowing the channel to contribute to the resting potential of muscle cells (Abbott et al., 2001). KCNE3 can also associate with  $K_v$ LQT1 with dramatic consequences. Its association leads to a constitutively open channel with nearly instantaneous activation and a linear voltage-current relationship (Schroeder et al., 2000b). The pharmacology and properties of heteromeric KCNE3/ $K_v$ LQT1 channels resemble those of a  $K^+$  current from intestinal crypt cells, and as mRNAs for both genes are expressed in these cells, KCNE3/ $K_v$ LQT1 has been proposed to underlie this current (Schroeder et al., 2000b).

Like other  $K^+$  channel regulatory subunits, association of minK with  $K^+$  channels dramatically alters their ion conducting properties. But minK may do more than just regulate  $K^+$  channels: it may also form part of the  $K^+$  conduction pathway (Wang et al., 1996a; Tai and Goldstein, 1998). Binding sites for methanethiosulfonate-ethylsulfonate (MTSES) or the thiol-reactive reagent cadmium were engineered on the transmembrane domain of minK by scanning cysteine mutagenesis and assayed for susceptibility to modification when complexed with the  $K_v$ LQT1 channel. Since three cysteine residues were protected from MTSES modification in the presence of TEA, a common  $K^+$  channel blocker, it has been hypothesized that minK lines the inner pore of the channel (Wang et al., 1996a). Consistent with this model, two consecutive cysteine residues in minK are susceptible to cadmium modification applied extracellularly or intracellularly respectively, indicating that these cysteines lie deep in the pore such that cadmium can access and modify them (Tai and Goldstein, 1998). However, an engineered high-

affinity site for TEA on  $K_v$ LQT1 channels does prevent modification of cysteine substitutions in the minK transmembrane domain in a TEA-dependent manner, suggesting that the previously observed TEA protection of minK cysteines may have been an indirect allosteric effect of TEA binding rather than a blocking of the pore (Kurokawa et al., 2001). Furthermore, a modeling study of  $K_v$ LQT1/minK complex based on the KcsA crystal structure predicts that minK lies adjacent to the S6 transmembrane domain of  $K_v$ LQT1 but outside of the pore (Tapper and George, 2001). This model is supported by the experimental confirmation of a predicted cadmium-binding site between a native cysteine in the S6 transmembrane helix of  $K_v$ LQT1 that faces away from the pore and an engineered cysteine in minK (Tapper and George, 2001). Although the precise location of minK relative to  $K_v$ LQT1 in the complex may be unresolved, its ability to modify the activity of multiple channels *in vivo* is well established.

### **SUR Regulatory Subunits**

The SUR1 and SUR2 proteins comprise the fourth class of  $K^+$  channel regulatory subunits. SUR1 was cloned by biochemical purification of the proposed hamster  $K_{ATP}$  channel, which regulates insulin secretion in  $\beta$ -cells, on the basis of its affinity for the sulfonylurea glyburide (Aguilar-Bryan et al., 1995) and found to belong to the ATP-Binding Cassette superfamily (Higgins, 1992). Expression of SUR1 in COS cells reconstitutes high-affinity glyburide binding but does not induce  $K^+$  currents (Aguilar-Bryan et al., 1995). Coexpression of a channel expressed in pancreatic islets,  $K_{ir}6.2$ , with SUR1 in COS cells or *Xenopus* oocytes reconstitute ATP-sensitive  $K^+$  currents (Inagaki et al., 1995; Sakura et al., 1995) and results in the formation of a detergent-soluble high-molecular weight complex with an estimated 1:1 channel to subunit ratio, a stoichiometry that has been confirmed by tandem fusion genes between channel and subunit (Clement et al., 1997). Consistent with its role in generating  $I_{KATP}$  in  $\beta$ -cells, mutations in SUR1 are associated with Familial Persistent Hyperinsulinemic Hypoglycemia of Infancy, a disorder in glucose homeostasis that is characterized by unregulated insulin secretion and severe hypoglycemia (Thomas et al., 1995). SUR2 was cloned based on its homology to SUR1, and found to reconstitute a  $K_{ATP}$  channel from muscle when coexpressed with  $K_{ir}6.2$  (Inagaki et al., 1996).  $K_{ir}6.2$  is not the only channel to associate with SUR proteins, as  $K_{ir}6.1$  also associates with either SUR1 or

SUR2 to generate nucleotide-sensitive channels (Ammala et al., 1996; Yamada et al., 1997).

The SUR proteins differ from the other K<sup>+</sup> channel regulatory subunits discussed thus far (K<sub>v</sub>, Slo β and minK) in that they are absolutely required for the channel activity of K<sub>ir</sub>6.1 and K<sub>ir</sub>6.2. A new ER trafficking signal has been identified in studies exploring the underlying requirement of SUR1 for K<sub>ir</sub>6.2 expression (Zerangue et al., 1999). A KRK motif near the C-terminus of K<sub>ir</sub>6.2 acts as an ER retention signal. Deletions of the C-terminal region of K<sub>ir</sub>6.2 or mutations within this tripeptide motif lead to channel expression on the cell surface. Association of K<sub>ir</sub>6.2 with SUR1 is proposed to occlude this signal and allow normal trafficking (Zerangue et al., 1999).

Because wildtype K<sub>ir</sub>6.1 and K<sub>ir</sub>6.2 do not express in the absence of SUR proteins, it is impossible to determine their intrinsic channel properties and compare them to those of channels complexed with SUR, thereby revealing the contribution of SUR subunits to channel properties. This difficulty has been circumvented by the use of channels with a deleted ER retention signal, thus achieving surface expression in the absence of SUR proteins (Tucker et al., 1997). Surprisingly, K<sub>ir</sub>6.2 K<sup>+</sup> currents are intrinsically sensitive to intracellular levels of ATP, and point mutations in K<sub>ir</sub>6.2 significantly reduce this modulation (Tucker et al., 1997; Tucker et al., 1998). This was a surprising finding because the Walker "A" and "B" ATP-binding domains of SUR1 had been assumed to confer ATP regulation to the channel complex (Aguilar-Bryan et al., 1995). Although ATP sensitivity may be intrinsic to these truncated K<sub>ir</sub> channels, coexpression of SUR1 does increase their sensitivity to ATP ten-fold (Tucker et al., 1997), and the Walker motifs of SUR1 are essential for conferring activation by Mg-ADP to K<sub>ir</sub>6.2 (Nichols et al., 1996; Gribble et al., 1997). Thus, SUR proteins regulate the surface expression of K<sub>ir</sub> channels, increase their sensitivity to ATP and confer regulation by ADP.

### **KchIPs Regulatory Subunits**

Three K<sub>v</sub> channel Interacting Proteins (KchIPs) were recently identified by two-hybrid screening for proteins that specifically bound to the N-terminal cytoplasmic domain of K<sub>v</sub>4 channels but not to the equivalent domain of K<sub>v</sub> channels from other families (An et al., 2000). KchIPs encode small proteins with distinct N-termini but with a similar core region containing four EF-like hand motifs shown to bind Ca<sup>2+</sup>. KchIPs coimmunoprecipitate with K<sub>v</sub>4.2 but not with K<sub>v</sub>2.1 channels from rat neocortex

membranes (An et al., 2000). When coexpressed with  $K_v4.2$  in CHO cells, all three KchIPs increased current density over ten-fold, shifted the midpoint of channel activation to more hyperpolarized potentials and slowed down inactivation kinetics four-fold compared to currents generated by  $K_v4.2$  alone. Point mutations in the EF-hand domain of KchIPs that abolish  $Ca^{2+}$  binding also abolish modulation of  $K_v4.2$  currents, but do not disrupt KchIP binding to the channel (An et al., 2000). In addition to its modulation of channel gating, KchIP1 confers regulation by arachidonic acid to  $K_v4.3$  channels (Holmqvist et al., 2001).

Characterization of an additional splice form of KchIP has provided an insight into the mechanism by which KchIPs may increase surface expression of  $K_v4$  channels (Bähring et al., 2001a). Deletion of the N-terminal domain of  $K_v4.2$  to which KchIP-2.2 binds increases the surface expression and current density of the channel. Since KchIP-2.2 binding to the full-length channel increased its surface expression 55-fold, this region may define a domain that normally inhibits trafficking of  $K_v4.2$ , such that upon binding of KchIP2.2 to this region the inhibition is relieved. This proposed mechanism is conceptually similar to the occlusion of the ER-retention KRK motif on  $K_{ir}6.2$  by the SUR-1 subunit (Zerangue et al., 1999) and may emerge as a common theme in channel trafficking.

A fourth KchIP conferring novel properties to  $K_v4$  channels has been reported (Holmqvist et al., 2002). Unlike KchIP1-3, KchIP4 coexpression with  $K_v4.3$  channels eliminated the fast inactivation of the channel. This activity is conferred by a modular domain at the N-terminus of KchIP4, as addition of this domain to KchIP1 is sufficient to confer it with the ability to remove fast inactivation (Holmqvist et al., 2002).

Comparison KchIP4 to the  $K_v\beta1$  subunit of  $K_v1$  channels reveals a striking functional divergence within a common structural framework. Both proteins are cytoplasmic regulatory subunits with modular N-terminal domains and a core C-terminal region that is conserved within their respective families. Both physically interact with the N-terminus of voltage-gated  $K^+$  channels and both profoundly alter the inactivation properties of the channels with which they associate. But while  $K_v\beta1$  transforms noninactivating delayed rectifier channels into A-rectifiers, KchIP4 turns A-rectifiers into delayed rectifiers.

## **K<sup>+</sup> Channel Associated Proteins**

In addition to regulatory channel subunits, a number of other proteins have been found to associate with K<sup>+</sup> channels *in vivo*. The criteria for classifying a protein as a channel regulatory subunit or simply as a protein that associates with K<sup>+</sup> channels has been inconsistent in the literature. Three such interacting proteins will be highlighted in this section, as they illustrate additional ways in which K<sup>+</sup> channel activity can be modulated and are relevant to the findings described in Chapters 2 and 3.

The cytoplasmic protein KchAP (K<sup>+</sup> channel Associated Protein) was identified through a two-hybrid screen for interactors of the voltage-gated K<sup>+</sup> channel subunit K<sub>v</sub>β1 (Wible et al., 1998). KchAP also interacts with the K<sub>v</sub>2.1 and K<sub>v</sub>1.5 channels directly by two-hybrid. Coexpression of KchAP with K<sub>v</sub>2.1 in *Xenopus* oocytes leads to a three-fold increase in K<sup>+</sup> current and to an increase in cell-surface expression of the channel, while having no effect on channel kinetics (Wible et al., 1998). KchAP additionally increases the currents of K<sub>v</sub>1.3 and K<sub>v</sub>4.3, but not those of K<sub>v</sub>3.1, K<sub>v</sub>2.2, HERG, KCNQ1 or other K<sub>v</sub>1.x family members (Kuryshv et al., 2000). As KchAP can co-immunoprecipitate K<sub>v</sub>2.1 and K<sub>v</sub>4.3 from rat heart lysates (Kuryshv et al., 2000), KchAP may act as a chaperone of distinct K<sup>+</sup> channels *in vivo*.

PSD-95 is a postsynaptic density protein belonging to the MAGUK (Membrane Associated Guanylate Kinase) family whose members contain an SH3 domain, a guanylate kinase domain and at least one PDZ domain (reviewed in Sheng, 2001). PSD-95 induces clustering of Shaker-type K<sup>+</sup> channels at the cell surface of doubly transfected cells, interacts *in vitro* and colocalizes with K<sub>v</sub>1.4 in rat nerve terminals (Kim et al., 1995). In addition, PSD-95 is required for the trafficking of K<sub>v</sub>1.4 to post-synaptic sites in rat cortex (Arnold and Clapham, 1999). Besides targeting Shaker-like channels, PSD-95 also coimmunoprecipitates with the inward rectifier channels K<sub>ir</sub>2.3 and K<sub>ir</sub>5.1 from rat brain lysates (Cohen et al., 1996; Tanemoto et al., 2002). PSD-95 coexpression with the inward-rectifier K<sup>+</sup> channel K<sub>ir</sub>5.1 is required for proper channel trafficking to the cell surface and generation of currents in transfected HEK cells (Tanemoto et al., 2002). Thus, PSD-95 and other PDZ domain-containing proteins may play important roles in regulating K<sup>+</sup> channel trafficking to their sites of action.

The Ca<sup>2+</sup> binding protein calmodulin plays an important role as a calcium sensor in many biological processes (Cohen and Klee, 1988). The small conductance SK channels of the brain are gated solely by calcium levels and are important for spike frequency adaptation in the brain (Kohler et al., 1996). Unlike the large conductance Slo channels which directly bind calcium through an intracellular C-terminal domain



(Schreiber and Salkoff, 1997), SK channels are indirectly gated by calcium through calmodulin (Xia et al., 1998). However, calmodulin is found constitutively bound to the SK channel, regardless of whether calcium is bound to it (Xia et al., 1998). The crystal structure of calmodulin bound to the C-terminal domain of SK2 reveals extensive contacts stabilizing their interaction (Schumacher et al., 2001). Thus, in the case of SK channels, a multipurpose calcium-binding protein has evolved into a permanent component of the functional channel. Thus, a compelling case can be made for calmodulin being a channel regulatory subunit even if it doubles as a  $\text{Ca}^{2+}$  sensor in many other processes.

### **Regulation of Channel-Subunit Interactions**

The previous section has highlighted the diversity in channel activity conferred by regulatory subunits. Surface expression, channel gating kinetics, sensitivity to channel modulators and regulation by novel molecules are all mechanisms by which regulatory subunits increase functional diversity from a single channel. But true diversity only arises when two populations of the same channel exist, one complexed with regulatory subunits and the other uncomplexed. This can be achieved through differential expression of subunits in only a subset of the cells in which their target channel is expressed, thus leading to two channel populations with distinct properties. Such regulated expression occurs for Slo  $\beta$  subunits in the cochlea hair cells of lower vertebrates and has been proposed as the basis for frequency discrimination (Ramanathan et al., 1999; Ramanathan and Fuchs, 2002).

Two additional mechanisms for creating distinct populations of channels through differential use of regulatory subunits have become evident. Dynamic control of  $\text{K}^+$  conductance has been achieved by regulating the channel/subunit functional interaction through phosphorylation of either the subunit or the channel. Coexpression of  $\text{K}_v\beta 1.3$  with  $\text{K}_v 1.5$  in *Xenopus* oocytes leads to fast inactivation of  $\text{K}_v 1.5$  currents (Kwak et al., 1999). PKA-mediated phosphorylation of  $\text{K}_v\beta 1.3$  at a serine residue in its N-terminal inactivation domain reduces its fast inactivation activity (Kwak et al., 1999). Likewise, phosphorylation of a serine residue in the  $\text{K}_v 1.1$  channel is required for its regulation by the  $\text{K}_v\beta 1.1$  subunit (Levin et al., 1996; Jing et al., 1999; Singer-Lahat et al., 1999). Thus phosphorylation of either component can regulate their interaction. This form of regulation has also been reported for Slo channels, where phosphorylation of the  $\beta 4$

subunit abrogates its effects on the activation and voltage dependence of Slo channels without altering their physical association (Jin et al., 2002).

A second mechanism for generating additional K<sup>+</sup> channel diversity through interactions with regulatory subunits occurs through the partial assembly of regulatory subunits with a channel. Under limiting concentrations, K<sub>v</sub>β1 and the Slo β1 and β2 subunits can partially assemble *in vitro* with their respective channels to form complexes with intermediate properties between those displayed by the channel alone and the fully titrated channel containing four bound subunits (Xu et al., 1998; Wang et al., 2002). Each additional Slo β subunit that binds to the Slo channel results in an incremental shift in the voltage dependence of gating (Wang et al., 2002). Studies with tandem fusion of KCNQ1 and minK indicate that minK may also be capable of assembling in multiple stoichiometries (Wang et al., 1998b). In addition to one subunit combining in different stoichiometries with a channel to generate populations of channels with distinct properties, the simultaneous assembly of two types of subunits with the same channel may generate novel K<sup>+</sup> conductances. K<sub>v</sub>β2 can compete with K<sub>v</sub>β1 in transfected mammalian cells for binding to Shaker-type channels (Xu and Li, 1997), raising the possibility of such mixed complexes *in vivo*.

### **K<sup>+</sup> Channels in *C. elegans***

The completed genome of the nematode *C. elegans* has allowed for the first time a survey of the full set of ion channels in a metazoan (Consortium, 1998). Such analysis indicates that *C. elegans* has over 70 K<sup>+</sup> channels, with all seven mammalian K<sup>+</sup> channel families represented by multiple members: K<sub>v</sub> (10), K<sub>v</sub>LQT (3), Eag (2), Slo (2), SK (4), K<sub>ir</sub> (3) and two-pore (~ 50) (Wei et al., 1996; Bargmann, 1998). The two-pore family is highly represented in *C. elegans* (68%) compared to other species. In *Drosophila*, 11 out of 26 (42%) predicted K<sup>+</sup> channels identified by genome analysis are two-pore channels (Littleton and Ganetzky, 2000), and only 14 out of 67 (21%) human channels are two-pore family (Goldstein et al., 2001 and I.P. and H.R.H., unpublished data). Surprisingly, the conservation of K<sup>+</sup> channel families in *C. elegans* does not extend to their regulatory subunits. No K<sub>v</sub>β, minK, Slo or KchIP regulatory subunits have been found in the *C. elegans* genome (Littleton and Ganetzky, 2000 and I.P. and H.R.H., unpublished data). SUR1-like genes are found in the *C. elegans* genome but it is presently unclear if they act as channel subunits or simply as ABC-transporters (I.P. and H.R.H. unpublished data). Thus, *C. elegans* appears to generate functional

diversity primarily by encoding additional two-pore channel genes rather than through coding regulatory subunits for each channel family. Alternative splicing of two-pore channels may be an alternative complementary mechanism for generating diversity in *C. elegans*. An analysis of the transcriptional unit of predicted two-pore channels *n2P16* and *n2P17* indicates that *n2P17* produces at least six alternatively spliced products (Wang et al., 1999).

*C. elegans* has been a fertile organism for the generation of both gain-of-function (gf) or loss-of-function (lf) mutations causing nervous system or muscle contraction defects, as even severely uncoordinated (Unc) or egg-laying defective (Egl) animals are viable (Trent et al., 1983; Park and Horvitz, 1986; Desai and Horvitz, 1989). Mutations in six K<sup>+</sup> channels from four different families have been identified through cloning of such mutants. These include the K<sub>v</sub> channels *exp-2* (Davis et al., 1999; Fleischhauer et al., 2000) and *egl-36* (Elkes et al., 1997; Johnstone et al., 1997), the HERG channels *egl-2* (Weinshenker et al., 1999) and *unc-103* (Reiner et al., 1999), the Slo channel *slo-1* (Yuan et al., 2000; Wang et al., 2001) and the two-pore channel *twk-18* (Kunkel et al., 2000). Comparison of the *in vivo* role of these channels in *C. elegans* with their counterparts of known function in humans has often revealed a functional conservation. Both the human HERG channel and the *C. elegans* HERG-like EGL-2 channel regulate muscle contraction and are both blocked by the drug imipramine (Weinshenker et al., 1999). In addition, a gain-of-function point mutation in *egl-2* leads to a shift in the midpoint of channel activation towards more hyperpolarized potentials. When this mutation is introduced into the mouse homolog, its midpoint of channel activation is also shifted (Weinshenker et al., 1999). These results are consistent with a functional conservation between *C. elegans* channels and their mammalian counterparts.

### ***sup-9, sup-10, sup-18 and unc-93 Interacting Genes***

The muscle-contraction regulatory genes *sup-9, sup-10, sup-18* and *unc-93* are the central focus of this work. *unc-93(e1500)* mutants are severely paralyzed, cannot lay eggs and display a characteristic rubber-band response: when prodded on the head, a wild-type animal will contract away from the touch and move away, while a rubberband worm will contract and relax along its entire body without moving backwards (Greenwald and Horvitz, 1980). Gene dosage studies indicate that *the unc-93(e1500)* mutation is neomorphic. Genetic screens for suppressors of the Unc phenotype of *unc-93(e1500)* mutants have defined two loci, *sup-9* and *sup-10*, and lf mutations in *unc-93*

itself (Greenwald and Horvitz, 1980; De Stasio et al., 1997). *sup-9(lf)* or *sup-10(lf)* mutations completely suppress the Unc and Egl phenotypes of *unc-93(e1500)* animals, while having a wild-type phenotype on their own. *sup-9(gf)* and *sup-10(gf)* mutants were subsequently identified that qualitatively displayed the same phenotypes as *unc-93(gf)* although with differing severity (Greenwald and Horvitz, 1986; Levin and Horvitz, 1993). As with *unc-93(gf)* mutations, the phenotypes of *sup-9(gf)* and *sup-10(gf)* mutants can be completely suppressed by *lf* in any of the three genes, indicating that they act at the same step genetically, possibly as subunits of a protein complex (Greenwald and Horvitz, 1986; Levin and Horvitz, 1993). Mosaic analysis of *sup-10* (Herman, 1984) and pharmacological characterization of *unc-93(gf)* mutants (Reiner et al., 1995) indicate that the phenotypes in these rubberband mutants are caused by muscle rather than neuronal dysfunction.

*sup-18(lf)* mutations suppress the defects of *sup-10(gf)* mutants completely while only partially those of *sup-9(gf)* or *unc-93(gf)* mutants, suggesting that *sup-10* may encode a nonessential regulator of the proposed complex. *unc-93* has been cloned and found to encode a novel multi-pass transmembrane protein with a highly charged N-terminal domain (Levin and Horvitz, 1992). The *unc-93(e1500)* mutation causes a glycine to arginine mutation in one of the predicted transmembrane domains. *sup-10* encodes a predicted novel type-one transmembrane protein (Cummins, Levin, Anderson and Horvitz, unpublished results). The *sup-10(n983)* mutation contains a late nonsense mutation predicted to delete the 10-amino acid intracellular domain of *sup-10*.

Chapter 2 will describe the molecular identification and characterization of *sup-9*, a two-pore K<sup>+</sup> channel. This identification suggests that two-pore channels are under regulation by regulatory subunits. Chapter 3 will describe the molecular identification of *sup-18* as a transmembrane nitroreductase and propose a molecular model by which two channel subunits, *sup-10* and *sup-18*, may coordinately regulate a two-pore channel. Finally, combined results from Chapter 3 and the appendices will explore the structural requirements in a two-pore channel for multiple activation by regulatory subunits.

## **Acknowledgments**

I would like to thank Megan Higginbotham and Eric Andersen for helpful comments concerning this chapter.

## References

Abbott, G. W., Butler, M. H., Bendahhou, S., Dalakas, M. C., Ptacek, L. J., and Goldstein, S. A. (2001). MiRP2 forms potassium channels in skeletal muscle with K<sub>v</sub>3.4 and is associated with periodic paralysis, *Cell* 104, 217-31.

Abbott, G. W., Sesti, F., Splawski, I., Buck, M. E., Lehmann, M. H., Timothy, K. W., Keating, M. T., and Goldstein, S. A. (1999). MiRP1 forms IKr potassium channels with HERG and is associated with cardiac arrhythmia, *Cell* 97, 175-87.

Accili, E. A., Kiehn, J., Wible, B. A., and Brown, A. M. (1997a). Interactions among inactivating and noninactivating K<sub>v</sub>beta subunits, and K<sub>v</sub>alpha1.2, produce potassium currents with intermediate inactivation, *J Biol Chem* 272, 28232-28236.

Accili, E. A., Kiehn, J., Yang, Q., Wang, Z., Brown, A. M., and Wible, B. A. (1997b). Separable K<sub>v</sub>beta subunit domains alter expression and gating of potassium channels, *J Biol Chem* 272, 25824-31.

Accili, E. A., Kuryshv, Y. A., Wible, B. A., and Brown, A. M. (1998). Separable effects of human K<sub>v</sub>beta1.2 N- and C-termini on inactivation and expression of human K<sub>v</sub>1.4, *J Physiol* 512, 325-336.

Adams, P. R., Constanti, A., Brown, D. A., and Clark, R. B. (1982). Intracellular Ca<sup>2+</sup> activates a fast voltage-sensitive K<sup>+</sup> current in vertebrate sympathetic neurones, *Nature* 296, 746-9.

Aguilar-Bryan, L., Nichols, C. G., Wechsler, S. W., Clement, J. P. t., Boyd, A. E., 3rd, Gonzalez, G., Herrera-Sosa, H., Nguy, K., Bryan, J., and Nelson, D. A. (1995). Cloning of the beta cell high-affinity sulfonylurea receptor: a regulator of insulin secretion, *Science* 268, 423-426.

Ammala, C., Moorhouse, A., and Ashcroft, F. M. (1996). The sulphonylurea receptor confers diazoxide sensitivity on the inwardly rectifying K<sup>+</sup> channel K<sub>ir</sub>6.1 expressed in human embryonic kidney cells, *J Physiol* 494, 709-14.

An, W. F., Bowlby, M. R., Betty, M., Cao, J., Ling, H. P., Mendoza, G., Hinson, J. W., Mattsson, K. I., Strassle, B. W., Trimmer, J. S., and Rhodes, K. J. (2000). Modulation of A-type potassium channels by a family of calcium sensors, *Nature* 403, 553-556.

Arnold, D. B., and Clapham, D. E. (1999). Molecular determinants for subcellular localization of PSD-95 with an interacting K<sup>+</sup> channel, *Neuron* 23, 149-57.

Ashmole, I., Goodwin, P. A., and Stanfield, P. R. (2001). TASK-5, a novel member of the tandem pore K<sup>+</sup> channel family, *Pflugers Arch* 442, 828-33.

Atkinson, N. S., Robertson, G. A., and Ganetzky, B. (1991). A component of calcium-activated potassium channels encoded by the *Drosophila slo* locus, *Science* 253, 551-5.

Bahring, R., Dannenberg, J., Peters, H. C., Leicher, T., Pongs, O., and Isbrandt, D. (2001a). Conserved K<sub>v</sub>4 N-terminal domain critical for effects of K<sub>v</sub> channel-interacting protein 2.2 on channel expression and gating, *J Biol Chem* 276, 23888-94.

Bahring, R., Milligan, C. J., Vardanyan, V., Engeland, B., Young, B. A., Dannenberg, J., Waldschutz, R., Edwards, J. P., Wray, D., and Pongs, O. (2001b). Coupling of voltage-dependent potassium channel inactivation and oxidoreductase active site of K<sub>v</sub>β subunits, *J Biol Chem* 276, 22923-9.

Bang, H., Kim, Y., and Kim, D. (2000). TREK-2, a New Member of the Mechanosensitive Tandem-pore K<sup>+</sup> Channel Family, *J Biol Chem* 275, 17412-17419.

Bargmann, C. I. (1998). Neurobiology of the *Caenorhabditis elegans* genome, *Science* 282, 2028-2033.

Barhanin, J., Lesage, F., Guillemare, E., Fink, M., Lazdunski, M., and Romey, G. (1996). K<sub>v</sub>LQT1 and IsK (minK) proteins associate to form the I<sub>Ks</sub> cardiac potassium current, *Nature* 384, 78-80.

Bezánilla, F. (2000). The voltage sensor in voltage-dependent ion channels, *Physiol Rev* 80, 555-92.

Bond, C. T., Maylie, J., and Adelman, J. P. (1999). Small-conductance calcium-activated potassium channels, *Ann N Y Acad Sci* 868, 370-8.

Brenner, R., Jegla, T. J., Wickenden, A., Liu, Y., and Aldrich, R. W. (2000a). Cloning and functional characterization of novel large conductance calcium-activated potassium channel beta subunits, hKCNMB3 and hKCNMB4, *J Biol Chem* 275, 6453-61.

Brenner, R., Perez, G. J., Bonev, A. D., Eckman, D. M., Kosek, J. C., Wiler, S. W., Patterson, A. J., Nelson, M. T., and Aldrich, R. W. (2000b). Vasoregulation by the beta1 subunit of the calcium-activated potassium channel, *Nature* 407, 870-6.

Broillet, M. C., and Firestein, S. (1999). Cyclic nucleotide-gated channels. Molecular mechanisms of activation, *Ann N Y Acad Sci* 868, 730-40.

Browne, D. L., Gancher, S. T., Nutt, J. G., Brunt, E. R., Smith, E. A., Kramer, P., and Litt, M. (1994). Episodic ataxia/myokymia syndrome is associated with point mutations in the human potassium channel gene, KCNA1, *Nat Genet* 8, 136-40.

Bruggemann, A., Pardo, L. A., Stuhmer, W., and Pongs, O. (1993). Ether-a-go-go encodes a voltage-gated channel permeable to K<sup>+</sup> and Ca<sup>2+</sup> and modulated by cAMP, *Nature* 365, 445-8.

Buckler, K. J., Williams, B. A., and Honore, E. (2000). An oxygen-, acid- and anaesthetic-sensitive TASK-like background potassium channel in rat arterial chemoreceptor cells, *J Physiol* 525 Pt 1, 135-142.

Butler, A., Tsunoda, S., McCobb, D. P., Wei, A., and Salkoff, L. (1993). mSlo, a complex mouse gene encoding "maxi" calcium-activated potassium channels, *Science* 261, 221-4.

Campomanes, C. R., Carroll, K. I., Manganas, L. N., Hershberger, M. E., Gong, B., Antonucci, D. E., Rhodes, K. J., and Trimmer, J. S. (2002). K<sub>v</sub> beta subunit oxidoreductase activity and K<sub>v</sub>1 potassium channel trafficking, *J Biol Chem* 277, 8298-305.

Catterall, W. A. (2000). Structure and regulation of voltage-gated  $Ca_{2+}$  channels, *Annu Rev Cell Dev Biol* 16, 521-55.

Chouinard, S. W., Wilson, G. F., Schlimgen, A. K., and Ganetzky, B. (1995). A potassium channel beta subunit related to the aldo-keto reductase superfamily is encoded by the *Drosophila hyperkinetic* locus, *Proc Natl Acad Sci USA* 92, 6763-6767.

Christie, M. J., Adelman, J. P., Douglass, J., and North, R. A. (1989). Expression of a cloned rat brain potassium channel in *Xenopus* oocytes, *Science* 244, 221-4.

Christie, M. J., North, R. A., Osborne, P. B., Douglass, J., and Adelman, J. P. (1990). Heteropolymeric potassium channels expressed in *Xenopus* oocytes from cloned subunits, *Neuron* 4, 405-11.

Clement, J. P. t., Kunjilwar, K., Gonzalez, G., Schwanstecher, M., Panten, U., Aguilar-Bryan, L., and Bryan, J. (1997). Association and stoichiometry of  $K_{ATP}$  channel subunits, *Neuron* 18, 827-38.

Cohen, N. A., Brenman, J. E., Snyder, S. H., and Brecht, D. S. (1996). Binding of the inward rectifier  $K^+$  channel  $K_{ir2.3}$  to PSD-95 is regulated by protein kinase A phosphorylation, *Neuron* 17, 759-67.

Cohen, P., and Klee, C. B. (1988). *Calmodulin* (Amsterdam ; New York, Elsevier).

Consortium, *C. e. S.* (1998). Genome sequence of the nematode *C. elegans*: a platform for investigating biology., *Science* 282, 2012-2018.

Covarrubias, M., Wei, A., Salkoff, L., and Vyas, T. B. (1994). Elimination of rapid potassium channel inactivation by phosphorylation of the inactivation gate, *Neuron* 13, 1403-12.

Curran, M. E., Splawski, I., Timothy, K. W., Vincent, G. M., Green, E. D., and Keating, M. T. (1995). A molecular basis for cardiac arrhythmia: HERG mutations cause long QT syndrome, *Cell* 80, 795-803.



Czirjak, G., and Enyedi, P. (2002). Formation of functional heterodimers between the TASK-1 and TASK-3 two-pore domain potassium channel subunits, *J Biol Chem* 277, 5426-32.

Davis, M. W., Fleischhauer, R., Dent, J. A., Joho, R. H., and Avery, L. (1999). A mutation in the *C. elegans* EXP-2 potassium channel that alters feeding behavior, *Science* 286, 2501-2504.

De Stasio, E., Lephoto, C., Azuma, L., C., H., Stanislaus, D., and Uttam, J. (1997). Characterization of Revertants of *unc-93(e1500)* in *Caenorhabditis elegans* Induced by N-ethyl-N-nitrosourea, *Genetics* 147, 597-608.

Decher, N., Maier, M., Dittrich, W., Gassenhuber, J., Bruggemann, A., Busch, A. E., and Steinmeyer, K. (2001). Characterization of TASK-4, a novel member of the pH-sensitive, two-pore domain potassium channel family, *FEBS Lett* 492, 84-9.

del Camino, D., Holmgren, M., Liu, Y., and Yellen, G. (2000). Blocker protection in the pore of a voltage-gated K<sup>+</sup> channel and its structural implications, *Nature* 403, 321-5.

Derst, C., Konrad, M., Kockerling, A., Karolyi, L., Deschenes, G., Daut, J., Karschin, A., and Seyberth, H. W. (1997). Mutations in the ROMK gene in antenatal Bartter syndrome are associated with impaired K<sup>+</sup> channel function, *Biochem Biophys Res Commun* 230, 641-5.

Desai, C., and Horvitz, H. R. (1989). *Caenorhabditis elegans* mutants defective in the functioning of the motor neurons responsible for egg laying, *Genetics* 121, 703-721.

Dick, G. M., Rossow, C. F., Smirnov, S., Horowitz, B., and Sanders, K. M. (2001). Tamoxifen activates smooth muscle BK channels through the regulatory beta 1 subunit, *J Biol Chem* 276, 34594-9.

Dick, G. M., and Sanders, K. M. (2001). (Xeno)estrogen sensitivity of smooth muscle BK channels conferred by the regulatory beta1 subunit: a study of beta1 knockout mice, *J Biol Chem* 276, 44835-40.

Doyle, D. A., Morais Cabral, J., Pfuetzner, R. A., Kuo, A., Gulbis, J. M., Cohen, S. L., Chait, B. T., and MacKinnon, R. (1998). The structure of the potassium channel: molecular basis of K<sup>+</sup> conduction and selectivity, *Science* *280*, 69-77.

Duprat, F., Lesage, F., Fink, M., Reyes, R., Heurteaux, C., and Lazdunski, M. (1997). TASK, a human background K<sup>+</sup> channel to sense external pH variations near physiological pH, *EMBO J* *16*, 5464-5471.

Elkes, D. A., Cardozo, D. L., Madison, J., and Kaplan, J. M. (1997). EGL-36 Shaw channels regulate *C. elegans* egg-laying muscle activity, *Neuron* *19*, 165-174.

Ellis, S. B., Williams, M. E., Ways, N. R., Brenner, R., Sharp, A. H., Leung, A. T., Campbell, K. P., McKenna, E., Koch, W. J., Hui, A., and et al. (1988). Sequence and expression of mRNAs encoding the alpha 1 and alpha 2 subunits of a DHP-sensitive calcium channel, *Science* *241*, 1661-4.

Engel, J. E., and Wu, C. F. (1998). Genetic dissection of functional contributions of specific potassium channel subunits in habituation of an escape circuit in *Drosophila*, *J Neurosci* *18*, 2254-67.

Ficker, E., Tagliatela, M., Wible, B. A., Henley, C. M., and Brown, A. M. (1994). Spermine and spermidine as gating molecules for inward rectifier K<sup>+</sup> channels, *Science* *266*, 1068-72.

Fink, M., Lesage, F., Duprat, F., Heurteaux, C., Reyes, R., Fosset, M., and Lazdunski, M. (1998). A neuronal two P domain K<sup>+</sup> channel stimulated by arachidonic acid and polyunsaturated fatty acids, *EMBO J* *17*, 3297-3308.

Fleischhauer, R., Davis, M. W., Dzhura, I., Neely, A., Avery, L., and Joho, R. H. (2000). Ultrafast inactivation causes inward rectification in a voltage-gated K<sup>+</sup> channel from *Caenorhabditis elegans*, *J Neurosci* *20*, 511-520.

Ganetzky, B., Robertson, G. A., Wilson, G. F., Trudeau, M. C., and Titus, S. A. (1999). The eag family of K<sup>+</sup> channels in *Drosophila* and mammals, *Ann N Y Acad Sci* *868*, 356-69.

Garcia-Calvo, M., Knaus, H. G., McManus, O. B., Giangiacomo, K. M., Kaczorowski, G. J., and Garcia, M. L. (1994). Purification and reconstitution of the high-conductance, calcium-activated potassium channel from tracheal smooth muscle, *J Biol Chem* *269*, 676-682.

Girard, C., Duprat, F., Terrenoire, C., Tinel, N., Fosset, M., Romey, G., Lazdunski, M., and Lesage, F. (2001). Genomic and functional characteristics of novel human pancreatic 2P domain K<sup>+</sup> channels, *Biochem Biophys Res Commun* *282*, 249-56.

Goldin, A. L. (1999). Diversity of mammalian voltage-gated sodium channels, *Ann N Y Acad Sci* *868*, 38-50.

Goldstein, S. A., Bockenhauer, D., O'Kelly, I., and Zilberberg, N. (2001). Potassium leak channels and the KCNK family of two-P-domain subunits, *Nat Rev Neurosci* *2*, 175-184.

Goldstein, S. A., and Miller, C. (1991). Site-specific mutations in a minimal voltage-dependent K<sup>+</sup> channel alter ion selectivity and open-channel block, *Neuron* *7*, 403-8.

Greenwald, I., and Horvitz, H. R. (1986). A visible allele of the muscle gene *sup-10X* of *C. elegans*, *Genetics* *113*, 63-72.

Greenwald, I. S., and Horvitz, H. R. (1980). *unc-93(e1500)*: A behavioral mutant of *Caenorhabditis elegans* that defines a gene with a wild-type null phenotype, *Genetics* *96*, 147-164.

Gribble, F. M., Tucker, S. J., and Ashcroft, F. M. (1997). The essential role of the Walker A motifs of SUR1 in K-ATP channel activation by Mg-ADP and diazoxide, *Embo J* *16*, 1145-52.

Grissmer, S. (1997). Potassium channels still hot, *Trends Pharmacol Sci* *18*, 347-50.

Gulbis, J. M., Mann, S., and MacKinnon, R. (1999). Structure of a voltage-dependent K<sup>+</sup> channel beta subunit, *Cell* *97*, 943-952.

Gulbis, J. M., Zhou, M., Mann, S., and MacKinnon, R. (2000). Structure of the cytoplasmic beta subunit-T1 assembly of voltage- dependent K<sup>+</sup> channels, *Science* 289, 123-7.

Hamill, O. P., Marty, A., Neher, E., Sakmann, B., and Sigworth, F. J. (1981). Improved patch-clamp techniques for high-resolution current recording from cells and cell-free membrane patches, *Pflugers Arch* 391, 85-100.

Hartshorne, R. P., and Catterall, W. A. (1981). Purification of the saxitoxin receptor of the sodium channel from rat brain, *Proc Natl Acad Sci U S A* 78, 4620-4.

Heginbotham, L., Lu, Z., Abramson, T., and MacKinnon, R. (1994). Mutations in the K<sup>+</sup> channel signature sequence, *Biophys J* 66, 1061-1067.

Heinemann, S. H., Rettig, J., Graack, H. R., and Pongs, O. (1996). Functional characterization of K<sub>v</sub> channel beta-subunits from rat brain, *J Physiol* 493, 625-633.

Herman, R. K. (1984). Analysis of genetic mosaics of the nematode *Caneorhabditis elegans*, *Genetics* 108, 165-180.

Higgins, C. F. (1992). ABC transporters: from microorganisms to man, *Annu Rev Cell Biol* 8, 67-113.

Hille, B. (1992). *Ionic Channels of Excitable Membranes*, Second edn (Sanderland, Sinauer).

Hirst, G. D., Johnson, S. M., and van Helden, D. F. (1985). The slow calcium-dependent potassium current in a myenteric neurone of the guinea-pig ileum, *J Physiol* 361, 315-37.

Ho, K., Nichols, C. G., Lederer, W. J., Lytton, J., Vassilev, P. M., Kanazirska, M. V., and Hebert, S. C. (1993). Cloning and expression of an inwardly rectifying ATP-regulated potassium channel, *Nature* 362, 31-8.

Hodgkin, A. L., Huxley, A.F. (1952). A quantitative description of membrane current and its application to conduction and excitation in nerve, *J, Physiol (Lond)* 117, 500-544.

Holmqvist, M. H., Cao, J., Hernandez-Pineda, R., Jacobson, M. D., Carroll, K. I., Sung, M. A., Betty, M., Ge, P., Gilbride, K. J., Brown, M. E., *et al.* (2002). Elimination of fast inactivation in K<sub>v</sub>4 A-type potassium channels by an auxiliary subunit domain, *Proc Natl Acad Sci U S A* *99*, 1035-40.

Holmqvist, M. H., Cao, J., Knoppers, M. H., Jurman, M. E., Distefano, P. S., Rhodes, K. J., Xie, Y., and An, W. F. (2001). Kinetic modulation of K<sub>v</sub>4-mediated A-current by arachidonic acid is dependent on potassium channel interacting proteins, *J Neurosci* *21*, 4154-61.

Hoshi, T., Zagotta, W. N., and Aldrich, R. W. (1990). Biophysical and molecular mechanisms of Shaker potassium channel inactivation, *Science* *250*, 533-8.

Inagaki, N., Gono, T., Clement, J. P., Wang, C. Z., Aguilar-Bryan, L., Bryan, J., and Seino, S. (1996). A family of sulfonylurea receptors determines the pharmacological properties of ATP-sensitive K<sup>+</sup> channels, *Neuron* *16*, 1011-7.

Inagaki, N., Gono, T., Clement, J. P. t., Namba, N., Inazawa, J., Gonzalez, G., Aguilar-Bryan, L., Seino, S., and Bryan, J. (1995). Reconstitution of I<sub>KATP</sub>: an inward rectifier subunit plus the sulfonylurea receptor, *Science* *270*, 1166-1170.

Inanobe, A., Horio, Y., Fujita, A., Tanemoto, M., Hibino, H., Inageda, K., and Kurachi, Y. (1999). Molecular cloning and characterization of a novel splicing variant of the K<sub>v</sub>3.2 subunit predominantly expressed in mouse testis, *J Physiol* *521 Pt 1*, 19-30.

Isom, L. L., De Jongh, K. S., Patton, D. E., Reber, B. F., Offord, J., Charbonneau, H., Walsh, K., Goldin, A. L., and Catterall, W. A. (1992). Primary structure and functional expression of the beta 1 subunit of the rat brain sodium channel, *Science* *256*, 839-42.

Jay, S. D., Ellis, S. B., McCue, A. F., Williams, M. E., Vedvick, T. S., Harpold, M. M., and Campbell, K. P. (1990). Primary structure of the gamma subunit of the DHP-sensitive calcium channel from skeletal muscle, *Science* *248*, 490-2.

Jentsch, T. J., Steinmeyer, K., and Schwarz, G. (1990). Primary structure of *Torpedo marmorata* chloride channel isolated by expression cloning in *Xenopus* oocytes, *Nature* *348*, 510-4.

Jiang, Y., Lee, A., Chen, J., Cadene, M., Chait, B. T., and MacKinnon, R. (2002a). Crystal structure and mechanism of a calcium-gated potassium channel, *Nature* *417*, 515-22.

Jiang, Y., Lee, A., Chen, J., Cadene, M., Chait, B. T., and MacKinnon, R. (2002b). The open pore conformation of potassium channels, *Nature* *417*, 523-6.

Jiang, Y., and MacKinnon, R. (2000). The barium site in a potassium channel by x-ray crystallography, *J Gen Physiol* *115*, 269-72.

Jin, P., Weiger, T. M., Wu, Y., and Levitan, I. B. (2002). Phosphorylation-dependent functional coupling of hSlo calcium-dependent potassium channel and its hbeta 4 subunit, *J Biol Chem* *277*, 10014-20.

Jing, J., Chikvashvili, D., Singer-Lahat, D., Thornhill, W. B., Reuveny, E., and Lotan, I. (1999). Fast inactivation of a brain K<sup>+</sup> channel composed of K<sub>v</sub>1.1 and K<sub>v</sub>beta1.1 subunits modulated by G protein beta gamma subunits, *Embo J* *18*, 1245-56.

Johnstone, D. B., Wei, A., Butler, A., Salkoff, L., and Thomas, J. H. (1997). Behavioral defects in *C. elegans egl-36* mutants result from potassium channels shifted in voltage-dependence of activation, *Neuron* *19*, 151-164.

Kaczorowski, G. J., Knaus, H. G., Leonard, R. J., McManus, O. B., and Garcia, M. L. (1996). High-conductance calcium-activated potassium channels; structure, pharmacology, and function, *J Bioenerg Biomembr* *28*, 255-67.

Kamb, A., Iverson, L. E., and Tanouye, M. A. (1987). Molecular characterization of Shaker, a *Drosophila* gene that encodes a potassium channel, *Cell* *50*, 405-13.

Kaplan, W. D., and Trout, W. E., 3rd (1969). The behavior of four neurological mutants of *Drosophila*, *Genetics* *61*, 399-409.

Ketchum, K. A., Joiner, W. J., Sellers, A. J., Kaczmarek, L. K., and Goldstein, S. A. (1995). A new family of outwardly rectifying potassium channel proteins with two pore domains in tandem, *Nature* 376, 690-5.

Kim, D., and Gnatenco, C. (2001). TASK-5, a new member of the tandem-pore K<sup>+</sup> channel family, *Biochem Biophys Res Commun* 284, 923-30.

Kim, E., Niethammer, M., Rothschild, A., Jan, Y. N., and Sheng, M. (1995). Clustering of Shaker-type K<sup>+</sup> channels by interaction with a family of membrane-associated guanylate kinases, *Nature* 378, 85-8.

Kim, Y., Bang, H., and Kim, D. (2000). TASK-3, a new member of the tandem pore K<sup>+</sup> channel family, *J Biol Chem* 275, 9340-9347.

Kindler, C. H., Yost, C. S., and Gray, A. T. (1999). Local anesthetic inhibition of baseline potassium channels with two pore domains in tandem, *Anesthesiology* 90, 1092-102.

Knaus, H. G., Folander, K., Garcia-Calvo, M., Garcia, M. L., Kaczorowski, G. J., Smith, M., and Swanson, R. (1994a). Primary sequence and immunological characterization of beta-subunit of high conductance Ca<sup>+2</sup>-activated K<sup>+</sup> channel from smooth muscle, *J Biol Chem* 269, 17274-17278.

Knaus, H. G., Garcia-Calvo, M., Kaczorowski, G. J., and Garcia, M. L. (1994b). Subunit composition of the high conductance calcium-activated potassium channel from smooth muscle, a representative of the *mSlo* and *slowpoke* family of potassium channels, *J Biol Chem* 269, 3921-3924.

Kofuji, P., Davidson, N., and Lester, H. A. (1995). Evidence that neuronal G-protein-gated inwardly rectifying K<sup>+</sup> channels are activated by G beta gamma subunits and function as heteromultimers, *Proc Natl Acad Sci U S A* 92, 6542-6.

Kohler, M., Hirschberg, B., Bond, C. T., Kinzie, J. M., Marrion, N. V., Maylie, J., and Adelman, J. P. (1996). Small-conductance, calcium-activated potassium channels from mammalian brain, *Science* 273, 1709-14.

- Kramer, J. W., Post, M. A., Brown, A. M., and Kirsch, G. E. (1998). Modulation of potassium channel gating by coexpression of  $K_v2.1$  with regulatory  $K_v5.1$  or  $K_v6.1$  alpha-subunits, *Am J Physiol* *274*, C1501-10.
- Krapivinsky, G., Gordon, E. A., Wickman, K., Velimirovic, B., Krapivinsky, L., and Clapham, D. E. (1995). The G-protein-gated atrial  $K^+$  channel  $I_{K_{ACH}}$  is a heteromultimer of two inwardly rectifying  $K^+$ -channel proteins, *Nature* *374*, 135-41.
- Kubisch, C., Schroeder, B. C., Friedrich, T., Lutjohann, B., El-Amraoui, A., Marlin, S., Petit, C., and Jentsch, T. J. (1999). KCNQ4, a novel potassium channel expressed in sensory outer hair cells, is mutated in dominant deafness, *Cell* *96*, 437-46.
- Kubo, Y., Baldwin, T. J., Jan, Y. N., and Jan, L. Y. (1993a). Primary structure and functional expression of a mouse inward rectifier potassium channel, *Nature* *362*, 127-33.
- Kubo, Y., Reuveny, E., Slesinger, P. A., Jan, Y. N., and Jan, L. Y. (1993b). Primary structure and functional expression of a rat G-protein-coupled muscarinic potassium channel, *Nature* *364*, 802-6.
- Kunkel, M. T., Johnstone, D. B., Thomas, J. H., and Salkoff, L. (2000). Mutants of a temperature-sensitive two-P domain potassium channel, *J Neurosci* *20*, 7517-7524.
- Kupersmidt, S., Snyders, D. J., Raes, A., and Roden, D. M. (1998). A  $K^+$  channel splice variant common in human heart lacks a C-terminal domain required for expression of rapidly activating delayed rectifier current, *J Biol Chem* *273*, 27231-5.
- Kurokawa, J., Motoike, H. K., and Kass, R. S. (2001). TEA<sup>+</sup>-sensitive KCNQ1 constructs reveal pore-independent access to KCNE1 in assembled  $I_{K_s}$  channels, *J Gen Physiol* *117*, 43-52.
- Kuryshv, Y. A., Gudz, T. I., Brown, A. M., and Wible, B. A. (2000). KChAP as a chaperone for specific  $K^+$  channels, *Am J Physiol Cell Physiol* *278*, C931-941.



Kwak, Y. G., Hu, N., Wei, J., George, A. L., Jr., Grobaski, T. D., Tamkun, M. M., and Murray, K. T. (1999). Protein kinase A phosphorylation alters K<sub>v</sub>β1.3 subunit-mediated inactivation of the K<sub>v</sub>1.5 potassium channel, *J Biol Chem* 274, 13928-32.

Leonoudakis, D., Gray, A. T., Winegar, B. D., Kindler, C. H., Harada, M., Taylor, D. M., Chavez, R. A., Forsayeth, J. R., and Yost, C. S. (1998). An open rectifier potassium channel with two pore domains in tandem cloned from rat cerebellum, *J Neurosci* 18, 868-877.

Lesage, F., Guillemare, E., Fink, M., Duprat, F., Lazdunski, M., Romey, G., and Barhanin, J. (1996a). TWIK-1, a ubiquitous human weakly inward rectifying K<sup>+</sup> channel with a novel structure, *EMBO J* 15, 1004-1011.

Lesage, F., Terrenoire, C., Romey, G., and Lazdunski, M. (2000). Human TREK2, a 2P domain mechano-sensitive K<sup>+</sup> channel with multiple regulations by polyunsaturated fatty acids, lysophospholipids, and G<sub>s</sub>, G<sub>i</sub>, and G<sub>q</sub> protein-coupled receptors, *J Biol Chem* 275, 28398-405.

Levin, G., Chikvashvili, D., Singer-Lahat, D., Peretz, T., Thornhill, W. B., and Lotan, I. (1996). Phosphorylation of a K<sup>+</sup> channel alpha subunit modulates the inactivation conferred by a beta subunit. Involvement of cytoskeleton, *J Biol Chem* 271, 29321-8.

Levin, J. Z., and Horvitz, H. R. (1992). The *Caenorhabditis elegans unc-93* gene encodes a putative transmembrane protein that regulates muscle contraction, *J Cell Biol* 117, 143-155.

Levin, J. Z., and Horvitz, H. R. (1993). Three new classes of mutations in the *Caenorhabditis elegans* muscle gene *sup-9*, *Genetics* 135, 53-70.

Lewis, A., Hartness, M. E., Chapman, C. G., Fearon, I. M., Meadows, H. J., Peers, C., and Kemp, P. J. (2001). Recombinant hTASK1 is an O<sub>2</sub>-sensitive K<sup>+</sup> channel, *Biochem Biophys Res Commun* 285, 1290-4.

Littleton, J. T., and Ganetzky, B. (2000). Ion channels and synaptic organization: analysis of the *Drosophila* genome, *Neuron* 26, 35-43.

- Liu, S. Q., Jin, H., Zacarias, A., Srivastava, S., and Bhatnagar, A. (2001). Binding of pyridine nucleotide coenzymes to the beta-subunit of the voltage-sensitive K<sup>+</sup> channel, *J Biol Chem* 276, 11812-20.
- Lopatin, A. N., Makhina, E. N., and Nichols, C. G. (1994). Potassium channel block by cytoplasmic polyamines as the mechanism of intrinsic rectification, *Nature* 372, 366-9.
- Lopes, C. M., Zilberberg, N., and Goldstein, S. A. (2001). Block of Kcnk3 by protons. Evidence that 2-P-domain potassium channel subunits function as homodimers, *J Biol Chem* 276, 24449-52.
- Lu, Z., Klem, A. M., and Ramu, Y. (2001). Ion conduction pore is conserved among potassium channels, *Nature* 413, 809-13.
- Lu, Z., and MacKinnon, R. (1994). Electrostatic tuning of Mg<sup>2+</sup> affinity in an inward-rectifier K<sup>+</sup> channel, *Nature* 371, 243-6.
- MacKinnon, R. (1991). Determination of the subunit stoichiometry of a voltage-activated potassium channel, *Nature* 350, 232-235.
- MacKinnon, R. (1995). Pore loops: an emerging theme in ion channel structure, *Neuron* 14, 889-892.
- MacKinnon, R., Cohen, S. L., Kuo, A., Lee, A., and Chait, B. T. (1998). Structural conservation in prokaryotic and eukaryotic potassium channels, *Science* 280, 106-9.
- Maingret, F., Fosset, M., Lesage, F., Lazdunski, M., and Honore, E. (1999a). TRAAK is a mammalian neuronal mechano-gated K<sup>+</sup> channel, *J Biol Chem* 274, 1381-1387.
- Maingret, F., Lauritzen, I., Patel, A. J., Heurteaux, C., Reyes, R., Lesage, F., Lazdunski, M., and Honore, E. (2000). TREK-1 is a heat-activated background K<sup>+</sup> channel, *EMBO J* 19, 2483-2491.
- Maingret, F., Patel, A. J., Lesage, F., Lazdunski, M., and Honore, E. (1999b). Mechano- or acid stimulation, two interactive modes of activation of the TREK-1 potassium channel, *J Biol Chem* 274, 26691-26696.

Majumder, K., De Biasi, M., Wang, Z., and Wible, B. A. (1995). Molecular cloning and functional expression of a novel potassium channel beta-subunit from human atrium, *FEBS Lett* *361*, 13-6.

Matsuda, H., Saigusa, A., and Irisawa, H. (1987). Ohmic conductance through the inwardly rectifying K channel and blocking by internal  $Mg^{2+}$ , *Nature* *325*, 156-9.

McCormack, K., Connor, J. X., Zhou, L., Ho, L. L., Ganetzky, B., Chiu, S. Y., and Messing, A. (2002). Genetic analysis of the mammalian  $K^+$  channel beta subunit  $K_{\beta}2$  (*Kcnab2*), *J Biol Chem* *277*, 13219-28.

McCormack, K., McCormack, T., Tanouye, M., Rudy, B., and Stuhmer, W. (1995). Alternative splicing of the human Shaker  $K^+$  channel beta 1 gene and functional expression of the beta 2 gene product, *FEBS Lett* *370*, 32-6.

McCormack, T., and McCormack, K. (1994). Shaker  $K^+$  channel beta subunits belong to an NAD(P)H-dependent oxidoreductase superfamily, *Cell* *79*, 1133-1135.

McManus, O. B., Helms, L. M., Pallanck, L., Ganetzky, B., Swanson, R., and Leonard, R. J. (1995). Functional role of the beta subunit of high conductance calcium-activated potassium channels, *Neuron* *14*, 645-650.

Meadows, H. J., and Randall, A. D. (2001). Functional characterisation of human TASK-3, an acid-sensitive two-pore domain potassium channel, *Neuropharmacology* *40*, 551-9.

Meera, P., Wallner, M., and Toro, L. (2000). A neuronal beta subunit (*KCNMB4*) makes the large conductance, voltage- and  $Ca^{2+}$ -activated  $K^+$  channel resistant to charybdotoxin and iberiotoxin, *Proc Natl Acad Sci U S A* *97*, 5562-7.

Melman, Y. F., Domenech, A., de la Luna, S., and McDonald, T. V. (2001). Structural determinants of  $K_{\nu}LQT1$  control by the KCNE family of proteins, *J Biol Chem* *276*, 6439-44.

Millar, J. A., Barratt, L., Southan, A. P., Page, K. M., Fyffe, R. E., Robertson, B., and Mathie, A. (2000). A functional role for the two-pore domain potassium channel TASK-1 in cerebellar granule neurons, *Proc Natl Acad Sci USA* *97*, 3614-3618.

Nagaya, N., and Papazian, D. M. (1997). Potassium channel alpha and beta subunits assemble in the Endoplasmic Reticulum, *J Biol Chem* *272*, 3022-7.

Neyton, J., and Miller, C. (1988a). Discrete Ba<sup>2+</sup> block as a probe of ion occupancy and pore structure in the high-conductance Ca<sup>2+</sup>-activated K<sup>+</sup> channel, *J Gen Physiol* *92*, 569-86.

Neyton, J., and Miller, C. (1988b). Potassium blocks barium permeation through a calcium-activated potassium channel, *J Gen Physiol* *92*, 549-67.

Nichols, C. G., Shyng, S. L., Nestorowicz, A., Glaser, B., Clement, J. P. t., Gonzalez, G., Aguilar-Bryan, L., Permutt, M. A., and Bryan, J. (1996). Adenosine diphosphate as an intracellular regulator of insulin secretion, *Science* *272*, 1785-7.

Niemeyer, M. I., Cid, L. P., Barros, L. F., and Sepulveda, F. V. (2001). Modulation of the two-pore domain acid-sensitive K<sup>+</sup> channel TASK-2 (KCNK5) by changes in cell volume, *J Biol Chem* *276*, 43166-74.

Noda, M., Shimizu, S., Tanabe, T., Takai, T., Kayano, T., Ikeda, T., Takahashi, H., Nakayama, H., Kanaoka, Y., Minamino, N., and et al. (1984). Primary structure of *Electrophorus electricus* sodium channel deduced from cDNA sequence, *Nature* *312*, 121-7.

Papazian, D. M., Schwarz, T. L., Tempel, B. L., Jan, Y. N., and Jan, L. Y. (1987). Cloning of genomic and complementary DNA from Shaker, a putative potassium channel gene from *Drosophila*, *Science* *237*, 749-53.

Parcej, D. N., and Dolly, J. O. (1989). Dendrotoxin acceptor from bovine synaptic plasma membranes. Binding properties, purification and subunit composition of a putative constituent of certain voltage-activated K<sup>+</sup> channels, *Biochem J* *257*, 899-903.

Parcej, D. N., Scott, V. E., and Dolly, J. O. (1992). Oligomeric properties of alpha-dendrotoxin-sensitive potassium ion channels purified from bovine brain, *Biochemistry* *31*, 11084-11088.

Park, E. C., and Horvitz, H. R. (1986). Mutations with dominant effects on the behavior and morphology of the nematode *Caenorhabditis elegans*, *Genetics* *113*, 821-852.

Patel, A. J., and Honore, E. (2001). Properties and modulation of mammalian 2P domain K<sup>+</sup> channels, *Trends Neurosci* *24*, 339-46.

Patel, A. J., Honore, E., Lesage, F., Fink, M., Romey, G., and Lazdunski, M. (1999). Inhalational anesthetics activate two-pore-domain background K<sup>+</sup> channels, *Nat Neurosci* *2*, 422-426.

Patel, A. J., Honore, E., Maingret, F., Lesage, F., Fink, M., Duprat, F., and Lazdunski, M. (1998). A mammalian two pore domain mechano-gated S-like K<sup>+</sup> channel, *EMBO J* *17*, 4283-4290.

Patton, D. E., Silva, T., and Bezanilla, F. (1997). RNA editing generates a diverse array of transcripts encoding squid K<sub>v</sub>2 K<sup>+</sup> channels with altered functional properties, *Neuron* *19*, 711-22.

Perez-Garcia, M. T., Lopez-Lopez, J. R., and Gonzalez, C. (1999). K<sub>v</sub>beta1.2 subunit coexpression in HEK293 cells confers O<sub>2</sub> sensitivity to k<sub>v</sub>4.2 but not to *Shaker* channels, *J Gen Physiol* *113*, 897-907.

Peri, R., Wible, B. A., and Brown, A. M. (2001). Mutations in the K<sub>v</sub>beta 2 binding site for NADPH and their effects on K<sub>v</sub>1.4, *J Biol Chem* *276*, 738-41.

Perozo, E., Cortes, D. M., and Cuello, L. G. (1999). Structural rearrangements underlying K<sup>+</sup>-channel activation gating, *Science* *285*, 73-78.

Piccini, M., Vitelli, F., Seri, M., Galletta, L. J., Moran, O., Bulfone, A., Banfi, S., Pober, B., and Renieri, A. (1999). KCNE1-like gene is deleted in AMME contiguous gene syndrome: identification and characterization of the human and mouse homologs, *Genomics* *60*, 251-7.

Plaster, N. M., Tawil, R., Tristani-Firouzi, M., Canun, S., Bendahhou, S., Tsunoda, A., Donaldson, M. R., Iannaccone, S. T., Brunt, E., Barohn, R., *et al.* (2001). Mutations in  $K_{ir}2.1$  cause the developmental and episodic electrical phenotypes of Andersen's syndrome, *Cell* 105, 511-9.

Pongs, O. (1992). Molecular biology of voltage-dependent potassium channels, *Physiol Rev* 72, S69-88.

Pongs, O., Kecskemethy, N., Muller, R., Krah-Jentgens, I., Baumann, A., Kiltz, H. H., Canal, I., Llamazares, S., and Ferrus, A. (1988). Shaker encodes a family of putative potassium channel proteins in the nervous system of *Drosophila*, *Embo J* 7, 1087-96.

Raab-Graham, K. F., and Vandenberg, C. A. (1998). Tetrameric subunit structure of the native brain inwardly rectifying potassium channel  $K_{ir}2.2$ , *J Biol Chem* 273, 19699-707.

Rajan, S., Wischmeyer, E., Karschin, C., Preisig-Muller, R., Grzeschik, K. H., Daut, J., Karschin, A., and Derst, C. (2000a). THIK-1 and THIK-2, a novel subfamily of tandem pore domain  $K^+$  channels, *J Biol Chem* 1, 1.

Rajan, S., Wischmeyer, E., Xin Liu, G., Preisig-Muller, R., Daut, J., Karschin, A., and Derst, C. (2000b). TASK-3, a Novel Tandem Pore Domain Acid-sensitive  $K^+$  Channel. AN EXTRACELLULAR HISTIDINE AS pH SENSOR, *J Biol Chem* 275, 16650-16657.

Ramanathan, K., and Fuchs, P. A. (2002). Modeling hair cell tuning by expression gradients of potassium channel beta subunits, *Biophys J* 82, 64-75.

Ramanathan, K., Michael, T. H., Jiang, G. J., Hiel, H., and Fuchs, P. A. (1999). A molecular mechanism for electrical tuning of cochlear hair cells, *Science* 283, 215-7.

Rehm, H., and Lazdunski, M. (1988). Purification and subunit structure of a putative  $K^+$ -channel protein identified by its binding properties for dendrotoxin I, *Proc Natl Acad Sci U S A* 85, 4919-23.

Reid, P. F., Pongs, O., and Dolly, J. O. (1992). Cloning of a bovine voltage-gated K<sup>+</sup> channel gene utilising partial amino acid sequence of a dendrotoxin-binding protein from brain cortex, *FEBS Lett* *302*, 31-4.

Reimann, F., and Ashcroft, F. M. (1999). Inwardly rectifying potassium channels, *Curr Opin Cell Biol* *11*, 503-508.

Reiner, D. J., Newton, E. M., Tian, H., and Thomas, J. H. (1999). Diverse behavioural defects caused by mutations in *Caenorhabditis elegans unc-43* CaM kinase II, *Nature* *402*, 199-203.

Reiner, D. J., Weinshenker, D., and Thomas, J. H. (1995). Analysis of dominant mutations affecting muscle excitation in *Caenorhabditis elegans*, *Genetics* *141*, 961-976.

Rettig, J., Heinemann, S. H., Wunder, F., Lorra, C., Parcej, D. N., Dolly, J. O., and Pongs, O. (1994). Inactivation properties of voltage-gated K<sup>+</sup> channels altered by presence of beta-subunit, *Nature* *369*, 289-294.

Reyes, R., Duprat, F., Lesage, F., Fink, M., Salinas, M., Farman, N., and Lazdunski, M. (1998). Cloning and expression of a novel pH-sensitive two pore domain K<sup>+</sup> channel from human kidney, *J Biol Chem* *273*, 30863-30869.

Robbins, J. (2001). KCNQ potassium channels: physiology, pathophysiology, and pharmacology, *Pharmacol Ther* *90*, 1-19.

Romey, G., Attali, B., Chouabe, C., Abitbol, I., Guillemare, E., Barhanin, J., and Lazdunski, M. (1997). Molecular mechanism and functional significance of the MinK control of the K<sub>v</sub>LQT1 channel activity, *J Biol Chem* *272*, 16713-16716.

Ruppertsberg, J. P., Schroter, K. H., Sakmann, B., Stocker, M., Sewing, S., and Pongs, O. (1990). Heteromultimeric channels formed by rat brain potassium-channel proteins, *Nature* *345*, 535-7.

Ruth, P., Rohrkasten, A., Biel, M., Bosse, E., Regulla, S., Meyer, H. E., Flockerzi, V., and Hofmann, F. (1989). Primary structure of the beta subunit of the DHP-sensitive calcium channel from skeletal muscle, *Science* *245*, 1115-8.

Sah, P. (1996).  $Ca^{2+}$ -activated  $K^+$  currents in neurones: types, physiological roles and modulation, *Trends Neurosci* *19*, 150-4.

Sakura, H., Ammala, C., Smith, P. A., Gribble, F. M., and Ashcroft, F. M. (1995). Cloning and functional expression of the cDNA encoding a novel ATP-sensitive potassium channel subunit expressed in pancreatic beta-cells, brain, heart and skeletal muscle, *FEBS Lett* *377*, 338-44.

Salinas, M., de Weille, J., Guillemare, E., Lazdunski, M., and Hugnot, J. P. (1997a). Modes of regulation of shab  $K^+$  channel activity by the  $K_v8.1$  subunit, *J Biol Chem* *272*, 8774-80.

Salinas, M., Duprat, F., Heurteaux, C., Hugnot, J. P., and Lazdunski, M. (1997b). New modulatory alpha subunits for mammalian Shab  $K^+$  channels, *J Biol Chem* *272*, 24371-9.

Salinas, M., Reyes, R., Lesage, F., Fosset, M., Heurteaux, C., Romey, G., and Lazdunski, M. (1999). Cloning of a new mouse two-P domain channel subunit and a human homologue with a unique pore structure, *J Biol Chem* *274*, 11751-11760.

Sanguinetti, M. C., Curran, M. E., Zou, A., Shen, J., Spector, P. S., Atkinson, D. L., and Keating, M. T. (1996). Coassembly of  $K_vLQT1$  and minK(IsK) proteins to form cardiac  $I_{Ks}$  potassium channel, *Nature* *384*, 80-83.

Sanguinetti, M. C., Jiang, C., Curran, M. E., and Keating, M. T. (1995). A mechanistic link between an inherited and an acquired cardiac arrhythmia: HERG encodes the  $I_{Kr}$  potassium channel, *Cell* *81*, 299-307.

Sano, Y., Mochizuki, S., Miyake, A., Kitada, C., Inamura, K., Yokoi, H., Nozawa, K., Matsushime, H., and Furuichi, K. (2002). Molecular cloning and characterization of  $K_v6.3$ , a novel modulatory subunit for voltage-gated  $K^+$  channel  $K_v2.1$ , *FEBS Lett* *512*, 230-4.



Schreiber, M., and Salkoff, L. (1997). A novel calcium-sensing domain in the BK channel, *Biophys J* 73, 1355-63.

Schreiber, M., Wei, A., Yuan, A., Gaut, J., Saito, M., and Salkoff, L. (1998). Slo3, a novel pH-sensitive K<sup>+</sup> channel from mammalian spermatocytes, *J Biol Chem* 273, 3509-16.

Schroeder, B. C., Hechenberger, M., Weinreich, F., Kubisch, C., and Jentsch, T. J. (2000a). KCNQ5, a novel potassium channel broadly expressed in brain, mediates M-type currents, *J Biol Chem* 275, 24089-95.

Schroeder, B. C., Kubisch, C., Stein, V., and Jentsch, T. J. (1998). Moderate loss of function of cyclic-AMP-modulated KCNQ2/KCNQ3 K<sup>+</sup> channels causes epilepsy, *Nature* 396, 687-90.

Schroeder, B. C., Waldegger, S., Fehr, S., Bleich, M., Warth, R., Greger, R., and Jentsch, T. J. (2000b). A constitutively open potassium channel formed by KCNQ1 and KCNE3, *Nature* 403, 196-9.

Schumacher, M. A., Rivard, A. F., Bachinger, H. P., and Adelman, J. P. (2001). Structure of the gating domain of a Ca<sup>2+</sup>-activated K<sup>+</sup> channel complexed with Ca<sup>2+</sup>/calmodulin, *Nature* 410, 1120-4.

Scott, V. E., Rettig, J., Parcej, D. N., Keen, J. N., Findlay, J. B., Pongs, O., and Dolly, J. O. (1994). Primary structure of a beta subunit of alpha-dendrotoxin-sensitive K<sup>+</sup> channels from bovine brain, *Proc Natl Acad Sci U S A* 91, 1637-41.

Sewing, S., Roeper, J., and Pongs, O. (1996). K<sub>v</sub> beta 1 subunit binding specific for shaker-related potassium channel alpha subunits, *Neuron* 16, 455-63.

Shao, L. R., Halvorsrud, R., Borg-Graham, L., and Storm, J. F. (1999). The role of BK-type Ca<sup>2+</sup>-dependent K<sup>+</sup> channels in spike broadening during repetitive firing in rat hippocampal pyramidal cells, *J Physiol* 521 Pt 1, 135-46.

Shen, N. V., and Pfaffinger, P. J. (1995). Molecular recognition and assembly sequences involved in the subfamily-specific assembly of voltage-gated K<sup>+</sup> channel subunit proteins, *Neuron* 14, 625-33.

Sheng, M. (2001). Molecular organization of the postsynaptic specialization, *Proc Natl Acad Sci U S A* 98, 7058-61.

Sheng, M., Liao, Y. J., Jan, Y. N., and Jan, L. Y. (1993). Presynaptic A-current based on heteromultimeric K<sup>+</sup> channels detected *in vivo*, *Nature* 365, 72-5.

Shi, G., Nakahira, K., Hammond, S., Rhodes, K. J., Schechter, L. E., and Trimmer, J. S. (1996). Beta subunits promote K<sup>+</sup> channel surface expression through effects early in biosynthesis, *Neuron* 16, 843-852.

Sigworth, F. J., and Neher, E. (1980). Single Na<sup>+</sup> channel currents observed in cultured rat muscle cells, *Nature* 287, 447-9.

Singer-Lahat, D., Dascal, N., and Lotan, I. (1999). Modal behavior of the K<sub>v</sub>1.1 channel conferred by the K<sub>v</sub>beta1.1 subunit and its regulation by dephosphorylation of K<sub>v</sub>1.1, *Pflugers Arch* 439, 18-26.

Smart, S. L., Lopantsev, V., Zhang, C. L., Robbins, C. A., Wang, H., Chiu, S. Y., Schwartzkroin, P. A., Messing, A., and Tempel, B. L. (1998). Deletion of the K<sub>v</sub>1.1 potassium channel causes epilepsy in mice, *Neuron* 20, 809-19.

Smith, P. L., Baukrowitz, T., and Yellen, G. (1996). The inward rectification mechanism of the HERG cardiac potassium channel, *Nature* 379, 833-6.

Stern, M., and Ganetzky, B. (1989). Altered synaptic transmission in *Drosophila hyperkinetic* mutants, *J Neurogenet* 5, 215-228.

Stuhmer, W., Ruppersberg, J. P., Schroter, K. H., Sakmann, B., Stocker, M., Giese, K. P., Perschke, A., Baumann, A., and Pongs, O. (1989). Molecular basis of functional diversity of voltage-gated potassium channels in mammalian brain, *Embo J* 8, 3235-44.

Stuhmer, W., Stocker, M., Sakmann, B., Seeburg, P., Baumann, A., Grupe, A., and Pongs, O. (1988). Potassium channels expressed from rat brain cDNA have delayed rectifier properties, *FEBS Lett* 242, 199-206.

Tai, K. K., and Goldstein, S. A. (1998). The conduction pore of a cardiac potassium channel, *Nature* 391, 605-608.

Takumi, T., Moriyoshi, K., Aramori, I., Ishii, T., Oiki, S., Okada, Y., Ohkubo, H., and Nakanishi, S. (1991). Alteration of channel activities and gating by mutations of slow ISK potassium channel, *J Biol Chem* 266, 22192-8.

Takumi, T., Ohkubo, H., and Nakanishi, S. (1988). Cloning of a membrane protein that induces a slow voltage-gated potassium current, *Science* 242, 1042-5.

Talley, E. M., Lei, Q., Sirois, J. E., and Bayliss, D. A. (2000). TASK-1, a two-pore domain K<sup>+</sup> channel, is modulated by multiple neurotransmitters in motoneurons, *Neuron* 25, 399-410.

Tanabe, T., Takeshima, H., Mikami, A., Flockerzi, V., Takahashi, H., Kangawa, K., Kojima, M., Matsuo, H., Hirose, T., and Numa, S. (1987). Primary structure of the receptor for calcium channel blockers from skeletal muscle, *Nature* 328, 313-8.

Tanemoto, M., Fujita, A., Higashi, K., and Kurachi, Y. (2002). PSD-95 mediates formation of a functional homomeric K<sub>v</sub>5.1 channel in the brain, *Neuron* 34, 387-97.

Tapper, A. R., and George, A. L., Jr. (2000). MinK subdomains that mediate modulation of and association with K<sub>v</sub>LQT1, *J Gen Physiol* 116, 379-90.

Tapper, A. R., and George, A. L., Jr. (2001). Location and orientation of minK within the I<sub>Ks</sub> potassium channel complex, *J Biol Chem* 276, 38249-54.

Tempel, B. L., Jan, Y. N., and Jan, L. Y. (1988). Cloning of a probable potassium channel gene from mouse brain, *Nature* 332, 837-9.

Tempel, B. L., Papazian, D. M., Schwarz, T. L., Jan, Y. N., and Jan, L. Y. (1987). Sequence of a probable potassium channel component encoded at *Shaker* locus of *Drosophila*, *Science* 237, 770-5.

Thomas, P., Ye, Y., and Lightner, E. (1996). Mutation of the pancreatic islet inward rectifier  $K_{ir}6.2$  also leads to familial persistent hyperinsulinemic hypoglycemia of infancy, *Hum Mol Genet* 5, 1809-12.

Thomas, P. M., Cote, G. J., Wohlk, N., Haddad, B., Mathew, P. M., Rabl, W., Aguilar-Bryan, L., Gagel, R. F., and Bryan, J. (1995). Mutations in the sulfonylurea receptor gene in familial persistent hyperinsulinemic hypoglycemia of infancy, *Science* 268, 426-9.

Trent, T., Tsung, N., and Horvitz, H. R. (1983). Egg-laying defective mutants of the nematode *Caenorhabditis elegans*, *Genetics* 104, 619-647.

Tucker, S. J., Gribble, F. M., Proks, P., Trapp, S., Ryder, T. J., Haug, T., Reimann, F., and Ashcroft, F. M. (1998). Molecular determinants of  $K_{ATP}$  channel inhibition by ATP, *Embo J* 17, 3290-6.

Tucker, S. J., Gribble, F. M., Zhao, C., Trapp, S., and Ashcroft, F. M. (1997). Truncation of  $K_{ir}6.2$  produces ATP-sensitive  $K^+$  channels in the absence of the sulphonylurea receptor, *Nature* 387, 179-83.

Valverde, M. A., Rojas, P., Amigo, J., Cosmelli, D., Orio, P., Bahamonde, M. I., Mann, G. E., Vergara, C., and Latorre, R. (1999). Acute activation of Maxi-K channels (hSlo) by estradiol binding to the beta subunit, *Science* 285, 1929-31.

Wallner, M., Meera, P., and Toro, L. (1996). Determinant for beta-subunit regulation in high-conductance voltage-activated and  $Ca^{2+}$ -sensitive  $K^+$  channels: an additional transmembrane region at the N terminus, *Proc Natl Acad Sci USA* 93, 14922-14927.

Wallner, M., Meera, P., and Toro, L. (1999). Molecular basis of fast inactivation in voltage and  $Ca^{2+}$ -activated  $K^+$  channels: a transmembrane beta-subunit homolog, *Proc Natl Acad Sci U S A* 96, 4137-42.

- Wang, H., Kunkel, D. D., Martin, T. M., Schwartzkroin, P. A., and Tempel, B. L. (1993). Heteromultimeric K<sup>+</sup> channels in terminal and juxtaparanodal regions of neurons, *Nature* **365**, 75-9.
- Wang, H. S., Pan, Z., Shi, W., Brown, B. S., Wymore, R. S., Cohen, I. S., Dixon, J. E., and McKinnon, D. (1998a). KCNQ2 and KCNQ3 potassium channel subunits: molecular correlates of the M-channel, *Science* **282**, 1890-3.
- Wang, K. W., Tai, K. K., and Goldstein, S. A. (1996a). MinK residues line a potassium channel pore, *Neuron* **16**, 571-577.
- Wang, Q., Curran, M. E., Splawski, I., Burn, T. C., Millholland, J. M., VanRaay, T. J., Shen, J., Timothy, K. W., Vincent, G. M., de Jager, T., *et al.* (1996b). Positional cloning of a novel potassium channel gene: K<sub>v</sub>LQT1 mutations cause cardiac arrhythmias, *Nat Genet* **12**, 17-23.
- Wang, W., Xia, J., and Kass, R. S. (1998b). MinK-K<sub>v</sub>LQT1 fusion proteins, evidence for multiple stoichiometries of the assembled IsK channel, *J Biol Chem* **273**, 34069-74.
- Wang, Y. W., Ding, J. P., Xia, X. M., and Lingle, C. J. (2002). Consequences of the stoichiometry of Slo1 alpha and auxiliary beta subunits on functional properties of large-conductance Ca<sup>2+</sup>-activated K<sup>+</sup> channels, *J Neurosci* **22**, 1550-61.
- Wang, Z., Kunkel, M., Wei, A., Butler, A., and Salkoff, L. (1999). Genomic organization of nematode 4TM K<sup>+</sup> channels. In *Ann. N.Y. Acad. Sci.*, pp. 286-303.
- Wang, Z. W., Saifee, O., Nonet, M. L., and Salkoff, L. (2001). SLO-1 potassium channels control quantal content of neurotransmitter release at the *C. elegans* neuromuscular junction, *Neuron* **32**, 867-81.
- Warmke, J. W., and Ganetzky, B. (1994). A family of potassium channel genes related to eag in *Drosophila* and mammals, *Proc Natl Acad Sci U S A* **91**, 3438-42.
- Washburn, C. P., Sirois, J. E., Talley, E. M., Guyenet, P. G., and Bayliss, D. A. (2002). Serotonergic raphe neurons express TASK channel transcripts and a TASK-like pH- and halothane-sensitive K<sup>+</sup> conductance, *J Neurosci* **22**, 1256-65.

Wei, A., Jegla, T., and Salkoff, L. (1996). Eight potassium channel families revealed by the *C. elegans* genome project, *Neuropharmacology* 35, 805-829.

Weinshenker, D., Wei, A., Salkoff, L., and Thomas, J. H. (1999). Block of an ether-a-go-go-like K<sup>+</sup> channel by imipramine rescues *egl-2* excitation defects in *Caenorhabditis elegans*, *J Neurosci* 19, 9831-9840.

Wible, B. A., Tagliatela, M., Ficker, E., and Brown, A. M. (1994). Gating of inwardly rectifying K<sup>+</sup> channels localized to a single negatively charged residue, *Nature* 371, 246-9.

Wible, B. A., Yang, Q., Kuryshev, Y. A., Accili, E. A., and Brown, A. M. (1998). Cloning and expression of a novel K<sup>+</sup> channel regulatory protein, KChAP, *J Biol Chem* 273, 11745-11751.

Wilson, G. F., Wang, Z., Chouinard, S. W., Griffith, L. C., and Ganetzky, B. (1998). Interaction of the K channel beta subunit, Hyperkinetic, with eag family members, *J Biol Chem* 273, 6389-6394.

Xia, X. M., Ding, J. P., and Lingle, C. J. (1999). Molecular basis for the inactivation of Ca<sup>2+</sup>- and voltage-dependent BK channels in adrenal chromaffin cells and rat insulinoma tumor cells, *J Neurosci* 19, 5255-64.

Xia, X. M., Fakler, B., Rivard, A., Wayman, G., Johnson-Pais, T., Keen, J. E., Ishii, T., Hirschberg, B., Bond, C. T., Lutsenko, S., *et al.* (1998). Mechanism of calcium gating in small-conductance calcium-activated potassium channels, *Nature* 395, 503-7.

Xu, J., and Li, M. (1997). K<sub>v</sub>beta2 inhibits the K<sub>v</sub>beta1-mediated inactivation of K<sup>+</sup> channels in transfected mammalian cells, *J Biol Chem* 272, 11728-35.

Xu, J., Yu, W., Jan, Y. N., Jan, L. Y., and Li, M. (1995). Assembly of voltage-gated potassium channels. Conserved hydrophilic motifs determine subfamily-specific interactions between the alpha- subunits, *J Biol Chem* 270, 24761-8.

Xu, J., Yu, W., Wright, J. M., Raab, R. W., and Li, M. (1998). Distinct functional stoichiometry of potassium channel beta subunits, *Proc Natl Acad Sci U S A* *95*, 1846-51.

Yamada, M., Isomoto, S., Matsumoto, S., Kondo, C., Shindo, T., Horio, Y., and Kurachi, Y. (1997). Sulphonylurea receptor 2B and K<sub>v</sub>6.1 form a sulphonylurea-sensitive but ATP-insensitive K<sup>+</sup> channel, *J Physiol* *499*, 715-20.

Yang, J., Jan, Y. N., and Jan, L. Y. (1995). Determination of the subunit stoichiometry of an inwardly rectifying potassium channel, *Neuron* *15*, 1441-7.

Yao, W. D., and Wu, C. F. (1999). Auxiliary Hyperkinetic beta subunit of K<sup>+</sup> channels: regulation of firing properties and K<sup>+</sup> currents in *Drosophila* neurons, *J Neurophysiol* *81*, 2472-84.

Yellen, G. (1998). The moving parts of voltage-gated ion channels, *Q Rev Biophys* *31*, 239-295.

Yu, W., Xu, J., and Li, M. (1996). NAB domain is essential for the subunit assembly of both alpha-alpha and alpha-beta complexes of *shaker*-like potassium channels, *Neuron* *16*, 441-453.

Yuan, A., Dourado, M., Butler, A., Walton, N., Wei, A., and Salkoff, L. (2000). SLO-2, a K<sup>+</sup> channel with an unusual Cl<sup>-</sup> dependence, *Nat Neurosci* *3*, 771-9.

Zagotta, W. N., Hoshi, T., and Aldrich, R. W. (1990). Restoration of inactivation in mutants of *Shaker* potassium channels by a peptide derived from ShB, *Science* *250*, 568-71.

Zerangue, N., Schwappach, B., Jan, Y. N., and Jan, L. Y. (1999). A new ER trafficking signal regulates the subunit stoichiometry of plasma membrane K<sub>ATP</sub> channels, *Neuron* *22*, 537-48.

Zhang, B. M., Kohli, V., Adachi, R., Lopez, J. A., Udden, M. M., and Sullivan, R. (2001). Calmodulin binding to the C-terminus of the small-conductance Ca<sup>2+</sup>-activated K<sup>+</sup> channel hSK1 is affected by alternative splicing, *Biochemistry* *40*, 3189-95.

Figure 1. Illustrated Timeline of Significant Developments in the Areas of K<sup>+</sup> Channel and Channel Regulatory Subunit Research

**1952** – In landmark paper, Hodgkin and Huxley propose that the inward and outward currents observed during depolarization of squid axons were caused by changes in discrete Na<sup>+</sup> and K<sup>+</sup> conductances, each with their own time constants and dependence on membrane potential; this work conceptualized the existence of K<sup>+</sup>-selective channels (Hodgkin, 1952).

**1980** – Improvements in patch-clamp recordings allow observation of currents from a single channel (Sigworth and Neher, 1980; Hamill et al., 1981).

**1981** – A Na<sup>+</sup> channel from rat brain is purified by chromatography based on its affinity for the scorpion toxin saxotoxin and found to consist of two polypeptides, indicating that ion channels may be formed by multiple subunits. (Hartshorne and Catterall, 1981).

**1984** – The first voltage-ion channel, the sodium channel from *Electrophorus electricus*, is cloned. Analysis of its primary structure reveals four homologous repeating units, each with six TMDs. The fourth TMD in each subunit contains positive charges and is suspected (and later confirmed experimentally) to act as a voltage sensor (Noda et al., 1984).

**1987** – The first K<sup>+</sup> channel is cloned: the voltage-gated Shaker channel from *Drosophila*. (Kamb et al., 1987; Papazian et al., 1987; Tempel et al., 1987; Pongs et al., 1988). The predicted structure of Shaker resembles one of the four repeats within the Na<sup>+</sup> channel, suggesting that the functional channel is a tetramer. The molecular identification allowed structure-function relationships through mutagenesis to be explored, enabled the study of channels in heterologous systems and facilitated the cloning of other K<sup>+</sup> channels through homology-based approaches.

**1987** – The first voltage-gated Ca<sup>2+</sup> channel is cloned and found to have a similar structure as the Na<sup>+</sup> channel (Tanabe et al., 1987).



**1988** – The first K<sup>+</sup> channel regulatory subunit is cloned from rat kidney mRNA (Takumi et al., 1988). For years minK was believed to encode a K<sup>+</sup> channel, as its expression in *Xenopus* oocytes resulted in K<sup>+</sup> selective currents. Later it was found to be a channel regulatory subunit (Barhanin et al., 1996; Sanguinetti et al., 1996) that when expressed in *Xenopus* oocytes activated an electrically silent endogenous channel.

**1988-9** – The four regulatory subunits of the voltage-gated Ca<sup>2+</sup> channel are cloned, representing the first regulatory subunits of any voltage-gated channel; beta subunit (Ruth et al., 1989); gamma subunit (Jay et al., 1990); alpha 1 and alpha 2/delta (Ellis et al., 1988).

**1988** – The dendrotoxin sensitive K<sup>+</sup> channel is purified from rat brain and found to consist of two polypeptides. This suggested that K<sup>+</sup> channels, like Na<sup>+</sup> and Ca<sup>2+</sup> channels, might also be regulated by subunits (Rehm and Lazdunski, 1988).

**1990** – The first voltage-gated Cl<sup>-</sup> channel is cloned, from *Torpedo marmorata*, and shown to produce Cl<sup>-</sup> currents when expressed in *Xenopus* oocytes (Jentsch et al., 1990).

**1994** – The first K<sup>+</sup> channel subunits (K<sub>v</sub>β1 and K<sub>v</sub>β2) are cloned by purification, proteolysis, sequencing, and degenerate PCR from cDNAs (Rettig et al., 1994; Scott et al., 1994). K<sub>v</sub>β1 is shown to modulate the inactivation properties of Shaker-like channels (Rettig et al., 1994).

**1995** – Yeast TOK-1 K<sup>+</sup> channel is cloned by analysis of genomic sequence. TOK1 defines a new structural family having eight transmembrane domains and two-pore domains (Ketchum et al., 1995). Although no additional K<sup>+</sup> channels with this unusual structure have been identified from any other organism, identification of TOK1 illustrated the structural diversity of K<sup>+</sup> channels and underscored the power of genomics for identification of new channels.

**1996** – The first human two-pore channel (TWIK-1) is cloned through EST database searches for cDNAs encoding proteins with K<sup>+</sup> channel P-domains (Lesage et al., 1996a). TWIK-1 generates background or “leak” currents with little voltage sensitivity.

**1998** – The completed sequence of the *C. elegans* genome reveals the first full set of K<sup>+</sup> channels in a metazoan (Consortium, 1998). *C. elegans* channels include members from all mammalian families, with an expansion of the two-pore family (Bargmann, 1998).

**1998** – In landmark study, the crystal structure of the bacterial KcsA 2TMD/1P channel is solved, marking the post-structural age of K<sup>+</sup> channel research (Doyle et al., 1998). The structure of KcsA resembles an inverted “teepee” with the gate located at the narrowest point where the helices cross. Backbone carbonyl groups are found to line multiple ion binding sites.

**1999** – The crystal structure of a K<sup>+</sup> channel regulatory subunit (K<sub>v</sub>β2) is solved (Gulbis et al., 1999). The oxidoreductase structure is confirmed suggesting possible metabolic coupling between channel and enzymatic activity. This structure also preceded the structure of the K<sub>v</sub>β2 subunit bound to the intracellular T1 domain of the Shaker channel (Gulbis et al., 2000).

**Figure 1**

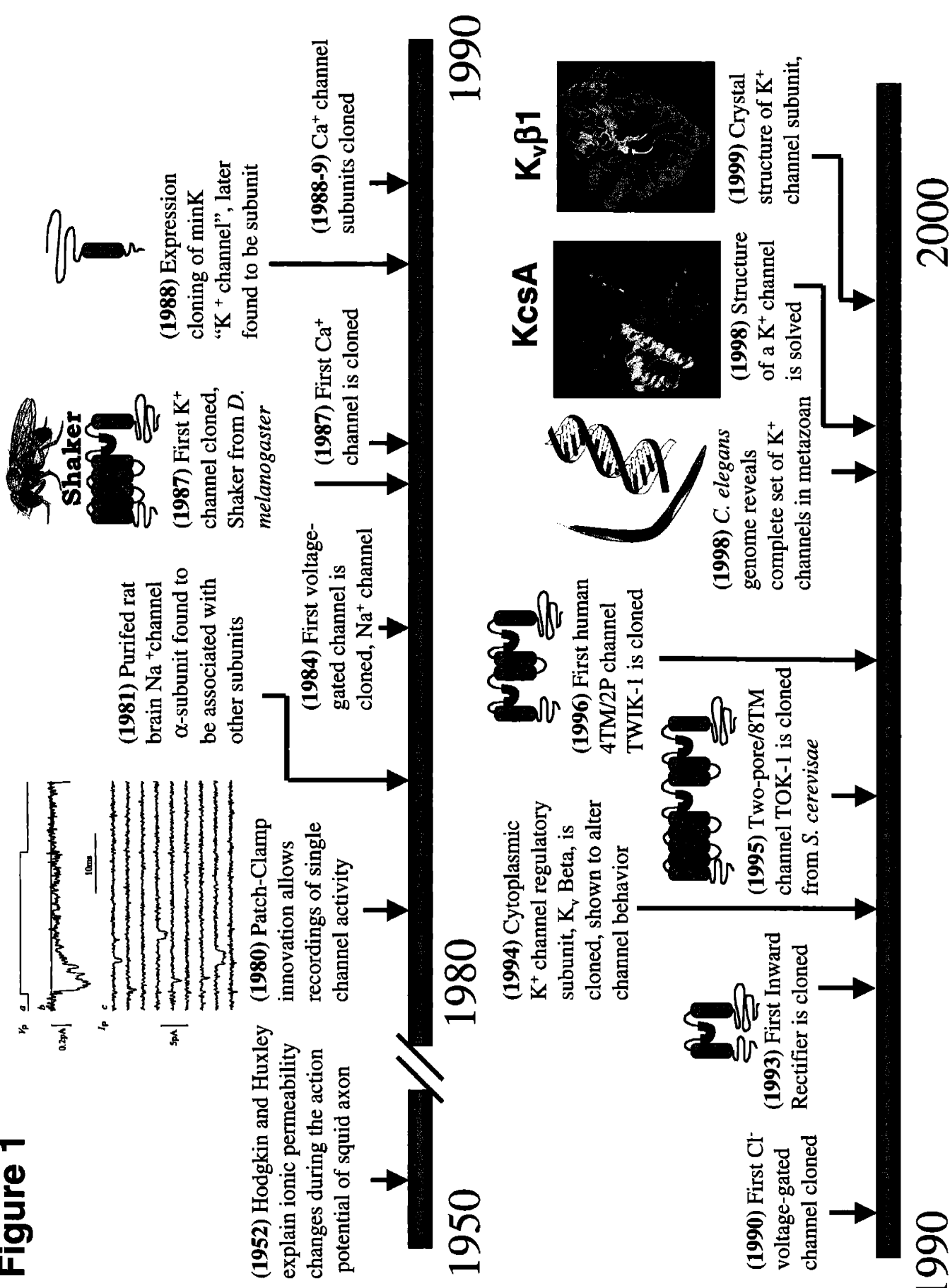
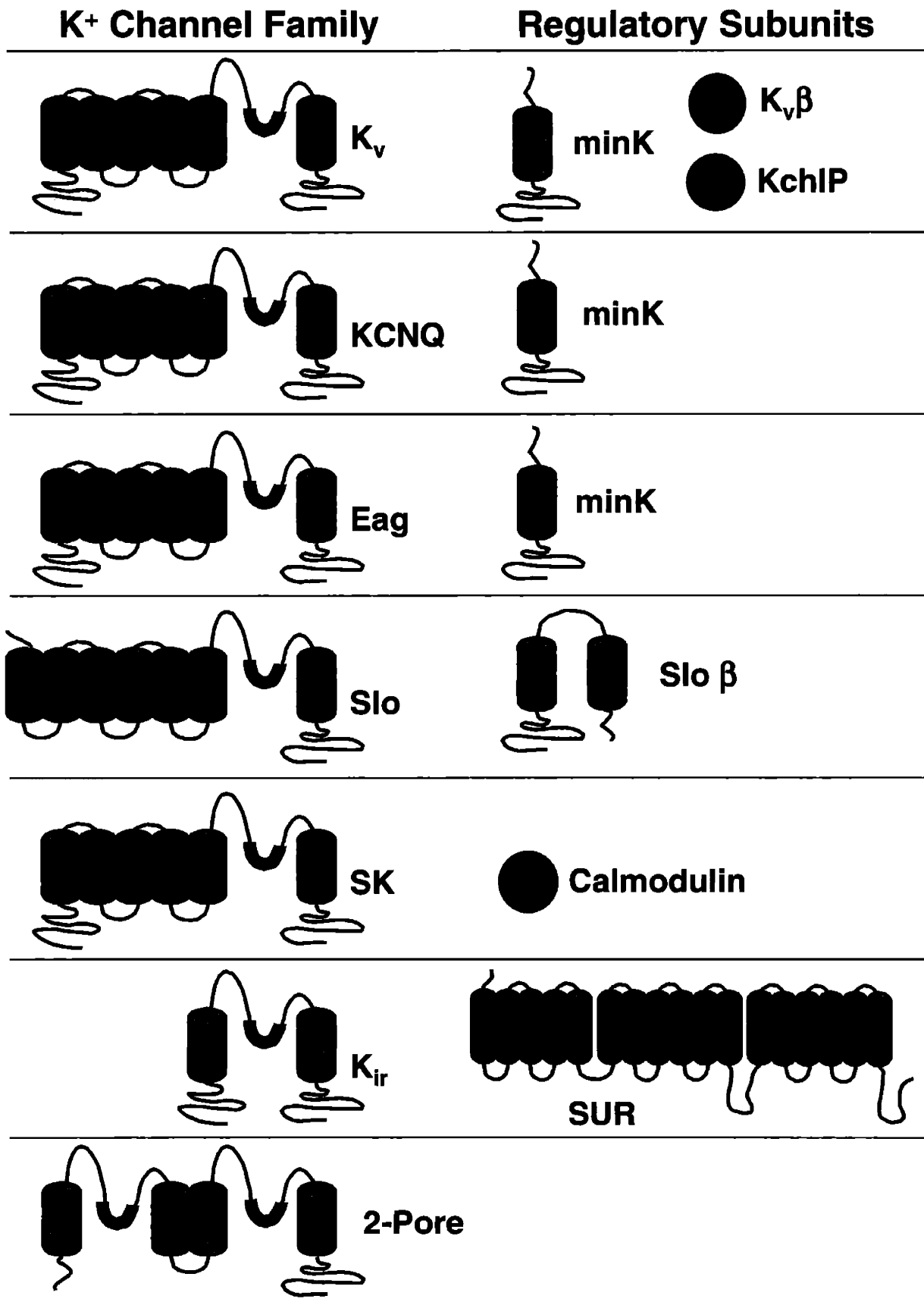


**Figure 2. Human K<sup>+</sup> Channel Families and their Associated Regulatory Subunits**

Representative membrane structure of K<sup>+</sup> channels (left) and their associated subunits (right). Cylinder, TMD; thick black line, P-Domain; circles, cytoplasmic protein.

**Figure 2**



## CHAPTER TWO

### ***sup-9* and *unc-93* May Encode Components of a Two-Pore K<sup>+</sup> Channel Required to Coordinate Muscle Contraction in *C. elegans***

Ignacio Perez de la Cruz and H. Robert Horvitz

(For submission to Neuron)

## Summary

Genetic studies of *sup-9*, *unc-93*, and *sup-10* suggest that these genes encode components of a multi-subunit protein complex that coordinates muscle contraction in *Caenorhabditis elegans*. Gain-of-function (gf) mutations in *sup-9*, *unc-93* or *sup-10* result in a relaxed body posture and a "rubberband" behavioral phenotype. We cloned *sup-9* and found that it encodes a two-pore K<sup>+</sup> channel. Pharmacologically hyperpolarizing muscle in wild-type animals caused a rubberband phenotype, suggesting these gf mutations abnormally open K<sup>+</sup> channels, leading to K<sup>+</sup> efflux and muscle hyperpolarization. All four *sup-9(gf)* alleles cause an alanine-236-threonine substitution in the fourth transmembrane domain. Mutations that suppress this A236T mutation cause amino acid substitutions in the third transmembrane domain, suggesting that interactions between the third and fourth transmembrane domains may be important in channel gating. We found that SUP-9 and UNC-93 were expressed in and function in muscle. UNC-93 co-localized with SUP-9 within muscle cells, consistent with the hypothesis that UNC-93 may be a regulatory subunit of a SUP-9 K<sup>+</sup> channel. UNC-93 is a member of a novel multi-gene family, which is conserved among *C. elegans*, *Drosophila* and humans. We propose that that SUP-9 and other two-pore K<sup>+</sup> channels function as multiprotein complexes and that UNC-93 defines a new class of channel regulatory proteins.

## Introduction

The activities of excitable cells are regulated by ion channels (Hille, 1992). Genetic analyses of *Caenorhabditis elegans* provides one approach towards the identification of genes important for distinct aspects of cell excitability, as mutants defective in neuronal and muscle function can be viable and are readily isolated (Brenner, 1974; Waterston et al., 1980; Trent et al., 1983). The *C. elegans* genome project has identified over 80 K<sup>+</sup> channels, approximately 50 of which belong to the two-pore structural class of background or “leak” channels (Wei et al., 1996; Bargmann, 1998). Mutations in several *C. elegans* voltage-gated K<sup>+</sup> channels have been characterized. These include the K<sub>v</sub> channels *exp-2* (Davis et al., 1999; Fleischhauer et al., 2000) and *egl-36* (Elkes et al., 1997; Johnstone et al., 1997), the HERG channels *egl-2* (Weinshenker et al., 1999) and *unc-103* (Reiner et al., 1999) and the large-conductance Ca<sup>2+</sup>-activated channel *slo-1* (Wang et al., 2001; Yuan et al., 2000). While two-pore channels comprise the largest family of K<sup>+</sup> channels, only one mutant in this family, *twk-18*, has been reported (Kunkel et al., 2000). Gf mutations in *twk-18* result in a muscle paralysis. TWK-18 gf channels conduct up to 30-fold larger K<sup>+</sup> currents than wild-type channels when expressed heterologously in *Xenopus* oocytes (Kunkel et al., 2000).

The *sup-9*, *sup-10*, and *unc-93* genes of *C. elegans* can affect the regulation of muscle contraction. Mutants carrying semidominant gf mutations in *sup-9*, *unc-93*, or *sup-10* move sluggishly, are defective in egg-laying and defecation, and display a rubberband uncoordinated (Unc) response when prodded on the head, a mutant worm contracts and then relaxes along its entire body without moving backwards, while a wild-type worm contracts its anterior end and moves away (Greenwald and Horvitz, 1980, 1986; Levin and Horvitz, 1993; Reiner et al., 1995). This behavior suggests that although capable of muscle contraction, these mutants are unable to mount a coordinated muscle response. By contrast, mutants defective in muscle structural genes are defective in muscle contraction (Waterston et al., 1980). Unlike wild-type animals, *sup-9(gf)*, *sup-10(gf)* and *unc-93(gf)* mutant animals are not stimulated to lay eggs in response to serotonin, which is believed to act on the egg-laying muscles, suggesting that the defect in these mutants is in their musculature (Trent et al., 1983, Reiner et al., 1995). Furthermore, mosaic analysis of *sup-10* indicates that it functions in muscle (Herman, 1984).

Genetic suppression screens revealed that lf mutations in any *sup-9*, *sup-10* or *unc-93* suppress the rubberband phenotype caused by gf mutations any of these three



genes (Greenwald and Horvitz, 1980, 1986; Levin and Horvitz, 1993). This mutual suppression indicates that these three genes act genetically at the same step. Worms with *lf* mutations in *sup-9*, *sup-10* or *unc-93* display no gross phenotypic abnormalities, suggesting that these genes have nonessential functions and may act in parallel to another gene or set of genes (Greenwald and Horvitz, 1980). Genetic studies exploring the interactions among *gf*, partial *lf*, and *lf* alleles of these three genes support a model in which the *sup-9*, *sup-10* and *unc-93* gene products physically interact (Greenwald and Horvitz, 1980, 1982; De Stasio et al., 1997; Levin and Horvitz, 1992).

A fourth gene, *sup-18*, was identified as a *lf* suppressor of the *sup-10(gf)* rubberband *Unc* phenotype and shown to be a partial suppressor of *sup-9(gf)* and *unc-93(gf)* rubberband *Unc* mutants (Greenwald and Horvitz, 1986). *sup-18* may encode a component, regulator or effector of a SUP-9/SUP-10/ UNC-93 complex.

*unc-93* encodes a novel, putative multi-pass transmembrane protein of unknown biochemical function (Levin and Horvitz, 1992). Here we report that *sup-9* encodes a two-pore K<sup>+</sup> channel with similarity to hTASK-1 and hTASK-3. TASK-1 and TASK-3 form a subfamily of two-pore channels that are activated by high pH (Kim et al., 2000; Lopes et al., 2001; Rajan et al., 2000), volatile anesthetic such as halothane and by neurotransmitters (Patel et al., 1999; Meadows and Randall, 2001; Czirjak and Enyedi, 2002; Talley and Bayliss, 2002). Our findings suggest that UNC-93 and SUP-10 act as regulatory subunits that associate with and modulate the activity of a SUP-9 K<sup>+</sup> channel.

## Results

### Molecular Cloning of *sup-9*

We cloned *sup-9* using transposon tagging. *sup-9(n1428)* was previously isolated as a suppressor of the dominant rubberband Unc phenotype caused by the *unc-93(e1500)* *gf* allele in the mutagenic *mut-2* background, where the spontaneous excision and transposition of the mariner-type transposable element Tc1 is greatly increased (Levin and Horvitz, 1992). We isolated a Tc1 insertion within the first exon of predicted gene F34D6.3 associated with the *sup-9(n1428)* mutation (See Experimental Procedures). To determine if F34D6.3 corresponded to *sup-9*, we performed transformation rescue experiments. As *sup-9(lf)* mutants have a wild-type phenotype, they cannot be used to assay *sup-9* wild-type activity. Instead, we used *sup-9(lf);sup-10(gf)* mutant, in which the *sup-10(gf)* Unc phenotype is suppressed by the *sup-9(lf)* mutation; this suppression can be eliminated by the addition of *sup-9* wild-type activity. Cosmid F19E8 as well as a 6.8 kb subclone of F19E8 containing the predicted gene F34D6.3 restored *sup-9* activity as transgenes in *sup-9(n180); sup-10(n983)* animals (Figure 1A).

### *sup-9* Encodes a Two-pore K<sup>+</sup> Channel

The *sup-9* minimal rescuing fragment contains a single complete predicted gene. Using RT-PCR and 5' and 3' Rapid Amplification of cDNA Ends (RACE) (Frohman et al., 1988), we cloned a full-length *sup-9* cDNA (Figure 1B). We found no evidence of alternative splicing or SL1/SL2 *trans*-splicing, which generates the 5' ends of some *C. elegans* transcripts (Krause and Hirsh, 1987). *sup-9* encodes a predicted protein of 329 amino acids with sequence similarity to the TASK subfamily of two-pore K<sup>+</sup> channels (Figure 1C). SUP-9 is 49 to 51% identical in amino acid sequence to human TASK-1 and TASK-3 and to two predicted *Drosophila* proteins. Human TASK-1 and TASK-3 behave as pH-sensitive background K<sup>+</sup> channels when expressed heterologously in mammalian cell lines (Duprat et al., 1997; Kim et al., 1998, 2000; Leonoudakis et al., 1998; Rajan et al., 2000b). Other human two-pore K<sup>+</sup> channels, such as TREK-1, share less than 30% amino acid identity with SUP-9. TWK-4 encodes the closest *C. elegans* homolog of SUP-9, with 42% amino acid identity, while other *C. elegans* two-pore K<sup>+</sup> channels share 25% or less amino acid identity, suggesting that SUP-9 and TWK-4 define a TASK-like subfamily of two-pore channels in *C. elegans*. Most of the amino acid identities among SUP-9 and the human TASK channels are restricted to the P domains, highly conserved loops that determine the ion selectivity of K<sup>+</sup> channels

(Heginbotham et al., 1994), and to the first, second, and fourth transmembrane domains, while the C-terminal tail and third transmembrane domain are poorly conserved.

### **Characterization of *sup-9* Mutant Alleles**

Suppressors of the rubberband Unc phenotypes of *sup-9*, *unc-93*, and *sup-10* *gf* mutants have defined many *sup-9* *lf* alleles. We have determined the sequences of the open reading frame and intron-exon boundaries of *sup-9* from 81 strains carrying *lf* mutations (Table 1). These mutations include 47 missense, 15 nonsense and 11 splice-site mutations as well as 3 deletions, one three base pair insertion and one Tc1 insertion. We did not find molecular lesions in three *sup-9* mutants; these alleles may contain mutations in the promoter region or in other regulatory elements not contained within the *sup-9* exons.

The identified *sup-9* missense mutations include lesions in all four transmembrane domains, the M1-P1 linker, which joins the first transmembrane domain and the first P domain, and both P domains. *sup-9(n2282)* encodes an isoleucine instead of the initiator methionine and thus is likely to be a null allele. Most of the missense mutations affecting the transmembrane domains result in the introduction of a charged amino, i.e. G22E, G106E, G106R, F109S, P119S, G121R, W165R, G172R, G172E, G173R, G230E, G230R and S235F.

The mutations V41A, V44E, D58V, I61S and A74V cause changes in the M1-P1 linker, which in the human TWIK-1 two-pore channel has been shown to act as a dimerization domain *in vitro* (Lesage et al., 1996b). Several mutations are found within the highly-conserved P domains, such as T195I. In the Shaker voltage-gated K<sup>+</sup> channel, the equivalent threonine in the P domain when mutated to alanine or valine (but not to serine) leads to the formation of channels that do not conduct currents when expressed in *Xenopus* oocytes (Heginbotham et al., 1994). A mutation in the Shaker channel similar to the *sup-9* mutation G202S results in nonselective channels that are equally permeable to K<sup>+</sup> and Na<sup>+</sup> (Heginbotham et al., 1994). Such a channel may cause a loss of function, since the charge carried by K<sup>+</sup> ions leaving the cell may be neutralized by Na<sup>+</sup> ions entering the cell.

No single *sup-9(lf)* missense mutations were located within the C-terminal cytoplasmic tail, suggesting that this region of SUP-9 may be dispensable for *in vivo* function. Similarly, no nonsense mutations leading to a truncation of only the C-terminal

domain were identified. *sup-9(n1028)* contains two point mutations, one in the second splice-donor site and the other causing a D278N substitution within the C-terminal domain. We suspect that the splice defect and not the missense mutation is responsible for the loss of function caused by this allele.

The *sup-9(n1550)* *gf* allele that leads to the rubberband Unc phenotype causes an A236T substitution in the fourth transmembrane domain. We determined the sequences of three additional independently isolated *sup-9* *gf* alleles. All three, *e2655*, *e2661*, and *n3310*, contain the same nucleotide change and therefore cause the same A236T substitution (Table 2).

The partial *lf* alleles *n2539*, *n2360*, *n2361* and *n2288*, which were isolated as suppressors of *sup-9(n1550)* (Levin and Horvitz, 1993), contain second-site mutations in addition to the A236T *sup-9 (n1550)* substitution (Table 2). *sup-9(n1550 n2360)* mutants do not display the rubberband Unc phenotype of *sup-9(n1550)* animals but rather appear wildtype. However, unlike both *sup-9(+)* and *sup-9(o)*, *sup-9(n1550 n2360)* partially suppresses the *sup-10(gf)* mutant phenotype, indicating that this allele is neither completely wild-type nor null. The *n2360* and *n2361* alleles contain a point mutation in the same codon mutated in *n1550* animals, leading to a substitution of methionine in place of the wild-type alanine and the *n1550* threonine, suggesting that it is the presence of a threonine at position 236 rather than the absence of an alanine that is responsible for the altered activity of the *sup-9(gf)* alleles. Two other partial *lf* alleles, *sup-9(n1550 n2288)* and *sup-9(n1550 n2359)*, contain missense mutations affecting the third transmembrane domain, G173E and A174T, respectively. These amino acid changes may suppress the *sup-9(n1550)* phenotype by altering an interaction between the third transmembrane domain and the mutant threonine in the fourth transmembrane domain.

### ***sup-9::gfp* Is Expressed in Muscles and a Subset of Neurons**

To study the expression of *sup-9* we constructed a translational fusion of SUP-9 to the Green Fluorescent Protein (GFP). This fusion included 2.9 kb of *sup-9* upstream promoter sequence and 0.8 kb of *sup-9* downstream sequence (see Experimental Procedures). When expressed in a *sup-9(lf); unc-93(gf)* mutant, the *sup-9::gfp* reporter could restore the rubberband Unc phenotype caused by an *unc-93(gf)* allele, indicating that this reporter fusion protein is functional.

We observed SUP-9::GFP expression along the surface of body-wall muscle cells, with a punctate stripe pattern characteristic of dense bodies (Figure 2A), structures functionally analogous to vertebrate Z-lines which connect the myofibril lattice to the cell membrane (Waterston et al., 1980). Additional staining was observed in muscle arms, which project from the muscle body toward neurons to form synapses (data not shown). The body-wall muscle staining became apparent at the 3.5-fold stage of embryogenesis, was most apparent in late embryos and L1 stage larvae and persisted to adulthood. All eight vulval muscles and the intestinal muscles also displayed GFP fluorescence (Figures 2B and C), consistent with the egg-laying and defecation defects of *sup-9(gf)* mutants. We observed weaker fluorescence in the anal depressor and anal sphincter muscles (data not shown). We also observed GFP expression in 12 to 15 head neurons in each animal (Figure 2D and data not shown) including the SIADL, SIADR, SIAVL, and SIAVR neurons (See experimental procedures).

To determine if the tissue and subcellular localization of SUP-9 is dependent on UNC-93, SUP-10 or SUP-18, we examined the expression of the *sup-9::gfp* reporter in *unc-93(lr12)*, *sup-10(n1008)* and *sup-18(n1030)* If mutants, all likely null alleles (De Stasio et al., 1997, and I.P and H.R.H., unpublished results). We found SUP-9::GFP was expressed and localized as in the wild-type background in all three mutants (data not shown), indicating that the SUP-9 K<sup>+</sup> channel can localize properly in the absence UNC-93, SUP-10 or SUP-18.

### ***unc-93::gfp* Is Expressed in Muscles and a Subset of Neurons**

To study the expression of *unc-93*, we created transgenic lines carrying an *unc-93::gfp* reporter containing 5.3 kb of *unc-93* upstream sequence, the entire *unc-93* coding region, and the *gfp* coding region fused just prior to the stop codon of *unc-93*. This construct restored the rubberband Unc phenotype caused by a *sup-10(gf)* mutation in an *unc-93(n234); sup-10(n983)* mutant, indicating that the fusion protein was functional. We found GFP expression in the body-wall muscle membranes and dense bodies (Figure 2E), as well as in all eight vulval and intestinal muscles (Figures 2F and G). As with the *sup-9::gfp* fusion, the *unc-93::gfp* fusion resulted in GFP expression (Figure 2H and data not shown), including the SIADL, SIADR, SIAVL, and SIAVR neurons. We tested the expression of this reporter in a *sup-9(n1913)* null background and found that the localization of UNC-93::GFP remained unchanged (data not shown).

### ***sup-9* and *unc-93* Function in Muscles**

Since the *sup-9::gfp* fusion was expressed in both neurons and muscle, we performed expression experiments to determine the site of action of *sup-9*. We overexpressed the *sup-9* cDNA under the *myo-3* muscle-specific promoter, which expresses in all non-pharyngeal muscle groups (Okkema et al., 1993). We tested if the *myo-3::sup-9* transgene was capable of restoring the sluggish movement and rubberband Unc phenotype of an *unc-93(gf)* allele in a *sup-9(lf); unc-93(gf)* mutant. We found that *sup-9(n1913); unc-93(e1500)* transgenic lines expressing SUP-9 in muscle exhibited a reduced locomotory rate compared to control transgenic lines expressing only GFP (Figure 3A). The rubberband Unc response was also restored to these lines but not to control lines expressing only GFP (data not shown). The reduction of locomotory rate by *sup-9* overexpression in muscle was not caused by a nonspecific effect of transgene overexpression but rather to an interaction between *sup-9* and *unc-93(gf)* since the *myo-3::sup-9* transgene in an *unc-93(+)* background did not cause a reduced locomotory rate (Figure 3B). In addition to displaying sluggish movement, *unc-93(gf)* animals are unable to lay eggs and instead form bags of worms as embryos hatch inside the parent (Greenwald and Horvitz, 1980). This phenotype is also suppressed by *sup-9(lf)* alleles. We assayed the *myo-3::sup-9* transgenic lines for restoration of the egg-laying defect of *unc-93(e1500)* animals and found that *sup-9* overexpression in muscle restored the egg-laying defect to a *sup-9(lf); unc-93(gf)* strain compared to *myo-3::gfp* control transgenic animals (Table 3).

By contrast, expression of *sup-9* under the control of the neuronal-specific *unc-76* promoter (Bloom and Horvitz, 1997) restored neither the locomotory nor the egg-laying defects to a *sup-9(lf); unc-93(gf)* mutant (Figure 3A; Table 3). These results together suggest that the *sup-9* channel functions in muscles to regulate locomotion and egg laying.

In similar experiments, we tested if *unc-93* expression in muscle would restore the *sup-10(gf)* phenotype to a *sup-9(gf); unc-93(lf)* mutant. Lines transgenic for *myo-3::unc-93* but not for *unc-76::unc-93* showed a severe locomotory defect as compared to control *myo-3::gfp* animals (Figure 3C and D), indicating that *unc-93* expression in muscle can result in a *sup-9(gf)* phenotype. Likewise, these lines formed bags of worms at a much higher frequency than did *myo-3::gfp* or *unc-76::gfp* transgenic animals (Table 3), suggesting that *unc-93* expression in vulval muscles is sufficient to

account for the egg-laying defect. We conclude that *unc-93*, like *sup-9*, functions in muscle cells.

### **SUP-9 and UNC-93 Colocalize Intracellularly**

If *sup-9* and *unc-93* encode components of a multisubunit K<sup>+</sup> channel complex, we expect them to colocalize within muscle membranes *in vivo*. To test for colocalization, we generated rabbit antibodies against SUP-9. Although these antibodies did not allow us to detect endogenous SUP-9 in whole-mount stainings of wild-type worms (I.P and H.R.H., unpublished observations), likely because of low expression, the antibodies yielded specific staining in transgenic worms overexpressing SUP-9 under the *myo-3* promoter (Figure 4A). Double-label whole-mount stainings of fixed worms with anti-SUP-9 and anti-GFP sera revealed an identical muscle membrane distributions of SUP-9 and UNC-93::GFP (Figure 4A). These proteins colocalized both to the dense bodies and more diffusely throughout the cell surface.

To test if the colocalization between SUP-9 and UNC-93::GFP was the result of overexpressing these proteins, we compared the localization of SUP-9 with that of PAT-3, an integrin beta subunit that is a structural component of dense bodies (Gettner et al., 1995). We found that although both SUP-9 and PAT-3::GFP were localized to dense bodies, their distribution patterns were only partially superimposable. Unlike PAT-3::GFP, SUP-9 was present in the spaces between adjacent dense bodies, was weakly diffused throughout the muscle membrane and was mainly excluded from the M-lines (Figure 4B).

Some muscle cells contained brightly-stainings clusters of SUP-9 protein, which may represent mislocalized protein resulting from overexpression. UNC-93::GFP co-segregated with SUP-9 in these clusters (Figure 4C), while PAT-3::GFP displayed a more diffuse staining near these clusters (Figure 4D). This result is consistent with the hypothesis that UNC-93, but not PAT-3, interacts with SUP-9 *in vivo*.

### **Muscimol Can Phenocopy the Rubberband Unc Phenotype**

We hypothesized that the rubberband Unc phenotype of *sup-9(gf)* and *unc-93(gf)* animals may be caused by an inappropriately open K<sup>+</sup> channel. Increased K<sup>+</sup> efflux from muscle would lead to an accumulation of negative charge inside the cell and could result in membrane hyperpolarization and reduced muscle contraction.

Electrophysiological patch-clamp recordings of *C. elegans* muscles reveal that

treatment of body-wall muscle cells with muscimol, a GABA Cl<sup>-</sup> channel agonist, leads to hyperpolarization by an inward Cl<sup>-</sup> flux that is dependent on the GABA receptor channel UNC-49 (Richmond and Jorgensen, 1999). We tested if pharmacologically hyperpolarizing the muscles of wild-type worms would result in a rubberband Unc phenotype similar to that of *sup-9(gf)*, *sup-10(gf)* or *unc-93(gf)* mutants.

Worms treated with muscimol displayed a rubberband Unc response in a concentration-dependent manner (Figure 5A). Saturation of the rubberband response was reached at a concentration of 2.5 mM muscimol (data not shown). The responses of wild-type animals at high drug concentrations resembled those of the strong *sup-9(n1550)* and *unc-93(e1500)* mutants, while lower doses resembled those of the weaker *sup-10(n983)* and *unc-93(n200)* mutants (Figure 5B). Additionally, worms treated with muscimol displayed uncoordinated movement and flaccid, extended body postures similar to those of the *sup-9(gf)* and *unc-93(gf)* mutants (data not shown).

We tested if *sup-9*, *unc-93*, *sup-10* or *sup-18* were required for the rubberband Unc response caused by muscimol. Worms carrying *lf* mutations in these genes all displayed the rubberband Unc response (Figure 6A). *sup-10(lf)* mutants were more sensitive to muscimol compared to wild-type animals. We presently cannot explain this extra sensitivity of *sup-10(lf)* mutants to muscimol, but it may be due to altered channel activity in the absence of a missing subunit. Nevertheless, these results establish that muscimol induces the rubberband response by a mechanism that is independent of *sup-9*, *unc-93*, *sup-10* and *sup-18*.

We tested if the effects of the rubberband Unc mutations and those induced by muscimol are additive. While *unc-93(n200)* mutants displayed a weak rubberband Unc response and wild-type worms in 1 mM muscimol displayed a strong rubberband Unc phenotype, treatment of *unc-93(n200)* worms with 1 mM muscimol resulted in a severe rubberband Unc phenotype similar to that observed at saturating concentrations of muscimol (Figure 6B). Likewise, a *sup-9(gf)/+* mutant in 1 mM muscimol displays a more severe rubberband Unc response than in the absence of drug and more severe than that of wild-type worms in the presence of 1 mM drug. A similar effect was seen for *sup-10(gf)* mutants (data not shown). We propose that an increase in K<sup>+</sup> conductance caused by *sup-9(gf)*, *sup-10(gf)* or *unc-93(gf)* sensitizes muscle cells to the hyperpolarizing effects of muscimol.



### ***unc-93* Belongs to a Large *C. elegans* Gene Family and Is Conserved in Flies and Mammals**

We searched the *C. elegans* genome for predicted genes with sequence similarities to UNC-93. We found that UNC-93 defines a family of 17 worm genes, of which UNC-93 is a relatively divergent member (Figure 7). UNC-93 contains a highly charged 245 amino acid N-terminal domain followed by 5-10 putative transmembrane domains (Levin and Horvitz, 1992). This N-terminal domain is unique to UNC-93 and appears not to be conserved in the other *C. elegans* members of this family.

In addition, by searching nucleotide and protein databases we identified four *Drosophila melanogaster*, three mouse, and three human genes with predicted products with sequence similarity to UNC-93 (Figure 7). Three pairs of mouse and human genes are likely orthologs as they are more closely related to each other than to other UNC-93-like genes in their respective species. While UNC-93 and the *Drosophila* and mammalian UNC-93-like genes cluster phylogenetically, mouse ET8 and human ET22 are more closely similar to the *C. elegans* predicted gene C27C12.4 than to UNC-93. Of the UNC-93-like genes, the human predicted gene 366N23.1/.2 is the most similar to UNC-93, sharing 30% amino acid identity. The existence of UNC-93-like genes in other organisms suggests that regulation of two-pore K<sup>+</sup> channels by regulatory subunits may be a common mechanism.

## Discussion

Although two-pore K<sup>+</sup> channels define the largest family of K<sup>+</sup> channels in *C. elegans*, little is known about the expression, regulation and *in vivo* function. The *C. elegans* gene *sup-9* encodes a two-pore K<sup>+</sup> channel similar to the mammalian TASK-1 and TASK-3 channels. To initiate structure-function studies of a two-pore K<sup>+</sup> channel, we determined the molecular lesions of 86 *sup-9* mutants. *sup-9* and *unc-93* function in muscle, and their protein products colocalize in muscle membranes. Genetic evidence has suggested that *sup-9*, *unc-93* and *sup-10* form a protein complex. We identified a large family of UNC-93-like genes in *C. elegans* as well as related genes in *Drosophila* and mammals. We propose that SUP-9, SUP-10, and UNC-93 form a multisubunit K<sup>+</sup> channel complex that regulates *C. elegans* muscle contraction and that the regulation of two-pore channels by auxiliary subunits is an evolutionarily conserved mechanism.

### SUP-9 and UNC-93 Probably Interact Physically

Genetic interactions among *sup-9*, *sup-10*, and *unc-93* suggest that their protein products assemble into a multisubunit protein complex (De Stasio et al., 1997; Greenwald and Horvitz, 1980, 1986; Levin and Horvitz, 1993). Allele-specific interactions between *sup-9* partial *lf* alleles and *unc-93(gf)* alleles are consistent with physical interactions between these two genes, as are interactions between *gf* mutants. For example, whereas the rubberband *Unc* phenotype of a *unc-93(n200); sup-10(n983)* mutant is more severe than that of either mutant alone, with the two *gf* mutations displaying an additive effect (Greenwald and Horvitz, 1986), an *unc-93(1500); sup-10(n983)* mutant displays a less severe rubberband *Unc* phenotype than either mutant alone. These results suggest that the two mutant proteins UNC-93(*e1500*) and SUP-10(*n983*) fail to properly interact physically to form a functional complex and therefore have reduced activity, whereas the UNC-93(*n200*) and SUP-10(*n983*) mutant proteins are compatible and their activation effects on SUP-9 activity are additive.

*sup-9::gfp* and *unc-93::gfp* gene fusions are both expressed in muscle cells and SUP-9 and UNC-93 proteins display indistinguishable membrane distributions in body-wall muscle cells. Since we performed these experiments using transgenic arrays, which contain multiple transgene copies (Mello et al., 1991), we expected the SUP-9 and UNC-93::GFP proteins to be overexpressed compared to their wild-type levels. Direct evidence that SUP-9 was indeed overexpressed in our experiments is indicated by the contrast between our inability to detect SUP-9 protein in whole-mount

immunostainings of wild-type animals and our ease in detecting a robust signal from *myo-3::sup-9* transgenic animals (I.P and H.R.H., unpublished results and Figure 4). It is likely that the superimposable patterns of SUP-9 and UNC-93::GFP expression we observed resulted from a direct physical interaction between these proteins, as any protein that mediated their interaction would probably be present at much lower concentration. We conclude that SUP-9 and UNC-93 proteins interact physically.

### **The SUP-9(gf) K<sup>+</sup> Channel May Be Stabilized in an Open Conformation**

The molecular identity of *sup-9* as a K<sup>+</sup> channel, together with the emergence of a rubberband Unc phenotype in wild-type animals treated with muscimol, suggests that the rubberband Unc paralysis of *sup-9(gf)* mutants is the result of increased K<sup>+</sup> efflux and hyperpolarization of muscle cells. Consistent with this model, gf mutations in the muscle two-pore K<sup>+</sup> channel *twk-18* result in a rubberband Unc paralysis that is indistinguishable from that of *sup-9(gf)* mutants (Kunkel et al., 2000). Heterologous expression of wt and mutant forms of *twk-18* channels in *Xenopus* oocytes reveals 30-fold greater K<sup>+</sup> currents for gf channels over wt channels (Kunkel et al., 2000). Thus, we propose that similar to *twk-18*, gf mutations in *sup-9* result in greater K<sup>+</sup> efflux and hyperpolarization of muscle cells.

What is the mechanism by which an amino acid substitution in SUP-9 might increase K<sup>+</sup> channel activity? Increased K<sup>+</sup> currents can arise by three distinct mechanisms: by an increase in the number of SUP-9 channels at the cell surface, by an increase in the unitary conductance of each channel or by an increase in the open probability of the channels. Because overexpression of wildtype SUP-9 under the *myo-3* promoter does not result in an Unc phenotype in transgenic animals (Figure 3), it is unlikely that the gf mutation in *sup-9* causes an Unc phenotype by increasing the number of channels on the cell surface. Thus, we postulate that the gf mutation in *sup-9* results in either a higher unitary conductance (channels pass more current when they are open) or in a higher open probability (more likely to open or to remain open for longer periods). TWK-18(gf) channels have comparable unitary conductance to wt channels, suggesting that the gf mutation stabilizes the TWK-18 in its open state (Kunkel et al., 2000).

We found that all four gf mutations in *sup-9* resulted in the same A236T amino acid substitution in the C-terminal half of the fourth transmembrane domain of SUP-9. The equivalent region in other K<sup>+</sup> channels, including the voltage-gated Shaker channel and K<sub>ir</sub> channels, undergoes conformational changes during channel opening, and thus is

believed to be critical for channel gating (Figure 8) (del Camino et al., 2000; Liu et al., 1997; Loussouarn et al., 2001). Site-directed spin-labeling techniques combined with electron paramagnetic resonance spectroscopy have been employed to compare the structures of the bacterial KcsA channel in the open and the closed state (Perozo et al., 1998, 1999). These studies reveal that when the channel opens, the transmembrane helices flanking the P domain undergo a counterclockwise rotation around the central pore of the channel, thereby widening the constriction at the base of the pore and allowing ion flow. A comparison of the crystal structures of the closed bacterial KcsA channel and the open MthK channel confirm a rearrangement of the transmembrane domains that follow the P-domain during channel opening (Figure 8) (Doyle et al., 1998, Jiang et al., 2002a; Jiang et al., 2002b). Since the *gf* alanine-to-threonine substitution occurs within this gating domain, we postulate that the mutant threonine may stabilize the fourth transmembrane domain in its rotated conformation, resulting in a SUP-9 channel that is constitutively open.

We determined that the second-site compensatory mutations *n2288* and *n2359*, which counteract the effects of the *gf* A236T substitution (Levin and Horvitz, 1993), affect adjacent amino acids, G173E and A174T, respectively, in the third transmembrane domain of SUP-9 (Table 2, Figure 8). In the two K<sup>+</sup> channels for which a crystal structure has been solved, KcsA and MthK, the transmembrane helices flanking the P-domain physically interact (Doyle et al., 1998, Jiang et al., 2002a). Thus, these compensatory mutations may counteract the effects of the *gf* threonine substitution by directly interacting with its side chain and neutralizing its stabilization of the open state. Alternatively, these second-site mutations may interact with other residues in the fourth transmembrane domain or induce a conformational change in the third transmembrane domain that stabilizes the closed conformation of the channel.

A yeast-based screen for gating mutants of the human channel K<sub>v</sub>3.2, composed of two transmembrane domains flanking a P domain, has identified a mutant with a substitution in the first transmembrane domain, N94H, that stabilized the open state of the channel (Yi et al., 2001). A substitution within the second transmembrane domain, V188I, suppressed the activating effects of the N94H mutation. These results, together with our analysis of *sup-9 gf* and compensatory mutations, suggest that an interaction between the two transmembrane domains that flank the P domains may play a role in K<sup>+</sup> channel gating.

### **SUP-10 and UNC-93 May Regulate SUP-9 K<sup>+</sup> Channel Activity**

Although 14 mammalian two-pore channels have been cloned and characterized thus far (Goldstein et al., 2001; Girard et al., 2001), no regulatory subunits have been reported for any of them. Three cloned mammalian two-pore channels, KCNK7, KCNK13 and KCNK15 have not produced K<sup>+</sup> currents when expressed in a heterologous system, suggesting that association with other proteins may be necessary for their functioning (Salinas et al., 1999; Rajan et al., 2000a; Ashmole et al., 2001; Kim and Gnatenco, 2001). Furthermore, beta subunits regulate K<sup>+</sup> channels from all other families (Pongs et al., 1999). K<sup>+</sup> channel regulatory beta subunits play diverse roles upon their association with the pore-forming alpha subunits. The cytoplasmic regulatory subunit K<sub>v</sub>β2 associates with Shaker-like K<sub>v</sub> channels and increases their surface expression in heterologous systems (Shi et al., 1996) while exerting small effects on channel activity (Heinemann et al., 1996; Rettig et al., 1994). By contrast, the transmembrane regulatory subunit minK not only causes a dramatic increase in the cell-surface channel density of K<sub>v</sub>LQT1 channels in heterologous expression systems but also leads to slower activation kinetics and a decrease in the single-channel conductance of the K<sub>v</sub>LQT1 channel (Barhanin et al., 1996; Romey et al., 1997; Sanguinetti et al., 1996). In addition to regulating K<sup>+</sup> channels through chaperone activity or altering gating kinetics, some channel subunits, such as the SUR1 subunit of Kir6.2 channels or the β1 subunits of slo channels alter the sensitivity of their associated channels to activating signals such as voltage, ATP or Ca<sup>2+</sup> (McManus et al., 1995; Tucker et al., 1997).

Two lines of evidence suggest that UNC-93 does not behave simply as a chaperone to increase SUP-9 surface expression but rather alters either the channel properties of SUP-9 or its sensitivity to a modulatory input. First, we have found that in an *unc-93(lf)* mutant SUP-9::GFP is expressed on the cell-surface of muscle cells, suggesting that association of SUP-9 with UNC-93 is not required for SUP-9 cell-surface expression. Second, if UNC-93 were simply a chaperone, then the hyperpolarization of the muscle membrane observed in *unc-93(gf)* would be the result of an increased level of wild-type SUP-9 on the cell surface. However, the overexpressing SUP-9 in muscle membranes using the *myo-3* promoter did not lead to an *unc-93(gf)* rubberband Unc phenotype, suggesting that the wild-type SUP-9 channel is in a closed or in an inactive state and that only a constitutively open mutant channel created by SUP-9(*gf*), UNC-93(*gf*) or

SUP-10(gf) results in sufficient hyperpolarization of the muscle membrane to cause the rubberband Unc phenotype.

The mammalian two-pore K<sup>+</sup> channel TREK-1 is activated by high temperature, arachidonic acid, lysophospholipids membrane stretch and low intracellular pH (Maingret et al., 1999, 2000a, 2000b; Patel et al., 1998). SUP-9 activity may similarly be responsive to multiple factors in muscle. UNC-93 may modulate the sensitivity of SUP-9 to one of these, such that an UNC-93(gf) mutant subunit may increase the sensitivity of SUP-9 to one of these inputs and cause the SUP-9 channel to open in response to basal levels of activator.

Direct evidence for the contributions of wild-type and mutant forms of SUP-10 and UNC-93 to SUP-9 channel activity awaits electrophysiological characterization of the proposed channel complex. We have attempted to express the wt and gf channel complexes in both *Xenopus* oocytes and in HEK cells. However, we have not detected K<sup>+</sup> selective currents with either system using patch-clamp techniques, although we have recorded pH-sensitive K<sup>+</sup> currents from the two-pore channel rTASK-1 in both systems (I.P. and H.R.H., unpublished data). Immunostaining of SUP-9 in transfected HEK cells indicates that it is not properly trafficked to the cell surface even when SUP-10, UNC-93 and SUP-18 are cotransfected (I.P. and H.R.H., unpublished data), suggesting a possible basis for the lack of detectable currents.

### **Implications for K<sup>+</sup> Channel Biology**

UNC-93 and SUP-10 represent may represent new classes of K<sup>+</sup> channels regulatory subunit. Seventeen other *C. elegans* genes encode proteins with sequence similarity to UNC-93. Members of this family could associate with the over 50 *C. elegans* two-pore channels (Wei et al., 1996; Bargmann, 1998) to create a stunning level of functional diversity. No interacting genes have been identified through genetic screens for the *C. elegans* two-pore K<sup>+</sup> channel encoded by *twk-18* (Kunkel et al., 2000), suggesting that unlike *sup-9*, some two-pore K<sup>+</sup> channels in *C. elegans* may function without regulatory subunits. Alternatively, such subunits might be either functionally redundant or essential, and for this reason not identified. The conservation of UNC-93-like genes in flies and humans suggests that UNC-93-like regulatory subunits represent a conserved mechanism for the regulation of two-pore K<sup>+</sup> channels. By contrast, we have found no genes with similarity to *sup-10* in the *C. elegans* genomic sequence or in mammalian EST or genomic databases, suggesting that SUP-10 may be a specialized regulatory

subunit specific to the SUP-9/UNC-93 channel complex (I.P. and H.R.H., unpublished data). Further studies of the interactions between two-pore K<sup>+</sup> channels and their presumptive regulatory subunits should enhance our understanding of this growing family of K<sup>+</sup> channels.

## Experimental Procedures

### Strains and Genetics

*C. elegans* strains were cultured as described (Brenner, 1974), except that *Escherichia coli* strain HB101 was used instead of OP50 as a food source. N2 was the wild-type strain (Brenner, 1974). Strains were grown at 20°C unless otherwise noted. The following mutations were used in this study: LGII: *lin-42*(n1089), *sup-9*(e2655gf, e2661gf, *lr1*, *lr100*, *lr11*, *lr129*, *lr142*, *lr30*, *lr35*, *lr38*, *lr45*, *lr57*, *lr73*, n180, n186, n188, n189, n190, n191, n213, n219, n222, n223, n229, n233, n241, n264, n266, n271, n292, n345, n350, n508, n659, n688, n1009, n1012, n1016, n1020, n1023, n1025, n1026, n1028, n1037, n1428, n1435, n1469, n1472, n1549, n1550gf, n1553, n1557, n1913, n1914, n2174, n2175, n2176, n2276, n2278, n2279, n2281, n2282, n2283, n2284, n2285, n2286, n2287, n2288, n2291, n2292, n2294, n2296, n2343, n2344, n2345, n2346, n2347, n2348, n2349, n2350, n2351, n2352, n2353, n2354, n2355, n2356, n2357, n2358, n2359, n2360, n2361, n3310gf), nP136, *lin-31*(n301); LGIII: *unc-93*(e1500gf, *lr12*, n200gf, n234), *nls124*, *sup-18*(n1030); LGX: *dpy-6*(e14), *sup-10*(n983gf, n1008), *lin-15*(n765ts). The sources of the *sup-9* alleles are indicated in Tables 1 and 2.

### Mapping of the *sup-9*(n1428) Tc1 Polymorphism

We found a 5.5 kb Tc1-containing *EcoRI* polymorphism, nP136, that co-segregated with the suppressed phenotype after nine back-crosses in *sup-9*(n1428); *unc-93*(e1500) mutants. We tested linkage of nP136 to *sup-9* by generating recombinants with the nearby loci *lin-42* and *lin-31*. *sup-9*(n1428) nP136; *unc-93*(e1500) males were crossed with *lin-42*(n1089) *lin-31*(n301); *unc-93*(e1500) hermaphrodites. F<sub>1</sub> non-Lin animals were allowed to self-fertilize, and F<sub>2</sub> non-Unc progeny were isolated to single plates. The F<sub>3</sub> progeny were scored for the Lin phenotypes to identify recombinants between *sup-9* and the flanking *lin* markers. All 15 *lin-42 sup-9* and all 8 *sup-9 lin-31* recombinants derived from *lin-42 + lin-31/+ sup-9 +* heterozygous parents retained nP136, indicating its tight linkage to *sup-9*. Using the polymerase chain reaction (PCR) (see Experimental Procedures), we cloned a 943 bp genomic fragment flanking the left arm of the Tc1 insertion. The sequence of this fragment was determined, and database searches of genomic sequence (*C. elegans* Sequencing Consortium, 1998) mapped it to the overlapping cosmids F34D6 and F19E8. DNA was isolated from each expanded



recombinant strain and linkage of *nP136* to *sup-9* was determined using Southern blots probed with Tc1 (Finney et al., 1988).

### **Cloning of *sup-9***

We cloned the DNA flanking the *nP136* polymorphism using a vectorette cloning approach (Korswagen et al., 1996) with the following modifications. We used an agarose gel to purify *EcoR* I-digested genomic DNA from the *sup-9(n1428) nP136; unc-93(e1500)* strain and ligated 40 ng to 10 pmol *EcoR* I vectorette in a 100  $\mu$ l volume; 3  $\mu$ l was used as template for a 100  $\mu$ l PCR reactions of 30 cycles using Tc1-specific primers L2 or R2 (Zwaal et al., 1993) and the universal vectorette primer 224 (Riley et al., 1990). Nested Polymerase Chain Reactions (PCRs) were performed with primer 224 and the Tc1 inverted-repeat primer N412 (Korswagen et al., 1996). PCR products generated from the L2 nested reaction were cloned into the *EcoR* I site of Bluescript (Stratagene). DNA sequences of both strands were determined using an automated ABI 373A DNA sequencer (Applied Biosystems).

### **Reverse Transcription PCR/ RACE**

The following primers were used in PCR reactions to amplify the *sup-9* cDNA from mixed-stage cDNA: 5'-GTGTGAGCTCAGCAGCTTCT-3' and 5'-TACTTCAAGAGATTGCAGC-3'. The cDNA was cloned into Bluescript, and its sequence determined. 5' and 3' Rapid Amplification of cDNA Ends (RACE) reactions were performed using 5' and 3' RACE Kits (Gibco-BRL).

### **Expression Constructs**

The *sup-9::gfp* fusion was obtained by subcloning the *Hpa* I-rescuing *sup-9* genomic fragment, which includes 2.9 kb of *sup-9* promoter sequence, into the *EcoR* V site of Bluescript. A *BamH* I site was introduced by PCR amplification immediately before the stop codon, and the genomic fragment subcloned into the *Sal* I/*BamH* I sites of the GFP expression vector pPD95.77 (provided by A. Fire), thereby fusing *gfp* at the C-terminal end of *sup-9* to create pIP201. To replace the *unc-54* 3'UTR from pPD95.77 with *sup-9* downstream sequence, an 808 bp region of genomic sequence immediately following the stop codon of *sup-9* was amplified by PCR using primers that introduced a *EcoR* I and *Spe* I linker at the 5' and 3' ends, respectively. This fragment was introduced into pPD95.77 at these sites, replacing the *unc-54* 3'UTR. A *BamH* I/*Spe* I fragment

containing the *gfp* coding sequence and the *sup-9* 3' region was subsequently excised and cloned into pIP201 at the same sites to create pIP210. Animals carrying the *sup-9::gfp* transgenic array were treated with gamma radiation to isolate a stable integrant (Fire, 1986). The resulting integrant, *nls124*, was mapped to LGIII by two-factor and three-factor mapping (data not shown).

The *unc-93::gfp* fusion was created by cloning a 12.9 kb *Sph* I/*Kpn* I genomic fragment from cosmid C46F11 containing 5.3 kb of *unc-93* upstream sequence, the entire coding sequence of *unc-93* and 3.2 kb of *unc-93* downstream region into the *Sph* I/*Kpn* I sites of pPD95.79 (provided by A. Fire), creating pIP314. A *Kpn* I site was introduced immediately preceding the *unc-93* stop codon using PCR, and the *Kpn* I fragment containing the *unc-93* 3' region was excised, creating plasmid pIP321, with a GFP fusion at the C-terminus of UNC-93.

To make the overexpression constructs, the *sup-9* cDNA was amplified by PCR from start to stop codons with the introduction of *Nhe* I/*Sac* I sites at the 5' and 3' ends, respectively, and subcloned into pPD95.86 (provided by A. Fire) to generate  $P_{myo-3}sup-9$ .  $P_{unc-76}sup-9$  was created by subcloning the *Nhe* I/*Sac* I fragment from  $P_{myo-3}sup-9$  into the *unc-76* expression vector, which contains 1 kb of *unc-76* promoter region (Bloom and Horvitz, 1997).

### **Transgenic Animals**

Germline transformation experiments were performed using standard methods (Mello et al., 1991). All transformations were done using strains carrying *lin-15(n765ts)* with the coinjection marker pL15EK(*lin-15*) (Clark et al., 1994) at 100 ng/ $\mu$ l, and the experimental DNA at 30-50 ng/ $\mu$ l. Transformants were recognized by their non-Muv phenotypes at 22.5°C.

### **Antibodies and Immunostaining**

Codons 1-118 of *sup-9* were fused to the GST gene (Smith and Johnson, 1988) in the vector pGEX-2T (Pharmacia), and codons 1-110 were fused to the Maltose Binding Protein (MBP) gene (di Guan et al., 1988) in the vector pMal-c2 (New England Biolabs). The GST fusion protein was expressed in *E. coli*, and the insoluble protein was purified by SDS-PAGE and used to immunize rabbits. Antisera were purified against the MBP fusion protein immobilized on nitrocellulose strips and eluted with 100 mM glycine-HCl (pH 2.5).

For immunofluorescence experiments, mixed-stage worms were fixed in 1% paraformaldehyde for 2 hours at 4°C and permeabilized as previously described (Finney and Ruvkun, 1990). For colocalization studies, transgenic lines were stained with anti-SUP-9 serum at 1:150 dilution and mouse anti-GFP serum at 1:100 dilution (Quantum Technologies). A secondary goat-anti-rabbit antibody conjugated to Texas Red (Jackson ImmunoResearch Laboratories) and a secondary goat-anti-rabbit antibody conjugated to FITC (Jackson ImmunoResearch Laboratories) were used at a 1:150 dilution. Worms were viewed using confocal microscopy.

### **Neuronal Cell Identifications**

To aid in the identification of neurons expressing SUP-9::GFP, we constructed a *sup-9::gfp* transcriptional containing the same promoter and 3'UTR region as the *sup-9::gfp* translational reporter described above but lacking any *sup-9* coding region. This reporter was brightly expressed in the cell bodies and processes of four of the approximately fifteen neurons that expressed the SUP-9 translational GFP fusion. Each neuron extended a single axonal processes into the nerve ring and turned posteriorly, two of them along the dorsal and two along the ventral cords, before ending in the posterior of the animal between the vulva and the anus. This axonal morphology was consistent with that of the four SIA interneurons (White et al., 1986). We confirmed this identification by immunostaining SUP-9::GFP (and UNC-93::GFP) -expressing animals with antisera raised against the homeodomain transcription factor CEH-17, which is expressed in the four SIA neurons and the ALA neuron (Pujol et al., 2000).

### **Muscimol and Rubberband Unc Assays**

Muscimol assays were done using 24-well plates (Costar). A 200 mM stock of muscimol (Sigma) was added to 1 ml melted NGM agar (Brenner, 1974). After four to six hours, HB101 bacteria were streaked in each well. Two hours later, 10-12 worms were placed into each well and allowed to equilibrate for one hour. The rubberband Unc response was scored by touching each worm with an eyelash across its body just posterior to the pharynx. Each worm was scored five or six times. The responses to touch were scored according to the presence of a contraction/relaxation cycle and backward movement in the following manner: 0, worms did not contract and relax but moved away from the touch; 1, worms quickly contracted and relaxed and moved away from the touch; 2, worms contracted and relaxed while concurrently generating a small

backward displacement (less than half a body-length); 3, worms contracted and relaxed but failed to move backwards; 4, worms incompletely contracted and relaxed and produced no displacement.

### **Acknowledgments**

We would like to thank J. Hodgkin for the *sup-9(e2655)* and *sup-9(e2661)* mutants, C. Ceol for the *sup-9(n3310)* mutant, B. DeStasio for the *sup-9(lr)* If mutants, B. Williams for supplying us with the *pat-3::gfp* plasmid, and A. Fire for worm expression plasmids. We would like to thank E. Jorgensen for making the initial observation that muscimol induces the rubberband Unc response, B. Castor for help with *sup-9* allele sequencing, R. Ranganathan, E. Speliotes and B. DeStasio for critically reading this manuscript, and members of the Horvitz laboratory for suggestions during the course of this work. This work was funded by NIH Grant No. 24663. I.P. was funded by an NIH predoctoral training grant. H. R. H. is an Investigator of the Howard Hughes Medical Institute.

## References

Ashmole, I., Goodwin, P. A., and Stanfield, P. R. (2001). TASK-5, a novel member of the tandem pore K<sup>+</sup> channel family, *Pflugers Arch* 442, 828-33.

Bargmann, C. I. (1998). Neurobiology of the *Caenorhabditis elegans* genome, *Science* 282, 2028-2033.

Barhanin, J., Lesage, F., Guillemare, E., Fink, M., Lazdunski, M., and Romey, G. (1996). K<sub>v</sub>LQT1 and IsK (minK) proteins associate to form the I<sub>Ks</sub> cardiac potassium current, *Nature* 384, 78-80.

Bloom, L., and Horvitz, H. R. (1997). The *Caenorhabditis elegans* gene *unc-76* and its human homologs define a new gene family involved in axonal outgrowth and fasciculation, *Proc. Natl. Acad. Sci. USA* 94, 3414-3419.

Brenner, S. (1974). The genetics of *Caenorhabditis elegans*, *Genetics* 77, 71-94.

Clark, S. G., Lu, X., and Horvitz, H. R. (1994). The *Caenorhabditis elegans* locus *lin-15*, a negative regulator of a tyrosine kinase signaling pathway, encodes two different proteins, *Genetics* 137, 987-997.

*C. elegans* Sequencing Consortium. (1998). Genome sequence of the nematode *C. elegans*: a platform for investigating biology., *Science* 282, 2012-2018.

Czirjak, G., and Enyedi, P. (2002). Formation of functional heterodimers between the TASK-1 and TASK-3 two-pore domain potassium channel subunits, *J Biol Chem* 277, 5426-32.

Davis, M. W., Fleischhauer, R., Dent, J. A., Joho, R. H., and Avery, L. (1999). A mutation in the *C. elegans* EXP-2 potassium channel that alters feeding behavior, *Science* 286, 2501-2504.

De Stasio, E., Lephoto, C., Azuma, L., C., H., Stanislaus, D., and Uttam, J. (1997). Characterization of Revertants of *unc-93(e1500)* in *Caenorhabditis elegans* Induced by N-ethyl-N-nitrosourea, *Genetics* 147, 597-608.

del Camino, D., Holmgren, M., Liu, Y., and Yellen, G. (2000). Blocker protection in the pore of a voltage-gated K<sup>+</sup> channel and its structural implications, *Nature* 403, 321-5.

di Guan, C., Li, P., Riggs, P. D., and Inouye, H. (1988). Vectors that facilitate the expression and purification of foreign peptides in *Escherichia coli* by fusion to maltose-binding protein, *Gene* 67, 21-30.

Doyle, D. A., Morais Cabral, J., Pfuetzner, R. A., Kuo, A., Gulbis, J. M., Cohen, S. L., Chait, B. T., and MacKinnon, R. (1998). The structure of the potassium channel: molecular basis of K<sup>+</sup> conduction and selectivity, *Science* 280, 69-77.

Duprat, F., Lesage, F., Fink, M., Reyes, R., Heurteaux, C., and Lazdunski, M. (1997). TASK, a human background K<sup>+</sup> channel to sense external pH variations near physiological pH, *EMBO J.* 16, 5464-5471.

Elkes, D. A., Cardozo, D. L., Madison, J., and Kaplan, J. M. (1997). EGL-36 Shaw channels regulate *C. elegans* egg-laying muscle activity, *Neuron* 19, 165-174.

Fink, M., Duprat, F., Lesage, F., Heurteaux, C., Romey, G., Barhanin, J., and Lazdunski, M. (1996). A new K<sup>+</sup> channel beta subunit to specifically enhance K<sub>v</sub>2.2 (CDRK) expression, *J. Biol. Chem.* 271, 26341-26348.

Finney, M., and Ruvkun, G. (1990). The *unc-86* gene product couples cell lineage and cell identity in *C. elegans*, *Cell* 63, 895-905.

Finney, M., Ruvkun, G., and Horvitz, H. R. (1988). The *C. elegans* cell lineage and differentiation gene *unc-86* encodes a protein with a homeodomain and extended similarity to transcription factors, *Cell* 55, 757-769.

Fire, A. (1986). Integrative transformation of *C. elegans*, *EMBO J.* 5, 2673-2680.

Fleischhauer, R., Davis, M. W., Dzhura, I., Neely, A., Avery, L., and Joho, R. H. (2000). Ultrafast inactivation causes inward rectification in a voltage-gated K<sup>+</sup> channel from *Caenorhabditis elegans*, *J. Neurosci.* *20*, 511-520.

Frohman, M. A., Dush, M. K., and Martin, G. R. (1988). Rapid production of full-length cDNAs from rare transcripts: amplification using a single gene-specific oligonucleotide primer, *Proc. Natl. Acad. Sci. USA* *85*, 8998-9002.

Gettner, S. N., Kenyon, C., and Reichardt, L. F. (1995). Characterization of beta *pat-3* heterodimers, a family of essential integrin receptors in *C. elegans*, *J. Cell. Biol.* *129*, 1127-1141.

Girard, C., Duprat, F., Terrenoire, C., Tinel, N., Fosset, M., Romey, G., Lazdunski, M., and Lesage, F. (2001). Genomic and functional characteristics of novel human pancreatic 2P domain K(+) channels, *Biochem Biophys Res Commun* *282*, 249-56.

Goldstein, S. A., Bockenhauer, D., O'Kelly, I., and Zilberberg, N. (2001). Potassium leak channels and the KCNK family of two-P-domain subunits, *Nat. Rev. Neurosci.* *2*, 175-184.

Greenwald, I., and Horvitz, H. R. (1986). A visible allele of the muscle gene *sup-10X* of *C. elegans*, *Genetics* *113*, 63-72.

Greenwald, I. S., and Horvitz, H. R. (1980). *unc-93(e1500)*: A behavioral mutant of *Caenorhabditis elegans* that defines a gene with a wild-type null phenotype, *Genetics* *96*, 147-164.

Greenwald, I. S., and Horvitz, H. R. (1982). Dominant suppressors of a muscle mutant define an essential gene of *Caenorhabditis elegans*, *Genetics* *101*, 211-225.

Heginbotham, L., Lu, Z., Abramson, T., and MacKinnon, R. (1994). Mutations in the K<sup>+</sup> channel signature sequence, *Biophys. J.* *66*, 1061-1067.



Heinemann, S. H., Rettig, J., Graack, H. R., and Pongs, O. (1996). Functional characterization of K<sub>v</sub> channel beta-subunits from rat brain, *J. Physiol.* *493*, 625-633.

Herman, R. K. (1984). Analysis of genetic mosaics of the nematode *Caneorhabditis elegans*, *Genetics* *108*, 165-180.

Hille, B. (1992). *Ionic Channels of Excitable Membranes*, (Sanderland, UK: Sinauer Associates).

Jiang, Y., Lee, A., Chen, J., Cadene, M., Chait, B. T., and MacKinnon, R. (2002a). Crystal structure and mechanism of a calcium-gated potassium channel, *Nature* *417*, 515-22.

Jiang, Y., Lee, A., Chen, J., Cadene, M., Chait, B. T., and MacKinnon, R. (2002b). The open pore conformation of potassium channels, *Nature* *417*, 523-6.

Johnstone, D. B., Wei, A., Butler, A., Salkoff, L., and Thomas, J. H. (1997). Behavioral defects in *C. elegans egl-36* mutants result from potassium channels shifted in voltage-dependence of activation, *Neuron* *19*, 151-164.

Kim, D., Fujita, A., Horio, Y., and Kurachi, Y. (1998). Cloning and functional expression of a novel cardiac two-pore background K<sup>+</sup> channel (cTBAK-1), *Circ. Res.* *82*, 513-518.

Kim, Y., Bang, H., and Kim, D. (2000). TASK-3, a new member of the tandem pore K<sup>+</sup> channel family, *J. Biol. Chem.* *275*, 9340-9347.

Kim, D., and Gnatenco, C. (2001). TASK-5, a new member of the tandem-pore K(+) channel family, *Biochem Biophys Res Commun* *284*, 923-30.

Knaus, H. G., Garcia-Calvo, M., Kaczorowski, G. J., and Garcia, M. L. (1994). Subunit composition of the high conductance calcium-activated potassium channel from smooth muscle, a representative of the *mSlo* and *slowpoke* family of potassium channels, *J. Biol. Chem.* *269*, 3921-3924.

Korswagen, H. C., Durbin, R. M., Smits, M. T., and Plasterk, R. H. (1996). Transposon Tc1-derived, sequence-tagged sites in *Caenorhabditis elegans* as markers for gene mapping, *Proc. Natl. Acad. Sci. USA* *93*, 14680-14685.

Krause, M., and Hirsh, D. (1987). A trans-spliced leader sequence on actin mRNA in *C. elegans*, *Cell* *49*, 753-761.

Kunkel, M. T., Johnstone, D. B., Thomas, J. H., and Salkoff, L. (2000). Mutants of a temperature-sensitive two-P domain potassium channel, *J. Neurosci.* *20*, 7517-7524.

Leonoudakis, D., Gray, A. T., Winegar, B. D., Kindler, C. H., Harada, M., Taylor, D. M., Chavez, R. A., Forsayeth, J. R., and Yost, C. S. (1998). An open rectifier potassium channel with two pore domains in tandem cloned from rat cerebellum, *J. Neurosci.* *18*, 868-877.

Lesage, F., Reyes, R., Fink, M., Duprat, F., Guillemare, E., and Lazdunski, M. (1996b). Dimerization of TWIK-1 K<sup>+</sup> channel subunits via a disulfide bridge, *EMBO J.* *15*, 6400-6407.

Levin, J. Z., and Horvitz, H. R. (1992). The *Caenorhabditis elegans unc-93* gene encodes a putative transmembrane protein that regulates muscle contraction, *J. Cell. Biol.* *117*, 143-155.

Levin, J. Z., and Horvitz, H. R. (1993). Three new classes of mutations in the *Caenorhabditis elegans* muscle gene *sup-9*, *Genetics* *135*, 53-70.

Liu, Y., Holmgren, M., Jurman, M. E., and Yellen, G. (1997). Gated access to the pore of a voltage-dependent K<sup>+</sup> channel, *Neuron* *19*, 175-184.

Lopes, C. M., Zilberberg, N., and Goldstein, S. A. (2001). Block of Kcnk3 by protons. Evidence that 2-P-domain potassium channel subunits function as homodimers, *J Biol Chem* *276*, 24449-52.

Loussouarn, G., Phillips, L. R., Masia, R., Rose, T., and Nichols, C. G. (2001). Flexibility of the Kir6.2 inward rectifier K(+) channel pore, *Proc. Natl. Acad. Sci. USA* *98*, 4227-32.

Maingret, F., Lauritzen, I., Patel, A. J., Heurteaux, C., Reyes, R., Lesage, F., Lazdunski, M., and Honore, E. (2000a). TREK-1 is a heat-activated background K<sup>+</sup> channel, *EMBO J.* *19*, 2483-2491.

Maingret, F., Patel, A. J., Lesage, F., Lazdunski, M., and Honore, E. (1999). Mechano- or acid stimulation, two interactive modes of activation of the TREK-1 potassium channel, *J. Biol. Chem.* *274*, 26691-26696.

Maingret, F., Patel, A. J., Lesage, F., Lazdunski, M., and Honore, E. (2000b). Lysophospholipids open the two-pore domain mechano-gated K<sup>+</sup> channels TREK-1 and TRAAK, *J. Biol. Chem.* *275*, 10128-10133.

McManus, O. B., Helms, L. M., Pallanck, L., Ganetzky, B., Swanson, R., and Leonard, R. J. (1995). Functional role of the beta subunit of high conductance calcium- activated potassium channels, *Neuron* *14*, 645-650.

Meadows, H. J., and Randall, A. D. (2001). Functional characterisation of human TASK-3, an acid-sensitive two-pore domain potassium channel, *Neuropharmacology* *40*, 551-9.

Mello, C. C., Kramer, J. M., Stinchcomb, D., and Ambros, V. (1991). Efficient gene transfer in *C. elegans*: extrachromosomal maintenance and integration of transforming sequences, *EMBO J.* *10*, 3959-3970.

Minor, D. L., Jr., Masseling, S. J., Jan, Y. N., and Jan, L. Y. (1999). Transmembrane structure of an inwardly rectifying potassium channel, *Cell* *96*, 879-891.

Okkema, P. G., Harrison, S. W., Plunger, V., Aryana, A., and Fire, A. (1993). Sequence requirements for myosin gene expression and regulation in *Caenorhabditis elegans*, *Genetics* *135*, 385-404.

Park, E. C., and Horvitz, H. R. (1986). Mutations with dominant effects on the behavior and morphology of the nematode *Caenorhabditis elegans*, *Genetics* 113, 821-852.

Patel, A. J., Honore, E., Maingret, F., Lesage, F., Fink, M., Duprat, F., and Lazdunski, M. (1998). A mammalian two pore domain mechano-gated S-like K<sup>+</sup> channel, *EMBO J.* 17, 4283-4290.

Patel, A. J., Honore, E., Lesage, F., Fink, M., Romey, G., and Lazdunski, M. (1999). Inhalational anesthetics activate two-pore-domain background K<sup>+</sup> channels, *Nat Neurosci* 2, 422-426.

Perozo, E., Cortes, D. M., and Cuello, L. G. (1998). Three-dimensional architecture and gating mechanism of a K<sup>+</sup> channel studied by EPR spectroscopy, *Nat. Struct. Biol.* 5, 459-469.

Perozo, E., Cortes, D. M., and Cuello, L. G. (1999). Structural rearrangements underlying K<sup>+</sup>-channel activation gating, *Science* 285, 73-78.

Pongs, O., Leicher, T., Berger, M., Roeper, J., Bähring, R., Wray, D., Giese, K. P., Silva, A. J., and Storm, J. F. (1999). Functional and molecular aspects of voltage-gated K<sup>+</sup> channel beta subunits, *Ann. NY Acad. Sci.* 868, 344-355.

Pujol, N., Torregrossa, P., Ewbank, J. J., and Brunet, J. F. (2000). The homeodomain protein CePHOX2/CEH-17 controls antero-posterior axonal growth in *C. elegans*, *Development* 127, 3361-71.

Rajan, S., Wischmeyer, E., Karschin, C., Preisig-Muller, R., Grzeschik, K. H., Daut, J., Karschin, A., and Derst, C. (2000a). THIK-1 and THIK-2, a novel subfamily of tandem pore domain K<sup>+</sup> channels, *J. Biol. Chem.* (in press).

Rajan, S., Wischmeyer, E., Xin Liu, G., Preisig-Muller, R., Daut, J., Karschin, A., and Derst, C. (2000b). TASK-3, a Novel Tandem Pore Domain Acid-sensitive K<sup>+</sup> Channel. AN EXTRACELLULAR HISTIDINE AS pH SENSOR, *J. Biol. Chem.* 275, 16650-16657.

Reiner, D. J., Weinschenker, D., and Thomas, J. H. (1995). Analysis of dominant mutations affecting muscle excitation in *Caenorhabditis elegans*, *Genetics* *141*, 961-976.

Rettig, J., Heinemann, S. H., Wunder, F., Lorra, C., Parcej, D. N., Dolly, J. O., and Pongs, O. (1994). Inactivation properties of voltage-gated K<sup>+</sup> channels altered by presence of beta-subunit, *Nature* *369*, 289-294.

Richmond, J. E., and Jorgensen, E. M. (1999). One GABA and two acetylcholine receptors function at the *C. elegans* neuromuscular junction, *Nat. Neurosci.* *2*, 791-797.

Riley, J., Butler, R., Ogilvie, D., Finniear, R., Jenner, D., Powell, S., Anand, R., Smith, J. C., and Markham, A. F. (1990). A novel, rapid method for the isolation of terminal sequences from yeast artificial chromosome (YAC) clones, *Nucleic Acids Res.* *18*, 2887-2890.

Romey, G., Attali, B., Chouabe, C., Abitbol, I., Guillemare, E., Barhanin, J., and Lazdunski, M. (1997). Molecular mechanism and functional significance of the Mink control of the K<sub>v</sub>LQT1 channel activity, *J. Biol. Chem.* *272*, 16713-16716.

Salinas, M., Reyes, R., Lesage, F., Fosset, M., Heurteaux, C., Romey, G., and Lazdunski, M. (1999). Cloning of a new mouse two-P domain channel subunit and a human homologue with a unique pore structure, *J. Biol. Chem.* *274*, 11751-11760.

Sanguinetti, M. C., Curran, M. E., Zou, A., Shen, J., Spector, P. S., Atkinson, D. L., and Keating, M. T. (1996). Coassembly of K<sub>v</sub>LQT1 and minK (IsK) proteins to form cardiac I(Ks) potassium channel, *Nature* *384*, 80-83.

Schafer, W. R., and Kenyon, C. J. (1995). A calcium-channel homologue required for adaptation to dopamine and serotonin in *Caenorhabditis elegans*, *Nature* *375*, 73-78.

Shi, G., Nakahira, K., Hammond, S., Rhodes, K. J., Schechter, L. E., and Trimmer, J. S. (1996). Beta subunits promote K<sup>+</sup> channel surface expression through effects early in biosynthesis, *Neuron* *16*, 843-852.

Smith, D. B., and Johnson, K. S. (1988). Single-step purification of polypeptides expressed in *Escherichia coli* as fusions with glutathione S-transferase, *Gene* 67, 31-40.

Talley, E. M., and Bayliss, D. A. (2002). Modulation of TASK-1 (Kcnk3) and TASK-3 (Kcnk9) Potassium Channels. Volatile anesthetics and neurotransmitters share a molecular site of action, *J Biol Chem* 277, 17733-42.

Thompson, J. D., Higgins, D. G., and Gibson, T. J. (1994). CLUSTAL W: improving the sensitivity of progressive multiple sequence alignment through sequence weighting, position-specific gap penalties and weight matrix choice, *Nucleic Acids Res.* 22, 4673-4680.

Trent, T., Tsung, N., and Horvitz, H. R. (1983). Egg-laying defective mutants of the nematode *Caenorhabditis elegans*, *Genetics* 104, 619-647.

Tucker, S. J., Gribble, F. M., Zhao, C., Trapp, S., and Ashcroft, F. M. (1997). Truncation of Kir6.2 produces ATP-sensitive K<sup>+</sup> channels in the absence of the sulphonylurea receptor, *Nature* 387, 179-83.

Waterston, R. H., Thomson, J. N., and Brenner, S. (1980). Mutants with altered muscle structure of *Caenorhabditis elegans*, *Dev. Biol.* 77, 271-302.

Wei, A., Jegla, T., and Salkoff, L. (1996). Eight potassium channel families revealed by the *C. elegans* genome project, *Neuropharmacology* 35, 805-829.

Weinshenker, D., Wei, A., Salkoff, L., and Thomas, J. H. (1999). Block of an ether-a-go-go-like K<sup>+</sup> channel by imipramine rescues *egl-2* excitation defects in *Caenorhabditis elegans*, *J. Neurosci.* 19, 9831-9840.

White, J. G., Southgate, E., Thomson, J. N., and Brenner, S. (1986). The structure of the nervous system of *Caenorhabditis elegans*, *Philos Trans R Soc Lond B Biol Sci* 314, 1-340.

Yi, B. A., Lin, Y., Jan, Y. N., and Jan, L. Y. (2001). Yeast screen for constitutively active mutant G protein-activated potassium channels, *Neuron* 29, 657-667.

Zwaal, R. R., Broeks, A., van Meurs, J., Groenen, J. T., and Plasterk, R. H. (1993). Target-selected gene inactivation in *Caenorhabditis elegans* by using a frozen transposon insertion mutant bank, *Proc. Natl. Acad. Sci. USA* 90, 7431-745.

Table 1. *sup-9* loss-of-function mutations

Allele	Mutation	Effect	Isolation Background	Mutagen
Nonsense Mutations				
<i>n345<sup>e</sup></i>	T <u>I</u> A to T <u>G</u> A	L20 Ochre	<i>unc-93(e1500)</i>	NTG
<i>n292<sup>e</sup></i>	<u>C</u> AG to <u>I</u> AG	Q37Amber	<i>unc-93(e1500)</i>	SPO
<i>n668<sup>a</sup></i>	<u>C</u> AG to <u>I</u> AG	Q42Amber	<i>unc-93(e1500); sup-18(n463)</i>	EMS
<i>n1012<sup>a</sup></i>	<u>C</u> AG to <u>I</u> AG	Q77Amber	<i>sup-10(n983)</i>	EMS
<i>n2276<sup>c</sup></i>	T <u>G</u> G to T <u>A</u> G	W78Amber	<i>sup-9(n1435); unc-93(e1500)</i>	EMS
<i>n2292<sup>c</sup></i>	T <u>G</u> G to T <u>A</u> G	W78Amber	<i>sup-9(n1550); sup-18(n1014)</i>	EMS
<i>n1549<sup>f</sup></i>	T <u>G</u> G to T <u>G</u> A	W78 Ochre	<i>sup-10(n983)</i>	EMS
<i>lr11<sup>b</sup></i>	<u>C</u> AG to <u>I</u> AG	Q126Amber	<i>unc-93(e1500)</i>	ENU
<i>n1023<sup>a</sup></i>	<u>C</u> GA to <u>I</u> GA	R131 Ochre	<i>sup-10(n983)</i>	EMS
<i>n2357<sup>c</sup></i>	T <u>G</u> G to T <u>G</u> A	W165 Ochre	<i>sup-9(n1550); sup-18(n1014)</i>	EMS
<i>n266<sup>e</sup></i>	T <u>G</u> G to T <u>A</u> G	W165Amber	<i>unc-93(e1500)</i>	EMS
<i>n1037<sup>a</sup></i>	<u>C</u> AA to <u>I</u> AA	Q208 Opal	<i>sup-10(n983)</i>	EMS
<i>lr73<sup>b</sup></i>	<u>C</u> AA to <u>I</u> AA	Q216 Opal	<i>unc-93(e1500)</i>	ENU
<i>lr57<sup>b</sup></i>	<u>C</u> AA to <u>I</u> AA	Q216 Opal	<i>unc-93(e1500)</i>	ENU
<i>n186<sup>e</sup></i>	<u>C</u> AA to <u>I</u> AA	Q216 Opal	<i>unc-93(e1500)</i>	EMS
Missense Mutations				
<i>n2282<sup>c</sup></i>	A <u>T</u> G to A <u>T</u> A	M1I	<i>sup-9(n1435); unc-93(e1500)</i>	EMS
<i>n213<sup>e</sup></i>	G <u>G</u> A to G <u>A</u> A	G22E	<i>unc-93(e1500)</i>	EMS
<i>lr129<sup>b</sup></i>	G <u>C</u> A to G <u>T</u> A	A23V	<i>unc-93(e1500)</i>	ENU
<i>n1472<sup>f</sup></i>	G <u>I</u> G to G <u>C</u> G	V41A	<i>sup-10(n983)</i>	GR
<i>n233<sup>e</sup></i>	G <u>I</u> G to G <u>A</u> G	V44E	<i>unc-93(e1500)</i>	DES
<i>n2291<sup>c</sup></i>	G <u>A</u> C to G <u>T</u> C	D58V	<i>sup-9(n1550)</i>	EMS
<i>lr35<sup>b</sup></i>	A <u>I</u> T to A <u>G</u> T	I61S	<i>unc-93(e1500)</i>	ENU
<i>n1025<sup>a</sup></i>	G <u>C</u> C to G <u>T</u> C	A74V	<i>sup-10(n983)</i>	EMS
<i>n1016<sup>a</sup></i>	A <u>T</u> C to A <u>A</u> C	I94N	<i>sup-10(n983)</i>	EMS
<i>n1020<sup>a</sup></i>	G <u>G</u> C to G <u>A</u> C	G95D	<i>sup-10(n983)</i>	EMS
<i>n2354<sup>c</sup></i>	G <u>G</u> C to G <u>A</u> C	G95D	<i>sup-9(n1550); sup-18(n1014)</i>	EMS
<i>n190<sup>e</sup></i>	<u>C</u> CA to <u>I</u> CA	P101S	<i>unc-93(e1500)</i>	EMS
<i>n508<sup>a</sup></i>	<u>C</u> CA to <u>I</u> CA	P101S	<i>sup-11(n406); unc-93(e1500)</i>	EMS
<i>n2353<sup>c</sup></i>	<u>C</u> CA to <u>I</u> CA	P101S	<i>sup-9(n1550); sup-18(n1014)</i>	EMS
<i>n2356<sup>c</sup></i>	<u>C</u> CA to <u>I</u> CA	P101S	<i>sup-9(n1550); sup-18(n1014)</i>	EMS
<i>n2347<sup>c</sup></i>	A <u>C</u> A to A <u>T</u> A	T103I	<i>sup-9(n1550); sup-18(n1014)</i>	EMS
<i>n1009<sup>a</sup></i>	G <u>G</u> A to G <u>A</u> A	G106E	<i>sup-10(n983)</i>	EMS
<i>n2351<sup>c</sup></i>	G <u>G</u> A to A <u>G</u> A	G106R	<i>sup-9(n1550); sup-18(n1014)</i>	EMS
<i>lr45<sup>b</sup></i>	T <u>I</u> C to T <u>C</u> C	F109S	<i>unc-93(e1500)</i>	ENU



<i>n2281</i> <sup>c</sup>	<u>C</u> CA to <u>T</u> CA	P119S	<i>sup-9(n1435); unc-93(e1500)</i>	EMS
<i>n2345</i> <sup>c</sup>	<u>C</u> CA to <u>T</u> CA	P119S	<i>sup-9(n1550); sup-18(n1014)</i>	EMS
<i>lr100</i> <sup>b</sup>	<u>G</u> GA to <u>A</u> GA	G121R	<i>unc-93(e1500)</i>	ENU
<i>n264</i> <sup>e</sup>	<u>C</u> TT to <u>I</u> TT	L122F	<i>unc-93(e1500)</i>	EMS
<i>lr38</i> <sup>b</sup>	<u>I</u> GG to <u>C</u> GG	W165R	<i>unc-93(e1500)</i>	ENU
<i>n2355</i> <sup>c</sup>	<u>G</u> GA to <u>A</u> GA	G172R	<i>sup-9(n1550); sup-18(n1014)</i>	EMS
<i>n219</i> <sup>e</sup>	<u>G</u> GA to <u>G</u> AA	G172E	<i>unc-93(e1500)</i>	UV
<i>n223</i> <sup>e</sup>	<u>G</u> GA to <u>A</u> GA	G172R	<i>unc-93(e1500)</i>	SPO
<i>n2294</i> <sup>c</sup>	<u>G</u> GA to <u>A</u> GA	G173R	<i>sup-9(n1550); sup-18(n1014)</i>	EMS
<i>n2296</i> <sup>c</sup>	<u>G</u> GA to <u>A</u> GA	G173R	<i>sup-9(n1550); sup-18(n1014)</i>	EMS
<i>n2350</i> <sup>c</sup>	<u>G</u> AA to <u>A</u> AA	E181K	<i>sup-9(n1550); sup-18(n1014)</i>	EMS
<i>n2352</i> <sup>c</sup>	<u>T</u> AC to <u>T</u> IC	Y190F	<i>sup-9(n1550); sup-18(n1014)</i>	EMS
<i>n2278</i> <sup>f</sup>	<u>A</u> CT to <u>A</u> IT	T195I	<i>sup-9(n1435)</i>	EMS
<i>n2343</i> <sup>c</sup>	<u>A</u> CT to <u>A</u> IT	T195I	<i>sup-9(n1550); sup-18(n1014)</i>	EMS
<i>n191</i> <sup>e</sup>	<u>G</u> GA to <u>G</u> AA	G200E	<i>unc-93(e1500)</i>	EMS
<i>n2286</i> <sup>c</sup>	<u>G</u> GA to <u>G</u> AA	G200E	<i>sup-9(n1550); sup-18(n1014)</i>	EMS
<i>n2283</i> <sup>c</sup>	<u>G</u> GA to <u>G</u> AA	G200E	<i>sup-9(n1435); unc-93(e1500)</i>	EMS
<i>n1469</i> <sup>f</sup>	<u>G</u> GT to <u>A</u> GT	G202S	<i>sup-10(n983)</i>	SPO
<i>n2344</i> <sup>c</sup>	<u>G</u> GT to <u>G</u> AT	G202D	<i>sup-9(n1550); sup-18(n1014)</i>	EMS
<i>lr1</i> <sup>b</sup>	<u>G</u> AC to <u>G</u> CC	D203A	<i>unc-93(e1500)</i>	ENU
<i>n2346</i> <sup>c</sup>	<u>G</u> AC to <u>A</u> AC	D203N	<i>sup-9(n1550); sup-18(n1014)</i>	EMS
<i>n2349</i> <sup>c</sup>	<u>G</u> AC to <u>A</u> AC	D203N	<i>sup-9(n1550); sup-18(n1014)</i>	EMS
<i>n1557</i> <sup>f</sup>	<u>T</u> IC to <u>T</u> CC	F226S	<i>sup-10(n983)</i>	EMS
<i>n2348</i> <sup>c</sup>	<u>G</u> GG to <u>A</u> GG	G230R	<i>sup-9(n1550); sup-18(n1014)</i>	EMS
<i>n2176</i> <sup>c</sup>	<u>G</u> GG to <u>G</u> AG	G230E	<i>sup-9(n1550)</i>	EMS
<i>n189</i> <sup>e</sup>	<u>T</u> CT to <u>T</u> IT	S235F	<i>unc-93(e1500)</i>	EMS
<i>n2358</i> <sup>c</sup>	<u>T</u> CT to <u>T</u> IT	S235F	<i>sup-9(n1550); sup-18(n1014)</i>	EMS
<i>lr142</i> <sup>b</sup>	<u>G</u> TG to <u>A</u> TG	V242M	<i>unc-93(e1500)</i>	ENU
<b>Splice Mutations</b>				
<i>n241</i> <sup>e</sup>	<u>A</u> Ggtaa to <u>A</u> Gctaa	1st donor	<i>unc-93(e1500)</i>	DES
<i>n659</i> <sup>a</sup>	<u>A</u> Ggtaa <u>A</u> Gctaa	1st donor	<i>sup-18(n463); unc-93(e1500)</i>	EMS
<i>n180</i> <sup>e</sup>	ttag <u>A</u> G to ttac <u>A</u> G	1st acceptor	<i>sup-10(n983)</i>	SPO
<i>n1028</i> <sup>a</sup>	<u>C</u> Ggtga to <u>C</u> Gatga	2nd donor	<i>sup-10(n983)</i>	EMS
	<u>G</u> AT to <u>A</u> AT	D278N		
<i>n2285</i> <sup>c</sup>	<u>T</u> Ggtga to <u>T</u> Gatga	3rd donor	<i>sup-9(n1550); sup-18(n1014)</i>	EMS
<i>n271</i> <sup>e</sup>	<u>A</u> Ggtat to <u>A</u> Gatat	4th donor	<i>unc-93(e1500)</i>	EMS
<i>n1553</i> <sup>c</sup>	<u>A</u> Ggtat to <u>A</u> Gatat	4th donor	<i>sup-10(n983)</i>	EMS
<i>n2175</i> <sup>c</sup>	tcag <u>G</u> A to tcaa <u>G</u> A	4th acceptor	<i>sup-9(n1550)</i>	EMS
<i>n2174</i> <sup>c</sup>	<u>T</u> Ggtga to <u>T</u> Gatga	5th donor	<i>sup-9(n1550)</i>	EMS

<i>n2279<sup>c</sup></i>	tcagAG to tcaaAG	6th acceptor	<i>sup-9(n1435); unc93(e1500)</i>	EMS
<i>n1026<sup>a</sup></i>	CGgtgg to CGatgg	7th donor	<i>sup-10(n983)</i>	EMS
Insertion, Deletion and Frameshift Mutations				
<i>n1913<sup>f</sup></i>	C to GAT	3+13aa Opal	<i>unc-93(e1500)</i>	GR
<i>n1428<sup>d</sup></i>	Tc1 insertion	17+insertion	<i>unc-93(e1500)</i>	SPO
<i>n2287<sup>c</sup></i>	155bp del.	94-127aa Del.	<i>sup-9(n1550); sup-18(n1014)</i>	EMS
<i>n1914<sup>f</sup></i>	1181 bp del.	94+11aa Opal	<i>unc-93(e1500)</i>	DEB
<i>n2284<sup>c</sup></i>	561 bp del.	95+1aa Ochre	<i>sup-9(n1435); unc-93(e1500)</i>	EMS
No Mutation Found				
<i>lr30<sup>b</sup></i>	No mutation found		<i>unc-93(e1500)</i>	ENU
<i>n188<sup>e</sup></i>	No mutation found		<i>unc-93(e1500)</i>	EMS
<i>n229<sup>e</sup></i>	No mutation found		<i>unc-93(e1500)</i>	DES

The sequence of the *sup-9* coding region including intron/exon boundaries, but not promoter or downstream regions, was determined. Isolation background indicates the strain in which a *sup-9* If allele was isolated as a suppressor. DEB, diepoxybutadiene; DES, diethyl sulfate; EMS, ethyl methanesulfonate; ENU, *N*-ethyl-*N*-nitrosourea; GR, gamma radiation; NTG, nitrosoguanidine; SPO, spontaneous; UV, ultraviolet light.

<sup>a</sup> Greenwald and Horvitz (1986)

<sup>b</sup> De Stasio et al.(1997)

<sup>c</sup> Levin and Horvitz (1993)

<sup>d</sup> Levin and Horvitz (1992)

<sup>e</sup> Greenwald and Horvitz (1980)

<sup>f</sup> J. Levin and H.R. Horvitz, unpublished

<sup>g</sup> I. Greenwald and H.R. Horvitz, unpublished

Table 2. *sup-9* altered-function mutations

Allele	Mutation	Effect	Isolation Background	Allele Type	Mutagen
<i>n1550</i>	<u>G</u> CG to <u>A</u> CG	A236T	wild-type	gf	EMS
<i>n3310</i>	<u>G</u> CG to <u>A</u> CG	A236T	wild-type	gf	EMS
<i>e2655</i>	<u>G</u> CG to <u>A</u> CG	A236T	wild-type	gf	EMS
<i>e2661</i>	<u>G</u> CG to <u>A</u> CG	A236T	wild-type	gf	EMS
<i>n2360</i>	<u>A</u> CG to <u>A</u> TG	T236M	<i>sup-9(n1550)</i>	Partial lf	EMS
<i>n2361</i>	<u>A</u> CG to <u>A</u> TG	T236M	<i>sup-9(n1550)</i>	Partial lf	EMS
<i>n2359</i>	<u>G</u> CA to <u>A</u> CA	A174T	<i>sup-9(n1550)</i>	Partial lf	EMS
<i>n2288</i>	<u>G</u> GA to <u>G</u> AA	G173E	<i>sup-9(n1550)</i>	Partial lf	EMS

The sequence of the *sup-9* coding region including intron/exon boundaries was determined. Isolation background indicates the gf mutant in which a *sup-9* allele was isolated. Alleles *n1550*, *n2360*, *n2361*, *n2359*, *n2288* and *n1435* have been previously described (Levin et al., 1993).

Table 3. Expression of *sup-9* and *unc-93* in muscle rescues their lf egg-laying defects

Genotype:	
<i>sup-9(n1913); unc-93(e1500)</i>	
Array	% bags of worms (animals scored) <sup>a</sup>
<i>myo-3::gfp</i>	0 (53)
<i>myo-3::gfp</i>	2 (53)
<i>myo-3::sup-9</i>	77 (44)
<i>myo-3::sup-9</i>	81 (47)
<i>myo-3::sup-9</i>	88 (56)
<i>unc-76::sup-9</i>	0 (44)
<i>unc-76::sup-9</i>	0 (44)
<i>unc-76::sup-9</i>	0 (37)
Genotype:	
<i>unc-93(n234); sup-9(e2655)</i>	
<i>myo-3::gfp</i>	0 (31)
<i>myo-3::gfp</i>	2 (61)
<i>myo-3::gfp</i>	0 (41)
<i>myo-3::unc-93</i>	96 (27)
<i>myo-3::unc-93</i>	94 (33)
<i>myo-3::unc-93</i>	97 (31)
<i>unc-76::unc-93</i>	18 (40)
<i>unc-76::unc-93</i>	15 (45)
<i>unc-76::unc-93</i>	9 (46)

Figure 1. Molecular Cloning, Genomic Structure, and Sequence of the *sup-9* Gene

(A) Schematic representation of the *sup-9* genomic region and the Tc1 insertion found in the *sup-9(n1428)* strain. Cosmid F19E8 as well as the 6.8 kb *Hpa* I subclone were tested for their abilities to rescue a *sup-9(n180); unc-93(e1500)* mutant by scoring the appearance of the rubberband Unc response. Numbers in parentheses indicate the number of rescued lines and the number of total transgenic lines scored.

(B) Intron/exon structure of *sup-9*. The structure of the *sup-9* gene was deduced by comparing its genomic sequence with the sequences of RT-PCR and RACE products. Closed boxes indicate coding regions. Open boxes indicate untranslated regions. The arrow indicates the direction of transcription.

(C) Alignment of SUP-9 with human TASK-1, human TASK-3, and *Drosophila* predicted proteins dCG9637 and dCG9361. Residues identical between SUP-9 and the other proteins are highlighted in gray. Closed bars indicate proposed transmembrane domains (M1, M2, M3 and M4), open bars indicate P domains (P1 and P2). If mutations in *sup-9* are indicated by the amino acids above the aligned sequences. The superscript indicates the number of alleles with that mutation. The closed triangle indicates the site of all four *gf* alleles. The open triangle indicates a potential N-glycosylation site. Genebank Accession numbers are as follows: SUP-9, (to be assigned); TASK-1, NP\_002237; TASK-3, NP\_057685; dCG9637, AAF54970; and dCG9361, AAF54374.



Figure 2. Expression of *sup-9::gfp* and *unc-93::gfp* Fusion Proteins  
Merged Nomarski and epifluorescence images of GFP expression in worms carrying a  
*sup-9::gfp* (A-D) or an *unc-93::gfp* (E-H) reporter transgene. Scale bars, 10  $\mu$ m.  
(A, E) Body-wall muscle cells. Short arrow indicates the cell membranes of adjacent  
body-wall muscle cells; long arrow indicates rows of dense bodies.  
(B, F) Vulval muscle cells. Arrow indicates the opening of the vulva.  
(C, G) Intestinal muscle cells (arrows).  
(D, H) Heads of adult animals expressing *gfp* in neurons (arrows).

Figure 2

*sup-9::gfp*

*unc-93::gfp*

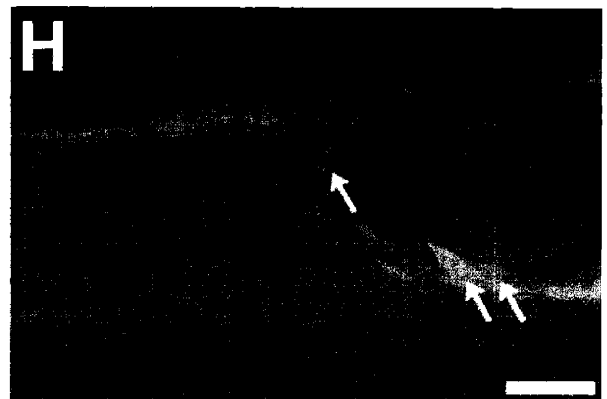
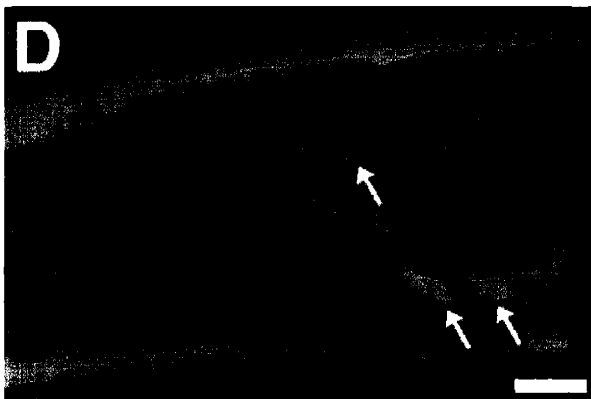
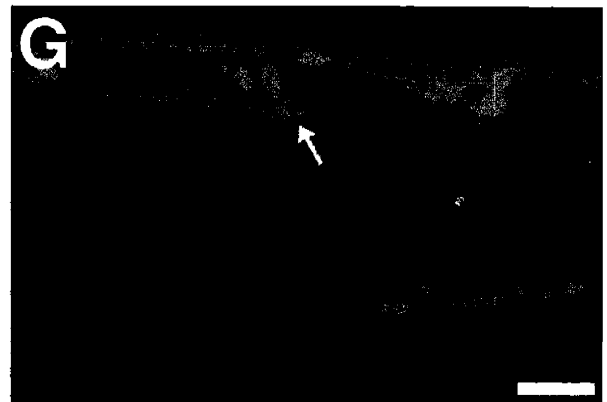
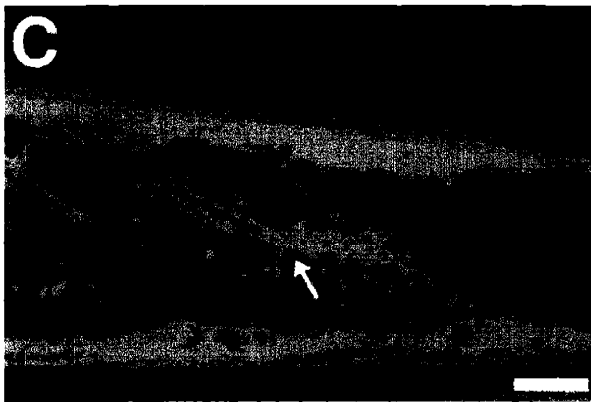
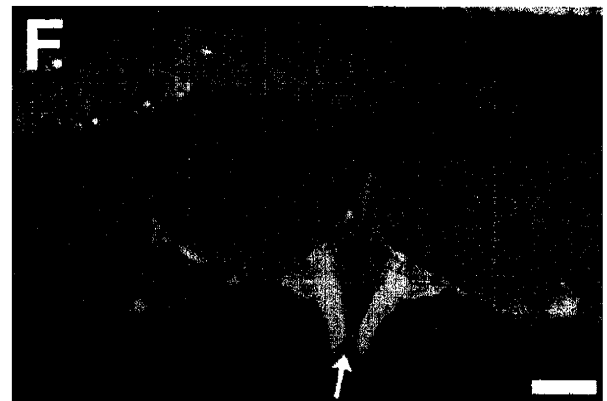
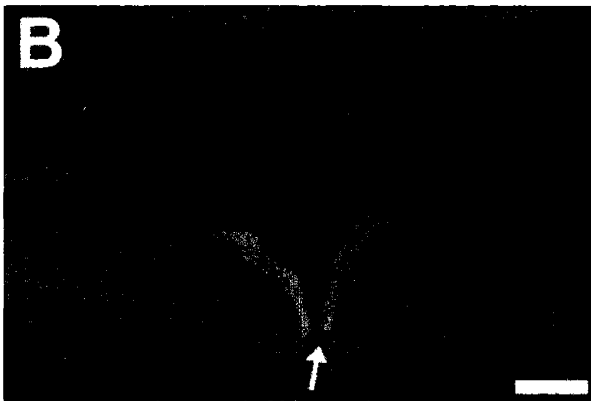
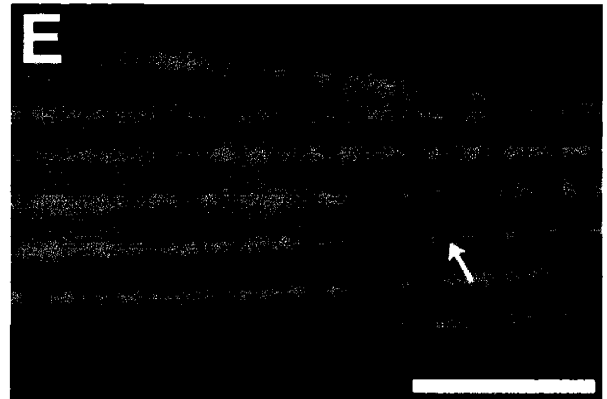
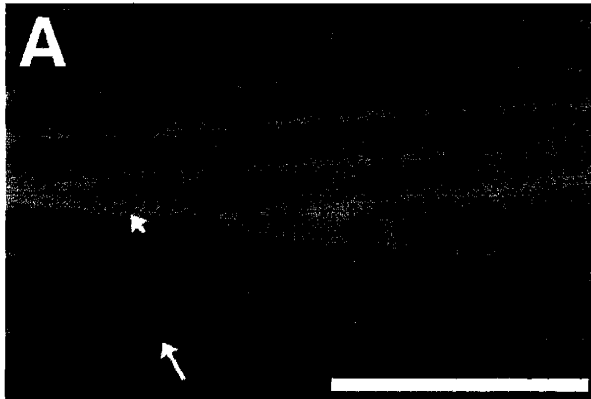




Figure 3. *sup-9* and *unc-93* Muscle-Specific Rescue of Locomotion Defects

Locomotion rates of young adult transgenic hermaphrodites were scored on a bacterial lawn during 60 second intervals. A body-bend is defined as a 360° sine wave. Each bar represents an independent transgenic line. All strains are *lin-15(n765)* and carry the wild-type *lin-15* gene as a transgene to aid in the identification of transgenic animals.

(A) Parental genotype: *sup-9(n1913); unc-93(e1500); lin-15(n765)*; n= 20-24 worms/transgenic line.

(B) Parental genotype: *lin-15(n765ts)*; n= 11-12.

(C) Parental genotype: *unc-93(e1500n234); sup-9(e2655) lin-15(n765)*; n= 16-17.

(D) Parental genotype: *lin-15(n765ts)*; n= 15-17.

Figure 3

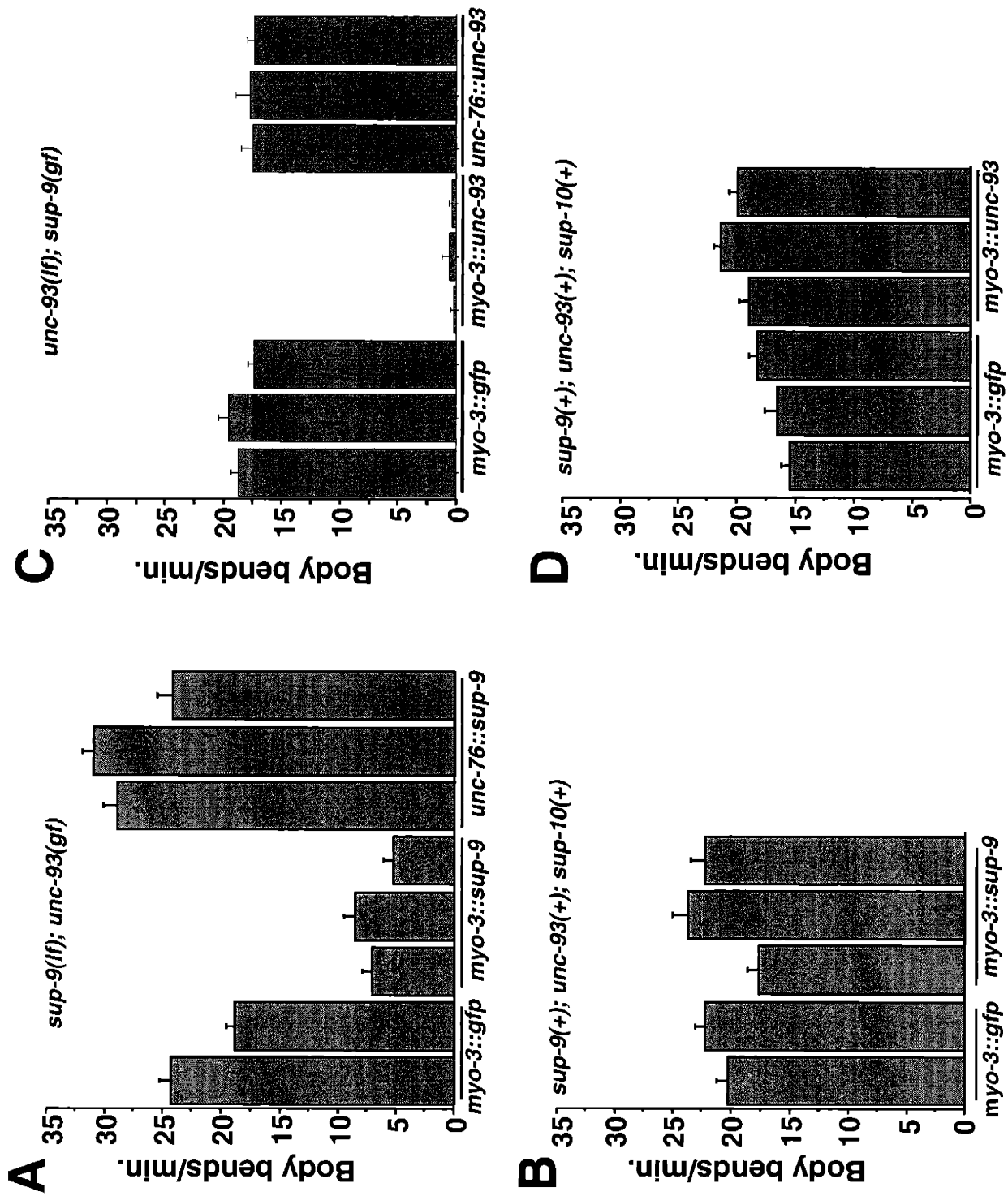


**Figure 4. Subcellular Colocalization of SUP-9 and UNC-93::GFP**

Transgenic lines expressing *sup-9* driven by the *myo-3* promoter and either an *unc-93::gfp* (A, C) or a *pat-3::gfp* (B, D) fusion were fixed and co-stained with anti-SUP-9 (red) and anti-GFP antisera (green). All panels display adult body-wall muscle cells analyzed by confocal microscopy for immunofluorescence. Scale bars, 10  $\mu\text{m}$ .

Figure 3

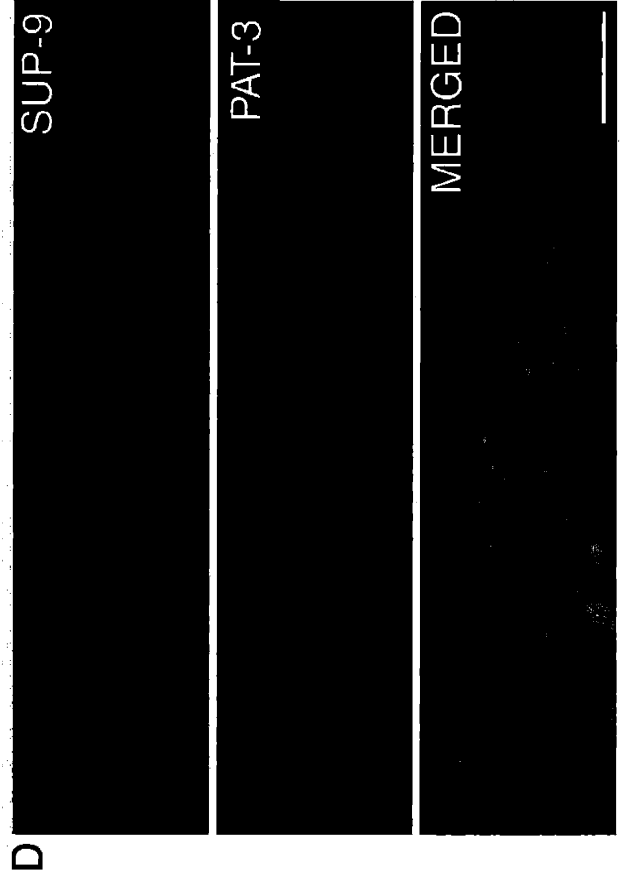
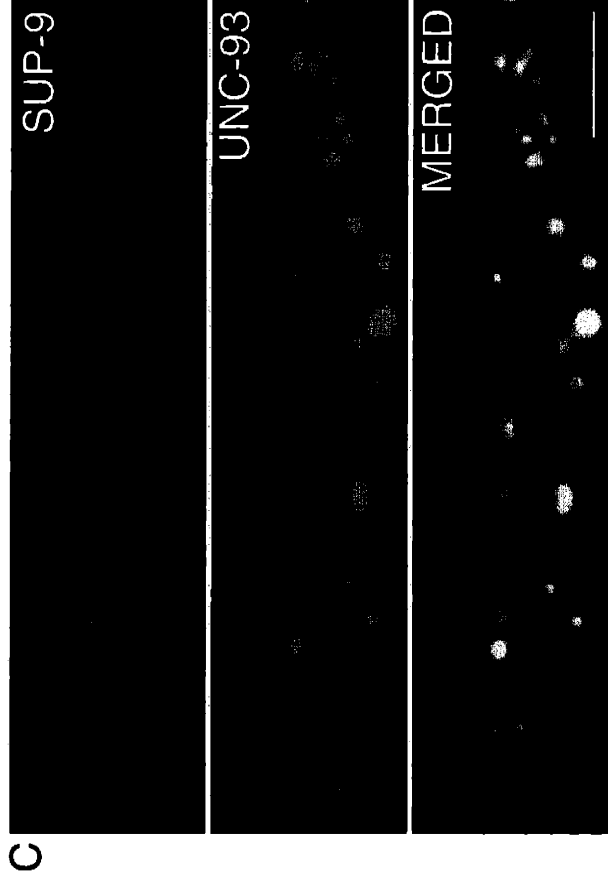
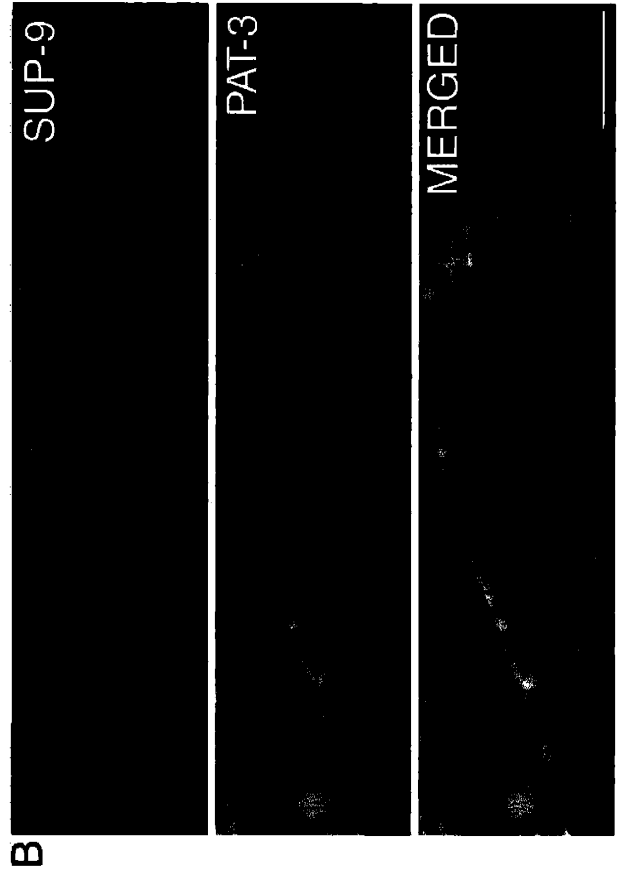
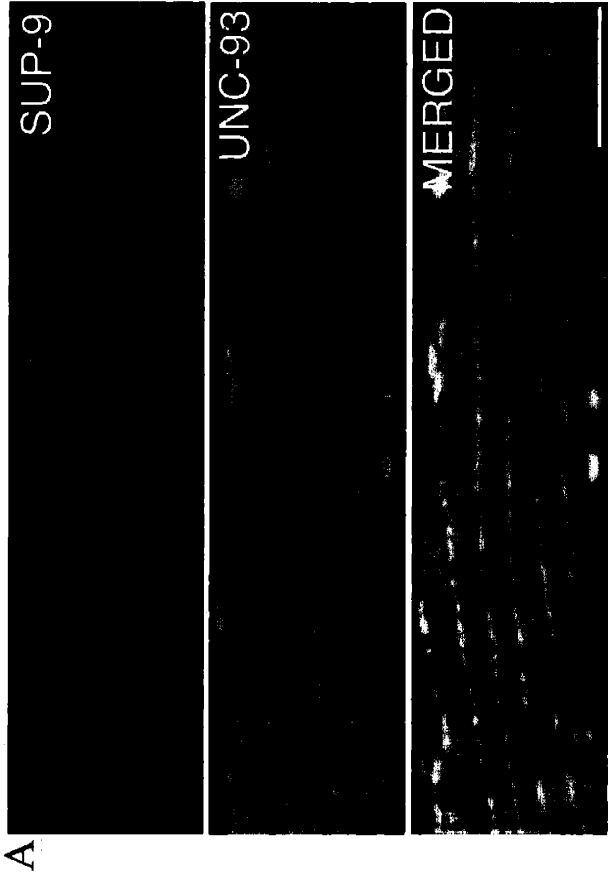


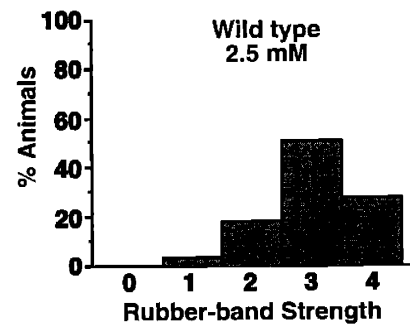
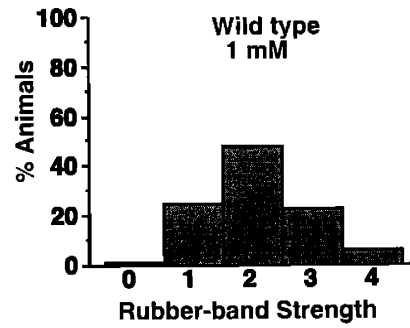
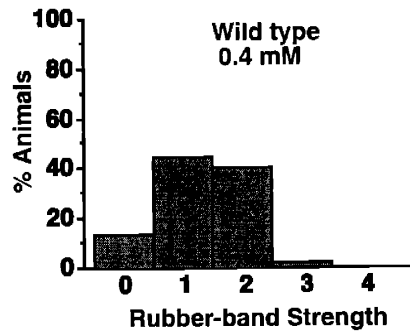
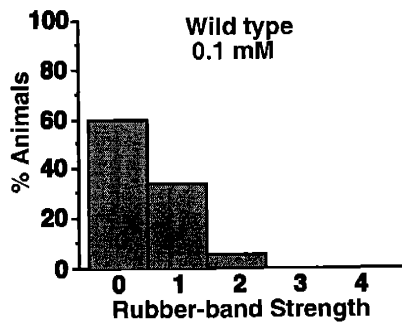
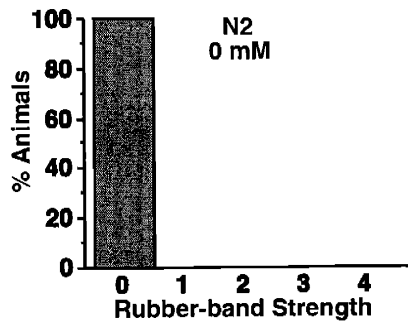
Figure 5. Muscimol Phenocopies the Rubberband Unc Phenotype of *sup-9(gf)*, *unc-93(gf)* and *sup-10(gf)* Mutants

(A) Wild-type (N2) worms were scored for the rubberband Unc response at the indicated concentrations of muscimol as defined in Experimental Procedures. n=170 for all concentrations except for 1 mM, in which case n=232.

(B) Rubberband mutants were scored for the rubberband Unc response in the absence of muscimol. n=300 for all genotypes except for *sup-9(n1550)*, in which case n=200.

Figure 5

**A**



**B**

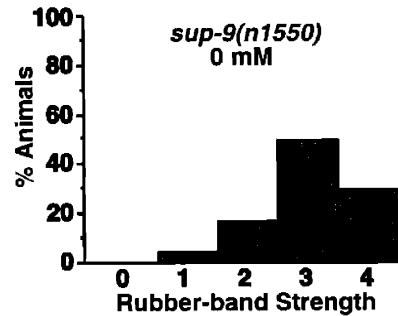
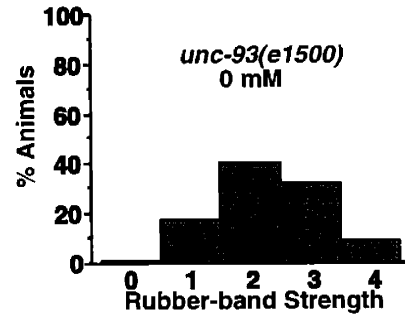
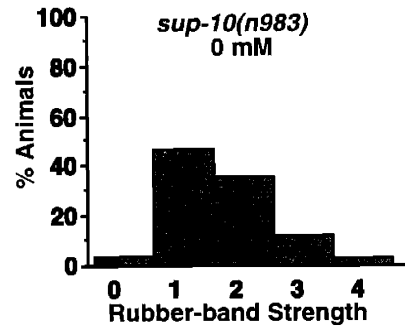
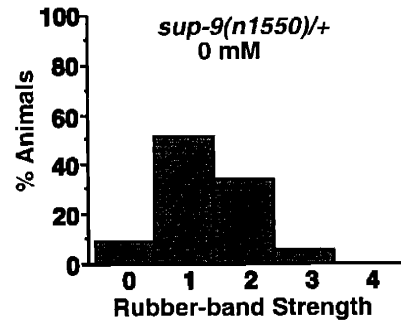
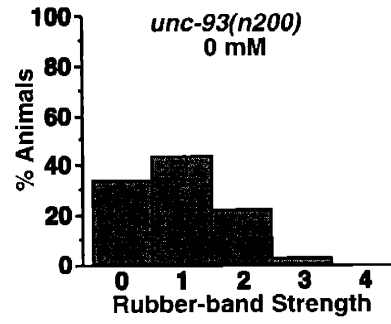


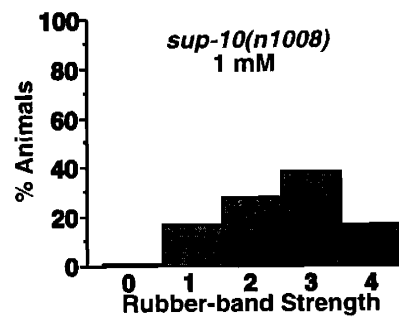
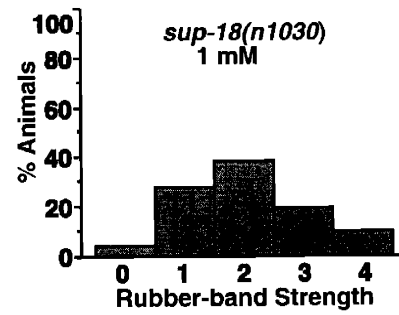
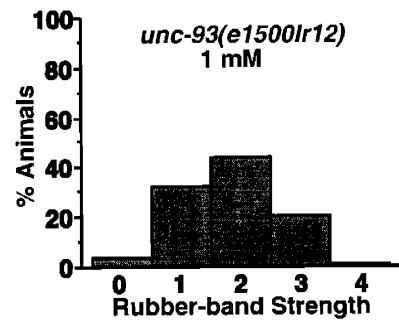
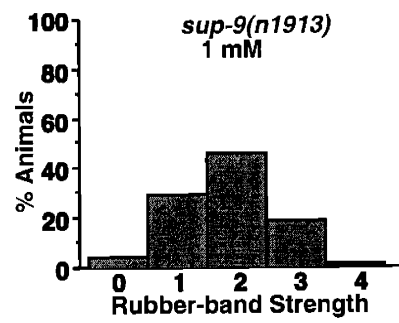
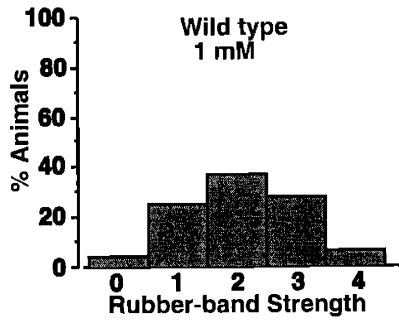
Figure 6. Muscimol Responses of *sup-9*, *sup-10*, *sup-18* and *unc-93* Mutants

(A) Wild-type (N2) and If mutant worms were scored for the rubberband Unc response in 1 mM muscimol. Number of responses scored were n= 979, n= 360, n= 300, n= 490 and n= 300, respectively. All graphs represent the results of at least three independent experiments.

(B) Rubberband Unc responses of *unc-93(n200)* and *sup-9(n1550)/+* worms were scored at the indicated muscimol concentrations; n=300, n=120, n=300 and n=300, respectively.

Figure 6

**A**



**B**

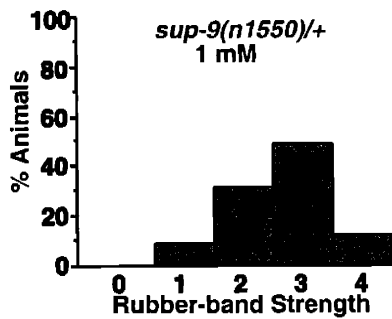
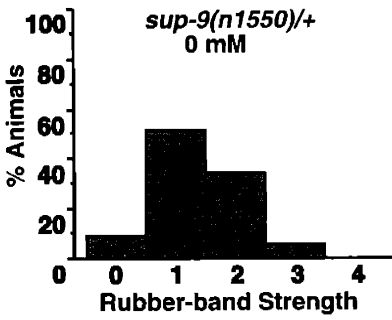
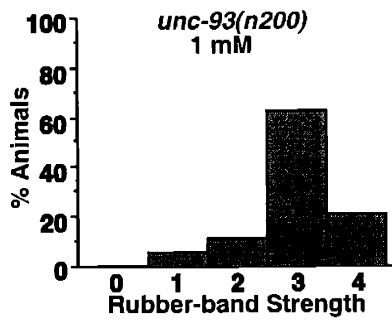
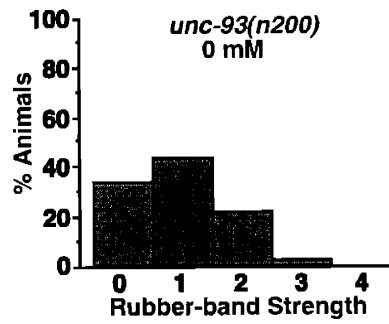
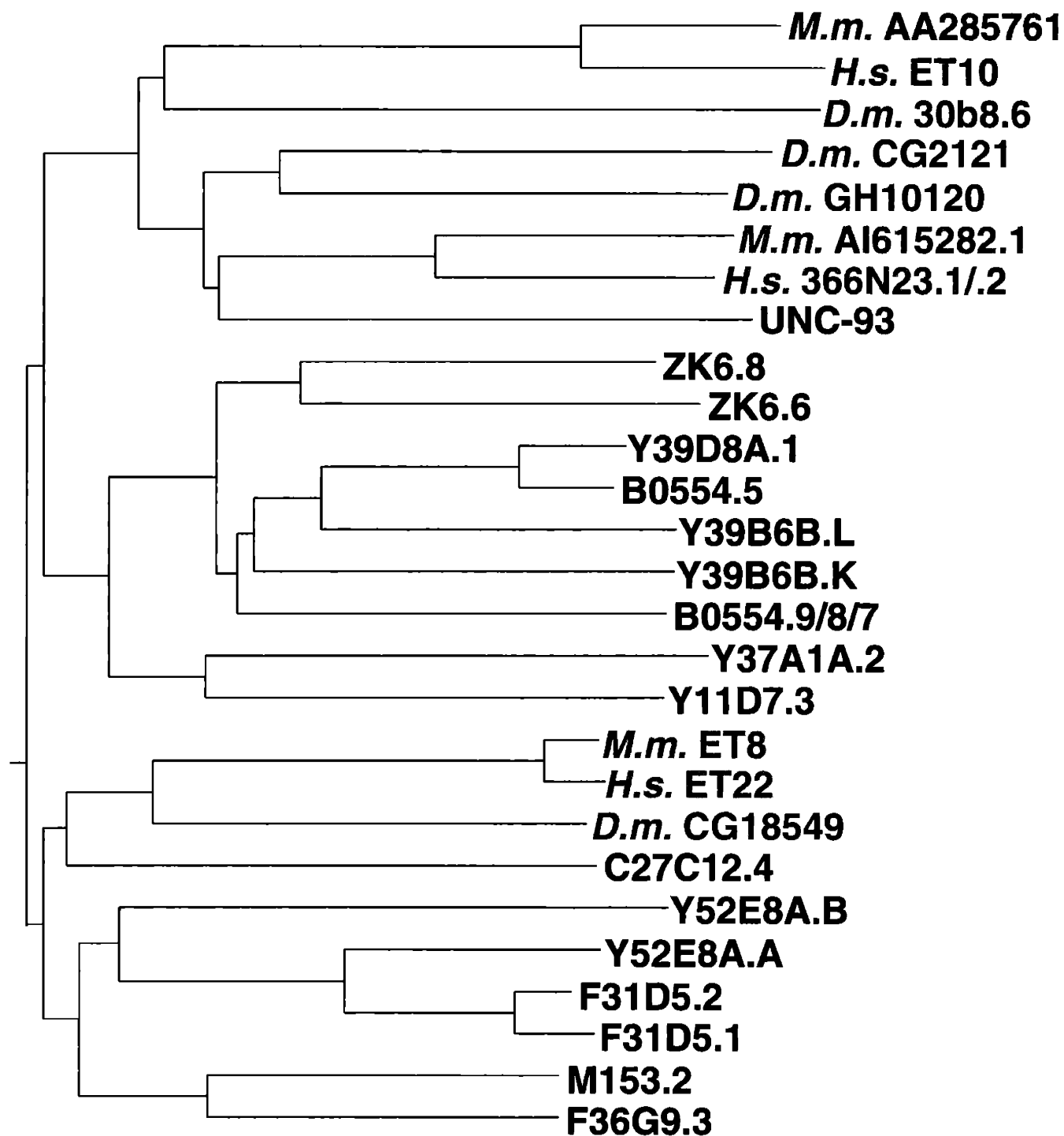




Figure 7. Phylogenetic Tree of UNC-93-like Genes from *C. elegans*, *Drosophila*, Mouse and Human

Protein alignments were generated using the ClustalW algorithm (Thompson et al., 1994). The horizontal length between each pair of branches represents the evolutionary distance between gene pairs as measured by number of substitutions per residue. The predicted sequences of *H.s.* dJ366N23.1 and *H.s.* dJ366N23.2 were used to create *H.s.* dJ366N23.1/.2, as these sequences likely represent the N- and C-terminal segments, respectively, of a single gene. *M.m.* AI615282 and *M.m.* 285761 are encoded by ESTs and likely represent partial sequences of their respective genes. B0554.9/.8/.7 contains the combined amino acid sequences of predicted genes B0554.9, B0554.8 and B0554.7, as these are likely portions of one gene. The Genbank accession numbers of the genes are as follows: *D.m.* 30B8.6, CAA15704; *D.m.* CG2121, AAF59099; *D.m.* GH10120, AF145657; *D.m.* CG18549, AAF54824; *H.s.* ET10, AF015185; *H.s.* dJ366N23.1/.2, AL021331; *H.s.* ET22, AF015186; *M.m.* AI615282, AI615282; *M.m.* ET8, AF015191; *M.m.* AA285761, AA285761; UNC-93, S23352; ZK6.8, AAC17687; ZK6.6, AAC17693; Y39D8A.1, AAC69224; B0554.5, AAB37612; Y39B6B.L, CAB60917; Y39B6B.K, CAB60916; B0554.9/.8/.7, AAB37619, AAB37618, AAB37616; Y37A1A.2, CAB16469; Y11D7A.3, CAA21581; C27C12.4, CAA93741; Y52E8A.B, AAF59523; Y52E8A.A, AAF59522; F31D5.2, AAC71105; F31D5.1, AAC71106; M153.2, CAA91944; F36G9.3, CAB04342. *H.s.*, *Homo sapiens*. *M.m.*, *Mus musculus*. *D.m.*, *Drosophila melanogaster*. All others are *C. elegans*.

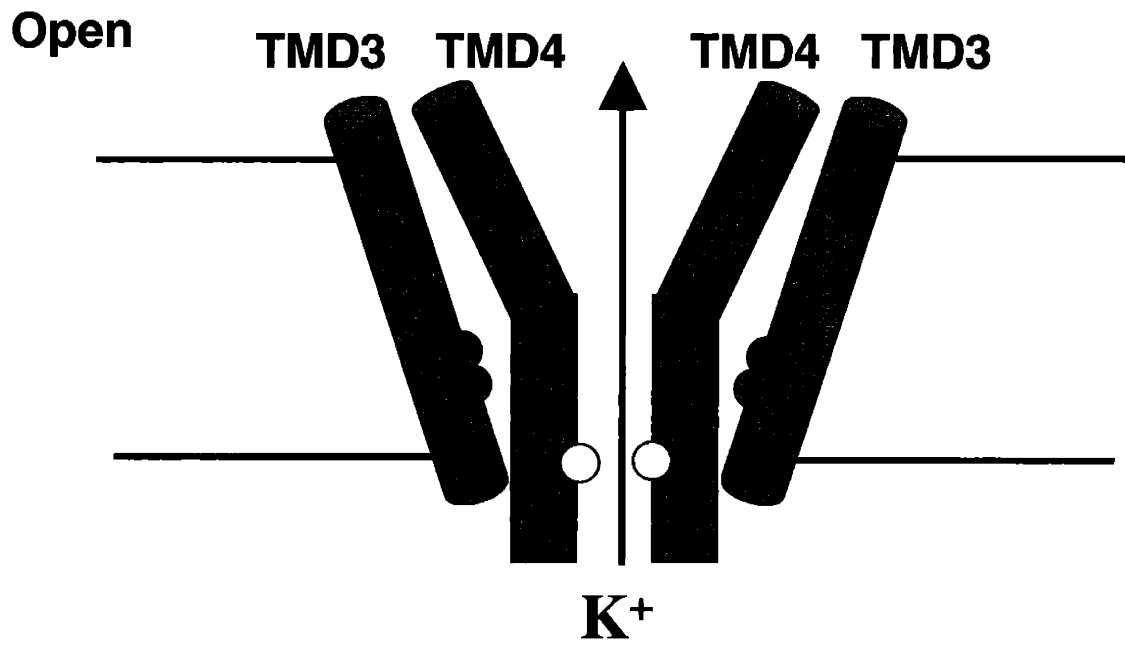
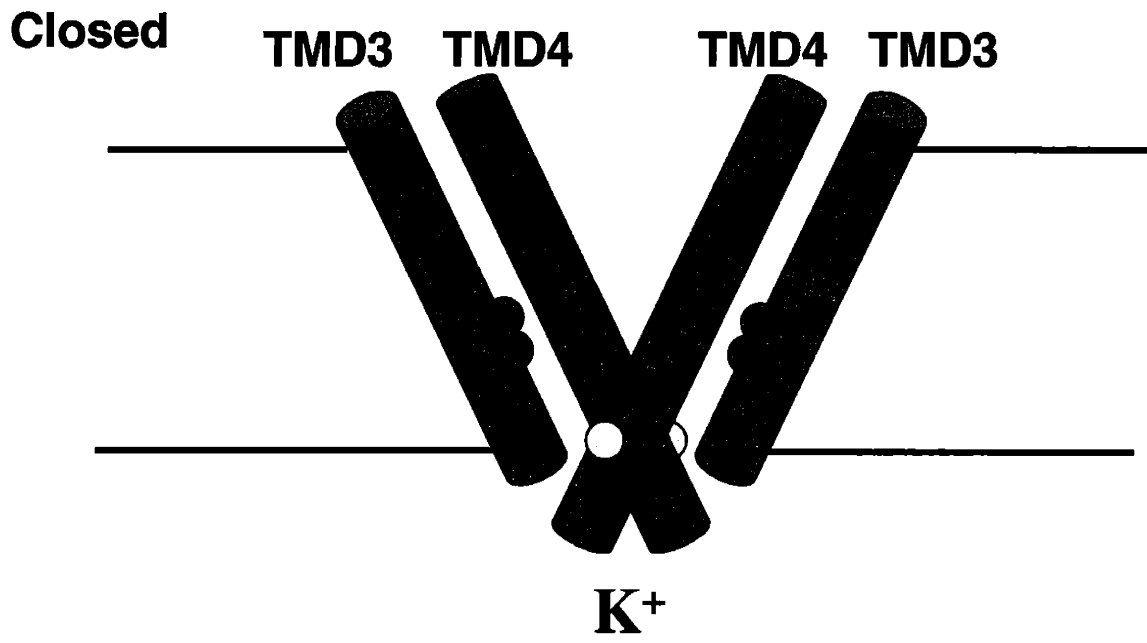


— 0.05 Substitutions/Residue

Figure 8. Proposed Conformational Changes in the Fourth Transmembrane Domain of SUP-9 Underlie Channel Gating

The third and fourth transmembrane domains (TMD) of a SUP-9 channel dimer are represented by cylinders. The first and second transmembrane domains from each SUP-9 molecule are not shown for clarity, but would reside above and below the plane of the page. Upon channel opening, the fourth transmembrane domains undergo a rotation around a proposed hinge region, allowing access of K<sup>+</sup> ions into the pore. Yellow circles represent the location of the *n1550* *gf* mutation, while the red circles represent the correctional alleles *n2288* and *n2359* which intragenically suppress the *gf* activity of *n1550*. Top and bottom panels represent the closed and open channels, respectively. Adapted from Jiang et al., 2002a.

**Figure 8**



## **Appendix to Chapter TWO**

## Introduction

In this appendix, I present supplementary results relevant to the function of the proposed *unc-93* channel regulatory subunit. These data support a model in which UNC-93 regulates SUP-9 channel properties and also indicate that *unc-93* and *sup-10* may be regulatory subunits specific to the *sup-9* K<sup>+</sup> channel and not to other *C. elegans* two-pore channels.

## Results/Discussion

### ***unc-93* Is Absolutely Required for Phenotypic Expression of *sup-9(gf)* Activity**

*sup-9(gf)* mutations result in a severe muscle paralysis that is completely suppressed by *lf* mutations in *unc-93* (Levin and Horvitz, 1993). Hyperpolarization of worm body-wall muscle cells with the GABA Cl<sup>-</sup> channel-agonist muscimol results in a rubberband *Unc* phenotype similar to that of *sup-9(gf)* mutants, suggesting that the *sup-9(gf)* defects are the result of increased K<sup>+</sup> currents through *sup-9*. *unc-93* is proposed to function as a regulatory subunit of the *sup-9* two pore K<sup>+</sup> channel (Chapter 2). Regulatory subunits have been described for other mammalian K<sup>+</sup> channel families. These include the K<sub>v</sub>β, slo β, minK, KchIPs and SUR subunits (reviewed in Chapter 1). Channel regulatory subunits can increase the K<sup>+</sup> currents flowing through channels by two general mechanisms: by acting as chaperones to increase the surface expression of channels or by altering channel properties such as removing inactivation, increasing single channel conductance or enhancing sensitivity to activating signals such as voltage or calcium (reviewed in Chapter 1).

We sought to determine the basis for the requirement of UNC-93 in supporting the *gf* activity of SUP-9. UNC-93 could be acting as a chaperone, such that a hyperactive channel generated by the *sup-9(n1550)* *gf* mutation cannot hyperpolarize muscle cells because it is inefficiently trafficked to the membrane in the absence of *unc-93*. Alternatively, the SUP-9(*gf*) channel may have been stabilized in the open state once it has opened, but still requires UNC-93 to open in response to an activating input.

To distinguish between these models, we overexpressed the *sup-9(n1550)* cDNA under the control of the *myo-3* muscle-specific promoter in transgenic arrays in an attempt to bypass the requirement for *unc-93*. Three independent lines overexpressing *sup-9(gf)* in an *unc-93(lr12)* null background displayed identical locomotion rates to the wild-type strain (26.6, 26.8 and 26.0 vs 26.3 bends/minute, respectively, Figure 1A), indicating that in the absence of UNC-93 excess amounts of SUP-9(*gf*) cannot

hyperpolarize muscle cells. Introduction of a single wild-type copy of *unc-93* into each transgenic strain resulted in a severe paralysis (0.5 to 1.5 bends/minute, Figure 1A), confirming that SUP-9(gf) overexpressed in muscle from a transgene can result in membrane hyperpolarization in the presence of the UNC-93 protein.

To confirm that the SUP-9(gf) channel was being overexpressed and trafficked to the membrane, we immunostained these transgenic lines with anti-SUP-9(N) antiserum (Figure 1B). As expected, a robust signal was obtained from animals carrying the transgenic array but not from their siblings who had lost the transgene (nontransgenic animals were easily recognized since they express a Multivulva phenotype when losing the *lin-15* coinjection marker). The cell-surface dense body localization of SUP-9 was similar to that previously reported for  $P_{myo-3}sup-9$  transgenic lines and for *sup-9::gfp* transgenes (Chapter 2).

The inability of SUP-9(gf) channels localized to the cell surface to hyperpolarize muscle membranes in the absence of UNC-93 suggests that UNC-93 is not behaving as a chaperone to increase cell-surface expression of SUP-9, but rather to alter channel properties as reported for regulatory subunits of other K<sup>+</sup> channels. The transmembrane  $\beta 1$  subunit of large-conductance Ca<sup>2+</sup>-activated K<sup>+</sup> (slo) channels greatly increases the sensitivity of the channels to Ca<sup>2+</sup> (McManus et al., 1995). In the mouse knockout of the slo  $\beta 1$  subunit, slo1 channels are expressed in the cell membranes of arterial muscle cells, but they remain closed because without the sensitivity conferred by the  $\beta 1$  subunit they cannot be opened by the low Ca<sup>2+</sup> concentrations found in these cells (Brenner et al., 2000). Two pore channels in mammals are gated by multiple cellular factors such as arachidonic acid, membrane stretch, pH, temperature and G-protein coupled receptors (reviewed by Goldstein et al., 2001). Although the cellular factors that activate the SUP-9 channel *in vivo* remain to be identified, UNC-93 may increase the sensitivity of SUP-9 to one of these factors, similar to the increase in Ca<sup>2+</sup> sensitivity conferred by slo  $\beta$  subunits to slo channels. Our results are consistent with a similar role for *unc-93* in the regulation of *sup-9*, and are further supported by the existence of an *unc-93(gf)* mutation that also results in paralysis (Greenwald and Horvitz, 1980). This mutation may increase the sensitivity of *sup-9* towards an activating factor even more, such that this hypersensitivity may result in excessive currents.

Finally, it should be noted that while our results do not support a primary role for *unc-93* in increasing total levels of *sup-9* channel on the cell surface, it remains possible

that *unc-93* may increase the efficiency of a post-translational modification, such as glycosylation, that might be absolutely required for channel activity. Such a model however, would need to explain how a mutation in *unc-93* leads to a rubberband Unc phenotype and why overexpression of wild-type *sup-9* or *unc-93* in muscle does not lead to a rubberband phenotype (Chapter 2).

### **The Paralysis of *twk-18(gf)* Mutants Is not Suppressed by *unc-93(lf)* or *sup-10(lf)* Mutations**

In chapter 2, we described the identification of a large gene family in *C. elegans* of *unc-93*-like genes. Since the initial report of *sup-9* as a two-pore K<sup>+</sup> channel, another rubberband Unc mutant, *unc-110*, has been cloned and found to encode a temperature-activated two-pore K<sup>+</sup> channel (Kunkel et al., 2000). *unc-110* has since been renamed *twk-18*. To test if *unc-93* or *sup-10* also acted as regulatory subunits of this two-pore channel, we tested whether the paralysis of *twk-18(cn110ts)* gf mutants could be suppressed by lf mutations in these two genes. We found that two *unc-93(lf)* mutations and one *sup-10(lf)* mutation were unable to suppress the severe paralysis of *twk-18(cn110ts)* mutants (Table 1), indicating that *unc-93* and *sup-10* do not encode essential units of *twk-18* and may be instead specific to the *sup-9* channel. *twk-18* expresses K<sup>+</sup>-selective temperature-sensitive currents when expressed in *Xenopus* oocytes, indicating that it may not require any regulatory subunits at all (Kunkel et al., 2000). These results suggest that some two-pore K<sup>+</sup> channels in *C. elegans* may not associate with regulatory subunits.

### **References**

Brenner, R., Perez, G. J., Bonev, A. D., Eckman, D. M., Kosek, J. C., Wiler, S. W., Patterson, A. J., Nelson, M. T., and Aldrich, R. W. (2000). Vasoregulation by the beta1 subunit of the calcium-activated potassium channel, *Nature* 407, 870-6.

Goldstein, S. A., Bockenhauer, D., O'Kelly, I., and Zilberberg, N. (2001). Potassium leak channels and the KCNK family of two-P-domain subunits, *Nat Rev Neurosci* 2, 175-184.

Greenwald, I. S., and Horvitz, H. R. (1980). *unc-93(e1500)*: A behavioral mutant of *Caenorhabditis elegans* that defines a gene with a wild-type null phenotype, *Genetics* 96, 147-164.



Kunkel, M. T., Johnstone, D. B., Thomas, J. H., and Salkoff, L. (2000). Mutants of a temperature-sensitive two-P domain potassium channel, *J Neurosci* *20*, 7517-7524.

Levin, J. Z., and Horvitz, H. R. (1993). Three new classes of mutations in the *Caenorhabditis elegans* muscle gene *sup-9*, *Genetics* *135*, 53-70.

McManus, O. B., Helms, L. M., Pallanck, L., Ganetzky, B., Swanson, R., and Leonard, R. J. (1995). Functional role of the beta subunit of high conductance calcium- activated potassium channels, *Neuron* *14*, 645-650.

Table 1. The rubberband Unc paralysis of *twk-18(cn110ts)* gf mutants cannot be suppressed by If mutations in *unc-93* or *sup-10*.

<b>Genotype</b>	<b>Bends/min <math>\pm</math> SEM</b>	<b>Range</b>
Wild-type	28.2 $\pm$ 1.3	(23.5-36)
<i>twk-18(cn110ts)</i>	0.1 $\pm$ 0.1	(0-0.5)
<i>unc-93(n392) dpy-17(e164); twk-18(cn110ts)</i>	0.0 $\pm$ 0.0	(0-0.5)
<i>unc-93(n394) dpy-17(e164); twk-18(cn110ts)</i>	0.1 $\pm$ 0.1	(0-1)
<i>twk-18(cn110ts) sup-10(e2127) lin-15(n7675)</i>	0.2 $\pm$ 0.2	(0-2)

Body-bends of young adults were scored during a 60 second interval at 30°C, since the *cn110ts* mutation is temperature sensitive. For all strains, n=12.

Figure 1. Overexpression of *sup-9(gf)* Cannot Bypass the Need for *unc-93*

A. Transgenic male animals were scored on a bacterial lawn for locomotory rate. All strains contained the *lin-15(n765)* mutation to enable the identification of transgenic animals by the nonMuv phenotype conferred by wildtype *lin-15* in the transgenic array. Transgenic lines were generated and locomotion assays were performed as described (Chapter 2). The *n1550* mutation was introduced into the  $P_{myo-3}$ *sup-9* plasmid (Chapter 2) using standard PCR techniques.

B. Confocal images of a representative adult transgenic animal (top) and its nontransgenic sibling (bottom). Epifluorescence images are on the left, Normarski images to the right. Scale bar is 10  $\mu$ m. Animals were fixed as described and stained with the SUP-9(N) antiserum (Chapter 2). This antiserum does not stain the endogenous SUP-9 channel in nontransgenic animals because its expression level is too low.

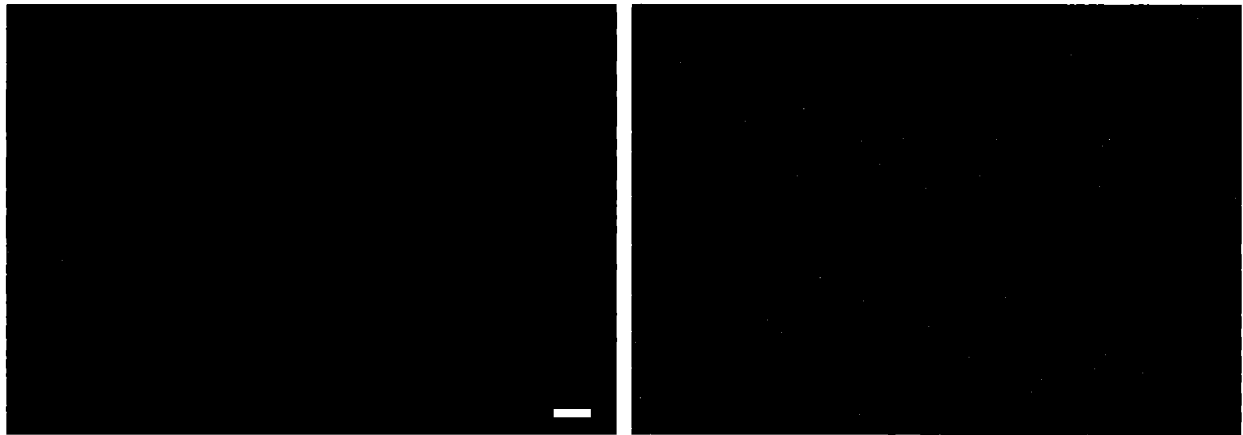
# Figure 1

A

Genotype	Locomotion (bends/min $\pm$ SEM)
wildtype	26.3 $\pm$ 1.8
<i>unc-93(lr12); nEx myo-3::sup-9(n1550)#1</i>	26.6 $\pm$ 1.6
<i>unc-93(lr12)/+; nEx myo-3::sup-9(n1550)#1</i>	0.5 $\pm$ 0.3
<i>unc-93(lr12); nEx myo-3::sup-9(n1550)#2</i>	26.8 $\pm$ 1.6
<i>unc-93(lr12)/+; nEx myo-3::sup-9(n1550)#2</i>	1.5 $\pm$ 0.4
<i>unc-93(lr12); nEx myo-3::sup-9(n1550)#3</i>	26.0 $\pm$ 1.2
<i>unc-93(lr12)/+; nEx myo-3::sup-9(n1550)#3</i>	0.7 $\pm$ 0.4

10 males of each phenotype were scored for locomotory rate

B



*unc-93(lr12); nEx P<sub>myo-3</sub>sup-9(n1550)*



*unc-93(lr12)*

## CHAPTER THREE

### Regulation of the *C. elegans* Two-pore K<sup>+</sup> Channel *sup-9* by a Nitroreductase-like Transmembrane Protein

Ignacio Perez de la Cruz and H. Robert Horvitz

## Summary

Loss-of-function mutations in the *C. elegans* gene *sup-18* suppress the muscle contraction defects conferred by gain-of-function mutations in either the *sup-9* two-pore K<sup>+</sup> channel or in its proposed regulatory subunits *sup-10* and *unc-93*. We have cloned *sup-18* and found it encodes a type-three transmembrane protein whose cytoplasmic domain is similar to oxygen-insensitive nitroreductases. Native SUP-18 and SUP-9 copurify from wildtype muscle membranes indicating that they may form a complex *in vivo*. Overexpression data indicate that the SUP-10 subunit acts together with SUP-18 to activate the SUP-9 channel through a pathway that is independent of the UNC-93 subunit. Through analysis of a rare channel mutant and site-directed mutagenesis, we have identified a domain in the C-terminal cytoplasmic domain of SUP-9 that is required for its specific activation by SUP-18 and is conserved in two human channels.

## Introduction

Leak or background K<sup>+</sup> channels play a key role in establishing the membrane potential of resting cells and modulating their response to neurotransmitters and second messengers (Belardetti and Siegelbaum, 1988; Hawkins et al., 1993). The first metazoan leak channels cloned, *Drosophila* ORK1 (Goldstein et al., 1996) and human TWIK-1 (Lesage et al., 1996a), defined a new structural class of K<sup>+</sup> channels having four transmembrane domains (TMD) and two P-domains, highly conserved loop structures that line the K<sup>+</sup>-selective pore (Doyle et al., 1998; Heginbotham et al., 1994). To date, fourteen human two-pore channels have been cloned (reviewed by Goldstein et al., 2001; Patel and Honore, 2001). The activity of two-pore channels can be regulated by multiple chemical and physical factors including temperature (Maingret et al., 2000), membrane stretch (Maingret et al., 1999; Patel et al., 1998) arachidonic acid (Fink et al., 1998), pH (Duprat et al., 1997; Leonoudakis et al., 1998) volatile anesthetics (Patel et al., 1999; Sirois et al., 2000) and neurotransmitters (Millar et al., 2000; Talley et al., 2000). Although K<sup>+</sup> channels from other families such as the voltage-gated or inward rectifiers are regulated through interactions with regulatory subunits (reviewed by Hanlon and Wallace, 2002; Pongs et al., 1999), no regulatory subunits have been reported for two-pore channels from any organism.

Genome analysis of the nematode *C. elegans* has revealed over 50 two-pore K<sup>+</sup> channels (Wang et al., 1999; Wei et al., 1996). Two of these channels, *twk-18* and *sup-9*, regulate muscle contraction and have been molecularly characterized ((Kunkel et al., 2000) and Chapter 2). *sup-9(gf)* mutants display a flaccid paralysis, are egg-laying defective and display a rubberband uncoordinated (Unc) response: when prodded on the head, a mutant worm contracts and relaxes along its entire body without moving backwards, while a wild-type worm contracts its anterior end and moves away (Levin and Horvitz, 1993). Loss-of-function (lf) mutations in two other genes, *sup-10* and *unc-93*, completely suppresses the *sup-9(gf)* defects (Levin and Horvitz, 1993) while having wild-type phenotypes on their own (Greenwald and Horvitz, 1980). In addition, *gf* mutations in *sup-10* and *unc-93* also induce a rubberband Unc paralysis, which in turn can be suppressed by lf mutations in *sup-9*, *sup-10* and *unc-93* (De Stasio et al., 1997; Greenwald and Horvitz, 1986; Greenwald and Horvitz, 1980). These and other genetic interactions support a model in which SUP-10 and UNC-93 form a protein complex with the SUP-9 two-pore K<sup>+</sup> channel *in vivo* and modulate its activity as channel regulatory subunits ((Greenwald and Horvitz, 1980) and Chapter 2). *unc-93*

encodes a proposed multi-pass transmembrane protein that shares amino acid similarities with predicted proteins encoded by several *Drosophila* and human ESTs, suggesting that two-pore K<sup>+</sup> channels in other species might also be modulated by regulatory subunits (Levin and Horvitz, 1992 and Chapter 2).

Lf mutations in the gene *sup-18* strongly suppress the muscle defects caused by a gf mutation in the proposed *sup-10* channel subunit while weakly suppressing those caused by gf mutations in *unc-93* or *sup-9*, indicating that *sup-18* may encode a positive effector of the proposed SUP-9/SUP-10/UNC-93 two-pore channel complex (Greenwald and Horvitz, 1986; Levin and Horvitz, 1993). In this study we have expanded the genetic analysis of *sup-18*-mediated channel activation and report the molecular cloning and characterization of *sup-18*. We find that *sup-18* encodes a nitroreductase-like transmembrane protein that associates with SUP-9 in muscle membranes. Gene dosage and overexpression data indicate that the gf mutation in the *sup-10* proposed subunit results in hypersensitivity to levels of *sup-18*. This and other genetic data support a model where the proposed channel subunit SUP-10 is bifunctional, serving both as an essential component of the channel complex and as a regulator of SUP-9 channel activation by SUP-18. In addition, we have identified two serine residues in the C-terminal intracellular domain of SUP-9 that are specifically required for channel activation by SUP-18 but not for activation by the UNC-93 regulatory subunit and are conserved in the human two-pore channels TASK-1 (KCNK3) and TASK-3 (KCNK9). Our findings indicate that two-pore channels can be regulated by multiple subunits *in vivo*, and that these subunits modulate channel activity through different mechanisms.



## Results

### ***sup-18* is Specifically Required for the Activation of the *sup-9* Channel by the Proposed *sup-10* Subunit**

Worms with the *n983 gf* mutation in the proposed *sup-10* channel subunit have a reduced locomotory rate compared to wild-type animals, as assayed by the body-bends they make per minute on a bacterial lawn (Table 1). Lf mutations in *sup-18* strongly suppress the locomotion defects of *sup-10(gf)* mutants (Table 1). By contrast, *sup-18(lf)* mutations only partially suppress the locomotion defects of a *gf* mutation in the *sup-9* channel or in the other proposed subunit *unc-93* (Greenwald and Horvitz, 1986; Levin and Horvitz, 1993) (Table 1). Although *sup-9(gf); sup-18(lf)* mutants are still severely paralyzed, these double mutants are healthier and can be maintained as a strain while *sup-9(gf)* mutants cannot be propagated, indicating that *sup-18(lf)* mutations do reduce the severity of the defects caused by the *sup-9(gf)* mutation.

We hypothesized that the *sup-18(lf)* mutation may be unable to suppress the defects caused by the *unc-93(gf)* or the *sup-9(gf)* mutations because the paralysis in these animals was very severe, while the comparatively weaker defects of *sup-10(gf)* mutants may be easier to suppress. To test this hypothesis, we examined the suppressor activity of *sup-18(lf)* mutations on an *unc-93(gf)* mutant whose severe paralysis had been alleviated. Lf mutations in the other essential channel subunit *sup-10* completely suppresses the paralysis of *unc-93(gf)* mutants (Greenwald and Horvitz, 1980). Thus, we reasoned that an *unc-93(gf)* mutant carrying only a partial lf mutation in *sup-10* would be partially suppressed. To isolate weak *sup-10* lf mutations, we performed an F<sub>2</sub> EMS genetic screen for partial suppressors of the locomotion defects of *unc-93(e1500) gf* mutants. From 17,500 haploid genomes screened, we isolated over 30 strong suppressors and seven weak suppressors. We assigned two of the seven weak suppressors, *n4025* and *n4026*, to the *sup-10* locus. *unc-93(e1500); sup-10(n4025)* and *unc-93(e1500); sup-10(n4026)* double mutants showed an improved locomotory rate over *unc-93(e1500)* animals (Table 1). Introduction of a *sup-18(lf)* mutation into these motile mutants improved their locomotion rates (from approximately 14 to 19 body-bends/minute), but they remained below those of either wild-type animals or *unc-93(e1500)* mutants carrying a null mutation in the *sup-9* channel (~27 body-bends/minute) (Table 1). These results indicate that the *sup-18* preferential suppression of *sup-10(gf)* over *unc-93(gf)* locomotion defects is not the result of

differences in the severity of their respective phenotypes, but rather reflects a requirement for *sup-18* in channel activation by the *sup-10(gf)* mutation.

Rather than reflecting a specific interaction between *sup-18* and *sup-10*, the observed differential suppression could alternatively be explained by an accumulation of multiple mutations on the channel complex. The channel complex may just barely be able to tolerate a physical disruption created by the *sup-10(gf)* mutation, but a second mutation in another component, *sup-18*, could further destabilize the complex resulting in loss of channel activity and full suppression. In this model, the *unc-93(gf)* mutation may be well tolerated, such that additional mutations in *sup-18* would only slightly destabilize the channel and therefore cause only a very weak suppression of its paralysis. To test this model, we introduced an activated *sup-9(gf)* channel into a *sup-18(lf); sup-10(gf)* background as a way to check the status of the channel complex. If the *sup-18(lf); sup-10(gf)* combination indeed had destabilized the channel complex then we expected the activated *sup-9(gf)* channel to be unable to induce paralysis. On the contrary, we found that the triple mutant was completely paralyzed (Table 1), indicating that an activated channel can function in a *sup-18(lf)* and *sup-10(gf)* mutant background. This result strongly suggests that the specific suppression of *sup-10(gf)* defects by mutations in *sup-18* is not the result of an accumulation of mutations on the channel complex.

### **In *sup-10(gf)* Mutants, the Activity of the SUP-9 Channel is Sensitive to Levels of SUP-18**

In addition to its absolute requirement for *sup-18* activity, we found that the severity of the paralysis in *sup-10(gf)* mutants was sensitive to *sup-18* levels. While *sup-10(gf)* males are severely Unc (4.7 bends/min) and *sup-18(n1030); sup-10(gf)* double mutants appear wild-type (31.7 bends/min), *sup-18(n1030)/+; sup-10(gf)* males show an intermediate phenotype (15.2 bends/min) (Table 2). This haploinsufficiency was observed for all *lf* alleles of *sup-18* tested (Table 2), including the null alleles *n1030* and *n1033* (see later), consistent with a sensitivity to gene dosage rather than a dominant negative effect by the *sup-18(n1030)* mutation. By contrast, the null channel mutation *sup-9(n1913)* behaved recessively in suppressing *sup-10(gf)* defects, indicating that *sup-10(gf)* mutants are specifically sensitive to levels of *sup-18* and not generally sensitive to the levels of any component of the proposed channel complex. We reasoned that while the paralysis caused by the *sup-10(gf)*-subunit was sensitive to

the levels of *sup-18* and not to those of the *sup-9* channel, this sensitivity could reflect a general effect of *sup-18* on any gf channel mutation. For instance, if SUP-18 were a rate-limiting component of the channel complex, then a reduction of SUP-18 levels by half would reduce the number of mutant channels and thus alleviate the paralysis. If this were the case then a reduction in SUP-18 levels would affect the severity of any channel mutation and not just that of *sup-10(gf)*. Thus, we tested if the severity of the locomotion defect of *unc-93(gf); sup-10(n4025)* mutants was sensitive to *sup-18* levels and found that it was not (Table 2). The locomotion rate of *unc-93(gf); sup-10(n4025)* males heterozygous for *sup-18(n1030)* (9.8 bends/min) was similar to that of worms wild-type for *sup-18* (10.0 bends/min) (Table 2). Therefore, we propose that the gf *n983* mutation in the *sup-10* subunit creates a hypersensitivity of SUP-9 channel activity to levels of SUP-18.

### **Molecular Cloning of *sup-18***

To understand the molecular mechanism by which SUP-18 increases the SUP-9 channel activity we cloned the gene using a positional mapping approach. *sup-18* had previously been mapped to the interval between *daf-4* and *unc-32* on LGIII (Greenwald and Horvitz, 1986). Using three-point mapping we further refined its map position to the interval between *ncl-1* and *unc-36* (see Experimental Procedures) (Figure 1A). Transformation rescue experiments with cosmids spanning the *ncl-1/unc-36* interval and with smaller cosmid subclones identified a 4.5 kb minimal rescuing fragment from cosmid C02C2 that restored the rubber-band Unc phenotype as a transgene to *sup-18(n1010); sup-10(n983)* mutants (Figure 1A). This rescuing fragment contained a single predicted gene, C02C2.5 (Consortium, 1998). We screened a mixed-stage cDNA library (Barstead and Waterston, 1989) using the smallest cosmid subclone and obtained a single partial cDNA of this predicted gene. We refined its gene structure through RT-PCR and through RACE experiments (see Experimental Procedures) (Figure 1B).

*sup-18* encodes a predicted protein of 325 amino acids with similarity to the “classical” oxygen-insensitive nitroreductases of enteric bacteria, including *E. coli* NfsB (Zenno et al., 1996), and to the *T. thermophilus* Nox oxidase (Park et al., 1992a) (Figure 1C). In addition, a *Drosophila* and a mouse predicted gene share significant amino acid homology with SUP-18 (Figure 1C), which we have named *dsup-18* and *msup-18* respectively. The partial genomic sequence of a predicted human gene of 184 amino

acids (Genebank Acc#CAA19772) is 91% identical to the mouse gene, indicating that *sup-18* also has a human counterpart. SUP-18, dSUP-18 and mSUP-18 all have a hydrophobic region preceding the nitroreductase domain that may serve as a transmembrane domain (Figure 1A). SUP-18 shares no amino acid similarity to the cytoplasmic regulatory subunits of voltage-gated K<sup>+</sup> channels, which are members of the NAD(P)H-dependent oxidoreductase superfamily (McCormack and McCormack, 1994).

The active site of nitroreductases contains a tightly-bound flavin cofactor (Hecht et al., 1995; Kobori et al., 2001; Koike et al., 1998; Lovering et al., 2001). The FMN binding site in *E. coli* NfsB, the minor oxygen-sensitive nitroreductase, is formed by the side chains of amino acids R10, S12, K14, N71, K74, K205 and R207 (Lovering et al., 2001), Figure 2C). Four of these residues are identical in SUP-18 (R10, S12, N71 and K205), while the other three, K14R, K74S and R207K, have substitutions to amino acids that predicted to retain hydrogen-bonding ability. The *T.t.*Nox oxidase contains a similar K14R substitution as SUP-18 relative to NfsB that preserves the hydrogen bond with the FMN cofactor as revealed by its crystal structure (Hecht et al., 1995). The K74 hydrogen bond in NfsB is also absent from the *T. thermophilus* enzyme. Residues S39 and N42 of NfsB provide van der Waals interactions to a bound nicotinic acid (Lovering et al., 2001), which represents the bound NAD(P)H substrate. These residues are conserved in SUP-18 as S163 and N167, respectively. The conservation of residues predicted to form the binding site for a flavin cofactor and for an NAD(P)H substrate suggest that SUP-18 may have nitroreductase activity *in vivo*.

### **Analysis of *sup-18* Mutations**

To confirm the identity of *sup-18* and to uncover structure-function relationships, we sequenced the *sup-18* coding sequence in mutant strains carrying If mutations in *sup-18*. We identified molecular lesions in all 18 mutant strains analyzed (Table 3, Figure 1C). The *sup-18(n1030)* and *sup-18(n1038)* mutations are predicted to delete the nitroreductase domain, while the *n1033* mutation leads to the substitution of the initiator methionine for an isoleucine. Since the next three ATG sequences in the *sup-18* cDNA are out of frame, any translational products would be nonfunctional. The other seven missense mutations disrupt residues within the nitroreductase domain. The *sup-18(n1471)* mutation results in a G259S substitution at a highly conserved glycine residue. In a genetic screen for *E. coli* mutants resistant to 5-nitrofurans derivatives

(Whiteway et al., 1998), If mutants in NfsB were identified including 17 missense mutations whose locations are indicated (Figure 1C). One of these mutations results in the same glycine to serine substitution as that caused by *sup-18(n1467)*. Other NfsB mutations include the FMN-binding N71 and R207 residues, which are conserved in SUP-18.

### **The *thermophilus* Nox Oxidase Carrying the Equivalent Mutation to *sup-18(n1010)* is Catalytically Inactive**

A missense mutation, *sup-18(n1010)*, results in an S137N substitution at a serine residue that in NfsB makes three hydrogen bonds with the FMN cofactor, two with the phosphate group and one with the ribityl tail, and thus such a mutation may disrupt enzymatic activity (Lovering et al., 2001). This serine also forms two hydrogen bonds with FMN in *T.t.NoX* (Figure 2A) (Hecht et al., 1995). To test the hypothesis that the *sup-18(n1010)* mutation would disrupt enzymatic activity, we generated GST and MBP fusions to the intracellular domain of SUP-18 and expressed them in *E. Coli*. Both fusion proteins were expressed poorly, partially degraded during purification and their protein preparations were contaminated with endogenous nitroreductases (I.P and H.R.H. unpublished data). Thus, we tested the effects of the *n1010* mutation on the related *T.t.NoX* enzyme (Figure 1A). The equivalent serine-to-asparagine mutation (S19N) into the *T.t.NoX* enzyme, which generates H<sub>2</sub>O<sub>2</sub> upon reduction of O<sub>2</sub> with NADH (Park et al., 1992b) and assayed its NADH oxidase activity from heat-denatured *E. coli* extracts. The lysates from cells expressing the mutant Nox consistently yielded 20-30% less Nox protein than those expressing the wild-type form (Figure 2B) along with a disproportionate 40-fold decrease in NADH oxidase activity (Figure 2C). These results suggest that if SUP-18 has an enzymatic activity *in vivo*, the *sup-18(n1010)* mutation results in a catalytic null.

### **SUP-18 Colocalizes with SUP-9 in Muscle Membranes**

To examine the expression pattern of *sup-18* we introduced the coding sequence of *gfp* between codons 88 and 89 of *sup-18* in its genomic context (see Experimental Procedures). Transgenic animals displayed GFP fluorescence in body-wall, vulval and defecation muscles (Figures 3A-C). In body-wall muscle cells the SUP-18::GFP fusion localized to dense body structures on the cell surface. Dense bodies are functionally analogous to vertebrate Z-lines which connect the myofibril lattice to the cell membrane

(Waterston et al., 1980). SUP-9 and UNC-93 have also been shown to localize to these structures (Chapter 2). In addition to muscle expression, three neurons in the head also displayed GFP staining (Figure 3D and data not shown). We have previously observed expression of a *sup-9::gfp* reporter in the four SIA interneurons (Chapter 2). We stained the *sup-18::gfp* transgenic lines with an anti-CEH-17 antibody, which labels the four SIA neurons and the ALA neuron (Pujol et al., 2000), and found that the neurons expressing the *sup-18::gfp* fusion were not the SIAs (data not shown).

We generated rabbit polyclonal antisera against amino acids 1 through 258 of recombinant SUP-18 (see Experimental Procedures). This antibody generated a robust signal in whole-mount immunostainings of transgenic animals that overexpress the *sup-18* cDNA under the muscle-specific *myo-3* promoter. However, it failed to give a signal above background in nontransgenic siblings, suggesting that endogenous *sup-18* is expressed at low levels (Figure 3E and data not shown). To test if SUP-18 colocalized with the SUP-9/SUP-10/UNC-93 channel complex *in vivo*, we generated transgenic animals carrying both a the  $P_{myo-3}sup-18$  and a *sup-10::gfp* transgene. SUP-18 and SUP-10::GFP colocalized in the dense bodies of muscle membranes (Figure 3E), as did SUP-9 and SUP-10::GFP, suggesting that SUP-18 may be a fourth component of the proposed SUP-9/SUP-10/UNC-93 complex *in vivo*.

### Protein Complex Formation

Since many NAD(P)H-binding proteins can be purified by pseudoaffinity chromatography with blue dextran sepharose (Thompson et al., 1975), we tested if native SUP-18 could bind to this resin. Detergent solubilized SUP-18 from wild-type worm membranes bound to the resin (Figure 4A) and could be eluted with buffer containing 1.2M NaCl but not with 1mM NADH, NADPH, FAD or ATP. This suggests that the interaction of SUP-18 with the resin is likely not the result of specific binding by an NAD(P)H-binding site.

We used this interaction between SUP-18 and blue sepharose in pulldown experiments to determine if, as their colocalization suggested, SUP-18 formed a complex *in vivo* with the SUP-9 channel. As detected by two anti-SUP-9 C-terminal and one anti-SUP-9 N-terminal antisera, SUP-9 co-purified with SUP-18 in the blue sepharose-bound fractions (Figure 4B). Although SUP-9 may bind to the resin directly and presently this possibility has not been tested, these results are consistent with the formation of a protein complex *in vivo*.

### **SUP-18 Membrane Topology**

Because SUP-18 lacks a signal sequence at its N-terminus, it may adopt either a type-two or type-three transmembrane topology with its nitroreductase domain residing extracellularly or intracellularly, respectively. To distinguish between these two models, we generated transgenic animals expressing SUP-18:: $\beta$ -Galactosidase gene fusions and assayed  $\beta$ -galactosidase activity *in vivo* in fixed animals (Figure 5). When  $\beta$ -galactosidase is expressed intracellularly it is enzymatically active, whereas expression extracellularly results in loss of activity (Froshauer et al., 1988; Silhavy and Beckwith, 1985). The use of  $\beta$ -galactosidase activity to elucidate membrane topology of *C. elegans* proteins *in vivo* has previously been reported for the presenillin SEL-12 protein (Li and Greenwald, 1996) and for the MEC-4 sodium channel subunit (Lai et al., 1996). Fixed transgenic animals expressing  $\beta$ -Galactosidase fused to either the C-terminal region of SUP-18 or immediately following its putative TMD showed robust  $\beta$ -Galactosidase activity (Figure 5). Introduction of a synthetic transmembrane domain between SUP-18 and  $\beta$ -Galactosidase in these chimeras reverses the membrane orientation of the  $\beta$ -Galactosidase and eliminates enzymatic activity (Figure 5).

These results suggest that the nitroreductase domain of SUP-18 resides intracellularly, but they do not formally distinguish between a type-three transmembrane protein and a cytoplasmic protein that simply localizes to the cell surface. To test directly if the putative transmembrane domain of SUP-18 can indeed behave as a transmembrane domain, we inserted a signal sequence at the N-terminus of SUP-18 (see Experimental Procedures). While the putative extracellular domain of SUP-18 lacking the TMD resides intracellularly as expected, introduction of a signal sequence leads to its secretion (Figure 5). In contrast, when either the SUP-18 putative transmembrane domain or the synthetic transmembrane domain is added to this SUP-18:: $\beta$ -Galactosidase fusion, enzymatic activity is restored. These results indicate that the putative transmembrane domain of SUP-18 can indeed serve as a transmembrane domain, and suggest that SUP-18 is likely a type-three integral membrane protein.

### **Overexpression of Catalytically-Impaired SUP-18(n1010) at the Cell Surface Fails to Rescue a *sup-18(lf)* Null Mutant**

To establish an assay for *in vivo sup-18* activity, we expressed the *sup-18* coding sequence under the control of the *myo-3* promoter in *sup-18(n1033); sup-10(n983)* mutant animals. While *sup-10(n983)* *gf* mutant animals have defective locomotion, double mutants carrying the *sup-18(n1033)* null mutation have improved locomotory rates (Figure 6A). Overexpression of  $P_{myo-3}gfp$  in these *sup-18(n1033); sup-10(n983)* animals had little effect on their locomotory rate, while overexpression of  $P_{myo-3}sup-18$  transgene restored *sup-18* activity and *sup-10(gf)*-induced paralysis (Figure 6A). In addition to their paralysis, all *sup-18* transgenic *sup-18(n1033); sup-10(n983)* animals assayed for locomotion also displayed the rubberband Unc response when prodded (n=48). These results further confirm the *gfp* expression data suggesting that *sup-18* functions in muscle to regulate the *sup-9* channel. Overexpression of two  $P_{myo-3}sup-18$  constructs containing the missense mutation *n1554* or the proposed catalytically-null mutation *n1010* did not restore *sup-18* activity to *sup-18(n1033); sup-10(n983)* mutants (Figure 6A), confirming that the rescue by overexpression of *sup-18* is dependent on its wildtype activity. Using anti-SUP-18 antiserum, we stained two of the transgenic lines overexpressing *sup-18(n1010)* to test if this putative catalytic null was expressed and localized properly. We found that overexpressed SUP-18(n1010) protein was localized to the dense bodies on the cell surface of muscle cells (Figure 6B). Thus, these transgenic lines have a functionally inactive form of SUP-18 localized to the cell surface. Together with our finding that *T.t.NoX* carrying the *sup-18(n1010)* catalytic mutation has impaired oxidase activity, this result argues that binding of a cofactor to SUP-18, and possibly an enzymatic activity dependent on the cofactor, is necessary for SUP-18 at the cell surface to activate the SUP-9 channel.

### **Mouse SUP-18 Cannot Substitute for SUP-18 *in vivo***

We further tested if *msup-18* (Figure 1C) was able to substitute for *sup-18* in worms. The locomotion rate of *sup-18(n1033); sup-10(n983)* animals transgenic for  $P_{myo-3}msup-18$  was indistinguishable from those transgenic for  $P_{myo-3}gfp$  alone (Figure 6A), indicating that mSUP-18 cannot function of *C. elegans*. To test if the inability of *msup-18* to substitute for *sup-18* was the result of poor heterologous expression, we tagged mSUP-18 with GFP at its C-terminus. Animals transgenic for this construct displayed GFP fluorescence in dense bodies of muscle cells (Figure 6C) similar to that observed for the SUP-18::GFP fusion (Figure 3A). These results suggest that



mSUP-18 is translated and localized to the cell surface properly but has lost an activity that prevents activation of the SUP-9 channel.

### **Overexpression of the Nitroreductase Domain of SUP-18 in Muscle Is Sufficient to Restore *sup-18* Activity *in vivo***

To confirm our membrane topology results and to determine the structural requirements of *sup-18* activity, we tested if overexpression of the *sup-18* intracellular domain was sufficient to restore *sup-18* activity to *sup-18(n1033); sup-10(n983)* mutants. Interestingly, transgenic expression of the intracellular nitroreductase domain alone induced a rubber-band Unc paralysis in *sup-18(n1033); sup-10(n983)* animals, albeit less severely than full-length *sup-18* (Figure 6A). This finding suggests that the extracellular and transmembrane domains of SUP-18 are dispensible for its *in vivo* function, and further confirms the intracellular assignment for the nitroreductase domain.

We reasoned that the SUP-18 intracellular domain was localizing to the cell surface in these rescued transgenic animals in order to activate the SUP-9. We tagged the intracellular domain of SUP-18 with GFP at its N-terminus and found that transgenic animals expressing this fusion protein displayed *gfp* fluorescence mostly in the cytoplasm of muscle cells, but some GFP::SUP-18(Intra) was localized to dense bodies (Figure 6D). A *gfp*-alone control was expressed solely in the cytoplasm and was excluded from the dense bodies (Figure 6D). We introduced the  $P_{myo-3}gfp::sup-18(intra)$  transgenic array into strains containing *sup-9(n1913)*, *sup-10(n3558)*, *unc-93(lr12)* or *sup-18(n1030)* null mutations and found that the membrane localization remained unchanged (data not shown). This suggests that SUP-18 may interact with another dense body protein that is independent of its proposed interaction with SUP-9.

### ***sup-18* Overexpression Specifically Enhances the Defects of *sup-10(gf)* but not those of *unc-93(gf)* Mutants**

Overexpression of *sup-18* in *sup-18(n1033); sup-10(n983)* animals rescued the *sup-18(lf)* mutation and restored the rubberband Unc paralysis caused by the *sup-10(gf)* mutation, but this paralysis was stronger than that of *sup-10(n983)* mutants alone (Figure 6A). This suggested that extra *sup-18* activity could enhance the paralysis caused by the *sup-10(gf)* mutation, consistent with our previous observation that *sup-18(lf)/+; sup-10(gf)* males lacking one copy of *sup-18* had an improved locomotory rate over *sup-10(gf)* animals having two wild-type copies of *sup-18* (Table 2). Thus, it

appeared that the severity of the paralysis in animals with a *gf* mutation in the *sup-10* subunit was directly correlated with *sup-18* levels. We hypothesized that SUP-18 normally activates the SUP-9 channel at a basal level, but in a *sup-10(gf)* mutant the channel becomes hypersensitive to SUP-18 activation such that a strict dependence between levels of *sup-18* and the severity of the observed paralysis is created.

To test if the hyperparalyzed phenotype of worms overexpressing *sup-18* was dependent on the *sup-10(gf)* mutation or was the result of a toxic effect arising from the overexpression of a nitroreductase-like transmembrane protein, we overexpressed *sup-18* in animals wildtype for *sup-9*, *sup-10*, *sup-18* and *unc-93*. *lin-15* transgenic lines overexpressing a *lin-15* coinjection marker either alone or together with  $P_{myo-3}sup-18$  had indistinguishable locomotion rates, indicating that both the overexpression of *sup-18* in itself is not toxic and that overexpressed *sup-18* cannot activate the *sup-9* channel and induce paralysis in a wild-type genetic background (Table 4). We introduced the extrachromosomal arrays containing the transgenes from these animals into *sup-10(n983) lin-15* double mutants by mating, so that each resulting strain would contain the same transgenes as the parent strain and therefore would overexpress *sup-18* to equivalent levels. *sup-18* overexpression induced a severe paralysis in *sup-10(n983) lin-15* animals relative to control transgenic animals expressing *lin-15* alone (0.1 and 0.0 vs. 5.7 and 5.4, bends/minute, respectively) (Table 4). By contrast, overexpression of the *sup-9* channel from a  $P_{myo-3}sup-9$  transgene in *sup-10(n983); lin-15* animals did not reduce their locomotion compared to animals expressing *lin-15* alone (6.0 and 5.1 vs 5.7 and 5.4 bends/minute, respectively), indicating that the paralysis caused by *sup-18* overexpression in *sup-10(gf)* mutants was specific and not the result of the *myo-3*-driven overexpression of a membrane protein. In addition, compared to control *sup-10(gf)* animals that overexpressed either no transgene, *lin-15* alone or the *lin-15 sup-9* combination, *sup-10(gf)* mutants overexpressing *lin-15-sup-18* were smaller in size (Figures 7A-D). Their smaller size resembled that of severely paralyzed mutants carrying a *sup-9(gf)* channel mutation (Figure 7E).

The results above indicate that overexpression of *sup-18* but not of *sup-9* creates a hyperparalysis in *sup-10(gf)* but not in *sup-10(+)* animals. To test if this hyperparalysis was specific to animals with a *gf* mutation in *sup-10* or was general to any channel *gf* mutation, we tested if overexpression of *sup-18* could induce a hyperparalysis in *unc-93(gf)* mutants. Overexpression of *sup-18* in these mutant animals had no effect on either their appearance (Figures 7F,G) or their locomotion rate

(Table 4) compared to control animals overexpressing *lin-15* alone; but because *unc-93(gf)* animals are already severely paralyzed a hyperparalysis would be difficult to score. Since *sup-10(gf)* and *unc-93(gf)* mutants have reduced brood sizes compared to wild-type animals (Levin and Horvitz, 1993), we assayed the transgenic lines for an enhancement of this phenotype by *sup-18*. Similar to its enhancement of locomotion defects, overexpression of *sup-18* reduces the brood size of *sup-10(gf)* mutants from an average of 74 and 75 to 27 and 17 progeny per animal, respectively (Table 4). These low brood sizes are comparable to those found in the severely paralyzed *sup-9(gf)*; *sup-18(lf)* mutants (Table 4). By contrast, the brood sizes of *unc-93(gf)* transgenic animals remained unchanged (35 and 43 vs. 37 and 40) upon *sup-18* overexpression (Table 4). Thus, overexpression of *sup-18* specifically enhances the phenotypes *sup-10(gf)* mutants (locomotion rate, body size and brood size), driving the severity of their defects past that of *unc-93(gf)* mutants and into the range of strains with a severe *sup-9(n1550) gf* mutation. These findings support a model where the *sup-10(gf)* mutation activates the *sup-9* channel by creating a hypersensitivity to *sup-18*.

#### ***sup-9(n1435)* Mutants Are Insensitive to *sup-10(gf)/sup-18*-Dependent Activation**

Lf mutations in the *sup-9* channel suppress the defects caused by gf mutations in the proposed subunits *sup-10* and *unc-93* equally well (Greenwald and Horvitz, 1986; Greenwald and Horvitz, 1980). This is expected, as mutations that eliminate SUP-9 channel activity would prevent channel activation by gf mutations in either of its regulatory subunits. By contrast, the *sup-9(n1435)* mutation preferentially suppresses defects caused by the *sup-10(gf)* over the *unc-93(gf)* mutation ((Levin and Horvitz, 1993) and Figure 8A). Thus, the mutant SUP-9(n1435) channel appears resistant to activation by one subunit but not by the other. We proposed earlier based on the *sup-18* gene dosage experiments that the *sup-10(gf)* mutation activates the *sup-9* channel by creating a hypersensitivity to *sup-18*. Thus, we reasoned that if *sup-9(n1435)* is resistant to activation by the *sup-10(gf)* mutation, then it should also be insensitive to activation by *sup-18*. If so, the partial suppressive effects of *sup-9(n1435)* and *sup-18(lf)* mutations on the defects of *unc-93(gf)* mutants would not be additive in the triple mutant, as in the absence of *sup-18* activity the *n1435* mutation conferring *sup-18* insensitivity would be irrelevant. Because the suppressive effect of these mutations on the locomotion rate of *unc-93(gf)* mutants is very weak (Table 1 and Figure 8B), detecting small additive effects by this assay is unreliable. To circumvent

this technical difficulty, we scored suppression of the low brood size of *unc-93(gf)* mutants. *unc-93(gf)* mutants have a low brood size that can be restored to wild-type levels by a null mutation in the *sup-9* channel (Figure 8B). The *sup-9(n1435)* and *sup-18(n1030)* mutations each increase the brood size of *unc-93(gf)* mutants two to three fold, but the triple mutant is no more suppressed than the *unc-93(gf); sup-18(n1030)* double mutant (Figure 8B). An unrelated missense mutation, *sup-9(n264)* also incompletely suppressed the low brood size of *unc-93(gf)* mutants, but unlike *sup-9(n1435)*, the triple mutant with *sup-18(n1030)* displays a strong additive suppressive effect, restoring their brood size to the level of *sup-9(null); unc-93(gf)* mutants (Figure 8B). The lack of an additive effect in their suppression of the *unc-93(gf)* brood size defect indicates that the *sup-9(n1435)* and *sup-18(n1030)* mutations suppress by the same mechanism, consistent with the model that *sup-9(n1435)* is insensitive to activation by *sup-18*.

We further tested the model that SUP-9(n1435) cannot be activated by SUP-18 through a second strategy that does not involve the *unc-93(gf)* mutation. In addition to its preferential suppression of *sup-10(gf)* defects, *sup-9(n1435)* is unusual in that it strongly suppressed the locomotion defects of *sup-10(gf)* animals as a heterozygote ((Levin and Horvitz, 1993) and Figure 8C). Since *sup-18(lf)* mutations also suppressed *sup-10(gf)* as heterozygotes, we asked if their suppressive effects as heterozygotes were additive. We reasoned that if the *sup-9(n1435)* channel mutation created an insensitivity to *sup-18*, then reducing SUP-18 levels in a *sup-9(n1435)/+; sup-10(n983)* mutant would have little effect in their locomotory rate. Indeed, *sup9(n1435)/+; sup-18(lf)/+; sup-10(gf)* mutant males moved only slightly better than *sup-9(n1435)/+; sup-10(gf)* animals ( $21.6 \pm 0.9$  vs  $23.7 \pm 0.6$ , mean  $\pm$  SEM, respectively) (Figure 8C). This small change is likely due to the presence of wild-type *sup-9* channels in these heterozygotes, which still would be responsive to *sup-18* activation. The control dominant negative allele of the *sup-9* channel *n3977* showed a strong enhancement by *sup-18(lf)/+* in the triple mutant strain *sup-9(n3977)/+; sup-18(lf)/+; sup-10(gf)* ( $21.3 \pm 0.6$  vs.  $28.5 \pm 0.5$  bends/minute, mean  $\pm$  SEM, respectively) (Figure 8C). These results indicate that as observed for its effect on *unc-93(gf)* brood size, the *n1435* channel mutation creates an indifference towards the activity of *sup-18* in *sup-10(gf)* mutants.

### **The *sup-9(n1435)* Mutation Affects a Conserved Region in the C-terminal Domain of SUP-9**

We sequenced the *sup-9* coding region in *sup-9(n1435)* mutants and identified a C-to-T transition within codon 292, resulting in a serine-to-phenylalanine substitution within the predicted intracellular C-terminal domain of SUP-9 (Figure 9A). Although *sup-9* is 41% to 47% identical in amino acid sequence over its entire region to several TASK-family two-pore K<sup>+</sup> channels, the C-terminal cytoplasmic domain of SUP-9 is poorly conserved with these channels (Figure 9A). However, the serine affected by the *n1435* mutation is contained within to a small region of similarity between these channels with the general structure SxxSCxC (Figure 9A). We have named this region the SC Box, for Serine-Cysteine-rich. The residues in the SC Box do not correspond to any reported motifs, including phosphorylation sites, as defined by the protein motif database PROSITE (Bucher and Bairoch, 1994). Variations of the SC Box are found in the human TASK-1 and TASK-3 channels and in two *Drosophila* two-pore channels (Figure 9A). We have not found an SC Box in other human two-pore channels (data not shown) or in TWK-4 (C40C9.1), a *C. elegans* two-pore channel of unknown function, that at 41% amino acid identity is the most closely related *C. elegans* channel to SUP-9 (Figure 9A).

### **Residue S289 in the SC Box of SUP-9 Is also Required for its Specific Activation by SUP-18**

To better understand how it mediates activation by *sup-10(gf)/sup-18*, we undertook an *in vivo* mutagenesis study of the SC Box. We singly mutated the residues S289, C293 and C295 to alanines and compared their ability to suppress the egg-laying defects of *sup-10(gf)* compared to *unc-93(gf)sup-18(lf)* mutants. We used egg-laying assays because they provide an alternative to locomotion assays that is well suited for quantitatively scoring suppression in a high-throughput fashion. When assayed over a three hour window, both mutant strains lay less than one egg per hour, while a null mutation in *sup-9* increased egg-laying behavior several fold in both strains (Figure 9B). Overexpression of a *sup-9* cDNA driven by the *myo-3* promoter ( $P_{myo-3}sup-9(wt)$ ) in either mutant background did not increase egg-laying in three independent transgenic lines. By contrast, overexpression of a *sup-9* cDNA containing the *n1435* mutation ( $P_{myo-3}sup-9(n1435)$ ) dominantly suppressed the egg-laying defects of *sup-10(gf)* mutants but not those of *unc-93(e1500)sup-18(n1030)* animals (Figure 9B). These results establish an *in vivo* assay for detecting mutations in *sup-9* that preferentially suppress *sup-10(gf)* over *unc-93(gf)* mutations and are consistent with the preferential

suppression of locomotion rates by *sup-9(n1435)*-containing strains described earlier (Figure 8).

Like  $P_{myo-3}sup-9(n1435)$ , a  $P_{myo-3}sup-9(S289A)$  transgene suppressed the defects caused by the *sup-10(gf)* but not the *unc-93(gf)sup-18(lf)* mutations. By contrast, the cysteine-to-alanine mutations at residues 293 and 295 suppressed both the *sup-10(gf)* and *unc-93(gf)sup-18(lf)* activities (Figures 9B). Since mutations in either cysteine suppressed both the defects caused by both *gf* mutations, these cysteines may be required to mediate channel activation by both *sup-10(gf)* and *unc-93(gf)*; alternatively they may be important for channel stability or structure, such that their disruption results in a nonfunctional SUP-9 channel that when overexpressed behaves as a dominant negative to the wild-type SUP-9. To distinguish these possibilities, we replaced the region of the *sup-9* cDNA encoding its C-terminal cytoplasmic domain with that of *twk-4*, which does not encode an SC Box (Figure 9A). We reasoned that if the cysteine residues of the SC Box were serving a structural role, the C-terminal domain of another two-pore channel may functionally substitute in this role. As a transgene, the *sup-9::twk-4* fusion suppressed the *sup-10(gf)* egg-laying defects, consistent with the requirement of an SC Box for *sup-10(gf)*-dependent channel activation. By contrast, the *sup-9::twk-4* transgene did not suppress the egg-laying defects of an *unc-93(gf)* mutant, indicating that the SUP-9::TWK-4 channel lacking cysteines 293 and 295 was competent for activation. These results indicate that the SC Box is dispensable for *unc-93(gf)*-dependent activation and that the cysteines in the SC box may serve an essential channel function distinct from activation by regulatory subunits.

## Discussion

### ***sup-18* Encodes a Muscle Transmembrane Protein with an Intracellular Nitroreductase Domain**

In this work, we have cloned a positive effector of the *C. elegans sup-9* two-pore K<sup>+</sup> channel and found it encodes a transmembrane protein with an intracellular nitroreductase domain. The regulation of mammalian K<sup>+</sup> channels from other families by regulatory subunits has been well studied (Hanlon and Wallace, 2002). Regulatory subunits have been characterized that associate with channels from the K<sub>v</sub>, slo, HERG, KCNQ, K<sub>ir</sub> and SK families (see Chapter 1). By contrast, only two subunits have been identified that regulate two-pore channels in any organism, those encoded by the *C. elegans* genes *unc-93* (Chapter 2) and *sup-10* (Cummins, Levin, Horvitz, Anderson, unpublished results). Although a physical interaction between SUP-18 and SUP-9 remains to be rigorously tested, our colocalization data and copurification of these two proteins are consistent with SUP-18 being a new channel regulatory subunit. The existence of *sup-18* and *unc-93* (Chapter 2) homologs in *Drosophila* and humans indicates that the regulation of two-pore K<sup>+</sup> channels by multiple regulatory subunits may be a common mechanism for increasing K<sup>+</sup> channel functional diversity.

Gf mutations in the proposed SUP-9/SUP-10/UNC-93 channel complex have been proposed to result in an excess K<sup>+</sup> efflux from muscle cells, causing membrane hyperpolarization and a rubberband-Unc paralysis (Chapter 2). Two lines of evidence support this model. First, pharmacological hyperpolarization of body-wall muscle cells with the GABA Cl<sup>-</sup> channel agonist muscimol induces a rubberband Unc response similar to that induced by gf mutations in the channel complex (Chapter 2). Secondly, gf mutations in the muscle two-pore K<sup>+</sup> channel *twk-18* result in both 30-fold larger K<sup>+</sup> currents when expressed in *Xenopus* oocytes and in a rubberband-Unc phenotype *in vivo*. Thus, pharmacological hyperpolarization of muscle and mutations in another muscle two-pore channel that increase its conductance both lead to a rubberband response. Since *sup-18(lf)* mutations reduce the severity of the rubberband Unc phenotypes of the *sup-9(gf)* and *unc-93(gf)* mutants, SUP-18 is likely required for full activation of the SUP-9 two-pore K<sup>+</sup> channel.

The molecular identification of *sup-18* provides an insight into the possible mechanism by which SUP-18 may increase SUP-9 channel activity and thus lead to paralysis in *sup-10(gf)* mutants. The nitroreductase domain of SUP-18 is similar to that of the “classical” oxygen-insensitive nitroreductases of enteric bacteria, such as *E. coli*

NfsB (Zenno et al., 1996) or a nitroreductase from *Salmonella typhimurium* (Watanabe et al., 1990). These enzymes reduce a wide variety of nitroaromatic, quinone and flavin compounds (Watanabe et al., 1998; Zenno et al., 1996). The NOX NADH oxidase from *Thermus thermophilus*, which reduces O<sub>2</sub> to generate H<sub>2</sub>O<sub>2</sub>, also shares similarity to SUP-18. The presence of an intracellular catalytic domain in SUP-18 with conserved cofactor binding residues suggests that SUP-18 may activate the SUP-9 channel through an enzymatic reaction involving O<sub>2</sub>, nitroaromatics, quinones or flavins. The importance of the nitroreductase domain in activating SUP-9 is underscored by the ability of the intracellular domain of SUP-18 alone to restore the locomotion defects of a *sup-18* null mutant in *sup-18(lf); sup-10(gf)* animals. Although full-length *sup-18* showed a more robust rescue than the intracellular domain, the intracellular domain was sufficient to confer a strong locomotion defect and a rubberband Unc response to transgenic animals similar to that of *sup-18(+); sup-10(gf)* animals. While the ability of full-length *sup-18* to induce a stronger locomotion defect may be indicative of a direct role for the extracellular and transmembrane domain in activating the SUP-9 channel, it is more likely that the role of these domains is simply to increase the concentration of SUP-18 at the cell surface. Neither dSUP-18 nor mSUP-18 contain a predicted extracellular domain, further suggesting that this domain in SUP-18 may be functionally irrelevant. Furthermore, no missense mutations were isolated that affected only the extracellular domain. Together, these findings indicate that the nitroreductase domain of SUP-18 is necessary and sufficient to activate the SUP-9 channel.

While the nitroreductase domain of SUP-18 may be sufficient to activate the SUP-9 channel, the mechanism by which this activation occurs is less clear. When the equivalent substitution to the serine-to-asparagine residue found in *sup-18(n1010)* was introduced into *T.t.NOX*, its NADH-oxidase activity was greatly reduced. Since this serine contacts the phosphate group of the bound FMN cofactor in *T.t.NOX* (Hecht et al., 1995), such a mutation likely disrupts the proper binding of FMN needed for catalysis. Antibody staining of overexpressed SUP-18(n1010) protein indicates that the protein is synthesized and trafficked to the plasma membrane. Since this mutant was localized to the membrane but could not activate SUP-9, we conclude that either cofactor binding and/or catalysis are required to activate the SUP-9 channel.

The binding of a flavin cofactor by a regulatory subunit as a prerequisite for activation of a channel raises the intriguing possibility that SUP-18 may couple the metabolic state of muscle cells with membrane excitability. The mammalian K<sub>v</sub>β



voltage-gated K<sup>+</sup> channel regulatory subunits (reviewed by Pongs et al., 1999), which belong to the aldo-keto reductase superfamily (Gulbis et al., 1999; McCormack and McCormack, 1994), have also been proposed to couple metabolic state with cell excitability based on indirect evidence. K<sub>v</sub>β2 has an NADP<sup>+</sup> cofactor bound in its active site and a catalytic triad spaced appropriately to engage in enzymatic activity (Gulbis et al., 1999). Although suggestive of an enzymatic activity, no substrate has been reported for K<sub>v</sub>β subunits. Disruption of NADPH-binding or catalytic residues alters the ability of K<sub>v</sub>β subunits to increase the surface expression or modify the gating kinetics of voltage-gated K<sup>+</sup> channels when both are coexpressed in heterologous systems (Bähring et al., 2001; Campomanes et al., 2002; Peri et al., 2001). However, while knockout mice for K<sub>v</sub>β2 have seizures and reduce lifespans, mice carrying a catalytic null mutation in K<sub>v</sub>β2 have a wild-type phenotype, suggesting that if an enzymatic activity for K<sub>v</sub>β2 did exist, it is functionally dispensable *in vivo* (McCormack et al., 2002). By contrast to the dispensability of K<sub>v</sub>β2 enzymatic activity *in vivo*, the catalytic mutant *sup-18(n1010)* behaves like a null mutation in worms in its inability to activate the SUP-9 channel, even though the SUP-18(n1010) protein is synthesized and localized to the cell surface of muscle cells.

### **SUP-10(gf) Likely Activates the SUP-9 Two-pore Channel by Creating a Hypersensitivity to SUP-18**

We found that *sup-10(gf)* mutants are hypersensitive to levels of *sup-18*, both by analyzing *sup-18* heterozygotes and by overexpressing *sup-18*. By contrast, *unc-93(gf)* mutants are not sensitive to changes in the levels of *sup-18* by these same criteria. We propose two alternate biochemical models to explain how the *sup-10(gf)* but not the *unc-93(gf)* mutation may lead to hyperactivation of SUP-9 by SUP-18 (Figure 10). SUP-10 and UNC-93 have an essential role in supporting channel activity, as *gf* mutations in *sup-9* are completely suppressed by *sup-10(lf)* and *unc-93(lf)* mutations (Levin and Horvitz, 1993). This activation is diagramed in both models as two parallel arrows from SUP-10 and UNC-93 to SUP-9, both of which must be present for SUP-9 channel activity. Because *sup-18(lf)* mutations only partially reduce the severity of the *sup-9(gf)* paralysis, a smaller input from SUP-18 to SUP-9 is indicated by a smaller arrow. In the SUP-10 repressor model, SUP-10 antagonizes the activation of SUP-9 by SUP-18 (Figure 10A). In a *sup-10(gf)* mutant, this repression is lost, and SUP-18 is unchecked to activate SUP-9 channel activity resulting in paralysis. In the *sup-10*

activator model, SUP-10 normally enhances SUP-18 activation of SUP-9 (Figure 10B). In a *sup-10(gf)* mutant, this enhancement is increased, resulting in excessive activation of SUP-9 by SUP-18. Both of these models account for both the hypersensitivity to *sup-18* gene dosage levels in *sup-10(gf)* mutants and for the indifference towards them in *unc-93(gf)* mutants.

Although our present data cannot conclusively distinguish between the two models, our data favors the repressor model. Overexpression of SUP-18 in a wild-type background did not result in paralysis (Table 4). This may be best explained by the repressor model, where wild-type SUP-10 would be present to inhibit any excessive hyperactivation. In these transgenic animals, the levels of SUP-18 are expected to far exceed those of SUP-10, as *sup-18* was overexpressed by the strong *myo-3* promoter from the extrachromosomal arrays having multiple copies of the expression plasmid. Therefore, we propose that this suppression likely would not occur through a direct interaction between SUP-10 and SUP-18, but rather through an interaction between SUP-10 and SUP-9 that prevents channel activation by SUP-18. SUP-10 is a predicted type-one transmembrane protein of 332 amino acids with a short 12 amino acid intracellular domain (Cummins, Levin, Horvitz and Anderson, unpublished results). The *gf* mutation in *sup-10(n983)* is a late nonsense mutation that deletes this intracellular domain. Therefore, we propose that this domain may inhibit the activation of SUP-9 by SUP-18, for instance, by blocking access to the SUP-9 SC Box region, such that in the SUP-10(*gf*) this domain is deleted and SUP-18 activation proceeds unchecked.

### **Activation of the SUP-9 Two-Pore Channel by Multiple Subunits Proceeds through Distinct Domains**

To better understand the mechanism by which multiple subunits regulate a two-pore channel, we have characterized the unusual *sup-9(n1435)* mutation and have described four of its important properties. First, SUP-9(*n1435*) channels cannot be activated by SUP-10(*gf*). Second, SUP-9(*n1435*) channels are insensitive to SUP-18 activity. Third, SUP-9(*n1435*) channels can be activated by UNC-93(*gf*). Fourth, heterodimeric channels of SUP-9(*n1435*) and wild-type proteins can not be activated by SUP-10(*gf*). Together, the first three properties of *sup-9(n1435)* provide strong evidence for our general models (Figure 10). The existence of a channel mutation that is insensitive to both SUP-18 and SUP-10(*gf*) indicates that these two inputs activate through a common mechanism as postulated. Furthermore, a mutant channel that can

be activated by UNC-93(gf) but not by SUP-10(gf) is also consistent with an independent pathway for SUP-9 activation by UNC-93.

Through our molecular analysis of the *sup-9(n1435)* lesion and through site-directed mutagenesis, we have defined a domain in SUP-9 that is required for SUP-10(gf)-specific activation. We have named this domain the SC Box. Although the SC Box is conserved in the human TASK-1 and TASK-3 channels, no function has yet been assigned to the SC Box in these channels. The ability of a SUP-9::TWK-4 chimera to differentially support the gf activity of *sup-10* over that of *unc-93* mutations confirms the importance of the SC Box in activation by SUP-10(gf)/SUP-18. The location of the gf mutations in *sup-10* and *unc-93* are consistent with their different sites of action on the SUP-9 channel. In the *sup-10(gf)* mutant, the intracellular domain of this type-one transmembrane protein is deleted, allowing the intracellular nitroreductase domain of SUP-18 to activate the SUP-9 channel through the intracellular SC Box; by contrast, the *unc-93(e1500)* gf mutation results in a glycine-to-arginine substitution at amino acid 388 in one of the putative TMDs (Levin and Horvitz, 1992) of this multipass transmembrane protein, and thus UNC-93(gf) may activate SUP-9 through a TMD to TMD interaction, irrespective of the SC Box or the rest of the cytoplasmic domain.

SUP-9 is closely related to the subfamily of two-pore K<sup>+</sup> channels formed by human TASK-1 and TASK-3 (Chapter 2). TASK-1 is activated by multiple factors including extracellular pH (Duprat et al., 1997; Leonoudakis et al., 1998; Lopes et al., 2000), inhalational anesthetics such as halothane (Patel et al., 1999) and oxygen (Lewis et al., 2001). TASK-1 is directly inhibited by sub-micromolar levels of anandamide (Maingret et al., 2001) and by the actions of neurotransmitters such as Thyrotropin Releasing Hormone (TRH) (Talley et al., 2000). The TASK-1 domains responsive to regulation by pH, halothane and TRH have been identified. A histidine residue in the first P-domain of TASK-1 modulates its sensitivity to pH (Lopes et al., 2001), while a six amino acid stretch following its fourth TMD is required for both halothane activation and TRH suppression (Patel et al., 1999; Talley and Bayliss, 2002). Interestingly, deletion of the TASK intracellular C-terminal domain, which contains the SC Box, does not change its basal activity or activation by halothane (Patel et al., 1999; Talley and Bayliss, 2002). Thus, the SC Box in TASK-1 may represent an activation domain that is required by one type of channel activator (human SUP-18) but not by others (halothane and pH).

Our finding that a two-pore channel is be regulated by two subunits through distinct domains is reminiscent of the regulation of Ca<sup>+2</sup>-activated voltage gated (or Slo)

channels. Slo channels are gated by two stimuli, voltage and calcium (McManus et al., 1995; Wallner et al., 1995). Voltage sensitivity is mediated by a positively charged transmembrane domain (Bezanilla, 2000), while activation by  $\text{Ca}^{+2}$  occurs through a domain on the intracellular C-terminal tail named the calcium bowl (Figure 11) (Schreiber and Salkoff, 1997). Likewise, SUP-9 is regulated in two ways. Much like voltage activation of Slo channels, UNC-93 likely stabilizes the open conformation of SUP-9 independently of the intracellular C-terminal domain and through interactions between their respective transmembrane domains, especially since the *unc-93(e1500)* mutation alters a glycine in a predicted transmembrane domain. Similar to Slo channel activation by  $\text{Ca}^{+2}$ , SUP-10/SUP-18 activate SUP-9 through the SC Box in the SUP-9 C-terminal cytoplasmic domain (Figure 11).

Another common feature of these two channels is the regulation of a channel activating input, SUP-18 or calcium, by a regulatory subunit, SUP-10 or Slo  $\beta$  subunits, respectively. The  $\beta 1$  or  $\beta 4$  subunits of Slo channels alter the endogenous sensitivity of Slo1 channels to activation by intracellular  $\text{Ca}^{2+}$  (Brenner et al., 2000a; Brenner et al., 2000b; McManus et al., 1995). Likewise, our data supports a model where SUP-10 regulates the sensitivity of the SUP-9 channel to SUP-18 activation, such that in the SUP-10(gf) mutant the SUP-9 channel is hypersensitive to SUP-18. Thus, both SUP-9 and Slo channels are able to set their activity levels after integrating two regulatory inputs, both of which are modulated by regulatory subunits.

## Experimental Procedures

### Strains and genetics

*C. elegans* strains were cultured as described (Brenner, 1974) except that *Escherichia Coli* strain HB101 was used instead of OP50 as a food source. Strains were grown at 20°C unless otherwise noted. The following mutations were used in this study:

LGII *sup-9*(n264, n1435, n1550, n1913, n3977).

LGIII *unc-93*(e1500sd), *sma-3*(e491), *mec-14*(u55), *ncl-1*(e1865), *unc-36*(e251).

*sup-18*(n463, n527, n528, n1010, n1014, n1015, n1022, n1033, n1030, n1035, n1036, n1038, n1471, n1539, n1548, n1554, n1556, n1558).

LGX *sup-10*(n983, n4025, n4026, n183, n1008), *lin-15*(n765ts).

### Mapping and Cloning of *sup-18*

34 *Sma* nonUnc and 23 Unc non-*Sma* progeny were isolated from a *sma-3 mec-14 ncl-1 unc-36/sup-18* parent. Scoring of the *ncl-1* and *sup-18* phenotypes yielded a recombination breakdown of *sma-3*(30/57) *ncl-1*(3/57) *sup-18*(24/57) *unc-36*. A pool of cosmids C33C3, C08C3, C27D11, C02C2, C39F10 and C44C9 at 1ng/μL and *rol-6* marker (Mello et al., 1991) at 80ng/μL was injected into *sup-18*(n1010); *sup-18*(n983) animals. Two Rol transgenic lines were obtained, one of which gave rubberband Unc animals. Cosmids were injected separately and C02C2 yielded (5/5) rescued lines, while transformation rescue with cosmids C08C3 (0/7), C27D11 (0/5) and C39F10 (0/9) showed no rescue.

RT-PCR was carried out on cDNA from the wild-type N2 strain using primers 5'-TTGAAAACCCCTGTAAATAC-3' and 5'-CGAGTTTCTAATAAAAATAAACC-3'. PCR products were cloned into pBSKII (Stratagene) and their sequence determined. 5' and 3' RACE was performed using their corresponding kits (Gibco).

### Molecular Biology

Genomic subclones of cosmid C02C2 were generated in pBSKII (Stratagene). The subclones, in the other they are shown (Figure 1), and spanned the following sequences (Genebank Acc#L23649): *Eco* RV (9,790) – *Eco* RV (21,098); *Pst* I (23,699) – *Pst* I (32,833); *Pst* I (23,699) – *Sac* I (28,185); *Bst* BI (24,448)– *Sac* I (28,185); and *Hind* III (24,671) – *Hind* III (27,169).

All PCR amplifications used in plasmid construction were performed using *Pfu* polymerase, and the sequence of their products determined to avoid introducing unintended mutations. The  $P_{myo-3}sup-18$  ectopic expression vector was generated by PCR-amplification of their respective coding regions from the cDNA using primers that introduced *Nhe* I and *Sac* I sites at the 5' and 3' ends respectively, and cloned into vector p95.86 (from A. Fire).  $P_{myo-3}sup-18(intra)$  was similarly constructed except that the 5' primer began at codon 66 of *sup-18*. The *gfp*-tagged version of this vector was created by PCR amplification of the *gfp* coding sequence from vector p95.77 (from A. Fire) and subcloned into  $P_{myo-3}sup-18(intra)$  just prior to the start codon of the *sup-18* sequence.

$P_{myo-3}msup-18$  was generated by PCR amplification of the coding region of the mouse cDNA (Gene Bank AK002363) with 5' and 3' primers containing *Nhe* I and *Eco* RV sites, respectively, and subcloning the PCR products into p95.86 at its *Nhe* I and *Sac* I (blunted) sites.  $P_{myo-3}msup-18::gfp$  was generated by a similar strategy using a 5' primer containing an *Nhe* I site and a 5' primer that did not include the stop codon of *msup-18* but instead contained a *Bam* HI site. The *myo-3* promoter from p95.86 was subcloned into p95.77, such that upon subcloning of the *msup-18* PCR fragment into the *Nhe* I and *Bam* HI sites of the vector the *myo-3* promoter drove expression of the *msup-18* gene fused in frame at its 3' end to *gfp*.

The GST::*sup-18*(N) and MBP::*sup-18*(N) fusions used to generate and purify rabbit polyclonal anti-SUP-18 antibodies were generated by PCR amplification of codons 1-258 from the *sup-18* cDNA and subcloning the products into the pGEX-2T (Pharmacia) and pMal-2c (NEB) vectors.

The *sup-18::gfp* genomic fusion was constructed by introducing *Sph* I sites at the ends of a *gfp* cassette by PCR amplification of plasmid pPD95.77 (from A. Fire) and subsequent subcloning into the single *Sph* I site contained within a 9.1 kb *Pst* I genomic *sup-18* rescuing fragment. The resulting fusion contained 6.5 kb of promoter sequence, the entire *sup-18* coding region with *gfp* inserted between the transmembrane and nitroreductase domains and 1.1 kb of 3' UTR and downstream sequence.

The *sup-10::gfp* fusion used in colocalization studies was constructed by subcloning a 7.3 kb *Mfe* I genomic fragment from cosmid C27G6 containing *sup-10* into the *Eco* R I site of pBSKII. A 6.4 kb *Pst* I fragment was subcloned from this vector into p95.77, which contained 3.5 kb of promoter sequence and the *sup-10* coding region.

Through PCR techniques, we introduced a *Sal*I site immediately preceding the stop codon of *sup-10* to create an in-frame fusion with the *gfp* coding sequence.

*sup-18::β-galactosidase* hybrid fusions were created by PCR amplification of 1869 bp of 5' *sup-18* promoter sequence and subcloning the product into the *Sph*I and *Pst*I sites of p34.110 (from A. Fire) to generate P<sub>*sup-18*</sub>TM-β-Gal, which contains a synthetic transmembrane sequence followed by the B-galactosidase coding sequence (Fire et al., 1990). *sup-18* genomic coding sequence spanning codons 1-42, 1-70 and 1-301 were PCR-amplified from the minimal rescuing fragment with 5' and 3' primers that contained *Pst*I and *Bam*HI sites respectively, and subcloned into these sites in P<sub>*sup-18*</sub>TM-β-Gal. The synthetic transmembrane domain was deleted from these plasmids by excising the *Kpn*I fragment containing this domain. A signal sequence (Perry et al., 1993) was inserted into these vectors by standard PCR techniques. *sup-9* constructs for the SC box.

The full-length *twk-4* cDNA was cloned by RT-PCR with primers 5'-CTCTGCTAGCAATGCATCAAATTGACGGAAAATCTGC-3' AND 5'-AGAGGATCCATATAGTTCAAGATCCACCAGATG-3' from wt mixed-stage RNA. The sequence of the *twk-4* cDNA obtained was in agreement with its predicted sequence (Genebank Acc#AF083646). The C-terminal cytoplasmic domain of *sup-9* from the P<sub>*myo-3*</sub>*sup-9* vector (lgs) codons (257-329) was replaced by *twk-4* codons (265-365) using standard ligation PCR techniques to generate P<sub>*myo-3*</sub>*sup-9::twk-4*. Site-directed mutagenesis of the SC Box in the P<sub>*myo-3*</sub>*sup-9* vector or of the *T.t. nox* expression vector pTNADOX (Park et al., 1992b) were likewise introduced.

### **Nox Enzymatic Assays**

*E. coli* BL21 cultures (15 ml) containing a control ampicillin resistance vector pPD95.77, the recombinant *T.t.NoX* vector pTNADOX or the pTNADOX vector containing the S19N mutation were induced with 1 mM IPTG at OD<sub>600</sub> = 0.6 and grown for an additional 3 hours at 37°C. Cell pellets were resuspended in 1 ml TEN buffer (50 mM Tris pH 7.5, 200 mM NaCl, 1 mM EDTA) and sonicated on ice to lyse cells. Cell debris was removed by centrifugation, and soluble protein was heat denatured at 72°C for 90 minutes. Insoluble proteins were removed by centrifugation and used directly in enzymatic assays. Assay mixtures contained 50 mM Tris pH 8.5, 165 μM NADH (Sigma) and 20 μL of enzyme mix. The change in absorbance of NADH at OD<sub>340</sub> was used to monitor the reaction rate during the first minute when reaction rates were linear.

To compare Nox protein levels between preparations, 200  $\mu$ L of lysate was incubated with 30  $\mu$ L Blue Sepharose beads in 1 ml total volume of 50mM Tris pH 8.5, allowed to bind for 10 minutes at room temperature, and washed three times with the same buffer. Proteins bound to Blue Sepharose were resuspended in 100  $\mu$ L total of 1X sample buffer and serial dilutions were resolved by SDS-PAGE and Coomassie Blue stainings.

### **Antibodies and Immunostaining**

The GST::SUP-18(N) fusion protein was expressed in *E. coli*, and the insoluble protein was purified by SDS-PAGE and used to immunize rabbits. Antisera was purified against the MBP::SUP-18 fusion immobilized on nitrocellulose strips, and eluted with 100mM glycine-HCL (pH 2.5).

For immunofluorescence experiments, mixed-stage worms were fixed in 1% paraformaldehyde for 2 hours at 4°C and permeabilized as previously described (Finney and Ruvkun, 1990). For colocalization studies, transgenic lines were stained with primary antibodies at 1:200 dilution, and a secondary goat-anti-rabbit antibody conjugated to Texas Red (Jackson Labs). Worms were viewed by indirect immunofluorescence microscopy and images captured with OpenLabs software or by viewed by confocal microscopy. Images were created using Photoshop software (Adobe Systems).

### ***In vivo* Pulldown Assays**

Wild-type membrane preps were obtained from 10 to 20 mL of frozen, packed, wild-type worms grown in liquid culture. All buffers used in the purification of membranes were supplemented with 1 mM DTT, 0.1% Aprotinin, 0.2 mM PMSF, 1 mM benzamidine and 1 mM Sodium Metabisulfite. Worms were lysed in 30 mL Homogenization Buffer (15 mM Hepes pH 7.6, 10 mM KCl, 5mM MgCl<sub>2</sub>, 0.1 mM EDTA, 0.5 mM EGTA and 350 mM sucrose) with 0.5 mm Glass beads (Biospec) in a Bead beater (Biospec) at 4°C for 15 minutes. Homogenate was filtered through two layers of Miracloth and centrifuged at 900 rpm in a SS34 rotor at 4°C for 15 minutes. NP-40 (0.2%) was added to the supernatant and centrifuged again at 8K in the same rotor. Pellets were dispersed with a glass Dounce using a B pestle in 5 mL homogenization buffer and centrifuged at 8K. Pellets were again dounced in 5mL of 1.5M sucrose buffer (15 mM Hepes pH 7.6, 60 mM KCl, 5mM MgCl<sub>2</sub>, 0.1 mM EDTA, 0.5 mM EGTA and 1.5M sucrose) and layered on tubes containing 5 mL of 2.1 M sucrose buffer (2.1 M



sucrose and the rest like 1.5M buffer). The remaining volume was made up with 1.5M sucrose buffer. Samples were centrifuged for 2 hours at 24.5K at 4°C. Membrane fractions were extracted from the interface between the sucrose layers (~ 2mL) and frozen at -20°C.

For pulldown experiments, 40  $\mu$ L of membrane fractions were added to 960  $\mu$ L of Binding Buffer (50 mM Tris pH 7.5, 200 mM NaCl, 1mM EDTA, 0.5 % NP-40) and rocked for 1 hour at 4°C. Samples were spun at 14K in a microcentrifuge and the supernatant was transferred to a fresh tube. 100  $\mu$ L fractions of solubilized membrane proteins were incubated with 20  $\mu$ L of Blue Sepharose Resin (Pharmacia) that had been washed extensively with Binding Buffer in 1 mL total of binding buffer for 1 hour at 4°C. Beads were washed five times with 1 mL of binding buffer for 10 minutes each, with low speed spins of 10 seconds at 3K to pellet beads. Beads were resuspended in 2X Sample Buffer (Chapter 2), resolved by SDS-PAGE, Western blotted onto nitrocellulose membranes and probed with anti-SUP-18 or anti-SUP-9(N) antisera. An HRP-Conjugated Goat-anti-Rabbit secondary was used (Pierce), and an enhanced chemiluminescence kit (Perkin-Elmer) was used to visualize proteins.

### **Transgenic Animals**

Germline transformation experiments were carried out using standard methods (Mello et al., 1991). Transgenes on strains carrying the *lin-15(n765ts)* mutation contained the coinjection marker pL15EK(*lin-15*) at 50 ng/ $\mu$ L (Clark et al., 1994) and transgenic animals were identified by their nonMuv phenotype at 22.5°C. The dominant *rol-6* plasmid was used at 100 ng/ $\mu$ L during cosmid rescue experiments, and transgenic animals were identified by their Rol phenotype. The dominant *myo-3::gfp* fusion vector p93.97 (from A fire) was used where indicated at 80 ng/ $\mu$ L, and transgenic animals were identified by *gfp* fluorescence. The experimental DNA was injected at 30-50 ng/ $\mu$ L.

## **Acknowledgments**

We thank Craig Ceol for critically reading this manuscript and for invaluable assistance in the purification of worm membrane fractions; Matthias Sprinzl for the plasmid pTNADOX; Andy fire for various *C. elegans* *gfp* and *LacZ* expression vectors; Beth Castor for assistance with allele sequencing; Beth DeStasio for her enthusiasm and discussions, and all the members of the Horvitz lab for their support. This work was funded by NIH Grant No. 24663. I.P. was funded by an NIH predoctoral training grant and an NSF Graduate Fellowship. H. R. H. is an Investigator of the Howard Hughes Medical Institute.

## References

- Bahring, R., Milligan, C. J., Vardanyan, V., Engeland, B., Young, B. A., Dannenberg, J., Waldschutz, R., Edwards, J. P., Wray, D., and Pongs, O. (2001). Coupling of voltage-dependent potassium channel inactivation and oxidoreductase active site of K<sub>v</sub>beta subunits, *J Biol Chem* 276, 22923-9.
- Barstead, R. J., and Waterston, R. H. (1989). The basal component of the nematode dense-body is vinculin, *J Biol Chem* 264, 10177-85.
- Belardetti, F., and Siegelbaum, S. A. (1988). Up- and down-modulation of single K<sup>+</sup> channel function by distinct second messengers, *Trends Neurosci* 11, 232-8.
- Bezanilla, F. (2000). The voltage sensor in voltage-dependent ion channels, *Physiol Rev* 80, 555-92.
- Brenner, R., Jegla, T. J., Wickenden, A., Liu, Y., and Aldrich, R. W. (2000a). Cloning and functional characterization of novel large conductance calcium-activated potassium channel beta subunits, hKCNMB3 and hKCNMB4, *J Biol Chem* 275, 6453-61.
- Brenner, R., Perez, G. J., Bonev, A. D., Eckman, D. M., Kosek, J. C., Wiler, S. W., Patterson, A. J., Nelson, M. T., and Aldrich, R. W. (2000b). Vasoregulation by the beta1 subunit of the calcium-activated potassium channel, *Nature* 407, 870-6.
- Brenner, S. (1974). The genetics of *Caenorhabditis elegans*, *Genetics* 77, 71-94.
- Bucher, P., and Bairoch, A. (1994). A generalized profile syntax for biomolecular sequence motifs and its function in automatic sequence interpretation, *Proc Int Conf Intell Syst Mol Biol* 2, 53-61.
- Campomanes, C. R., Carroll, K. I., Manganas, L. N., Hershberger, M. E., Gong, B., Antonucci, D. E., Rhodes, K. J., and Trimmer, J. S. (2002). K<sub>v</sub> beta subunit oxidoreductase activity and K<sub>v</sub>1 potassium channel trafficking, *J Biol Chem* 277, 8298-305.

Clark, S. G., Lu, X., and Horvitz, H. R. (1994). The *Caenorhabditis elegans* locus *lin-15*, a negative regulator of a tyrosine kinase signaling pathway, encodes two different proteins, *Genetics* 137, 987-997.

Consortium, *C. e. S.* (1998). Genome sequence of the nematode *C. elegans*: a platform for investigating biology., *Science* 282, 2012-2018.

De Stasio, E., Lephoto, C., Azuma, L., C., H., Stanislaus, D., and Uttam, J. (1997). Characterization of Revertants of *unc-93(e1500)* in *Caenorhabditis elegans* Induced by N-ethyl-N-nitrosourea, *Genetics* 147, 597-608.

Doyle, D. A., Morais Cabral, J., Pfuetzner, R. A., Kuo, A., Gulbis, J. M., Cohen, S. L., Chait, B. T., and MacKinnon, R. (1998). The structure of the potassium channel: molecular basis of K<sup>+</sup> conduction and selectivity, *Science* 280, 69-77.

Duprat, F., Lesage, F., Fink, M., Reyes, R., Heurteaux, C., and Lazdunski, M. (1997). TASK, a human background K<sup>+</sup> channel to sense external pH variations near physiological pH, *EMBO J* 16, 5464-5471.

Fink, M., Lesage, F., Duprat, F., Heurteaux, C., Reyes, R., Fosset, M., and Lazdunski, M. (1998). A neuronal two P domain K<sup>+</sup> channel stimulated by arachidonic acid and polyunsaturated fatty acids, *EMBO J* 17, 3297-3308.

Finney, M., and Ruvkun, G. (1990). The *unc-86* gene product couples cell lineage and cell identity in *C. elegans*, *Cell* 63, 895-905.

Fire, A. (1992). Histochemical techniques for locating *Escherichia coli* beta-galactosidase activity in transgenic organisms, *Genet Anal Tech Appl* 9, 151-8.

Fire, A., Harrison, S. W., and Dixon, D. (1990). A modular set of lacZ fusion vectors for studying gene expression in *Caenorhabditis elegans*, *Gene* 93, 189-98.

Froshauer, S., Green, G. N., Boyd, D., McGovern, K., and Beckwith, J. (1988). Genetic analysis of the membrane insertion and topology of MalF, a cytoplasmic membrane protein of *Escherichia coli*, *J Mol Biol* 200, 501-11.

Goldstein, S. A., Bockenhauer, D., O'Kelly, I., and Zilberberg, N. (2001). Potassium leak channels and the KCNK family of two-P-domain subunits, *Nat Rev Neurosci* 2, 175-184.

Goldstein, S. A., Price, L. A., Rosenthal, D. N., and Pausch, M. H. (1996). ORK1, a potassium-selective leak channel with two pore domains cloned from *Drosophila melanogaster* by expression in *Saccharomyces cerevisiae*, *Proc Natl Acad Sci USA* 93, 13256-13261.

Greenwald, I., and Horvitz, H. R. (1986). A visible allele of the muscle gene *sup-10X* of *C. elegans*, *Genetics* 113, 63-72.

Greenwald, I. S., and Horvitz, H. R. (1980). *unc-93(e1500)*: A behavioral mutant of *Caenorhabditis elegans* that defines a gene with a wild-type null phenotype, *Genetics* 96, 147-164.

Gulbis, J. M., Mann, S., and MacKinnon, R. (1999). Structure of a voltage-dependent K<sup>+</sup> channel beta subunit, *Cell* 97, 943-952.

Hanlon, M. R., and Wallace, B. A. (2002). Structure and function of voltage-dependent ion channel regulatory beta subunits, *Biochemistry* 41, 2886-94.

Hawkins, R. D., Kandel, E. R., and Siegelbaum, S. A. (1993). Learning to modulate transmitter release: themes and variations in synaptic plasticity, *Annu Rev Neurosci* 16, 625-65.

Hecht, H. J., Erdmann, H., Park, H. J., Sprinzl, M., and Schmid, R. D. (1995). Crystal structure of NADH oxidase from *Thermus thermophilus*, *Nat Struct Biol* 2, 1109-1114.

Heginbotham, L., Lu, Z., Abramson, T., and MacKinnon, R. (1994). Mutations in the K<sup>+</sup> channel signature sequence, *Biophys J* 66, 1061-1067.

Kobori, T., Sasaki, H., Lee, W. C., Zenno, S., Saigo, K., Murphy, M. E., and Tanokura, M. (2001). Structure and site-directed mutagenesis of a flavoprotein from *Escherichia coli* that reduces nitrocompounds: alteration of pyridine nucleotide binding by a single amino acid substitution, *J Biol Chem* *276*, 2816-23.

Koike, H., Sasaki, H., Kobori, T., Zenno, S., Saigo, K., Murphy, M. E., Adman, E. T., and Tanokura, M. (1998). 1.8 Å crystal structure of the major NAD(P)H:FMN oxidoreductase of a bioluminescent bacterium, *Vibrio fischeri*: overall structure, cofactor and substrate-analog binding, and comparison with related flavoproteins, *J Mol Biol* *280*, 259-73.

Kunkel, M. T., Johnstone, D. B., Thomas, J. H., and Salkoff, L. (2000). Mutants of a temperature-sensitive two-P domain potassium channel, *J Neurosci* *20*, 7517-7524.

Lai, C. C., Hong, K., Kinnell, M., Chalfie, M., and Driscoll, M. (1996). Sequence and transmembrane topology of MEC-4, an ion channel subunit required for mechanotransduction in *Caenorhabditis elegans*, *J Cell Biol* *133*, 1071-81.

Leonoudakis, D., Gray, A. T., Winegar, B. D., Kindler, C. H., Harada, M., Taylor, D. M., Chavez, R. A., Forsayeth, J. R., and Yost, C. S. (1998). An open rectifier potassium channel with two pore domains in tandem cloned from rat cerebellum, *J Neurosci* *18*, 868-877.

Lesage, F., Guillemare, E., Fink, M., Duprat, F., Lazdunski, M., Romey, G., and Barhanin, J. (1996a). TWIK-1, a ubiquitous human weakly inward rectifying K<sup>+</sup> channel with a novel structure, *EMBO J* *15*, 1004-1011.

Levin, J. Z., and Horvitz, H. R. (1992). The *Caenorhabditis elegans unc-93* gene encodes a putative transmembrane protein that regulates muscle contraction, *J Cell Biol* *117*, 143-155.

Levin, J. Z., and Horvitz, H. R. (1993). Three new classes of mutations in the *Caenorhabditis elegans* muscle gene *sup-9*, *Genetics* *135*, 53-70.

Lewis, A., Hartness, M. E., Chapman, C. G., Fearon, I. M., Meadows, H. J., Peers, C., and Kemp, P. J. (2001). Recombinant hTASK1 is an O<sub>2</sub>-sensitive K<sup>+</sup> channel, *Biochem Biophys Res Commun* 285, 1290-4.

Li, X., and Greenwald, I. (1996). Membrane topology of the *C. elegans* SEL-12 presenilin, *Neuron* 17, 1015-21.

Lopes, C. M., Gallagher, P. G., Buck, M. E., Butler, M. H., and Goldstein, S. A. (2000). Proton block and voltage gating are potassium-dependent in the cardiac leak channel *kcnk3*, *J Biol Chem* 275, 16969-16978.

Lopes, C. M., Zilberberg, N., and Goldstein, S. A. (2001). Block of Kcnk3 by protons. Evidence that 2-P-domain potassium channel subunits function as homodimers, *J Biol Chem* 276, 24449-52.

Lovering, A. L., Hyde, E. I., Searle, P. F., and White, S. A. (2001). The structure of *Escherichia coli* nitroreductase complexed with nicotinic acid: three crystal forms at 1.7 Å, 1.8 Å and 2.4 Å resolution, *J Mol Biol* 309, 203-13.

Maingret, F., Fosset, M., Lesage, F., Lazdunski, M., and Honore, E. (1999). TRAAK is a mammalian neuronal mechano-gated K<sup>+</sup> channel, *J Biol Chem* 274, 1381-1387.

Maingret, F., Lauritzen, I., Patel, A. J., Heurteaux, C., Reyes, R., Lesage, F., Lazdunski, M., and Honore, E. (2000). TREK-1 is a heat-activated background K<sup>+</sup> channel, *EMBO J* 19, 2483-2491.

Maingret, F., Patel, A. J., Lazdunski, M., and Honore, E. (2001). The endocannabinoid anandamide is a direct and selective blocker of the background K<sup>+</sup> channel TASK-1, *Embo J* 20, 47-54.

McCormack, K., Connor, J. X., Zhou, L., Ho, L. L., Ganetzky, B., Chiu, S. Y., and Messing, A. (2002). Genetic analysis of the mammalian K<sup>+</sup> channel beta subunit K<sub>v</sub>beta 2 (*Kcnab2*), *J Biol Chem* 277, 13219-28.

McCormack, T., and McCormack, K. (1994). Shaker K<sup>+</sup> channel beta subunits belong to an NAD(P)H-dependent oxidoreductase superfamily, *Cell* 79, 1133-1135.

McManus, O. B., Helms, L. M., Pallanck, L., Ganetzky, B., Swanson, R., and Leonard, R. J. (1995). Functional role of the beta subunit of high conductance calcium-activated potassium channels, *Neuron* 14, 645-650.

Mello, C. C., Kramer, J. M., Stinchcomb, D., and Ambros, V. (1991). Efficient gene transfer in *C. elegans*: extrachromosomal maintenance and integration of transforming sequences, *EMBO J* 10, 3959-3970.

Millar, J. A., Barratt, L., Southan, A. P., Page, K. M., Fyffe, R. E., Robertson, B., and Mathie, A. (2000). A functional role for the two-pore domain potassium channel TASK-1 in cerebellar granule neurons, *Proc Natl Acad Sci USA* 97, 3614-3618.

Park, H. J., Kreutzer, R., Reiser, C. O., and Sprinzl, M. (1992a). Molecular cloning and nucleotide sequence of the gene encoding a H<sub>2</sub>O<sub>2</sub>-forming NADH oxidase from the extreme thermophilic *Thermus thermophilus* HB8 and its expression in *Escherichia coli*, *Eur J Biochem* 205, 875-879.

Park, H. J., Reiser, C. O., Kondruweit, S., Erdmann, H., Schmid, R. D., and Sprinzl, M. (1992b). Purification and characterization of a NADH oxidase from the thermophile *Thermus thermophilus* HB8, *Eur J Biochem* 205, 881-885.

Patel, A. J., and Honore, E. (2001). Properties and modulation of mammalian 2P domain K<sup>+</sup> channels, *Trends Neurosci* 24, 339-46.

Patel, A. J., Honore, E., Lesage, F., Fink, M., Romey, G., and Lazdunski, M. (1999). Inhalational anesthetics activate two-pore-domain background K<sup>+</sup> channels, *Nat Neurosci* 2, 422-426.

Patel, A. J., Honore, E., Maingret, F., Lesage, F., Fink, M., Duprat, F., and Lazdunski, M. (1998). A mammalian two pore domain mechano-gated S-like K<sup>+</sup> channel, *EMBO J* 17, 4283-4290.



Peri, R., Wible, B. A., and Brown, A. M. (2001). Mutations in the K<sub>v</sub>beta 2 binding site for NADPH and their effects on K<sub>v</sub>1.4, *J Biol Chem* 276, 738-41.

Perry, M. D., Li, W., Trent, C., Robertson, B., Fire, A., Hageman, J. M., and Wood, W. B. (1993). Molecular characterization of the *her-1* gene suggests a direct role in cell signaling during *Caenorhabditis elegans* sex determination, *Genes Dev* 7, 216-28.

Pongs, O., Leicher, T., Berger, M., Roeper, J., Bähring, R., Wray, D., Giese, K. P., Silva, A. J., and Storm, J. F. (1999). Functional and molecular aspects of voltage-gated K<sup>+</sup> channel beta subunits, *Ann N Y Acad Sci* 868, 344-355.

Pujol, N., Torregrossa, P., Ewbank, J. J., and Brunet, J. F. (2000). The homeodomain protein CePHOX2/CEH-17 controls antero-posterior axonal growth in *C. elegans*, *Development* 127, 3361-71.

Schreiber, M., and Salkoff, L. (1997). A novel calcium-sensing domain in the BK channel, *Biophys J* 73, 1355-63.

Silhavy, T. J., and Beckwith, J. R. (1985). Uses of lac fusions for the study of biological problems, *Microbiol Rev* 49, 398-418.

Sirois, J. E., Lei, Q., Talley, E. M., Lynch, C., 3rd, and Bayliss, D. A. (2000). The TASK-1 two-pore domain K<sup>+</sup> channel is a molecular substrate for neuronal effects of inhalation anesthetics, *J Neurosci* 20, 6347-54.

Talley, E. M., and Bayliss, D. A. (2002). Modulation of TASK-1 (Kcnk3) and TASK-3 (Kcnk9) Potassium Channels. Volatile anesthetics and neurotransmitters share a molecular site of action, *J Biol Chem* 277, 17733-42.

Talley, E. M., Lei, Q., Sirois, J. E., and Bayliss, D. A. (2000). TASK-1, a two-pore domain K<sup>+</sup> channel, is modulated by multiple neurotransmitters in motoneurons, *Neuron* 25, 399-410.

Thompson, S. T., Cass, K. H., and Stellwagen, E. (1975). Blue dextran-sepharose: an affinity column for the dinucleotide fold in proteins, *Proc Natl Acad Sci U S A* 72, 669-72.

Wallner, M., Meera, P., Ottolia, M., Kaczorowski, G. J., Latorre, R., Garcia, M. L., Stefani, E., and Toro, L. (1995). Characterization of and modulation by a beta-subunit of a human maxi KCa channel cloned from myometrium, *Receptors Channels* 3, 185-99.

Wang, Z., Kunkel, M., Wei, A., Butler, A., and Salkoff, L. (1999). Genomic organization of nematode 4TM K<sup>+</sup> channels. In *Ann. N.Y. Acad. Sci.*, pp. 286-303.

Watanabe, M., Ishidate, M., Jr., and Nohmi, T. (1990). Nucleotide sequence of *Salmonella typhimurium* nitroreductase gene, *Nucleic Acids Res* 18, 1059.

Watanabe, M., Nishino, T., Takio, K., Sofuni, T., and Nohmi, T. (1998). Purification and characterization of wild-type and mutant "classical" nitroreductases of *Salmonella typhimurium*. L33R mutation greatly diminishes binding of FMN to the nitroreductase of *S. typhimurium*, *J Biol Chem* 273, 23922-8.

Waterston, R. H., Thomson, J. N., and Brenner, S. (1980). Mutants with altered muscle structure of *Caenorhabditis elegans*, *Dev Biol* 77, 271-302.

Wei, A., Jegla, T., and Salkoff, L. (1996). Eight potassium channel families revealed by the *C. elegans* genome project, *Neuropharmacology* 35, 805-829.

Whiteway, J., Koziarz, P., Veall, J., Sandhu, N., Kumar, P., Hoecher, B., and Lambert, I. B. (1998). Oxygen-insensitive nitroreductases: analysis of the roles of nfsA and nfsB in development of resistance to 5-nitrofurantoin derivatives in *Escherichia coli*, *J Bacteriol* 180, 5529-39.

Zenno, S., Koike, H., Tanokura, M., and Saigo, K. (1996). Gene cloning, purification, and characterization of NfsB, a minor oxygen-insensitive nitroreductase from *Escherichia coli*, similar in biochemical properties to FRase I, the major flavin reductase in *Vibrio fischeri*, *J Biochem (Tokyo)* 120, 736-44.

Table 1. *sup-18(lf)* mutations specifically suppress *sup-10(gf)* locomotion defects

Genotype	Locomotion Rate (Bends/min. $\pm$ SEM)	Animals Assayed
<i>Wild-type</i>	27.3 $\pm$ 0.5	n = 36
<i>sup-10(n983)</i>	5.1 $\pm$ 0.5	n = 16
<i>sup-18(n1030); sup-10(n983)</i>	26.4 $\pm$ 0.6	n = 16
<sup>a</sup> <i>sup-9(n1550)</i>	0.0 $\pm$ 0.0	n = 12
<i>sup-9(n1550); sup-18(n1030)</i>	0.0 $\pm$ 0.0	n = 12
<i>unc-93(e1500)</i>	0.2 $\pm$ 0.1	n = 32
<i>unc-93(e1500); sup-18(n1030)</i>	1.0 $\pm$ 0.3	n = 35
<i>unc-93(e1500); sup-10(n4025)</i>	13.9 $\pm$ 0.6	n = 30
<i>unc-93(e1500); sup-18(n1030); sup-10(n4025)</i>	19.1 $\pm$ 0.4	n = 30
<i>unc-93(e1500); sup-10(n4026)</i>	14.9 $\pm$ 0.5	n = 30
<i>unc-93(e1500); sup-18(n1030); sup-10(n4026)</i>	19.6 $\pm$ 0.4	n = 30
<i>sup-9(n1913); unc-93(e1500)</i>	27.1 $\pm$ 0.5	n = 11
<i>sup-9(n1550)/+; sup-18(n1030)</i>	6.3 $\pm$ 0.2	n = 12
<i>sup-9(n1550)/+; sup-18(n1030); sup-10(n983)</i>	0.0 $\pm$ 0.0	n = 12

Young adult hermaphrodites were assayed for the number of bends they make on a bacterial lawn in a one-minute interval.

<sup>a</sup>homozygote animals are inviable and were generated from *sup-9(n1550)/+* parent.

Table 2. *sup-18(lf)* mutations are haploinsufficient for suppression of *sup-10(gf)* but not *unc-93(gf)* locomotion defects

Genotype	Locomotion Rate (Bends/min. $\pm$ SEM)	Animals Assayed
<i>Wild-type</i>	33.0 $\pm$ 1.2	n = 36
<i>sup-10(n983)</i>	4.7 $\pm$ 0.9	n = 25
<i>sup-18(n1030)/+; sup-10(n983)</i>	15.2 $\pm$ 0.7	n = 25
<i>sup-18(n1030); sup-10(n983)</i>	31.7 $\pm$ 0.7	n = 15
<i>sup-9(n1913)/+; sup-10(n983)</i>	5.6 $\pm$ 0.6	n = 20
<i>sup-9(n1913); sup-10(n983)</i>	33.2 $\pm$ 1.1	n = 15
<i>sup-18(n1033)/+; sup-10(n983)</i>	13.8 $\pm$ 0.6	n = 25
<i>sup-18(n1014)/+; sup-10(n983)</i>	14.6 $\pm$ 0.6	n = 25
<i>sup-18(n1036)/+; sup-10(n983)</i>	12.3 $\pm$ 0.7	n = 25
<i>sup-18(n1471)/+; sup-10(n983)</i>	14.0 $\pm$ 0.7	n = 25
<i>unc-93(e1500); sup-10(n4025)</i>	10.0 $\pm$ 0.5	n = 30
<i>unc-93(e1500) sup-18(n1030)/+; sup-10(n4025)</i>	9.8 $\pm$ 0.7	n = 20
<i>unc-93(e1500) sup-18(n1030); sup-10(n4025)</i>	17.5 $\pm$ 0.9	n = 30

Young adult males were assayed for the number of bends they make on a bacterial a one-minute interval.

Table 3. *sup-18* loss-of-function mutations

Allele	Mutation	Effect	Mutagen	Background
<i>n1033</i>	AT <u>G</u> to AT <u>T</u>	M1I	EMS	<i>sup-10(n983)</i>
<i>n1030</i>	<u>C</u> GA to <u>T</u> GA	R63S STOP	EMS	<i>sup-10(n983)</i>
<i>n1038</i>	916 bp deletion	97aa + frameshift	EMS	<i>unc-93(e1500)</i>
<i>n527</i>	13 bp deletion	154 _ frameshift	Spo	<i>unc-93(e1500)</i>
<i>n1548</i>	T <u>G</u> G to T <u>A</u> G	W170 STOP	EMS	<i>sup-10(n983)</i>
<i>n463</i>	4 bp deletion	175 + frameshift	Spo	<i>unc-93(e1500)</i>
<i>n1539</i>	Tc3 Insertion	320 + frameshift	Spo	<i>sup-10(n983)</i>
<i>n1036</i>	ag <u>G</u> T to aa <u>G</u> T	3 <sup>th</sup> splice acceptor	EMS	<i>sup-10(n983)</i>
<i>n1035</i>	ag <u>G</u> C to aa <u>G</u> C	5 <sup>th</sup> splice acceptor	EMS	<i>sup-10(n983)</i>
<i>n1015</i>	GT <u>g</u> t to GT <u>a</u> t	8 <sup>th</sup> splice donor	EMS	<i>sup-10(n983)</i>
<i>n1558</i>	ag <u>A</u> T to aa <u>A</u> T	8 <sup>th</sup> splice acceptor	EMS	<i>sup-10(n983)</i>
<i>n1010</i>	AGT to AAT	S137N	EMS	<i>sup-10(n983)</i>
<i>n1554</i>	<u>G</u> GC to <u>A</u> GC	G258D	EMS	<i>sup-10(n983)</i>
<i>n1471</i>	<u>G</u> GC to <u>G</u> AC	G258S	Gamma	<i>sup-10(n983)</i>
<i>n1556</i>	<u>A</u> CT to <u>A</u> TT	T271I	EMS	<i>sup-10(n983)</i>
<i>n1014</i>	<u>G</u> GA to <u>A</u> GA	G280R	EMS	<i>sup-10(n983)</i>
<i>n1022</i>	<u>A</u> GG to <u>A</u> AG	R289K	EMS	<i>sup-10(n983)</i>
<i>n528</i>	<u>A</u> CC to <u>C</u> CC	T322P	Spo	<i>unc-93(e1500)</i>

DNA sequence was determined for both strands of *sup-18* exons and intron/exon boundaries in each mutant. For splice-junction mutants, the intron sequence is indicated by lowercase lowercase, for exons as uppercase. EMS, Ethyl-methylsulfonate; Spo, Spontaneous;

Table 4. Overexpression of *sup-18* in muscle enhances the defects of *sup-10(gf)* but not *unc-93(gf)* mutants

Genotype	Locomotion Rate	
	(Bends/min. $\pm$ SEM)	Broodsize
<i>wild-type</i>	26.8 $\pm$ 0.4	ND
<i>lin-15; nEx(lin-15#1)</i>	26.5 $\pm$ 0.9	ND
<i>lin-15; nEx(lin-15#2)</i>	27.3 $\pm$ 0.7	ND
<i>lin-15; nEx(lin-15;sup-18#1)</i>	27.1 $\pm$ 0.8	ND
<i>lin-15; nEx(lin-15;sup-18#2)</i>	26.9 $\pm$ 0.8	ND
<i>sup-10(n983) lin-15; nEx(lin-15#1)</i>	5.7 $\pm$ 0.4	74 $\pm$ 5
<i>sup-10(n983) lin-15; nEx(lin-15#2)</i>	5.4 $\pm$ 0.4	75 $\pm$ 4
<i>sup-10(n983) lin-15; nEx(lin-15; sup-18#1)</i>	0.1 $\pm$ 0.1	27 $\pm$ 3
<i>sup-10(n983) lin-15; nEx(lin-15; sup-18#2)</i>	0.0 $\pm$ 0.0	17 $\pm$ 3
<i>sup-10(n983) lin-15; nEx(lin-15; sup-9#1)</i>	6.0 $\pm$ 0.6	ND
<i>sup-10(n983) lin-15; nEx(lin-15; sup-9#2)</i>	5.1 $\pm$ 0.4	ND
<i>unc-93(e1500); lin-15; nEx(lin-15#1)</i>	0.0 $\pm$ 0.0	35 $\pm$ 2
<i>unc-93(e1500); lin-15; nEx(lin-15#2)</i>	0.0 $\pm$ 0.0	43 $\pm$ 2
<i>unc-93(e1500); lin-15; nEx(lin-15; sup-18#1)</i>	0.0 $\pm$ 0.0	37 $\pm$ 2
<i>unc-93(e1500); lin-15; nEx(lin-15; sup-18#2)</i>	0.0 $\pm$ 0.0	40 $\pm$ 3
<i>sup-9(n1550); sup-18(n1030)</i>	0.0 $\pm$ 0.0	24 $\pm$ 1
<i>sup-10(n183) lin-15; nEx(lin-15#1)</i>	? $\pm$ 0.4	ND
<i>sup-10(n183) lin-15; nEx(lin-15#2)</i>	? $\pm$ 0.4	ND
<i>sup-10(n183) lin-15; nEx(lin-15; sup-18#1)</i>	? $\pm$ 0.1	ND
<i>sup-10(n183) lin-15; nEx(lin-15; sup-18#2)</i>	? $\pm$ 0.0	ND

Locomotion rate for all strains represents the mean of 12 animals. The broodsize represents the mean of 10 animals. Four extrachromosomal arrays (nEx) were generated, two containing *lin-15* alone and two containing both *lin-15* and *sup-18*, as indicated by the text in parenthesis. These extrachromosomal arrays were introduced into the different genetic backgrounds by mating to ensure consistent gene dosage between experiments.

Figure 1. *sup-18* Encodes a Protein with Amino Acid Similarity to Bacterial Nitroreductases

(A) Top, genetic map of the *sup-18* region in linkage group III (LG III). Horizontal lines below *sup-18* represent the cosmids tested for rescue of *sup-18(n1010)*; *sup-10(n983)* mutants. Bottom, physical map of cosmid C02C2. Open boxes, coding regions; horizontal brackets, cosmid subclones. Rescued lines indicate the number of independently derived transgenic lines over the total number of lines scored. Rescue was scored as the appearance of a rubberband Unc paralysis.

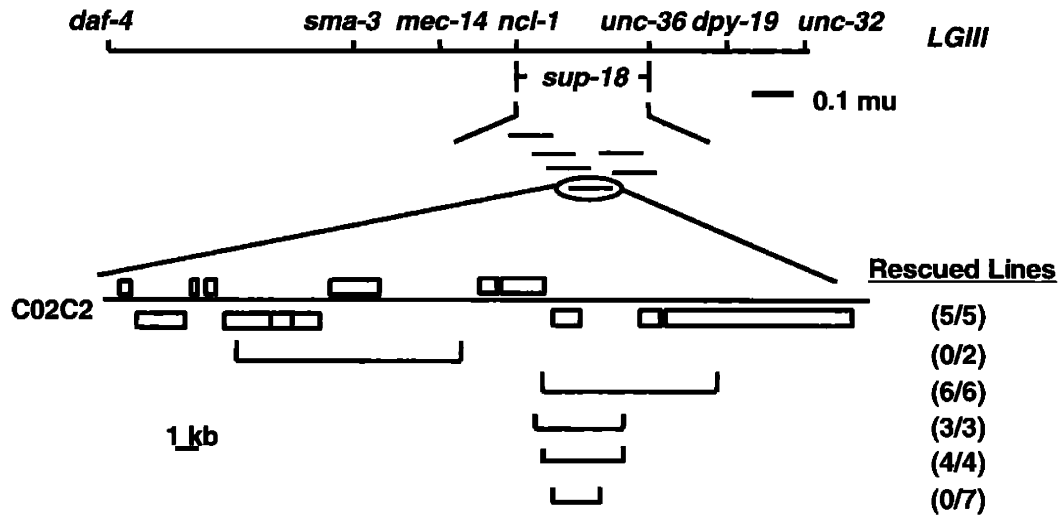
(B) Intron-exon structure of *sup-18* as inferred by comparison of cDNA and genomic sequences. Closed boxes, coding regions; open boxes, untranslated region; arrow, direction of transcription. The *sup-18* open reading frame is 978bp, the 5' UTR is 57 bp and the 3'UTR is 44 bp.

(C) Sequence alignment of SUP-18 and similar proteins from other species. Amino acids conserved between at least three of the aligned proteins are highlighted in black boxes. (▼) *sup-18* missense mutation. (\*) FMN cofactor-binding residues in the *E. coli* NfsB nitroreductase. (△) Lf mutations in NfsB identified genetically (Whiteway et al., 1998). A putative transmembrane domain (TMD) of SUP-18 is indicated by an open rectangle.

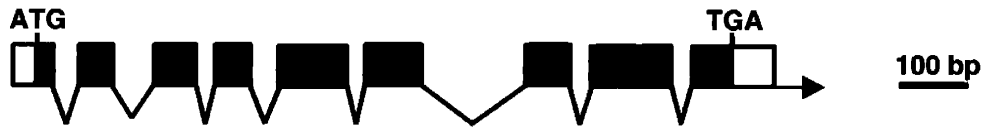
Genebank accession numbers are as follows: SUP-18, (to be assigned); *M. musculus*, AAH23358, *Drosophila*, AAM11009; *T.t.NOX*, CAA42707; *E. coli* NfsB. NP\_41511.

# Figure 1

## A



## B



## C

			TM	
SUP-18	1	MKKHTHHKA YGDSTGKEPLIDLQSIKWLNSFGNOGHSSEAVLNLVFLTGLVILFVIYQVA		60
M.m. SUP-18	1		MFLFTPVLVAVVCILVVWVFK	21
D.m. SUP-18	1		MDVDELISSSKLLKHWP SLFI	21
T.l. NOX	1			0
E. c. NfsB	1			0
SUP-18	61	SLLHRMNKRVEKQLESRTKQRKVEVADKHVGD	EMVFTDLHENVIRERMI	120
M.m. SUP-18	22	NADRNLEKKKEEAQVQPWVDEDLKDSTEDLQV	EDAEEWQEAESVEHI	81
D.m. SUP-18	22	TLALIWIWKRLFFKGNRVLKTYNLDEQVEEEV	EHFADLGD ELQPALEDK	81
T.l. NOX	1			ME 2
E. c. NfsB	1			0
SUP-18	121	TLRNSQIFVEEMKRRSCRFSSRDVP	LKVIQNLKTAGTSPSPVGN	179
M.m. SUP-18	82	MRMRSQEFYELLNKRRSVRFISSEHVP	MEVIEENVIKAAAGTAPSGAHT	140
D.m. SUP-18	82	NPNGAKRLYELMRGRRSIRSFNSHP	KPDLSSVIEDCIRAAGTAPSGAHT	141
T.l. NOX	3	ATLPVLDAKTAA LKRHSIRRYRKDP	VP EGLLREILEAALRA PSAWN	61
E. c. NfsB	1	MDIISVALKRHSITKAFDASKKLTPEQA	EQIKTLLQYSPSSTNSQPWHFI	55
			* * *	
SUP-18	180	IKTMIKRILEADERDNYVSRKKGAS	WVVDVVSQIQDT--WRRPYITD	229
M.m. SUP-18	141	MKHKIREIIEEEEEINYMKR-MGKR	WVTDLKKLR TN--WIKKEYLDT	189
D.m. SUP-18	142	LKRSIREIIEEELVNYSQRMHPQ	WVTDLRR LQTN--HVKEYLTE	190
T.l. NOX	62	TKRALREAAFGQAHVEEAPVVLVLYAD	LEDALAHLD--EV IHPGVQ	111
E. c. NfsB	58	GKARVAKSAAGNYVFNERKMLDASHV	VVFCAKTAMDVWV LKLVVDQEDADGRFAT	115
			* * *	
SUP-18	230	VCHEIFRDVHSKT--ERVFHYNQIST	SIAYVGI LLAAIIONVGLSTV	285
M.m. SUP-18	190	IFKQVHGFANGK--KVVHYNEISV	SIACGG LLAAALONAGLVTV	245
D.m. SUP-18	191	IFKQTYGLSENGKR--MRRHYNEIS	SIACGG ILLCALQAAGLASLV	247
T.l. NOX	112	QKQAIQRAFAAMGQ--EARKAWASG	QSYLLG YLLLLLEAYGLGS	167
E. c. NfsB	116	ANDKGRKFFADMHHRKDLHDDAEWMA	KQVYLVN VGNFLLGVAA LGLDA	174
			* * *	
SUP-18	286	ILRRPEN-ESILLLPLLGYASEDV--	LVPDLKR KRPVEHITKLY	325
M.m. SUP-18	246	LLGRPSH-EKLLLVLLLPVGYPSRDA--	TVPDLKR KALDQIMVT	285
D.m. SUP-18	248	LLGRPVN-EKLLI LLLPVGYPKDGC--	TVPDLA RKNLSNIMVT	287
T.l. NOX	168	ILGLPSR-AAIPALVALGYPAEEG--	-YPSH RLP LERVVLR	205
E. c. NfsB	175	EFG LKEKGYTSLVVVPVGHHSVED	FNA TLPKS RLPQNI TLTEV	217



Figure 2. *T.t.*NOX Carrying an S19N Mutation Equivalent to *sup-18(n1010)* Has Greatly Reduced NADH Oxidase Activity

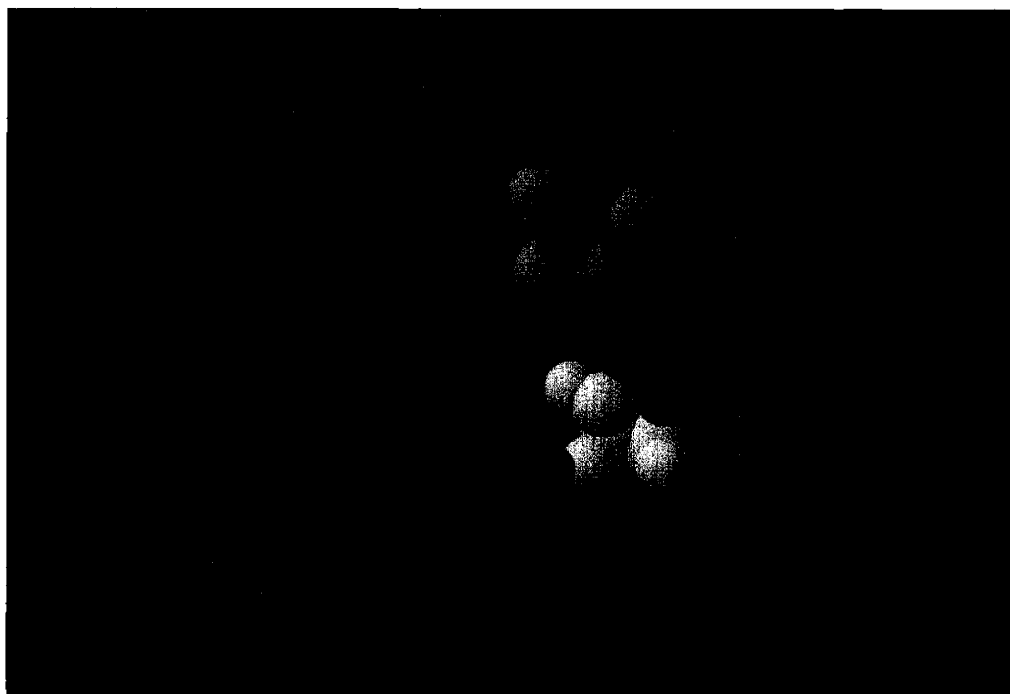
A. Crystal structure of *T.t.*NOX monomer showing the proximity of serine 19, which is equivalent to serine 137 of SUP-18 (see Figure 1 alignment), and a bound FMN cofactor as described (Hecht et al., 1995). Serine 19 is colored yellow.

B. SDS-PAGE of heat-shocked *E. coli* proteins bound to blue sepharose. Nox- refers to protein from *E. coli* carrying a control ampicillin resistance plasmid, whereas wild-type and S19N refer to the wild-type and mutant NOX proteins, respectively.

C. Relative NADH oxidase activity of control, wildtype and S19N mutant lysates. Arbitrary units are relative and indicate the change in NADH concentration per unit time as measured by its change in absorbance at OD<sub>340</sub>. Legends are as in (B). Bars represent mean  $\pm$  SEM of triplicate experiments.

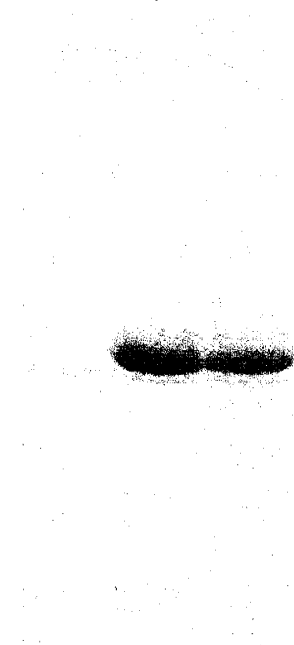
**Figure 2**

**A**



**B**

Nox -  
wt  
S19N



**C**

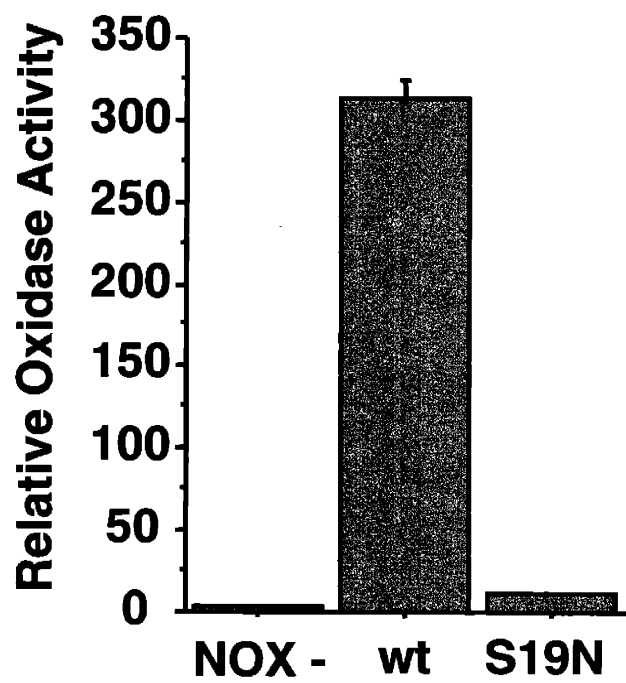


Figure 3. *sup-18* Is Expressed Predominantly in Muscle Membranes and Colocalizes with SUP-10::GFP

Epifluorescence and Normarski images of worms carrying a *sup-18::gfp* reporter transgene (A - D). Confocal images of immunostained fixed-worms carrying a *sup-10::gfp* reporter and either a  $P_{myo-3}sup-9$  (E) or a  $P_{myo-3}sup-18$  (F) transgene. Scale bars are 10  $\mu$ m.

(A) Muscle cell displaying GFP fluorescence in the dense bodies as dotted lines on the cell surface.

(B) Ventral view of egg-laying muscles. Animal is mosaic and is not expressing *gfp* in the uppermost muscle cell.

(C) Tail region of hermaphrodite showing fluorescence in the anal depressor muscle (arrow).

(D) Head of adult animal with expression in a neuron (arrow).

(E, F) Serial images of fixed, immunostained transgenic animals; muscle cell in transgenic animals overexpressing a SUP-10::GFP translational reporter and either SUP-9 driven by the *myo-3* promoter (left) or SUP-18 driven by the same promoter (right). FITC channel showing GFP fluorescence (top), rhodamine channel displaying antibody staining of SUP-9 or SUP-18 as indicated (middle) and merged images (bottom).

Figure 3

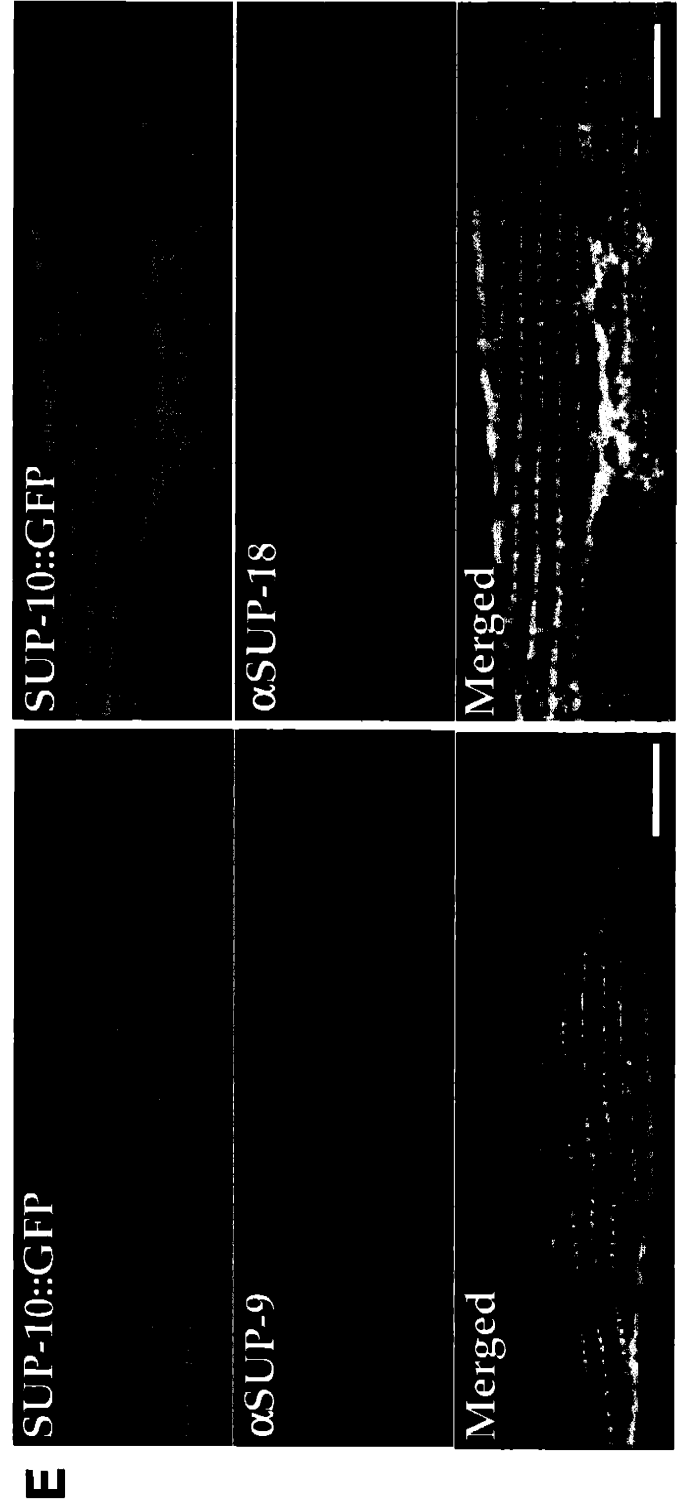
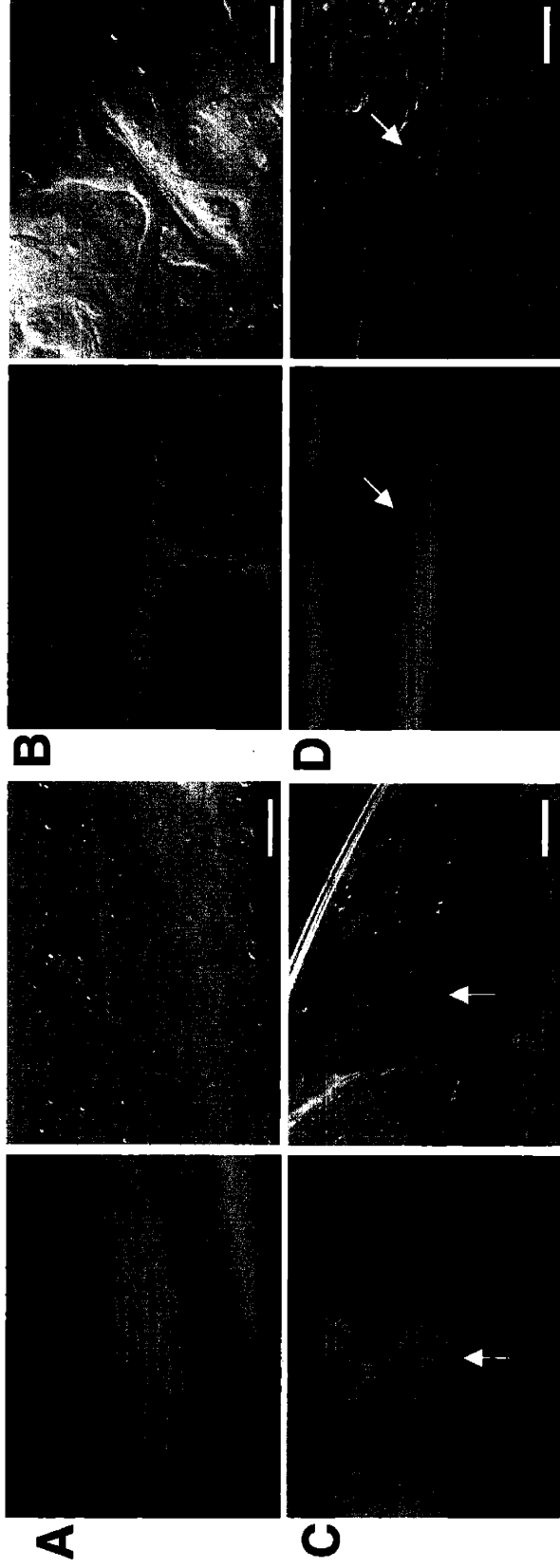


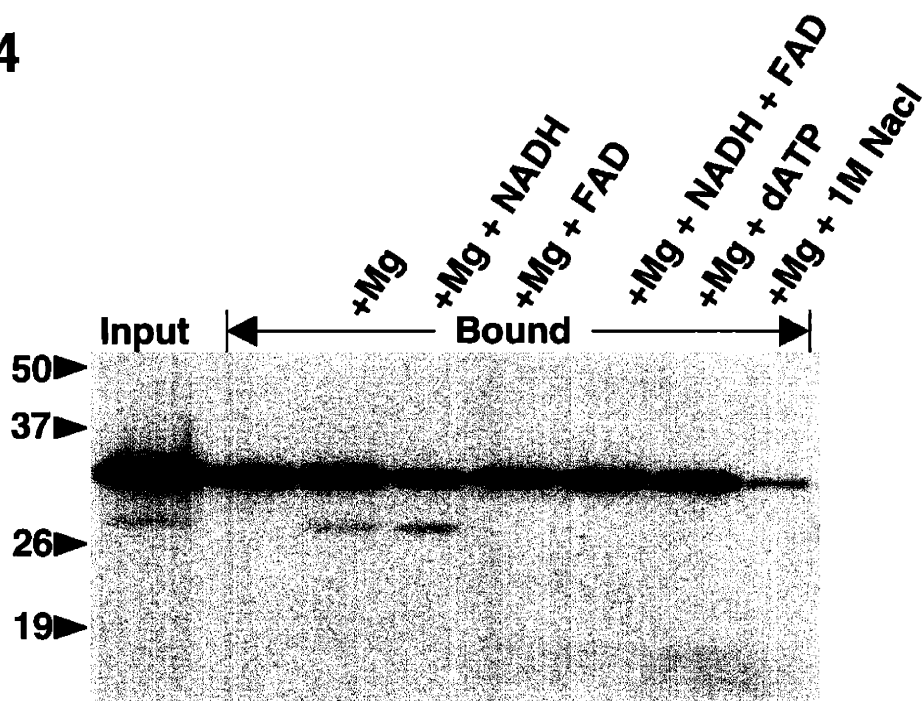
#### Figure 4. Native SUP-18 and SUP-9 Copurify from Worm Membranes

(A) Solubilized membrane extracts (see methods) were incubated with blue sepharose resin and washed five times with wash buffer, where the last wash was supplemented with 5 mM MgCl<sub>2</sub>, 1 mM NADH, 1 mM FAD 1 mM ATP or 1M NaCl as indicated. Proteins retained by the beads were resolved by SDS-PAGE, transferred to nitrocellulose and immunoblotted with antiSUP-18 antiserum on western blots. The input lane represents 1/3 of bound material.

(B) Proteins bound to blue sepharose from wild-type solubilized membrane extracts was resolved by SDS-PAGE and immunostained as above using either anti-SUP-18 (amino acids 1-258), anti-SUP-9(C) (amino acids 258-329) or anti-SUP-9(N) (amino acids 1-110) antisera. SUP-9 has a predicted molecular weight of 37.0 kDa, while SUP-18 is predicted to be 37.3 kDa. The input lane represents 1/3 of bound material.

**Figure 4**

**A**



**B**

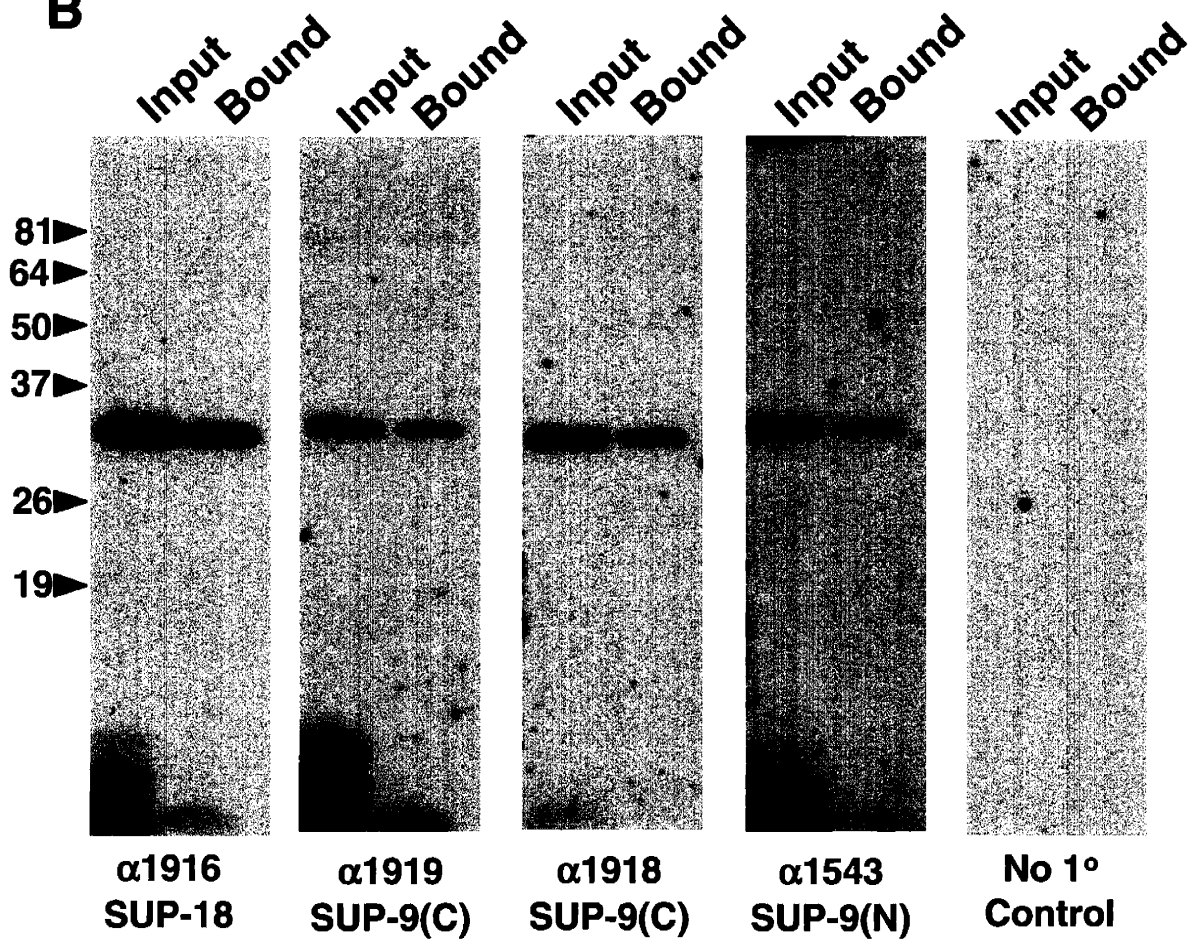


Figure 5. SUP-18 Is a Type-one Transmembrane Protein whose Nitroreductase Domain Resides Intracellularly

Transgenic animals expressing *sup-18::B-galactosidase* gene fusions were generated in wild-type animals using the dominant *rol-6* coinjection marker. *B-galactosidase* assays were carried as described (Fire, 1992). At least 100 animals were scored for each transgenic line using Normarski optics. Quantification was performed as follows: staining in adult vulval muscles and larvae easily observed at 10X magnification in > 30% of animals (++), staining in 3-30% of animals (+) or staining in less than 3% of animals (-). Open boxes, SUP-18 TMD; closed boxes, synthetic TMD; "SS", signal sequence.

**Figure 5**

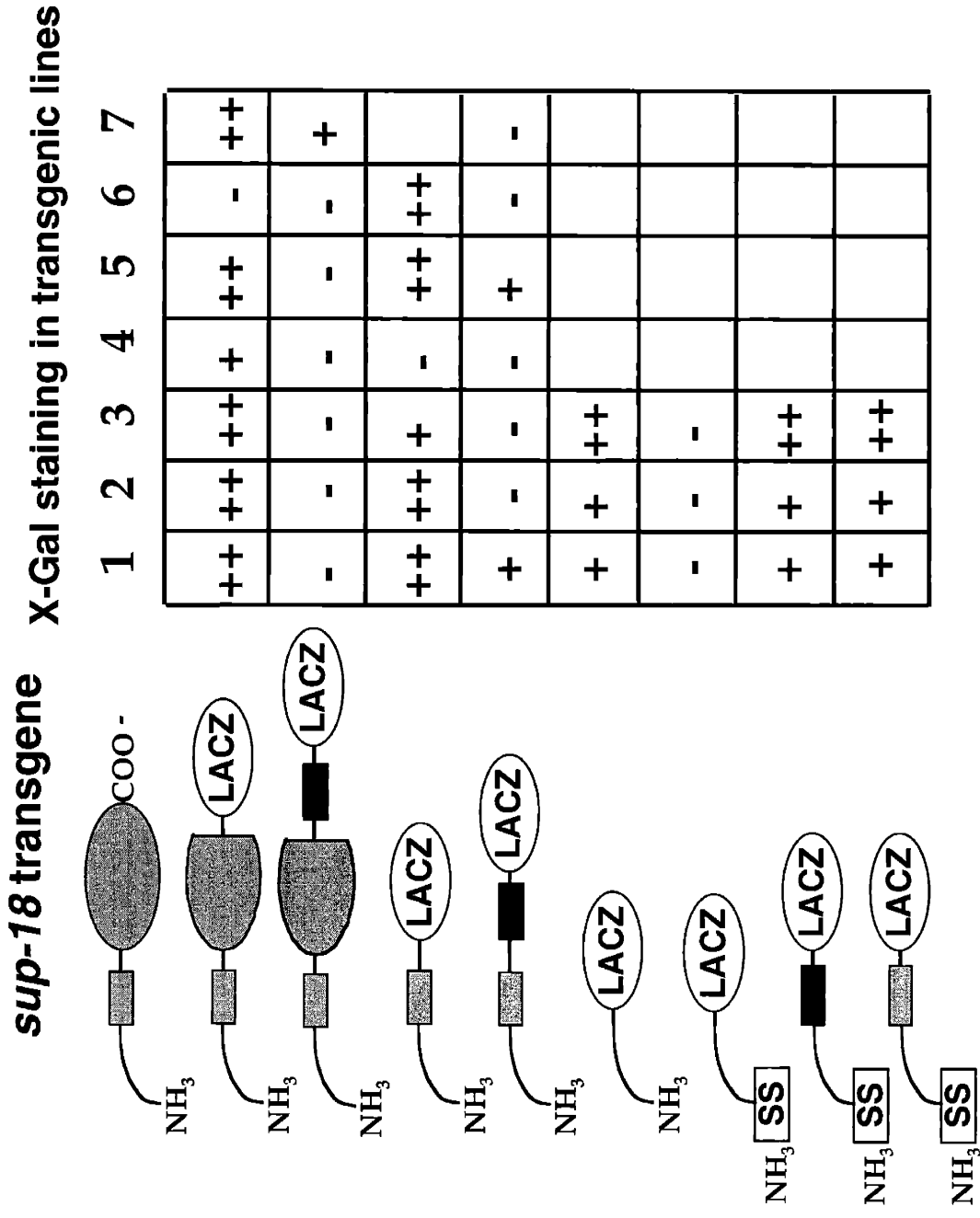




Figure 6. Overexpression of SUP-18 or of its Intracellular Domain Restores a Rubberband-Unc paralysis to *sup-18(lf); sup-10(gf)* Animals

(A) Transgenic *sup-18(n1033); sup-10(gf)* animals carrying *myo-3*-driven arrays, as indicated by the text below the dark horizontal lines, were scored for locomotory rates.  $P_{myo-3}gfp$  was used as a coinjection marker to allow the identification of transgenic animals by their *gfp* fluorescence. Non-transgenic *sup-10(n983)* and *sup-10(n1033); sup-10(n983)* mutants were also scored as controls. Bars indicate mean  $\pm$  SEM;  $n = 12$  for each transgenic line or control genotype.

(B) Epifluorescence photographs of a muscle cell from *sup-18(n1033); sup-10(gf)* animals transgenic for  $P_{myo-3}sup-18(n1010)$  and a *myo-3::gfp* coinjection marker. Animals were stained with anti-SUP-18(N) antisera and a Texas Red-conjugated secondary antibody (Chapter 2). Transgenic animals were identified by their *gfp* fluorescence, and photographs using a rhodamine filter. The proposed catalytic null SUP-18(n1010) protein is localized to dense bodies. Scale bar is 10  $\mu$ m.

(C) Epifluorescence photographs of a muscle cell in *lin-15* animals transgenic for  $P_{myo-3}msup-18::gfp$  and a *lin-15* coinjection marker. mSUP-18::GFP is localized to dense bodies. Scale bar is 10  $\mu$ m.

(D) Epifluorescence photographs of a muscle cell in animals transgenic for  $P_{myo-3}gfp::sup-18(intra)$  (Top) or for  $P_{myo-3}gfp$  alone (Bottom). Scale bars are 10  $\mu$ m.

Figure 6

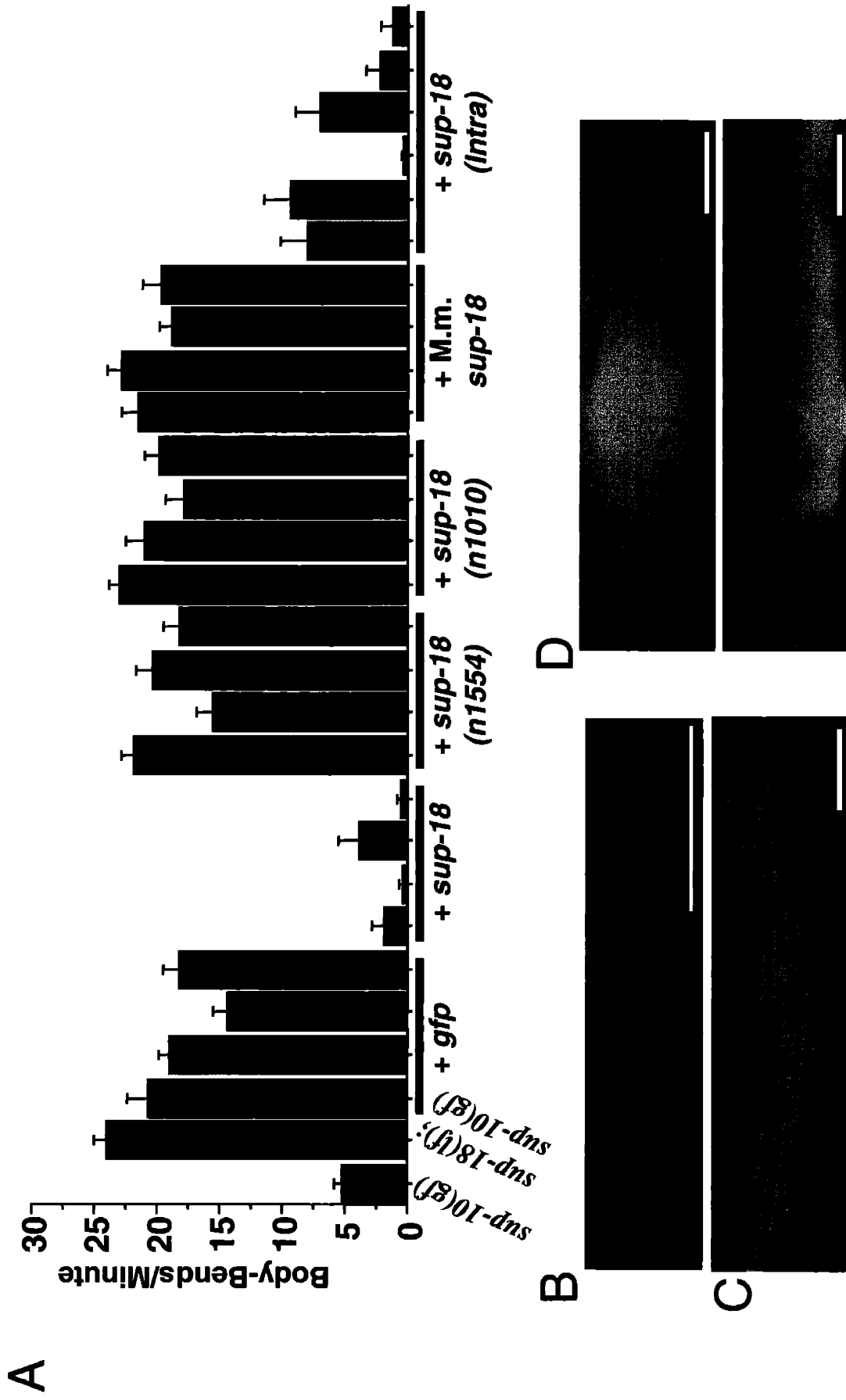


Figure 7. Overexpression of a *sup-18* Transgene in *sup-10(gf)* but not in *unc-93(gf)*  
Mutnats Enhances the Rubberband-Unc Phenotype

All hermaphrodites were photographed after at least a two-minute delay after being placed on a fresh petri plate to allow animals that can move to leave tracks on the bacterial lawn. Scale bar for all figures is 100  $\mu$ m. Genotypes are as follows:

(A) *sup-10(n983)*

(B) *sup-18(n1030); sup-9(n1550)*

(C) *sup-10(n983); lin-15(n765); nEx(lin-15)*

(D) *sup-10(n983); lin-15(n765); nEx(lin-15, P<sub>myo-3</sub>sup-18)*

(E) *sup-10(n983); lin-15(n765); nEx(lin-15, P<sub>myo-3</sub>sup-9)*

(F) *unc-93(e1500); lin-15(n765); nEx(lin-15)*

(G) *unc-93(e1500); lin-15(n765); nEx(lin-15, P<sub>myo-3</sub>sup-18)*

**Figure 7**

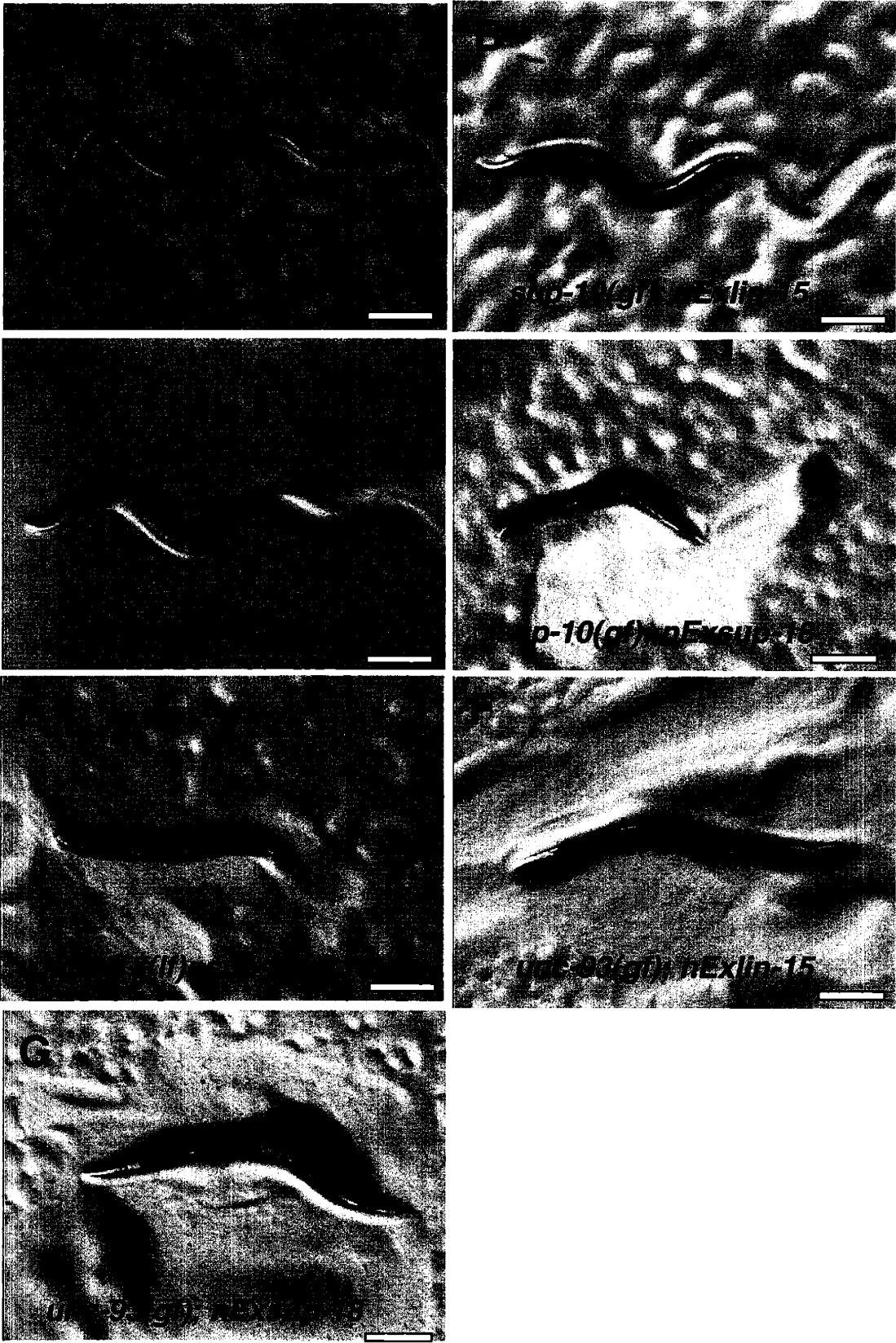


Figure 8. The *sup-9(n1435)* Mutation Confers Resistance to Channel Activation by *sup-18*

(A) The SUP-9(n1435) channel cannot be activated by the SUP-10(gf) subunit but is activated by UNC-93(gf). Body-bend assays of young hermaphrodites: wt (n = 16), *sup-10(n983)* (n = 16), *sup-9(n1435); sup-10(n983)* (n = 12); *unc-93(e1500)* (n = 32) and *sup-9(n1435); unc-93(e1500)* (n = 16). Bars indicate mean  $\pm$  SEM.

(B) The suppressive effects of *sup-9(n1435)* and *sup-18(lf)* mutations on the brood size defects of *unc-93(gf)* mutants are not additive. Brood sizes of hermaphrodites were determined by picking L4 hermaphrodites to single plates and passaging them: *unc-93(e1500)* (n = 30), *sup-9(n1913); unc-93(e1500)* (n = 11), *sup-9(n1435); unc-93(e1500)* (n = 29), *unc-93(e1500) sup-18(n1030)* (n = 29); *sup-9(n1435); unc-93(e1500) sup-18(n1030)* (n = 29), *sup-9(n264); unc-93(e1500)* (n = 13) and *sup-9(n264); unc-93(e1500) sup-18(n1030)* (n = 15).

(C) Body bend assays of young males: wildtype (n = 15), *sup-10(n983)* (n = 25), *sup-9(n1435); sup-10(n983)* (n = 25); *sup-9(n1435)/+; sup-10(n983)* (n = 17), *sup-18(n1030)/+; sup-10(n983)* (n = 25), *sup-9(n1435)/+; sup-18(n1030)/+; sup-10(n983)* (n = 45), *sup-9(n264)/+; sup-10(n983)* (n = 45), *sup-9(n264)/+; sup-18(n1030)/+; sup-10(n983)* (n = 45). Bars indicate mean  $\pm$  SEM.

**Figure 8**

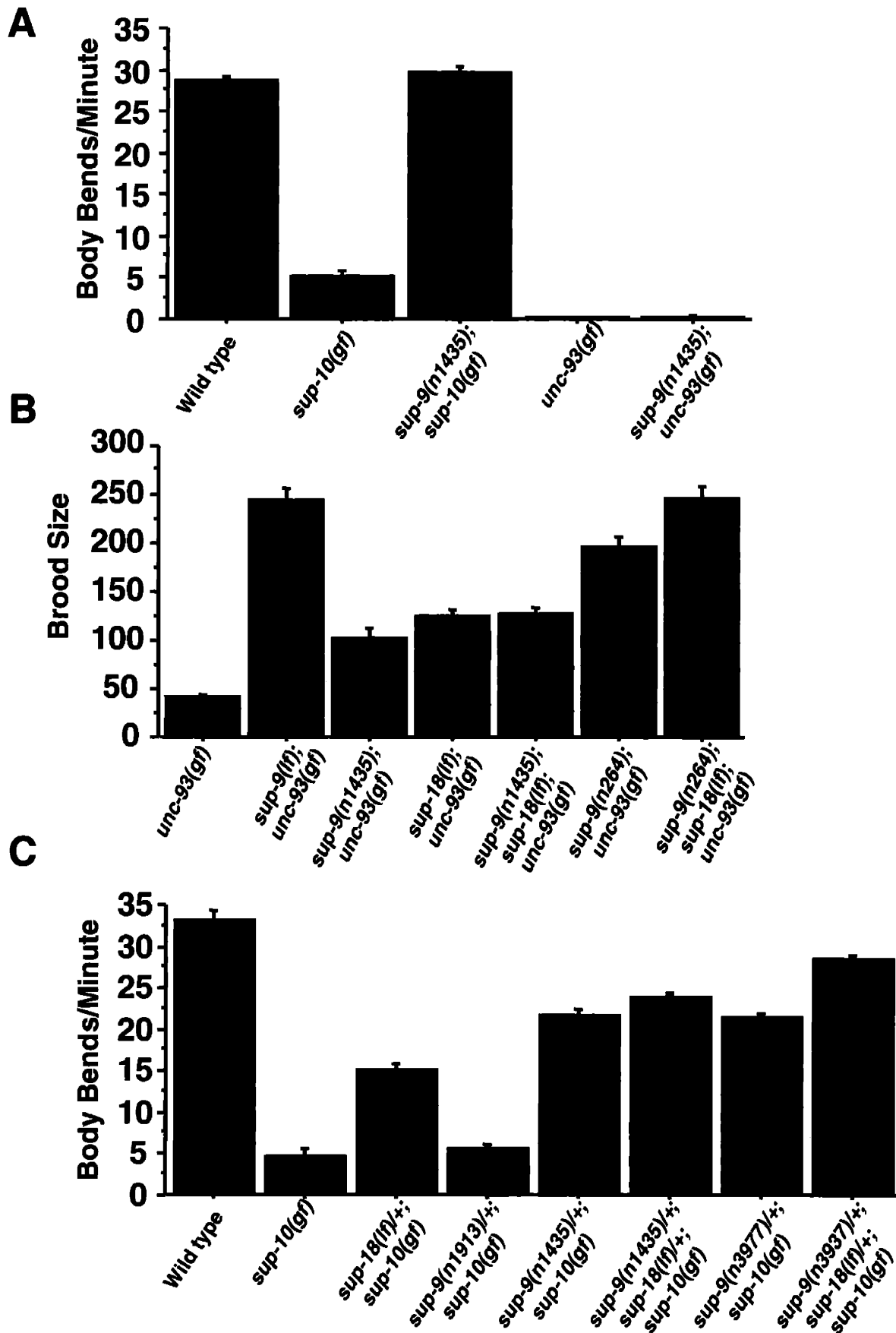


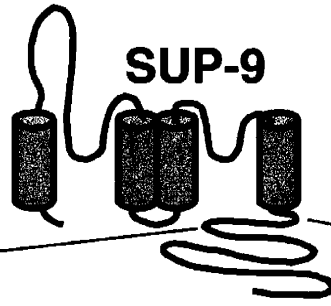
Figure 9. Serines 289 and 292 in the Cytoplasmic C-terminal Domain of SUP-9 Are Required for Activation by the SUP-10(gf) Subunit

(A) Top, schematic diagram of the proposed structure of the SUP-9 channel. Middle, alignment of the C-terminal cytoplasmic tail of SUP-9 (amino acids 247-329) and related channels: human TASK-1 (248-394) Genebank Acc#NP\_002237; human TASK-3 (248-374) Genebank Acc#Q9NPC2; *Drosophila* predicted protein CG9637 (238-398) Genebank Acc# AAF54970; *Drosophila* predicted protein CG9361 (249-340) Genebank Acc# AAF54374; *C. elegans* TWK-4 (255-334) Genebank Acc#AAC32857. Residues conserved among at least four of the channels are shaded. Open box, SC Box; closed triangle, site of *n1435* mutation; open triangle, site of SUP-9::TWK-4 C-terminal fusion. Bottom, alignment of SC Box from SUP-9 and related channels. Residues conserved between SUP-9 and at least one other channel are shaded.

(B) Mutant animals of the indicated genotypes were assayed for egg-laying rate. Abbreviated genotypes are as follows: *sup-10(gf), n983*; *sup-9(lf), n1913*; *unc-93(gf), e1500*; *sup-18(lf), n1030*. Young adult hermaphrodites were allowed to lay eggs for three hours on a bacterial lawn and eggs or larvae on the plate were counted. Independently-derived transgenic lines of *sup-10(n983) lin-15* (top) or *unc-93(e1500) sup-18(n1030); lin-15* animals (bottom) contained both a *lin-15*-rescuing transgene and the indicated  $P_{myo-3}$ *sup-9* derivative as text below the heavy black lines. Bars indicate mean  $\pm$  SEM of at least 14 animals.

**Figure 9**

**A**



```

SUP-9      1  TERNYEDERKREGEAIIAAGGLVLR...VGDPTADDDFG...RLPLSDNV...LA...S...VQLPD...54
hTASK-1   1  TERNYEDERKREAEHRAALLTRNGQAGGGGGGSAHTTDTASBTAAGGGGFRNVYAEVLHFC...LWYKRSREKLYSIPMIIPRDLSTBD  90
hTASK-3   1  TERNYEDERKREAEERASL...GMRNS...MVIHIDETPRPR...YKADVDLDC...LWYKRSQD...YGGRSVAPOMSFAK  74
dCG9361   1  TERNYEDERKREEDDAQNL...GNAQP...VTFDDESTYNNHGKLLN...NYTTENDETA...LWYKRSQD...YGGRSVAPOMSFAK  63
dCG9637   1  TERNYEDERKREEDDAQNL...GNAQP...VTFDDESTYNNHGKLLN...NYTTENDETA...LWYKRSQD...YGGRSVAPOMSFAK  65
TWK-4     1  A SNADLVTAADREPPSAIVLER...FTRNSLVDS...QIFNIQKHSTVGVLPGRP...  49
    
```

```

SUP-4      55  --EKLRHRRHKHTEPHG-QP...PTFSGMTTTPKY  83
hTASK-1   91  TCVEQSHSRPQGGGRYDTPRRRCLCSGAPRSAISSV...STQLHSLSTFRGLMKR...SSV  147
hTASK-3   75  LAPHYFHSISYKIEEISPTLKNLFP...SPISSI...SPQLHSFTDHRMLKR...KSV  127
dCG9361   64  ---CLNHEQFVDDPDPFTDIEESTLCL...K...ASV  92
dCG9637   66  LRQSPTHIRHLLPEVYPMODLNYDYDQSLHTLADRGTMDSSYMGVDMADMGDTGSMELRPHTLLKRNVSLLSIRI  161
TWK-4     50  --RRKKEHPGHCLLWFGTKATKASVFT...YS...KAY  80
    
```

**B**

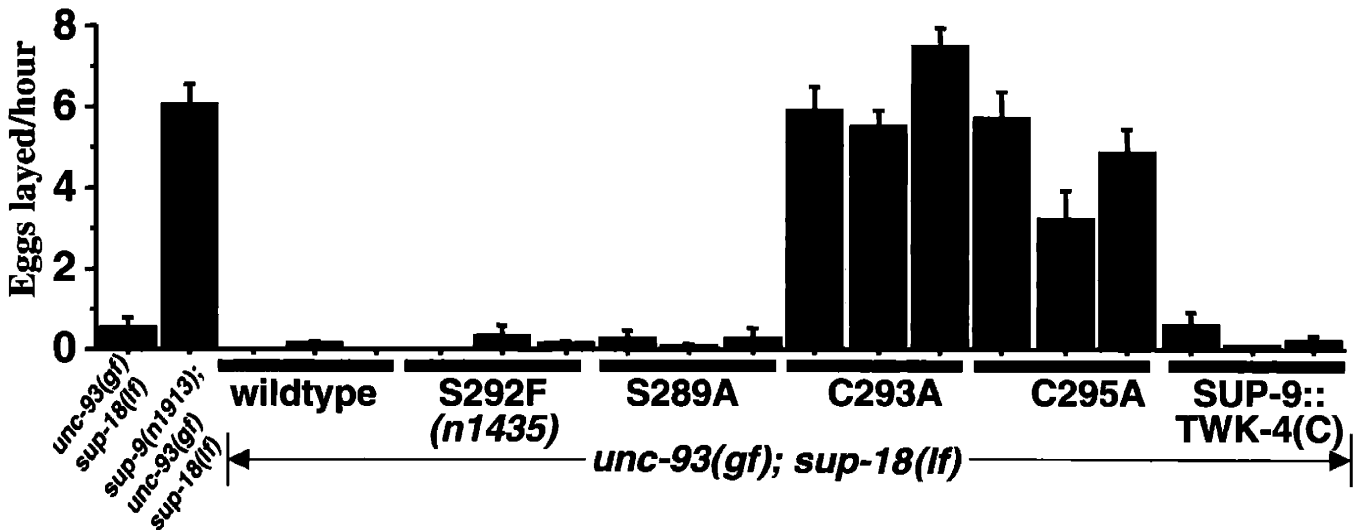
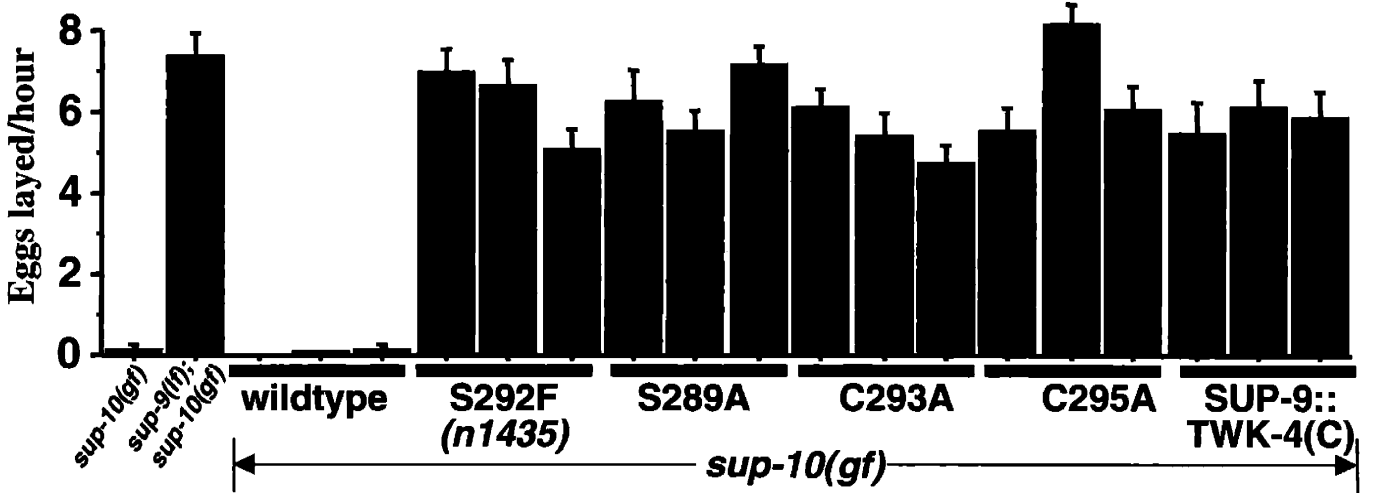
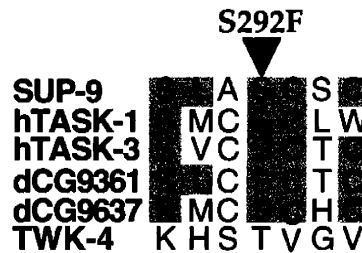




Figure 10. Biochemical Models for Activation of the SUP-9 Channel by Multiple Subunits

SUP-10(gf) May Confer SUP-18 Hypersensitivity to SUP-9 either by Losing a SUP-18 Inhibitory Function (A) or by Hyperactivating SUP-18 (B). The size of the arrows pointing at SUP-9 are representative of their relative importance in sustaining gf activity, with thicker arrows representing a larger contribution.

(A) SUP-10 normally enhances activation of SUP-9 by SUP-18, and this enhancement is increased in a SUP-10(gf) mutant, leading to SUP-18 hyperactivity.

(B) SUP-10 normally represses activation of SUP-9 by SUP-18. This repression is lost in a SUP-10(gf) mutant allowing normal SUP-18 activity to activate SUP-9.

**Figure 10**

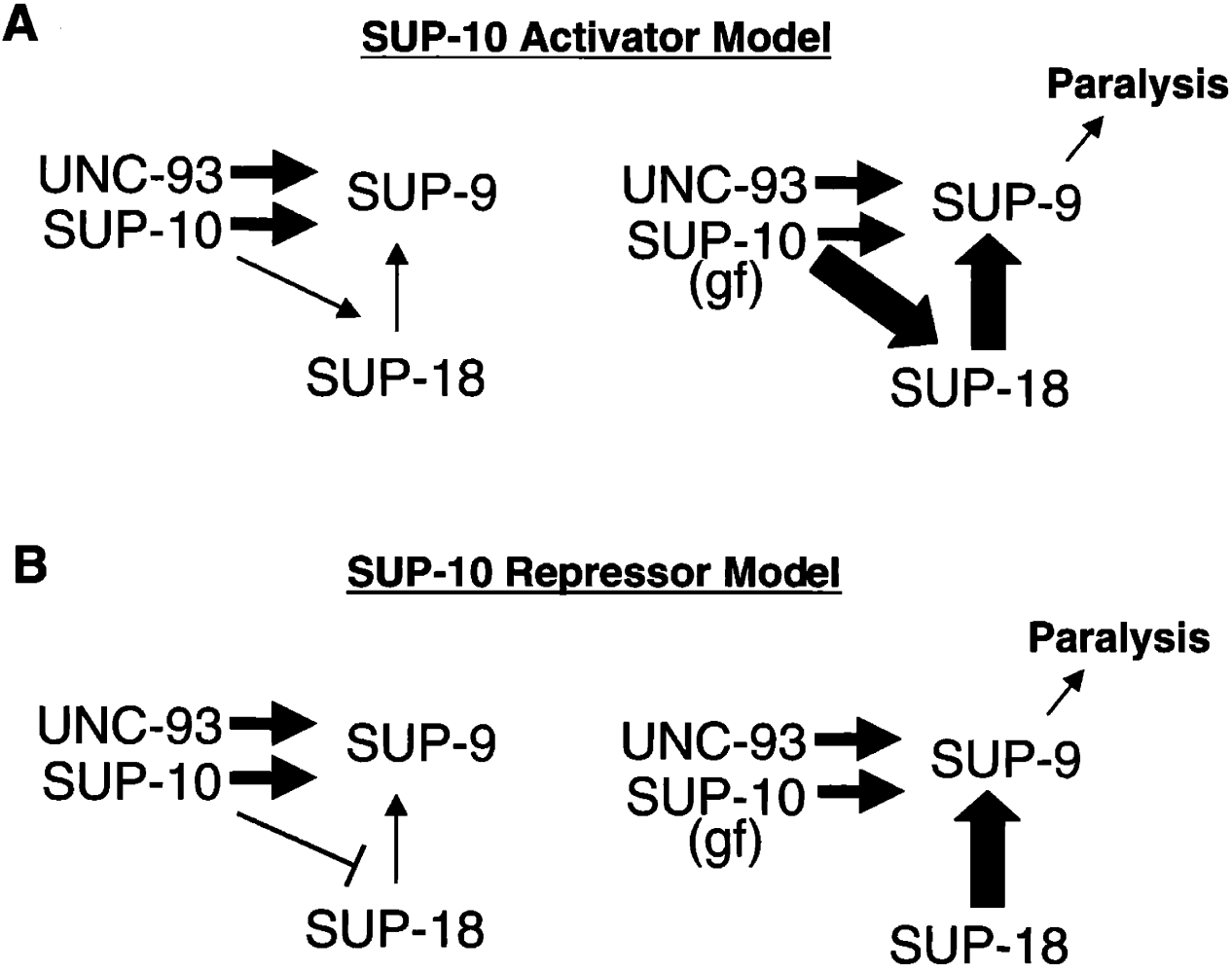


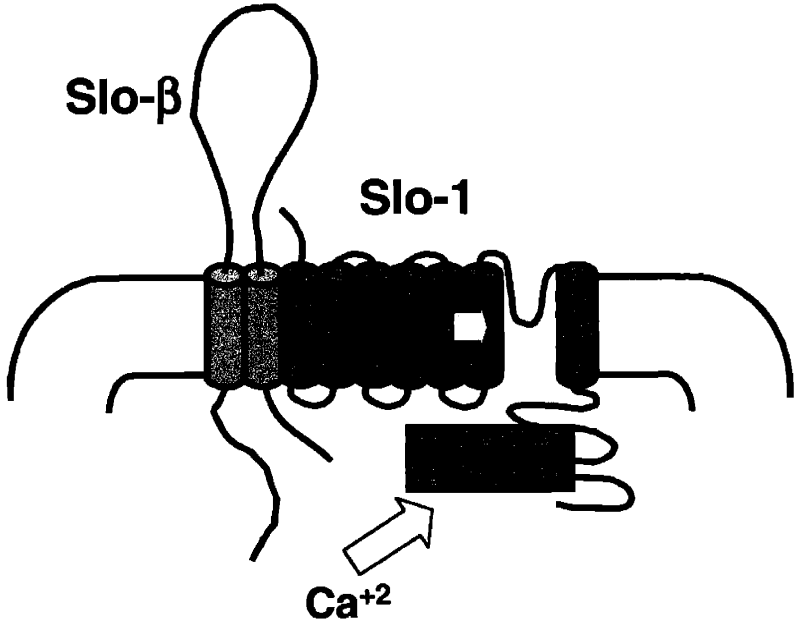
Figure 11. Activation of K<sup>+</sup> Channels through Multiple Regulatory Inputs

(A) The SUP-9 two-pore K<sup>+</sup> channel receives two regulatory inputs, from UNC-93 through interactions between their transmembrane domains and from SUP-10/SUP-18 through the SC Box in the SUP-9 C-terminal tail.

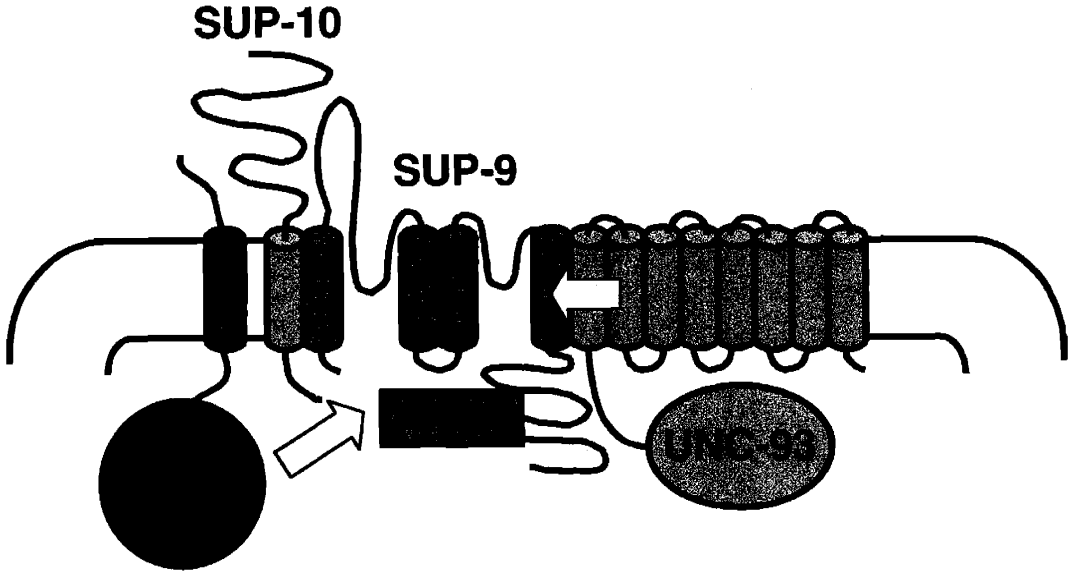
(B) The Slo1 channel receives two inputs from membrane voltage through its positively charged transmembrane domain and from Ca<sup>+2</sup> through a domain named the calcium bowl. The Slo-β subunit increases the sensitivity of the channel to calcium.

**Figure 11**

**A**



**B**



## **Appendix to Chapter THREE**

## Introduction

The intracellular domain of SUP-18 shares amino acid similarity with two classes of enzymes: oxygen-insensitive nitroreductases such as *E. Coli* NfsB, which utilize NADH to reduce nitroaromatic compounds (Zenno et al., 1996b) and the *Thermus thermophilus* NOX enzyme (*T.t.NOX*), which catalyzes the oxidation of NAD(P)H with molecular oxygen to generate hydrogen peroxide (Park et al., 1992b). Both of these enzymes are homodimers and bind an FMN cofactor group in their catalytic sites (Park et al., 1992a; Park et al., 1992b; Zenno et al., 1996b). The crystal structures of both of these proteins indicate that the two enzymes have very similar secondary and tertiary structures (Hecht et al., 1995; Lovering et al., 2001). The similarity of SUP-18 to these enzymes suggests that SUP-18 may regulate the SUP-9 channel *in vivo* through an enzymatic activity. Attempts at detecting a biochemical activity for recombinant SUP-18 fusions with GST or MBP have been unsuccessful due to poor protein expression in *E. coli* and contaminating nitroreductase activity from endogenous *E. coli* genes (I.P. and H.R.H. unpublished data). This section will describe efforts using *T.t.NOX* to explore a possible H<sub>2</sub>O<sub>2</sub>-forming activity for SUP-18 *in vivo*.

## Results/Discussion

To test if SUP-18 activates the SUP-9 channel through the generation of H<sub>2</sub>O<sub>2</sub>, we constructed a *sup-18::nox* chimeric gene that encoded the extracellular and transmembrane domains of SUP-18 and the catalytic domain of *T.t.NOX* (Figure 1A). Overexpression of SUP-18 driven by the *myo-3* promoter in transgenic arrays restored the locomotion defect to *sup-18(n1033); sup-10(gf)* mutants, while overexpression of GFP by the same promoter has little effect on locomotion rate (Figure 1B). The *sup-18(n1033)* mutation changes the initiator methionine to an isoleucine and is predicted to eliminate SUP-18 protein (Chapter 3). By contrast, overexpression of the SUP-18::NOX chimera in these mutants had no effect on their locomotion rate compared to animals overexpressing GFP (Figure 1B). To test if the inability of SUP-18::NOX to substitute for SUP-18 was the result of poor heterologous expression, we immunostained the transgenic animals that presumptively overexpressed SUP-18::NOX using an anti-SUP-18(N) antiserum that recognizes the first 258 amino acids of SUP-18 when it is overexpressed in worms (Chapter 3). SUP-18::NOX was properly localized to the dense bodies in muscle cells of transgenic animals (Figure 1C), while nontransgenic

animals displayed no staining (data not shown). This pattern of dense body localization is similar to that previously observed for SUP-18 (Chapter 3).

While SUP-18::NOX was localized to the cell membrane in muscle cells, it is possible that NOX may be enzymatically inactive due to the fusion of SUP-18 sequence at its N-terminus. Overexpression of the intracellular domain of SUP-18 which contains the nitroreductase domain is sufficient to rescue *sup-18(lf)* mutants, although not as strongly as SUP-18 (Chapter 3 and Figure 2). Thus, we tested if overexpression of NOX could also rescue *sup-18(lf)* in *sup-18(lf); sup-10(gf)* mutants. Transgenic lines overexpressing NOX had reduced locomotory rates (Figure 2), but none of these animals displayed the rubberband Unc touch response of *sup-10(gf)* (n=96), suggesting that the locomotion defect of these animals was likely the result of toxicity by *T.t.NOX*. If the locomotion defect was due to the nonspecific effect of overexpressing an NADH oxidase in muscle, we hypothesized that the toxic effect would be independent of the *sup-10(gf)* mutation. Indeed, when the *sup-10(gf)* mutation was outcrossed from one of the Unc transgenic lines, the impaired locomotion rate of the resulting strain did not change ( $5.6 \pm 1.5$  vs.  $5.0 \pm 1.6$ , respectively, n=12 for each).

Finally, we hypothesized that while SUP-18 may activate SUP-9 through an H<sub>2</sub>O<sub>2</sub>-forming activity, a physical interaction between the proteins may also be required for channel activation. Therefore, overexpressed NOX may provide the required H<sub>2</sub>O<sub>2</sub>- but it cannot reconstitute the parallel physical interaction. To test this hypothesis, we assayed the ability of NOX to rescue the proposed *sup-18(n1010)* putative catalytic null mutant rather than the *sup-18(n1033)* molecular null. The *n1010* mutation results in a serine-to-asparagine mutation in a residue proposed to bind an FMN cofactor, and introduction of the *n1010* mutation into the equivalent serine in *T.t.NOX* severely reduces its enzymatic activity (Chapter 3). Overexpression of *T.t.NOX* in *sup-18(n1010); sup-10(gf)* mutants reduced their locomotory rate as it had in *sup-18(n1033); sup-10(gf)* mutants (Figure 2), and also failed to induce the rubberband Unc response in these animals (n=84).

Our results indicate that the introduction of an H<sub>2</sub>O<sub>2</sub>-forming enzyme in *C. elegans* muscle is unable to restore *sup-18* activity. Although *T.t. Nox* may be catalytically inactive in *C. elegans*, the toxicity conferred by its overexpression suggests that it likely has enzymatic activity in *C. elegans*. NOX displays robust NADH-oxidase activity even at room temperature (Chapter 3 and Park et al., 1992b). The activation of SUP-9 by SUP-18 may require an enzymatic activity that is not provided by *T.t.NOX*.

Besides its similarity to NOX, SUP-18 is similar to the oxygen-insensitive nitroreductases, which catalyze the reductions of a wide variety of quinones and nitroaromatic compounds (Zenno et al., 1996a; Zenno et al., 1996b). Thus, the ability of an oxygen-insensitive nitroreductase such as NfsB to substitute for SUP-18 *in vivo* may uncover an enzymatic role for SUP-18 in its activation of the SUP-9 two-pore channel, but the identification of the *in vivo* substrate will likely remain more elusive.

## References

Hecht, H. J., Erdmann, H., Park, H. J., Sprinzl, M., and Schmid, R. D. (1995). Crystal structure of NADH oxidase from *Thermus thermophilus*, *Nat Struct Biol* 2, 1109-1114.

Lovering, A. L., Hyde, E. I., Searle, P. F., and White, S. A. (2001). The structure of *Escherichia coli* nitroreductase complexed with nicotinic acid: three crystal forms at 1.7 Å, 1.8 Å and 2.4 Å resolution, *J Mol Biol* 309, 203-13.

Park, H. J., Kreutzer, R., Reiser, C. O., and Sprinzl, M. (1992a). Molecular cloning and nucleotide sequence of the gene encoding a H<sub>2</sub>O<sub>2</sub>-forming NADH oxidase from the extreme thermophilic *Thermus thermophilus* HB8 and its expression in *Escherichia coli*, *Eur J Biochem* 205, 875-879.

Park, H. J., Reiser, C. O., Kondruweit, S., Erdmann, H., Schmid, R. D., and Sprinzl, M. (1992b). Purification and characterization of a NADH oxidase from the thermophile *Thermus thermophilus* HB8, *Eur J Biochem* 205, 881-885.

Zenno, S., Koike, H., Kumar, A. N., Jayaraman, R., Tanokura, M., and Saigo, K. (1996a). Biochemical characterization of NfsA, the *Escherichia coli* major nitroreductase exhibiting a high amino acid sequence homology to Frp, a *Vibrio harveyi* flavin oxidoreductase, *J Bacteriol* 178, 4508-14.

Zenno, S., Koike, H., Tanokura, M., and Saigo, K. (1996b). Gene cloning, purification, and characterization of NfsB, a minor oxygen-insensitive nitroreductase from *Escherichia coli*, similar in biochemical properties to FRase I, the major flavin reductase in *Vibrio fischeri*, *J Biochem (Tokyo)* 120, 736-44.



Figure 1. A SUP-18::NOX Chimera Does not Rescue *sup-18(lf)* Mutants

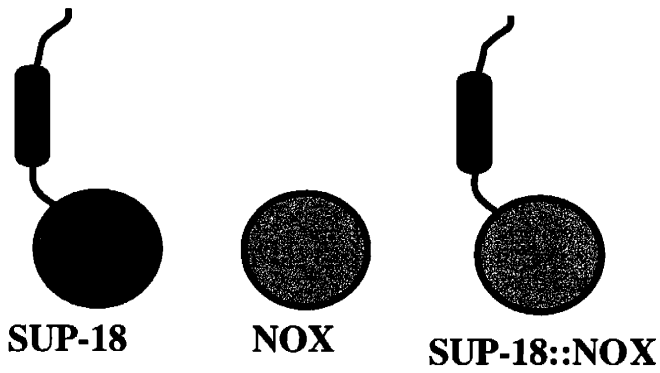
A. Schematic representation of SUP-18 (blue), *T.t.NOX* (gray) and the SUP-18::NOX Chimera. Cylinders, transmembrane domain; circle, catalytic domain. In the chimera, the *T.t.nox* coding sequence was introduced after codon 109 of *sup-18* in the  $P_{myo-3}sup-18$  vector using standard PCR techniques (Chapter 3).

B. Locomotion assays of transgenic lines and control strains in *sup-18* rescue experiments. All transgenic lines were generated using the coinjection marker  $P_{myo-3}gfp$  at 70ng/ $\mu$ L and the experimental plasmid at 30ng/ $\mu$ L. Transgenic hermaphrodites were identified by their GFP fluorescence and assayed for the number of body-bends they make on a bacterial lawn as previously described (Chapter 3). The *sup-10(gf)* allele is *n983* and the *sup-18(lf)* allele is the molecular null *n1033*. All bars represent mean  $\pm$  SEM of independent lines; n=12 for all strains.

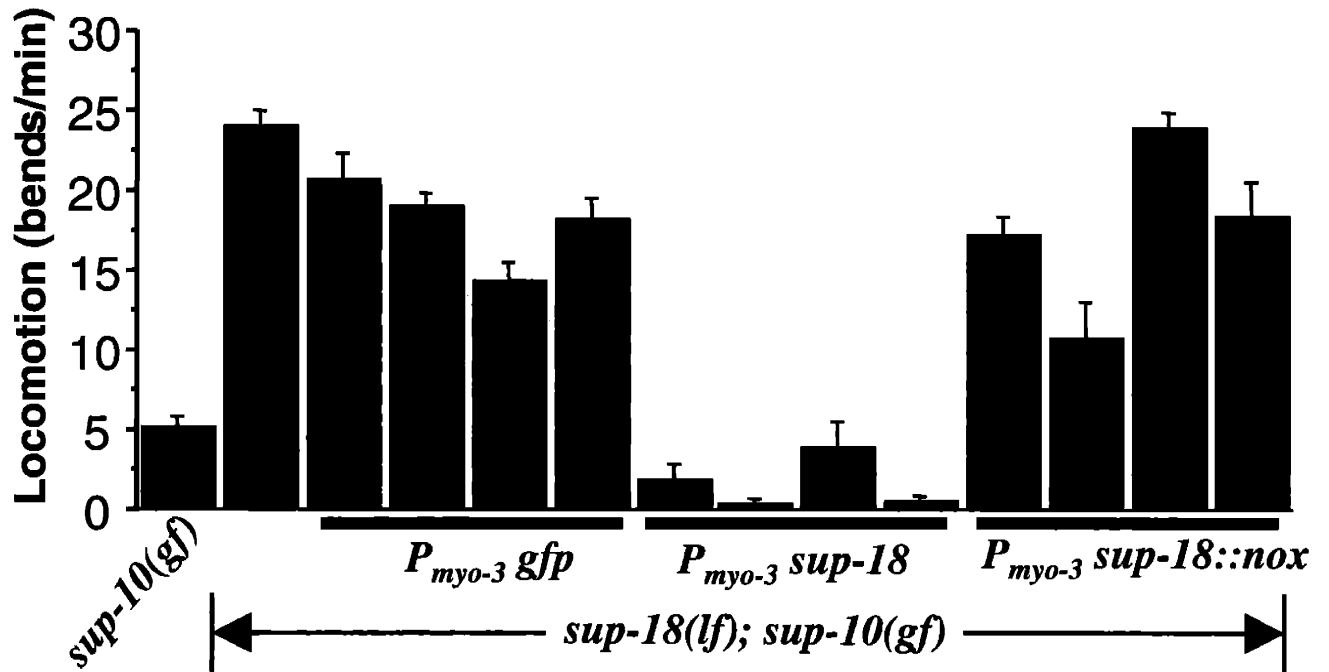
C. Representative immunostaining of muscle cell from an adult hermaphrodite transgenic for  $P_{myo-3}sup-18::nox$ . Transgenic animals from were fixed, permeabilized and immunostained using the SUP-18(N) antiserum and a goat-anti-rabbit Texas Red-conjugated secondary antibody as previously described (Chapter 3). Scale bar, 10 $\mu$ m.

**Figure 1**

**A**



**B**



**C**

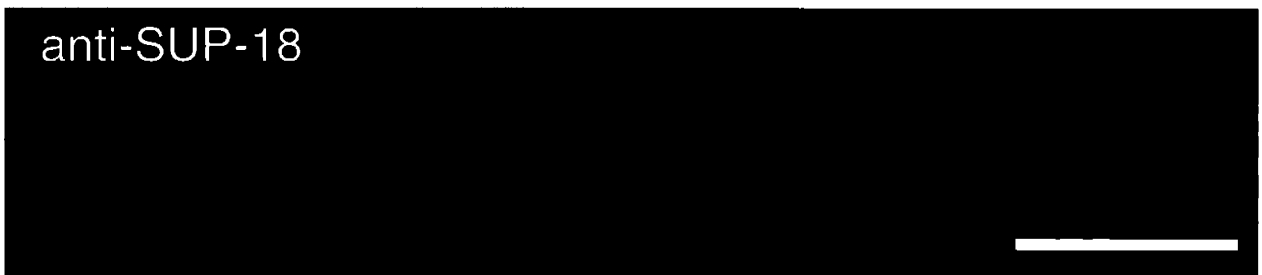
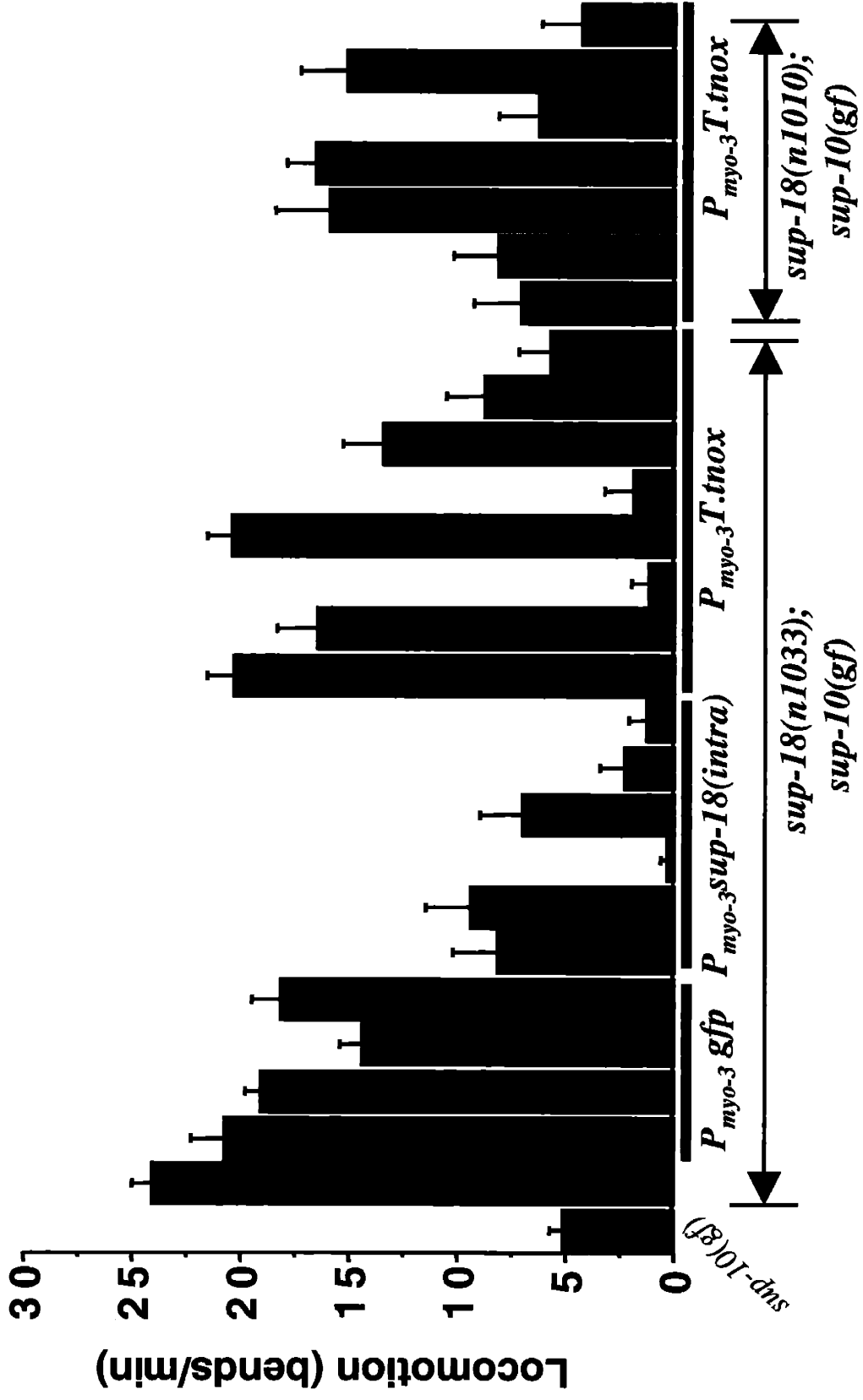


Figure 2. Overexpression of *T.t.NOX* in *sup-18(lf); sup-10(gf)* is Toxic

Locomotion assays of transgenic lines and control strains. All transgenic lines were generated as in Figure 1. The complete coding sequence of *T.t.nox* was subcloned into the *myo-3* expression vector pD95.86 (provided by A. Fire) using standard PCR techniques. The *sup-18* allele used in rescue experiments is indicated below the bars. All bars represent mean  $\pm$  SEM; n=12 for all strains.

**Figure 2**



## **CHAPTER FOUR**

### **Additional Findings**

## The *sup-9(n3935)* Mutation Reveals a Convergence of Activating Signals from Multiple Regulatory Subunits

### Introduction

The mutant SUP-9(n1435) two-pore K<sup>+</sup> channel is resistant to activation by its proposed regulatory subunits SUP-10(gf) and SUP-18, but can support the gf activity of its mutant UNC-93(gf) subunit (Chapter 3). The *sup-9(n1435)* mutation results in a serine-to-phenylalanine substitution within a short conserved region within the intracellular C-terminal region of SUP-9. Serine 289 was identified through site-directed mutagenesis as additionally required for activation of SUP-9 by the SUP-10(gf)/SUP-18 activation pathway but not by UNC-93(gf) (Chapter 3). Both of these serine residues are conserved in the mammalian TASK-1 and TASK-3 two-pore channels but are not found in other mammalian or *C. elegans* two-pore K<sup>+</sup> channels.

Studies on the bacterial KcsA channel (Perozo et al., 1998; Perozo et al., 1999), the Shaker voltage-gated channel (Holmgren et al., 1998) and on CNG channels (Flynn and Zagotta, 2001; Johnson and Zagotta, 2001), which are structurally related to the Shaker channel and have P-domains, all implicate a rotation of the TMDs that follow the P-domains during channel gating. The *sup-9(n1550)* gf mutation results in an alanine-to-threonine substitution within this transmembrane domain (Chapter 2), consistent with the proposed role of this transmembrane domain in channel gating. We hypothesize that additional residues in SUP-9 may be required for an activating SUP-18 signal originating in the SC Box to be transmitted to the transmembrane domains and result in channel opening. These residues may lie in the C-terminal domain of SUP-9 where the SC Box is found or within the transmembrane domains. Site-directed mutagenesis of residues in *sup-9* coupled with rescue experiments in worms would allow the identification of such residues, as was done in the identification of S289 (Chapter 3). However, such an approach is limited by the subjectivity with which candidate residues are selected for mutagenesis. To identify such residues through a nonbiased approach, we have performed a large-scale genetic screen for semidominant suppressors of the locomotion defects of *sup-10(gf)* mutants.

## Results

### Screen Rationale

A genetic strategy for isolating mutant SUP-9 channels that are specifically resistant to activation by SUP-10(gf)/SUP-18 would be to perform an F<sub>2</sub> screen for suppressors of *sup-10(gf)* locomotion defects and then test which ones cannot suppress the defects of *unc-93(gf)* mutants. Most of the *sup-9* alleles isolated from such a screen would be *lf* and null mutations in *sup-9*, rather than the rare alleles that would result in a SUP-9 protein specifically impaired in SUP-10(gf)/SUP-18 activation. We therefore opted for an alternate strategy based on the semidominance of the *sup-9(n1435)* mutation to enrich for this rare class of mutants. While the *sup-9* null mutations, such as *n1913*, recessively suppress the locomotion defects of *sup-10(gf)* mutants, the *sup-9(n1435)* mutation displays a strong semidominant suppression (Figure 1, black bars). As two pore K<sup>+</sup> channels are homodimers (Czirjak and Enyedi, 2002; Lopes et al., 2001), this semidominance likely reflects the formation of nonfunctional heterodimers composed of *n1435* and wildtype *sup-9* proteins. The strength of this semidominance (~23 vs. ~5 bends/minute for *sup-9(n1435)/+*; *sup-10(gf)* vs. *sup-10(gf)* mutants, respectively) formed the basis for an F<sub>1</sub> screen for suppressors of *sup-10(n983)* locomotion defects.

### Isolation of *sup-9* Alleles

*sup-10(gf)* L4 hermaphrodites were mutagenized with EMS and approximately 550,000 F1 progeny (1.1 million genomes) were screened for improved locomotion on agar plates. From 89 candidate suppressors, 35 mutants retested in the next generation, representing at least 31 independent mutants. To quantitate the semidominant character of each of these mutants, wildtype males were crossed into homozygous mutant hermaphrodites to generate *sup/+*; *sup-10(gf)* males, and their locomotion rate was scored (Figure 1). Because *sup-10* is on the X chromosome, this strategy generates males hemizygous for *sup-10(gf)* while heterozygous for other mutations not on the X chromosome, providing a convenient assay of semidominance. Four mutations were completely dominant in males with locomotion rates very similar to wt animals (~ 33 bends/minute). We reasoned that these four mutants were likely *lf* alleles of *sup-10*, as such animals would be hemizygous for *sup-10* and thus appear dominant in males. We confirmed such an assignment by sequencing the *sup-10* locus and found mutations in all four strains (See appendix II, Table 1).

For the stronger remaining mutants, we performed complementation tests with *sup-9*, *sup-18* and *unc-93* strains and identified seven semidominant alleles of *sup-9*: *A-71-1*, *D-7-2*, *n3935*, *n3942*, *n3975*, *n3976* and *n3977* (Figure 1). As heterozygotes, five of these mutants had similar suppressive activity as *sup-9(n1435)/+* (~23 bends/minute), while the other two mutations were weaker (Figure 1). We identified the molecular lesions in all seven *sup-9* alleles and found that *n3942*, *D-7-2* and *A-71-1* contained the same C to T transition as *sup-9(n1435)*, and therefore the same S292F substitution (Figure 2A). The other alleles contained missense mutations affecting four different regions of SUP-9 (Figure 2A) including the first and second transmembrane domains, the first P-domain and the beginning of the C-terminal cytoplasmic domain.

To determine if these four *sup-9* mutations conferred resistance to *sup-18* activation or if they were simply dominant negative mutations, we tested their responsiveness to changes in *sup-18* levels. As shown previously (Chapter 3), the strength of the locomotion defect in *sup-10(gf)* mutants is sensitive to the levels of *sup-18*: *sup-18(lf)/+; sup-10(gf)* mutants have a greatly improved locomotion over *sup-10(gf)* mutants (Figure 2A), indicating that the wild-type SUP-9 in these strains is competent for SUP-18 activation and thus sensitive to SUP-18 levels. By contrast, *sup-9(n1435)/+; sup18(lf)/+; sup-10(gf)* mutants have only a very weakly improved locomotory rate over *sup-9(n1435)/+; sup-10(gf)* mutants, consistent with the model that SUP-9(n1435) cannot be activated by SUP-18 and thus is not responsive to changes in its levels. A small improvement in locomotory rate was expected, as one quarter of the SUP-9 dimers in these mutants would contain two wildtype subunits and would be fully responsive to *sup-18*. By this *sup-18* sensitivity assay, *sup-9(n3935)/+* animals showed an identical response to *sup-9(n1435)/+* animals, while *n3975/+*, *n3976/+* and *n3977/+* mutants showed a significant improvement in locomotory rate in response to a change in *sup-18* levels. Thus, the channels generated by these three mutations have impaired ability to generate K<sup>+</sup> currents but retain regulation by SUP-18.

Because it suppressed the *sup-10(gf)* defects semidominantly and was insensitive to *sup-18* levels, *sup-9(n3935)* behaved like the original *sup-9(n1435)*. In addition to its *sup-18* insensitivity, *sup-9(n1435)* is only a weak suppressor of *unc-93(gf)* locomotion defects while the null mutation *sup-9(n1913)* completely suppresses the *unc-93(gf)* defects (Figure 2C and Chapter 3). We found that unlike the *sup-9(n1435)* mutation, *sup-9(n3935)* completely suppressed the locomotion defects of *unc-93(gf)* animals, indicating that *sup-9(n3935)* was not only insensitive to *sup-18* but also



resistant to the activating effects of *unc-93(gf)*. Thus, *sup-9(n3935)* defines a new class of *sup-9* mutations that prevents gf channel activation by all of its subunits.

## Discussion

Through a genetic screen for semidominant suppressors of *sup-10(gf)* mutants we have isolated seven alleles of *sup-9*. Three *sup-9* alleles are resistant to activation by *sup-18* and are identical to the original *n1435* mutation, three are dominant-negative *sup-9* alleles that retain sensitivity to *sup-18* and one defines a new class of channel mutants that cannot be activated by any subunit. In addition to these four mutants, four *lf* mutations in *sup-10* and at least six in both *sup-18* and *unc-93* were isolated.

The three suppressors that were specifically resistant to *sup-18* activation all contained a mutation identical to the original *sup-9(n1435)* mutation. This suggests there may be no EMS-mutable residues in addition to serine 292 that can confer specific resistance to SUP-18. The S289A mutation identified through mutagenesis as conferring resistance to *sup-10(gf)* channel activation would not have been isolated through EMS mutagenesis since it would require a T-to-G nucleotide change, and T-to-G changes are very rarely induced by EMS in *C. elegans* (Anderson, 1995). Although the inability to identify new mutations that behave like *sup-9(n1435)* may be in part to the limited mutagenic range of EMS, our results suggest that the target for SUP-18 activation in SUP-9 is small and might be truly limited to the SC Box where these serines are found. The mechanism by which SUP-18 activates SUP-9 channel activity is still unclear (Chapter 3). SUP-18 may activate SUP-9 through an enzymatic product or through a protein-protein interaction. If the later is the mode of activation *in vivo*, then our results suggests that the binding interface between these two proteins may be small, such that disruption of this interface by mutation is limited only to serines 289 and 292.

## The Post-4TMD Region of Two-Pore Channels Integrates Multiple Inputs

The *sup-9(n3935)* mutation contains an arginine-to-tryptophan substitution at amino acid 244, just after the last transmembrane domain of SUP-9 (Figure 3A). The *sup-9(n1550)* *gf* mutation results in an alanine-to-threonine substitution at residue 236 within the fourth transmembrane domain on SUP-9 (Chapter 2). Thus, activation of SUP-9 by SUP-18 may occur through the relay of an activating signal from the SC Box to this domain to this post 4-TMD region (Figure 3A), resulting in helix rotation and

channel opening. Our results suggest that the post 4-TMD region in SUP-9 may integrate multiple activation signals, from SUP-18 and UNC-93, that result in channel opening (Figure 3A).

The human TASK-1 channel can be activated by high pH (Duprat et al., 1997), volatile anesthetics including halothane (Duprat et al., 1997; Leonoudakis et al., 1998; Patel et al., 1999) and can be inhibited by neurotransmitters such as thyrotropin releasing hormone (TRH) (Talley and Bayliss, 2002; Talley et al., 2000). A six amino acid domain (Figure 3B) has been identified through deletion analysis of human TASK-1 that is required for its activation by halothane when expressed heterologously in cell culture (Patel et al., 1999; Talley and Bayliss, 2002). In addition, the same domain is required for inhibition of TASK-1 activity by the neurotransmitter TRH (Talley and Bayliss, 2002). Thus, this region of TASK-1 integrates both activating and inhibitory modulatory signals that drive channel gating (Figure 3B). Sequence alignment between SUP-9 and TASK-1 (Chapter 2) indicates that the arginine residue mutated in *sup-9(n3935)* is equivalent to the arginine within this six-residue domain *i.e.* SUP-9 R244 corresponds to R245 of TASK-1 (Figure 3A,B). Thus, our findings suggest that regulation of two-pore channels by multiple inputs, including neurotransmitters, anesthetics and regulatory subunits, occurs through a conserved region post 4-TMD in both *C. elegans* and humans.

### **Acknowledgments**

I would like to thank Ewa Davidson for helpful comments concerning this work.

### **References**

- Anderson, P. (1995). Mutagenesis. In *Caenorhabditis elegans* : modern biological analysis of an organism, H. F. Epstein, and D. C. Shakes, eds. (San Diego, Academic Press), pp. 31-58.
- Brenner, S. (1974). The genetics of *Caenorhabditis elegans*, *Genetics* 77, 71-94.
- Czirjak, G., and Enyedi, P. (2002). Formation of functional heterodimers between the TASK-1 and TASK-3 two-pore domain potassium channel subunits, *J Biol Chem* 277, 5426-32.

Duprat, F., Lesage, F., Fink, M., Reyes, R., Heurteaux, C., and Lazdunski, M. (1997). TASK, a human background K<sup>+</sup> channel to sense external pH variations near physiological pH, *EMBO J* 16, 5464-5471.

Flynn, G. E., and Zagotta, W. N. (2001). Conformational changes in S6 coupled to the opening of cyclic nucleotide-gated channels, *Neuron* 30, 689-98.

Holmgren, M., Shin, K. S., and Yellen, G. (1998). The activation gate of a voltage-gated K<sup>+</sup> channel can be trapped in the open state by an intersubunit metal bridge, *Neuron* 21, 617-621.

Johnson, J. P., Jr., and Zagotta, W. N. (2001). Rotational movement during cyclic nucleotide-gated channel opening, *Nature* 412, 917-21.

Leonoudakis, D., Gray, A. T., Winegar, B. D., Kindler, C. H., Harada, M., Taylor, D. M., Chavez, R. A., Forsayeth, J. R., and Yost, C. S. (1998). An open rectifier potassium channel with two pore domains in tandem cloned from rat cerebellum, *J Neurosci* 18, 868-877.

Lopes, C. M., Zilberberg, N., and Goldstein, S. A. (2001). Block of Kcnk3 by protons. Evidence that 2-P-domain potassium channel subunits function as homodimers, *J Biol Chem* 276, 24449-52.

Patel, A. J., Honore, E., Lesage, F., Fink, M., Romey, G., and Lazdunski, M. (1999). Inhalational anesthetics activate two-pore-domain background K<sup>+</sup> channels, *Nat Neurosci* 2, 422-426.

Perozo, E., Cortes, D. M., and Cuello, L. G. (1998). Three-dimensional architecture and gating mechanism of a K<sup>+</sup> channel studied by EPR spectroscopy, *Nat Struct Biol* 5, 459-469.

Perozo, E., Cortes, D. M., and Cuello, L. G. (1999). Structural rearrangements underlying K<sup>+</sup>-channel activation gating, *Science* 285, 73-78.

Talley, E. M., and Bayliss, D. A. (2002). Modulation of TASK-1 (Kcnk3) and TASK-3 (Kcnk9) Potassium Channels. Volatile anesthetics and neurotransmitters share a molecular site of action, *J Biol Chem* 277, 17733-42.

Talley, E. M., Lei, Q., Sirois, J. E., and Bayliss, D. A. (2000). TASK-1, a two-pore domain K<sup>+</sup> channel, is modulated by multiple neurotransmitters in motoneurons, *Neuron* 25, 399-410.

Figure 1. Gene Assignments of Semidominant Suppressors of *sup-10(gf)*

Wild-type males were mated into wt, *sup-10(n983)*, *sup-9(n1913); sup-10(n983)*, *sup-9(n1435); sup-10(n983)* hermaphrodites and to hermaphrodites of each suppressed strain to generate *sup/+;sup-10(gf)* cross-progeny males (*sup-10* is on the X-chromosome so males will be hemizygous for the *sup-10(gf)* mutation). At least 14 cross-progeny males of each genotype were scored for locomotory rate as previously described (Chapter 3). The colors on the bars indicate the gene assignment of each suppressor according to transmission tests and complementation tests using wild-type or *sup-9(n1913); sup-10(n983)* or *unc-93(lr12)* or *sup-18(n1030); sup-10(n983)* males. Bars denote mean  $\pm$  SEM. Mutagenesis was performed as previously described (Brenner, 1974).

**Figure 1**

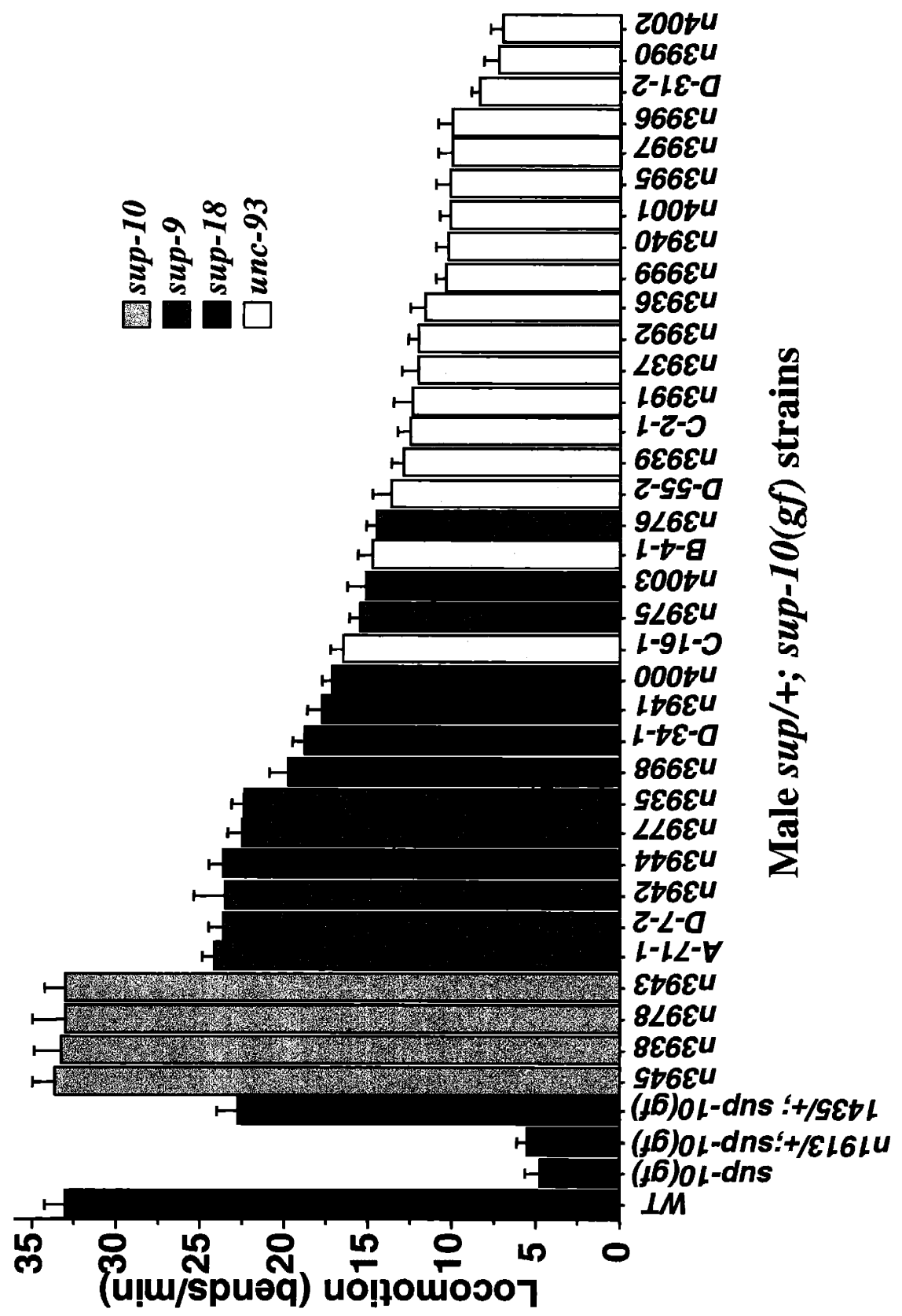


Figure 2. The *sup-9(n3935)* Mutation in the Post-4-TMD Region of SUP-9 Confers Resistance to Activation by *sup-18* and *unc-93(gf)*

A. Schematic diagram of SUP-9 showing the allele, location and amino acid substitution for each of the seven semidominant suppressors. The *n3932*, *A-71-1* and *D-7-2* mutations result in the same S292F mutation as that found in *sup-9(n1435)*. All DNA sequencing was performed on both strand as described (Chapter 2). Cylinders, TMDs; black circles, site of mutation.

B. Locomotion assays of males carrying various combinations of *sup-9* semidominant mutations and *sup-18(lf)* mutations. Wild-type males were mated into *wt*, *sup-10(n983)* or mutant *sup-9(sd); sup-10(gf)* hermaphrodites to generate *sup/+;sup-10(gf)* cross-progeny males. At least 16 males of each genotype were scored. Bars denote mean  $\pm$  SEM.

C. Locomotion assays of young-adult *unc-93(e1500) gf* hermaphrodites carrying different alleles of *sup-9*. At least 20 animals of each genotype were scored. Bars denote mean  $\pm$  SEM.

Figure 2

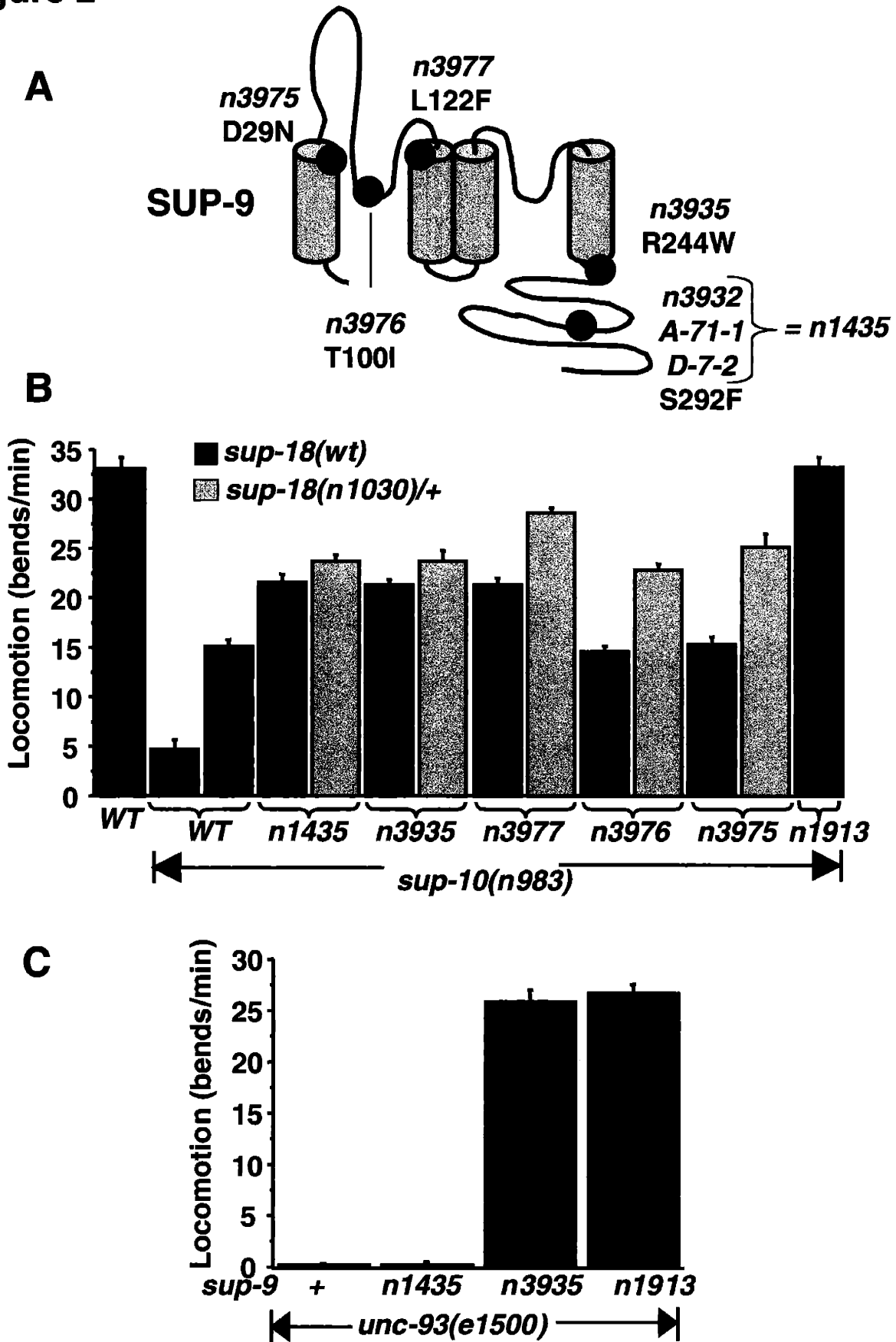


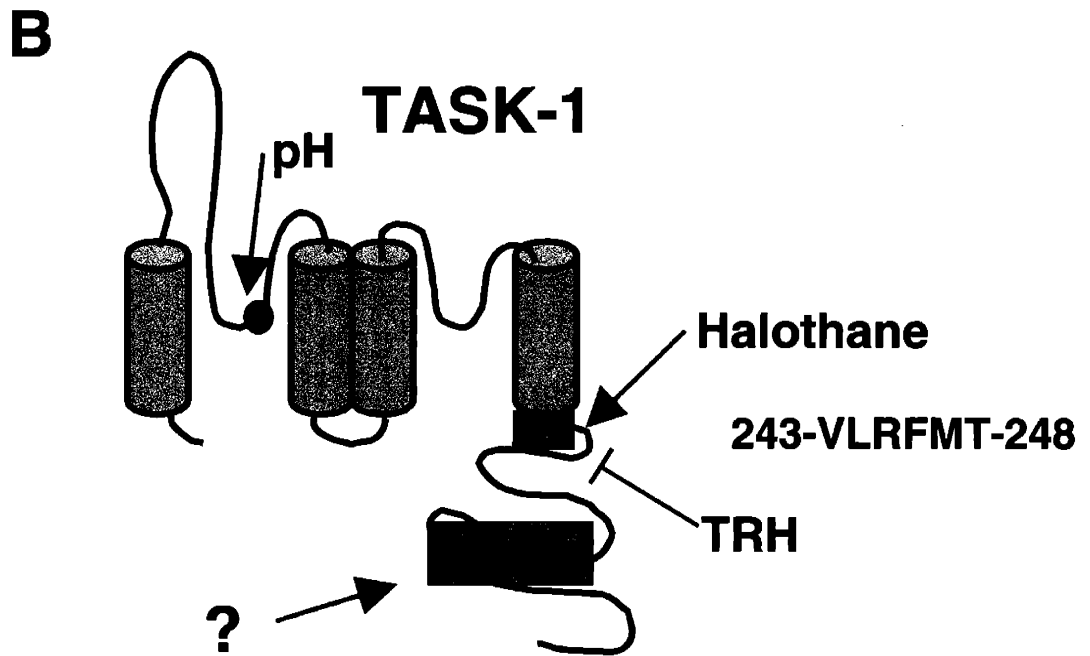
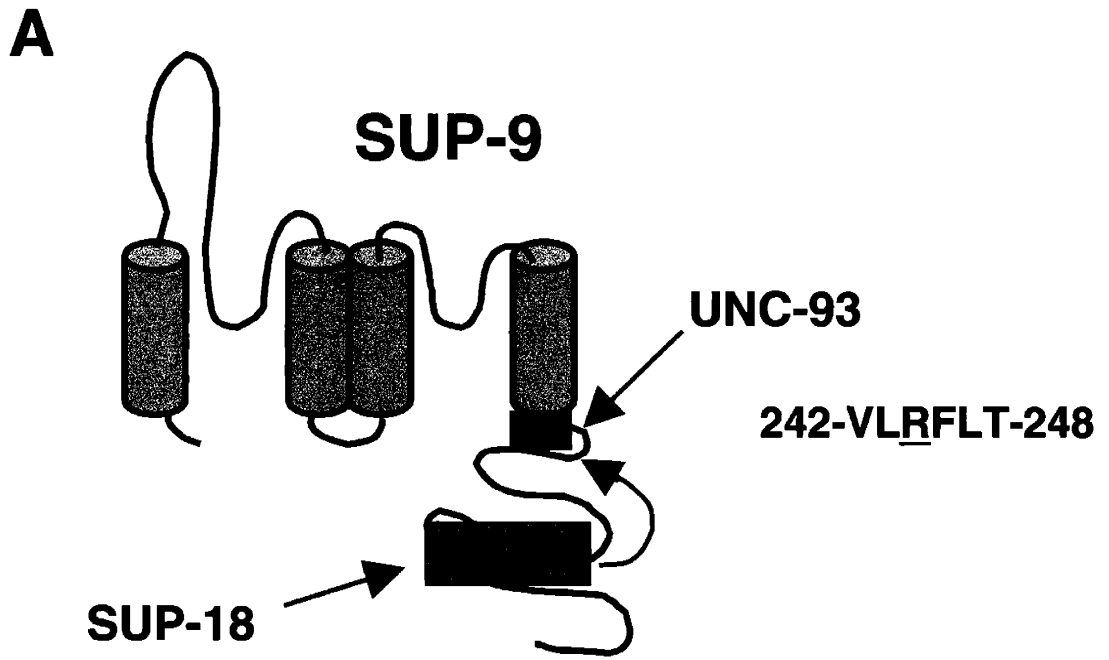


Figure 3. *C. elegans* and Mammalian Two-Pore K<sup>+</sup> channels Integrate Multiple Regulatory Inputs Through a Common Mechanism

A. Schematic diagrams of SUP-9 activation by the SUP-18 and UNC-93 regulatory subunits. The blue box refers to the location of the *sup-9(n3935)* mutation. The amino acid sequence surrounding the arginine residue mutated in *n3935* is indicated.

B. Schematic diagram of human TASK-1 modulation by multiple inputs. TRH, Thyrotropin Releasing Hormone; the blue box denotes the six amino acid stretch required for modulation by halothane and TRH, and its sequence is shown to the right.

**Figure 3**



## **Analysis of Two-Pore K<sup>+</sup> Channel Function and Membrane Localization in *C. elegans***

### **Introduction**

Analysis of the completed *C. elegans* genome has revealed over 70 K<sup>+</sup> channels, including over 50 from the two-pore (twk) family (Bargmann, 1998; Wei et al., 1996). Two twk channels, *sup-9* and *twk-18*, have been defined by gf mutations that lead to a characteristic rubberband-Unc muscle paralysis (Chapter 2 and (Kunkel et al., 2000; Levin and Horvitz, 1993)). Although the functions of other two-pore channels have yet to be defined by forward or reverse genetics, some progress has been made in molecularly characterizing these channels (Salkoff et al., 2001; Wang et al., 1999). Transcriptional GFP reporters of twenty two-pore channel promoters have defined predicted expression patterns (Salkoff et al., 2001). Some of these promoters drive expression in single cells, while others affect neurons, muscle, intestinal or hypodermal cells more broadly (Salkoff et al., 2001).

Among the 50 predicted twk channels, TWK-4 shares significant amino acid similarity (41%) with SUP-9 indicating that they form a subfamily, while the other channels all share less than 30% identity with SUP-9 or TWK-4 (Figure 1 and data not shown). SUP-9 and TWK-4 are both similar to the human TASK-1 and TASK-3 channels (Duprat et al., 1997; Kim et al., 2000; Leonoudakis et al., 1998). TASK-1 and TASK-3 form a subfamily of two-pore channels that are activated by high pH through a histidine in their first P-domain (Kim et al., 2000; Lopes et al., 2001; Rajan et al., 2000) and are also regulated by both the volatile anesthetic halothane and by neurotransmitters (Czirjak and Enyedi, 2002; Meadows and Randall, 2001; Patel et al., 1999; Talley and Bayliss, 2002). Not only are TASK-1 and TASK-3 similar in their sequence and regulation, they can also form heterodimeric channels when expressed heterologously in cell culture (Czirjak and Enyedi, 2002). Thus, we hypothesized that *twk-4* may have a similar function in *C. elegans* to *sup-9* in regulation muscle contraction. Consistent with this hypothesis is the finding that a *twk-4* transcriptional reporter is expressed in muscle cells (Salkoff et al., 2001).

In this appendix, we have explored a functional role for *twk-4* in muscle contraction and present a comparison of the membrane localization of the three muscle channels SUP-9, TWK-4 and TWK-18.

## Results/Discussion

### Overexpression of Wildtype or Mutant TWK-4 in Worm Muscle Has no Effect on Locomotion Rates

*sup-9(lf)* mutants have a wildtype phenotype (Greenwald and Horvitz, 1980), whereas *sup-9(gf)* mutants display a characteristic rubberband Unc paralysis (Chapter 2 and (Levin and Horvitz, 1993)). To test if *twk-4* hyperactivity could also result in a rubberband Unc paralysis we overexpressed a *twk-4* transgene in muscle. Overexpression of a *myo-3::twk-4* transgene in *lin-15* animals (a *lin-15*-containing plasmid was used as a coinjection marker) did not alter the locomotion rate of three independently derived transgenic lines when compared to nontransgenic animals (Table 1), indicating that additional *twk-4* activity in muscle does not hyperpolarize muscle membranes. Overexpression of wild-type *sup-9* in muscle does not result in membrane hyperpolarization (Chapter 2), but overexpression of *sup-9(n1550)* induces a severe paralysis (Chapter 2-Appendix). The *sup-9(n1550)* *gf* mutation results in an alanine-to-serine substitution at amino acid 236 (Chapter 2 and Figure 1). This serine is conserved in TWK-4 (Figure 1). We introduced the *gf n1550* mutation into the *twk-4* cDNA and overexpressed it as a transgene in muscle. Animals overexpressing TWK-4(n1550) had locomotion rates indistinguishable from either wild-type animals or those overexpressing TWK-4. Thus, in spite of their amino acid similarity and reported muscle expression, *twk-4* and *sup-9* may have different functions in the regulation of muscle contraction in *C. elegans*. Since *twk-4(lf)* mutations have not been isolated in suppressor screens of the rubberband Unc phenotype of *sup-9(gf)* (Levin and Horvitz, 1993), *unc-93(gf)* (De Stasio et al., 1997; Greenwald and Horvitz, 1980) or *sup-10(gf)* (Greenwald and Horvitz, 1986) mutants, it is unlikely that TWK-4 physically interacts with the proposed SUP-9/SUP-10/UNC-93 channel complex. Furthermore, TWK-4 does not have an SC Box (Chapter 3) and its C-terminal domain did not support the *gf* activity of *sup-10(n983)* as a SUP-9::TWK-4 chimera (Chapter 3), further supporting a distinct form of regulation for this channel. However, *twk-4* may associate with one of the UNC-93-like proteins predicted from the genome (Chapter 2).

### TWK-18::GFP Has a Strikingly Different Membrane Localization on Muscle Membranes Compared to TWK-4::GFP and SUP-9

SUP-9 is localized to the cell membrane when overexpressed in muscle and immunostained with antiSUP-9 antisera (Chapter 2 and Figure 1A) or when tagged with

GFP and expressed as a transgene under its own promoter (Chapter 2). SUP-9 staining is concentrated in dense bodies, structures functionally analogous to vertebrate Z-lines that connect the myofibril lattice to the cell membrane (Waterston et al., 1980). The cell surface localization of other K<sup>+</sup> channels has not been reported, except for the high-conductance Ca<sup>2+</sup>-activated K<sup>+</sup> channel Slo-1 which also localizes to dense bodies (Wang et al., 2001). To determine if TWK-4 is localized to dense bodies, we introduced the coding sequence of *gfp* just prior to the stop codon of *twk-4* in the *myo-3* driven vector used in the above overexpression experiments. We found that when overexpressed in muscle, TWK-4::GFP also colocalized to dense body structures (Figure 2B). To determine if dense body localization was a general phenomena for muscle K<sup>+</sup> channels, we examined the expression pattern of a TWK-18::GFP fusion. Contrary to SUP-9 and TWK-4::GFP, TWK-18::GFP was excluded from the dense bodies and from the M-lines, the sites of stacking between thick filaments (Waterson, 1988), but showed an otherwise uniform distribution on the cell surface. The localization pattern of TWK-18 on the membrane was the reverse of that observed for the integrin beta subunit PAT-3::GFP (Figure 1D and (Gettner et al., 1995)). We also compared the membrane distribution TWK-18::GFP to that of SUP-18::GFP and of GFP alone. As previously reported (Chapter 3), SUP-18::GFP localized to dense bodies like SUP-9 (Figure 2E). GFP alone was expressed cytoplasmically as expected, but the GFP proximal to the membrane was excluded from the M-lines but not from the dense bodies. These results indicate that the *twk* channels SUP-9 and TWK-18 are differentially localized to distinct domains on the surface of *C. elegans* muscle cells.

To our knowledge, this represents the first report of differential membrane targeting of two-pore K<sup>+</sup> channels expressed within the same cell for any organism. Although at present the functional significance of this differential targeting of K<sup>+</sup> channels to distinct domains of the cell is unknown, our findings establish a powerful model for the study of this differential trafficking. Chimeras between SUP-9 and TWK-18 may identify the domains in these channels that regulate differential targeting. In mammals, proteins such as PSD-95, a postsynaptic density protein which contains PDZ domains and belongs to the MAGUK family (Membrane Associated GUanylate Kinase), target voltage-gated and K<sub>ir</sub> channels to post-synaptic sites (Arnold and Clapham, 1999; Cohen et al., 1996; Kim et al., 1995; Tanemoto et al., 2002). At least 30 proteins containing PDZ domains are found in the *C. elegans* genome (Bargmann,

1998). Genetic screens for mistargeted SUP-9::GFP or TWK-18::GFP reporters may identify genes involved in the trafficking of these channels.

## References

Arnold, D. B., and Clapham, D. E. (1999). Molecular determinants for subcellular localization of PSD-95 with an interacting K<sup>+</sup> channel, *Neuron* 23, 149-57.

Bargmann, C. I. (1998). Neurobiology of the *Caenorhabditis elegans* genome, *Science* 282, 2028-2033.

Cohen, N. A., Brenman, J. E., Snyder, S. H., and Brecht, D. S. (1996). Binding of the inward rectifier K<sup>+</sup> channel Kir 2.3 to PSD-95 is regulated by protein kinase A phosphorylation, *Neuron* 17, 759-67.

Czirjak, G., and Enyedi, P. (2002). Formation of functional heterodimers between the TASK-1 and TASK-3 two-pore domain potassium channel subunits, *J Biol Chem* 277, 5426-32.

De Stasio, E., Lephoto, C., Azuma, L., C., H., Stanislaus, D., and Uttam, J. (1997). Characterization of Revertants of *unc-93(e1500)* in *Caenorhabditis elegans* Induced by N-ethyl-N-nitrosourea, *Genetics* 147, 597-608.

Duprat, F., Lesage, F., Fink, M., Reyes, R., Heurteaux, C., and Lazdunski, M. (1997). TASK, a human background K<sup>+</sup> channel to sense external pH variations near physiological pH, *EMBO J* 16, 5464-5471.

Fire, A., Harrison, S. W., and Dixon, D. (1990). A modular set of lacZ fusion vectors for studying gene expression in *Caenorhabditis elegans*, *Gene* 93, 189-98.

Gettner, S. N., Kenyon, C., and Reichardt, L. F. (1995). Characterization of beta *pat-3* heterodimers, a family of essential integrin receptors in *C. elegans*, *J Cell Biol* 129, 1127-1141.

Greenwald, I., and Horvitz, H. R. (1986). A visible allele of the muscle gene *sup-10X* of *C. elegans*, *Genetics* 113, 63-72.

Greenwald, I. S., and Horvitz, H. R. (1980). *unc-93(e1500)*: A behavioral mutant of *Caenorhabditis elegans* that defines a gene with a wild-type null phenotype, *Genetics* 96, 147-164.

Kim, E., Niethammer, M., Rothschild, A., Jan, Y. N., and Sheng, M. (1995). Clustering of Shaker-type K<sup>+</sup> channels by interaction with a family of membrane-associated guanylate kinases, *Nature* 378, 85-8.

Kim, Y., Bang, H., and Kim, D. (2000). TASK-3, a new member of the tandem pore K<sup>+</sup> channel family, *J Biol Chem* 275, 9340-9347.

Kunkel, M. T., Johnstone, D. B., Thomas, J. H., and Salkoff, L. (2000). Mutants of a temperature-sensitive two-P domain potassium channel, *J Neurosci* 20, 7517-7524.

Leonoudakis, D., Gray, A. T., Winegar, B. D., Kindler, C. H., Harada, M., Taylor, D. M., Chavez, R. A., Forsayeth, J. R., and Yost, C. S. (1998). An open rectifier potassium channel with two pore domains in tandem cloned from rat cerebellum, *J Neurosci* 18, 868-877.

Levin, J. Z., and Horvitz, H. R. (1993). Three new classes of mutations in the *Caenorhabditis elegans* muscle gene *sup-9*, *Genetics* 135, 53-70.

Lopes, C. M., Zilberberg, N., and Goldstein, S. A. (2001). Block of Kcnk3 by protons. Evidence that 2-P-domain potassium channel subunits function as homodimers, *J Biol Chem* 276, 24449-52.

Meadows, H. J., and Randall, A. D. (2001). Functional characterisation of human TASK-3, an acid-sensitive two-pore domain potassium channel, *Neuropharmacology* 40, 551-9.

Okkema, P. G., Harrison, S. W., Plunger, V., Aryana, A., and Fire, A. (1993). Sequence requirements for myosin gene expression and regulation in *Caenorhabditis elegans*, *Genetics* 135, 385-404.

Patel, A. J., Honore, E., Lesage, F., Fink, M., Romey, G., and Lazdunski, M. (1999). Inhalational anesthetics activate two-pore-domain background K<sup>+</sup> channels, *Nat Neurosci* 2, 422-426.

Rajan, S., Wischmeyer, E., Xin Liu, G., Preisig-Muller, R., Daut, J., Karschin, A., and Derst, C. (2000). TASK-3, a Novel Tandem Pore Domain Acid-sensitive K<sup>+</sup> Channel. AN EXTRACELLULAR HISTIDINE AS pH SENSOR, *J Biol Chem* 275, 16650-16657.

Salkoff, L., Butler, A., Fawcett, G., Kunkel, M., McArdle, C., Paz-y-Mino, G., Nonet, M., Walton, N., Wang, Z. W., Yuan, A., and Wei, A. (2001). Evolution tunes the excitability of individual neurons, *Neuroscience* 103, 853-9.

Talley, E. M., and Bayliss, D. A. (2002). Modulation of TASK-1 (Kcnk3) and TASK-3 (Kcnk9) Potassium Channels. Volatile anesthetics and neurotransmitters share a molecular site of action, *J Biol Chem* 277, 17733-42.

Tanemoto, M., Fujita, A., Higashi, K., and Kurachi, Y. (2002). PSD-95 mediates formation of a functional homomeric Kir5.1 channel in the brain, *Neuron* 34, 387-97.

Wang, Z., Kunkel, M., Wei, A., Butler, A., and Salkoff, L. (1999). Genomic organization of nematode 4TM K<sup>+</sup> channels. In *Ann. N.Y. Acad. Sci.*, pp. 286-303.

Wang, Z. W., Saifee, O., Nonet, M. L., and Salkoff, L. (2001). SLO-1 potassium channels control quantal content of neurotransmitter release at the *C. elegans* neuromuscular junction, *Neuron* 32, 867-81.

Waterson, R. H. (1988). Muscle. In *The Nematode Caenorhabditis Elegans*, W. B. Wood, ed. (New York, Cold Spring Harbor Laboratory), pp. 281-336.



Waterston, R. H., Thomson, J. N., and Brenner, S. (1980). Mutants with altered muscle structure of *Caenorhabditis elegans*, *Dev Biol* 77, 271-302.

Wei, A., Jegla, T., and Salkoff, L. (1996). Eight potassium channel families revealed by the *C. elegans* genome project, *Neuropharmacology* 35, 805-829.

Table 1. Overexpression of *twk-4* in muscle does not result in an paralysis

Transgene	Bends/min $\pm$ SEM	Range
No transgene	25.2 $\pm$ 1.2	(18-30)
<i>twk-4(wt)</i> #1	24.9 $\pm$ 0.9	(21-29)
<i>twk-4(wt)</i> #2	26.0 $\pm$ 1.0	(22-30)
<i>twk-4(wt)</i> #3	25.7 $\pm$ 0.7	(22-29)
<i>twk-4(n1550)</i> #1	23.9 $\pm$ 1.1	(18-28)
<i>twk-4(n1550)</i> #2	24.8 $\pm$ 1.1	(20-29)
<i>twk-4(n1550)</i> #3	25.6 $\pm$ 1.3	(21-31)

Locomotion rates of *lin-15(n765)* transgenic young adults were scored for 60 seconds as described (Chapter 2). The coinjection marker was *lin-15*; n=10 for all lines. The *twk-4* cDNA (Chapter 3) was subcloned into the pPD95.86 vector (a gift of A. Fire) which contains a *myo-3* promoter driving expression in muscle (Okkema et al., 1993). The *n1550* mutation was introduced into the *twk-4* cDNA by standard PCR methods. Transgenic animals were generated as previously described (Chapter 2).

Figure 1. Sequence alignment of SUP-9, TWK-4 and TWK-18 Two-Pore K<sup>+</sup> Channels

Amino acids conserved among at least two of the channels are shaded. Amino acid identities are as follows: SUP-9/TWK-4, 41%; SUP-9/TWK-18, 18%; TWK-4/TWK-18, 14%. The transmembrane domains (TMDs) of SUP-9 are indicated by gray bars. The location of the alanine-to-threonine substitution found in the *sup-9(n1550)* gf rubberband-Unc mutant is indicated by an open triangle. Genebank accession numbers are as follows: SUP-9, (not yet assigned, Chapter 2); TWK-4, AAC32857; TWK-18, NP\_509697.

# Figure 1

**TMD1**

SUP-9 1 V K R Q N . . . . . I R T L S L V C T L T Y L L V G A I A V F D A L S E T E N E . . . . . I L Q R K L V Q R 43  
 TWK-4 1 P H Q I D G . . . . . K S A R A L L L L S T F T Y L L F G A M V F D K L E S E K D . . . . . T W V R D E I E R 46  
 TWK-18 1 V A I V A Q G V S T I L T T F Q K T F K G L L P L I I L V A Y T L L G A W T F W M T E G E N S E R E M L T E Q Q K E R D E 60

SUP-9 44 V R E K L K T K Y N M S N A D . . . . . Y E I L E A T I V K S V P H K A G Y Q W K F S G A F 84  
 TWK-4 47 I T D P L K H K Y K F S E R D . . . . . L H L F E A I A ; K S I P Q Q A G Y Q W Q F A G A F 87  
 TWK-18 61 L I R R T V Y K I N Q L Q I K R Q R R L M T A E E Y N R T A K V L T T F Q E T L G I V P A D M D K D I H W T F L G S I 120

**TMD2**

SUP-9 85 V F A T V T I I G Y G H S T P M T D A G K V F C W L Y A L A G P L G L M F Q S G E R M N T F A A K L R F I J R 144  
 TWK-4 88 V F A T V T I I V G Y G H S A P S T N A G K L F C I F A L F G V P M G L M F Q S G E R V N T F I A Y S L H K F R 147  
 TWK-18 121 F Y C M T V Y T I I G Y G N T V P G T G W G R F A T I L V A F I G T P L T V L S L Y C L G S L F A K G C K M E W R F F L 180

**TMD3**

SUP-9 145 R A A G K O . . . . . P I V I S S D L I I F C T G W G G L I F G . . . . . 172  
 TWK-4 148 D S L H Q Q G F T C L . . . . . Q E V I P T H L L M V S L T ; G F M V L V S . . . . . 180  
 TWK-18 181 K S T R V S K D L S N K I S E A A D N I E E G T T A I T P S A E K T E N N D D D L L S F P I S G L L L I T V I W V I F 240

**TMD4**

SUP-9 173 G A F M F S S Y E N W T Y F D A V Y C F V T L T T G F G D Y V A L O K R G S L O T O P E Y V F F S L V F L F G T 232  
 TWK-4 181 G T Y F H T I E K W S I F D A Y Y F C M T F S T G F G D L V P L Q Q V N A L Q D O P L Y V F A T I M F L T G S A 240  
 TWK-18 241 C A V L F T L E E W D F G T S L Y F T L S F T G F G D I L P S . . . . . D Y D F M P I V G V L L L I G S 292

**TMD5**

SUP-9 233 V I S A A E N L L V I R F L T M N T E D E R R D E Q E A I L A A Q G L V R V G . . . . . D P T A D D D F G R L P L S D 286  
 TWK-4 241 V F S A C V N L L V L G F M A S N A D E V T A A Q R E P P S A I V L E R F T R . . . . . N S L V D S Q I F N I Q K H S 294  
 TWK-18 293 L V S T V M T L I Q Q Q I E A L A S G M K D N I D Q E Y A R A L N E A R E D G E V D E H V D P E E D P E N N K K S F D A 352

SUP-9 287 N V S L A S C S C . . . . . Y Q L P D E K . . . . . L R 304  
 TWK-4 295 T V G V L P G . . . . . R P R R M . . . . . K E 308  
 TWK-18 353 V I S R M N W S K R G L Y L P D S Q K K E L A K Q S E K K M G R K S I K I Q T D N D L L E T L I R E E I L K A E L N 412

SUP-9 305 H R H R K H T E P H G - G P P T F S G M T T R P K Y 329  
 TWK-4 309 H P G H C L L W M F Q - T K A I K A S V F T Y S K A Y 334  
 TWK-18 413 N E M H K Y T A P R S S H O P K L L V Y S D V R E K E V P I E V V R V E H F N H G N E D Y L E H D I 461

Figure 2. Muscle Expression Patterns in Transgenic Animals Overexpressing GFP Translational Fusions of Various Genes.

All transgenic animals were generated in the *lin-15(n765)* strain with a *lin-15*-rescuing plasmid as a coinjection marker as previously described (Chapter 2). All photographs are of body-wall muscle cells from adult hermaphrodites. Scale bars, 10 $\mu$ m.

(A) SUP-9: SUP-9 was overexpressed under the *myo-3* promoter (Chapter 2).

Transgenic animals were fixed and stained with anti-SUP-9 antiserum and a Texas Red-conjugated secondary antibody as previously described (Chapter 2).

(B) TWK-14::GFP: The coding sequence of *gfp* was introduced just prior to the stop codon of *twk-4* in the *myo-3* expression vector (described in Table 1) using standard PCR techniques.

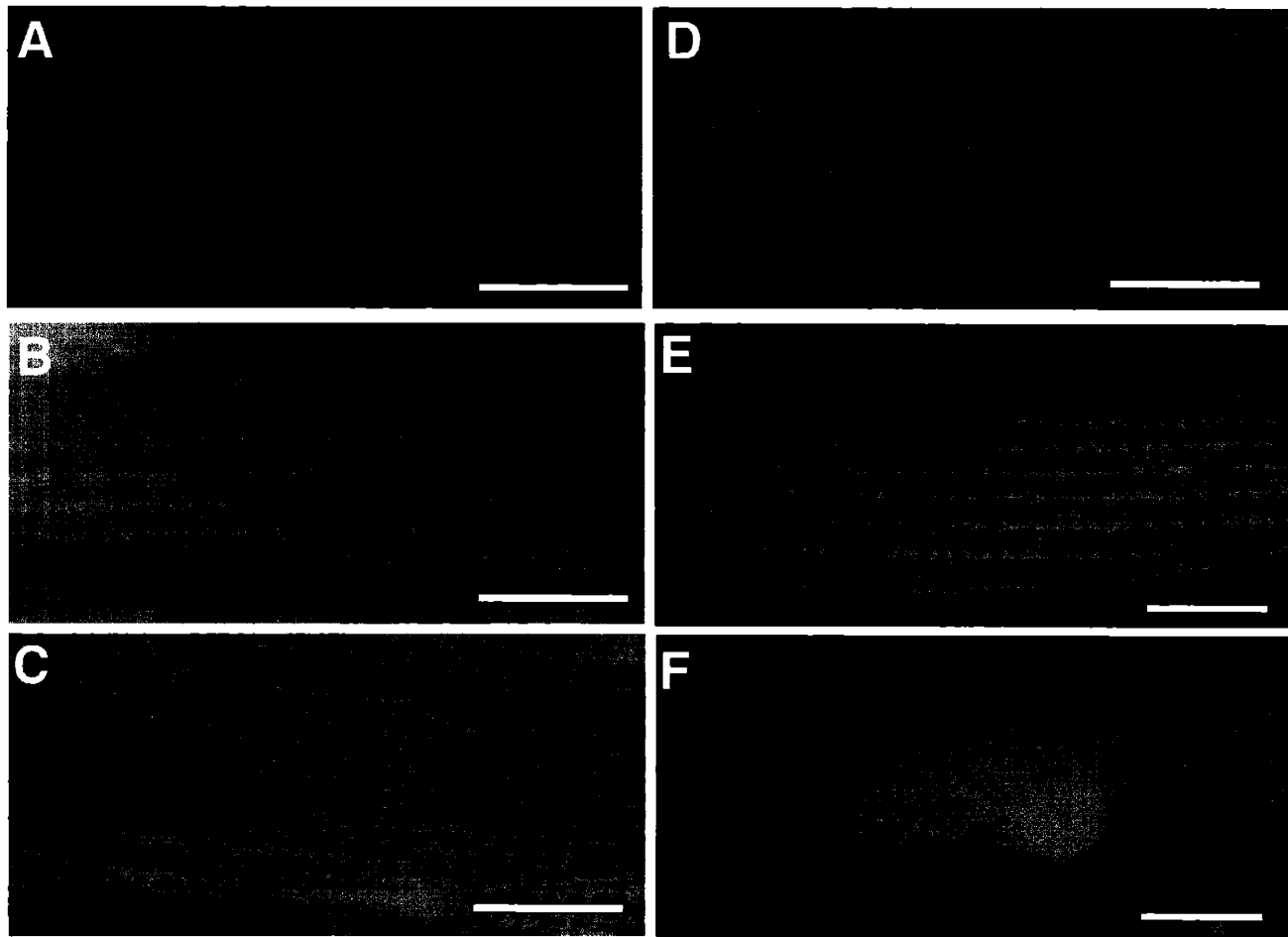
(C) TWK-18::GFP: The *twk-18::gfp* vector was kindly provided by L. Salkoff (unpublished reagent). The *gfp* coding region is fused at the C-terminus of *twk-18* in a genomic rescuing plasmid (Kunkel et al., 2000).

(D) PAT-3::GFP: A *pat-3::gfp* fusion gene was kindly provided by B. Williams (Gettner et al., 1995).

(E) SUP-18::GFP: A genomic *sup-18::gfp* fusion with *gfp* inserted between the transmembrane and nitroreductase domains of *sup-18* as previously described (Chapter 3).

(F) GFP: The *myo-3::gfp* vector pPD93.97 was kindly provided by A. Fire (Fire et al., 1990).

**Figure 2**



## Molecular Analysis of *sup-10* and *unc-93* Mutations

In this section, the identification of molecular lesions in *sup-10* and *unc-93* will be described.

### Mutational Analysis of *sup-10*

*sup-10* encodes a putative single-pass transmembrane protein of 332 amino acids with a short predicted intracellular domain of 10-12 amino acids (Cummins, Levin, Horvitz, Anderson unpublished results). The gf rubberband mutation *sup-10(n983)* contains a nonsense mutation at tryptophan 322 that deletes the last 10 amino acids of *sup-10*. While the molecular lesion in the gf allele of *sup-10* has been identified, the identities of lf mutations had not been determined.

We have identified the molecular lesions in 17 strong *sup-10(lf)* alleles isolated through various suppression screens of rubberband Unc mutants (Table 1). In addition, we have identified the mutations in the two *sup-10* partial lf alleles, *n4025* and *n4026*, that we generated to study the mode of suppression of *sup-18* (Chapter 3, Table 1). All of the nonsense, frameshift and splicing mutations are predicted to disrupt the C-terminal transmembrane domain of *sup-10*, and therefore the truncated proteins would be secreted and likely nonfunctional. The six missense mutations identified all affect residues within the extracellular domain of *sup-10*, except for the *sup-10(n240)* mutation which causes a glycine-to-arginine substitution at residue 323 at the beginning of the predicted intracellular domain. The *sup-10(n240)* mutation was isolated as a suppressor of the rubberband Unc phenotype of *unc-93(1500)* gf mutants. The double gf mutant *unc-93(e1500); sup-10(n983)* has a much weaker gf phenotype than either gf mutant alone (Greenwald and Horvitz, 1986; Levin and Horvitz, 1993). This mutual suppression between two gf mutations suggests that the two mutations may be incompatible within the proposed channel complex and thus their gf effects are mutually suppressive rather than additive. Since the glycine mutated in *sup-10(n240)* lies within the 10 amino acid stretch deleted by the *sup-10(n983)* gf nonsense mutation, we hypothesized that *sup-10(n240)* might also be a gf mutation that also mutually suppresses the *unc-93(e1500)* paralysis, thus enabling its initial isolation. We therefore separated the *sup-10(n240)* mutation away from *unc-93(e1500)*, but contrary to our prediction, *sup-10(n240)* animals had wild-type movement (data not shown). In addition, *sup-10(n240)* animals do not display a rubberband response when prodded ( $n > 50$ ). Thus, the *sup-10(n240)* mutation behaves as a lf mutation by both its

suppression of *unc-93(e1500)* defects and by the lack of a rubberband Unc phenotype on its own.

### **Mutational Analysis of Second-Site Partial Suppressors of *unc-93(e1500)***

We have identified the molecular lesions of three second-site mutations of *unc-93(e1500)* that partially reduce the strength of its rubberband Unc phenotype (Table 2). These alleles were isolated during an F<sub>2</sub> screen for weak suppressors of the locomotion defects of *unc-93(e1500)* gf mutants (Chapter 3) and may be useful in future structure-function studies.

### **References**

Greenwald, I., and Horvitz, H. R. (1986). A visible allele of the muscle gene *sup-10X* of *C. elegans*, *Genetics* 113, 63-72.

Levin, J. Z., and Horvitz, H. R. (1992). The *Caenorhabditis elegans unc-93* gene encodes a putative transmembrane protein that regulates muscle contraction, *J Cell Biol* 117, 143-155.

Levin, J. Z., and Horvitz, H. R. (1993). Three new classes of mutations in the *Caenorhabditis elegans* muscle gene *sup-9*, *Genetics* 135, 53-70.



Table 1. *sup-10* loss-of-function mutations

Allele	Mutation	Effect	Mutagen	Background
<i>n1017</i>	G56A	W19STOP	EMS	<i>sup-10(n983)</i>
<i>n1008</i>	C1832T	Q99 STOP	EMS	<i>sup-10(n983)</i>
<i>n2297</i>	G2173A	W139 STOP	EMS	<i>sup-9(n1550)</i>
<i>n1626</i>	A2264T	K170 STOP	Gamma	<i>sup-10(n983)</i>
<i>n3555</i>	49-133 del, 85 bp	16 + frameshift	UV-TMP	<i>unc-93(e1500)</i>
<i>n3558</i>	778-876 del, 99 bp	34 + frameshift	UV-TMP	<i>unc-93(e1500)</i>
<i>n183</i>	53 bp del, A1987G	128 + frameshift	Spo	<i>unc-93(e1500)</i>
<i>n1468</i>	2164 Tc1 insertion	136 + frameshift	Spo	<i>sup-10(n983)</i>
<i>e2127</i>	1847 Tc1 insertion	103 + frameshift	Spo	<i>wild type</i>
<i>n3978</i>	Large deletion	End points N.D.	EMS	<i>sup-10(n983)</i>
<i>n1007</i>	G1747A cagATT	Exon 3 Donor	EMS	<i>sup-10(n983)</i>
<i>n250</i>	T3045A GTTgtg	Exon 5 Donor	Gamma	<i>unc-93(e1500)</i>
<i>n342</i>	T3045A GTTgtg	Exon 5 Donor	NTG	<i>unc-93(e1500)</i>
<i>n619</i>	G1799A	E88K	EMS	<i>unc-93(e1500)</i>
<i>n3945</i>	C1874T	P113S	EMS	<i>sup-10(n983)</i>
<i>n4025<sup>a</sup></i>	G2896T	V200F	EMS	<i>unc-93(e1500)</i>
<i>n4026<sup>a</sup></i>	C2960T	L221F	EMS	<i>unc-93(e1500)</i>
<i>n3943</i>	C3250T	P300L	EMS	<i>sup-10(n983)</i>
<i>n240</i>	G3318A	G323R	DES	<i>unc-93(e1500)</i>

Both DNA strands were sequenced for each mutant. Location of mutation refers to the distance in nucleotides from the first base of the *sup-10* coding sequence within its genomic context. For splice mutations, intron sequence is represented in lowercase, exon in uppercase. EMS, ethyl-methylsulfonate; Spo, spontaneous; UV-TMP, ultraviolet and trimethylpsoralen; NTG, nitrosoguanidine; DES, diethyl sulfate. N.D., not determined.

<sup>a</sup> Allele is partial loss-of-function

Table 2. *unc-93* partial loss-of-function mutations

Allele	Mutation	Effect	Mutagen	Background
<i>e1500n4027</i>	G2400A	G306E	EMS	<i>unc-93(e1500)</i>
<i>e1500n4029</i>	G3708A	M540I	EMS	<i>unc-93(e1500)</i>
<i>e1500n4030</i>	C3884T	L566F	EMS	<i>unc-93(e1500)</i>

All mutations are second-site mutations in *unc-93(e1500)* that reduce the severity of the rubberband Unc phenotype but do not eliminate it. Both DNA strands were sequenced for each mutant. Location of mutations refers to the numbering as previously described (Levin and Horvitz, 1992). EMS, ethyl-methylsulfonate.